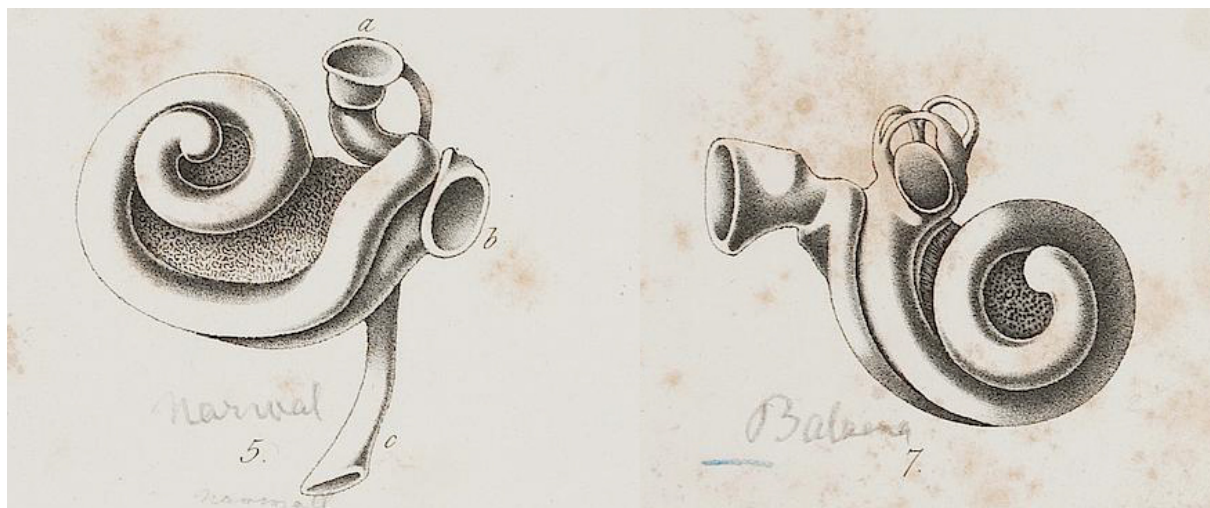# MONASH University

The evolution of hearing in Neoceti, with an emphasis on toothed mysticetes

Cochlea of a narwhal and a bowhead whale. Illustrations from Hyrtl 1845, used under a CC-BY license from Heidelberg University Library

Travis Park
BBSc (Hons)

A thesis submitted for the degree of Doctor of Philosophy at
Monash University in February 2017
School of Biological Sciences

Under the supervision of

Dr. Alistair R. Evans – Monash University
Dr. Erich M.G. Fitzgerald – Museums Victoria

For Heather & Lenox

Here's to sharing my love of the natural world with you.

For David Pickering

Without whom I would not be where I am today. Cheers mate.

Copyright notice

Abstract

Hearing is the primary means by which cetaceans (whales and dolphins) perceive their surroundings. The two extant cetacean groups Odontoceti (toothed whales) and Mysticeti (baleen whales) display a clear dichotomy in their acoustic biology, with odontocetes hearing and producing ultrasonic signals for echolocation, and mysticetes possessing low frequency or infrasonic hearing and vocalisations. However, the timing and pattern of when and how this dichotomy was established remains one of the critical gaps in our knowledge of cetacean evolution. In particular, virtually nothing is known about the hearing abilities of the earliest mysticetes, whose small stature and toothed jaws emphasize their disparity to modern giant baleen whales. By dividing the auditory system of toothed mysticetes into three functional modules — the mandible, basicranium and the inner ear — this thesis investigates their hearing abilities and establishes baseline sound sensitivities for the group. Informing these conclusions are new data on the hearing abilities of contemporaneous early odontocetes, a poorly known modern mysticete, as well as the influence of hearing ability on mandible shape.

I found that toothed mysticetes possess a cochlear morphology very similar to that of basilosaurids and modern mysticetes, including the inner ear of the previously undescribed pygmy right whale (*Caperea*), indicating that they could detect low frequency sounds and lacked the ability to echolocate. This plesiomorphic morphology is mirrored in the basicranium of toothed mysticetes, but contrasts with that of modern mysticetes, with significant modifications to both the extent of the air sinuses around the earbones and the level of articulation of the earbones with the skull. Additionally, quantitative shape analysis suggests a weak relationship between mandibular shape and what sounds an animal can detect. Together, these data suggest that overall; mysticete hearing has remained relatively unchanged over the last 34 million years, having low frequency hearing prior to the evolution of other signature mysticete characteristics including filter feeding, baleen and giant body size, with the high frequency hearing of odontocetes being the derived condition. The infrasonic hearing seen in modern mysticetes likely only became possible once the changes in the mysticete basicranium and mandible took place.
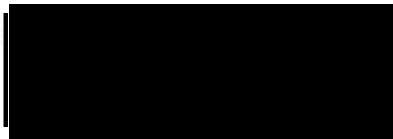
I also establish that the derived condition of odontocetes evolved very early on in their evolution. By examining the cochlea of an Oligocene xenorophid, one of the earliest diverging stem odontocete groups, I show that archaic odontocetes had a cochlea specialized for sensing high-frequency sound, indicating that the most archaic toothed whales possessed a functional biosonar system, contrasting with the plesiomorphic low frequency cochleae seen in early mysticetes.

Declaration

This thesis contains no material which has been accepted for the award of any other degree or diploma at any university or equivalent institution and that, to the best of my knowledge and belief, this thesis contains no material previously published or written by another person, except where due reference is made in the text of the thesis.

Signature:

Print Name: Travis Park

Date: 24/06/2017

Publications during enrolment

- **Park T.** 2014. Redescription of the Miocene penguin *Pseudaptenodytes macraei* Simpson (Aves: Sphenisciformes) and redefinition of the taxonomic status of ?*Pseudaptenodytes minor* Simpson. Alcheringa 38, 450–454.

- **Park T,** Fitzgerald EMG, Evans AR. 2016. Ultrasonic hearing and echolocation in the earliest toothed whales. Biology Letters 12, 20160060.

- **Park T,** Fitzgerald EMG, Gallagher SJ, Tomkins E, Allan T. 2016. New Miocene Fossils and the History of Penguins in Australia. PLoS ONE 11, e0153915.

- Marx FG, Hocking DP, **Park T,** Ziegler T, Evans AR, Fitzgerald EMG. 2016. Suction feeding preceded filtering in baleen whale evolution. Memoirs of Museum Victoria 75, 71–82.

- **Park T,** Evans AR, Gallagher SJ, Fitzgerald EMG. 2017. Low-frequency hearing preceded the evolution of giant body size and filter feeding in baleen whales. Proceedings of the Royal Society B: Biological Sciences 284, 20162528.

Thesis including published works declaration

I hereby declare that this thesis contains no material which has been accepted for the award of any other degree or diploma at any university or equivalent institution and that, to the best of my knowledge and belief, this thesis contains no material previously published or written by another person, except where due reference is made in the text of the thesis.

This thesis includes two original paper published in peer reviewed journals and one submitted publication. The core theme of the thesis is investigating the hearing abilities of cetaceans, with an emphasis on the archaic toothed mysticetes. The ideas, development and writing up of all the papers in the thesis were the principal responsibility of me, the student, working within the School of Biological Sciences under the supervision of Dr. Alistair Evans and Dr. Erich Fitzgerald.

The inclusion of co-authors reflects the fact that the work came from active collaboration between researchers and acknowledges input into team-based research.

In the case of chapters two, three and six my contribution to the work involved the following:

Thesis Chapter	Publication Title	Status *(published, in press, accepted or returned for revision, submitted)*	Nature and % of student contribution	Co-author name(s) Nature and % of Co-author's contribution*	Co-author(s), Monash student Y/N*
2	Low frequency hearing preceded the evolution of giant body size and filter feeding in baleen whales	Published	75%. Conceived the study, data processing & analysis, wrote manuscript.	1) Erich Fitzgerald: 10%. Conceived the study, guided data analysis, wrote manuscript. 2) Alistair Evans: 10%. Guided data analysis, wrote manuscript. 3) Stephen Gallagher: 5%. Provided information on specimen stratigraphy and age.	No
3	The cochlea of the enigmatic pygmy right whale *Caperea marginata* (Cetacea, Mysticeti)	Published	70%. Conceived the study, data processing & analysis, wrote manuscript.	1) Felix Marx: 10%. Conceived the study, specimen photography, guided data analysis, wrote manuscript. 2) Erich Fitzgerald: 10%. Conceived the study, guided data analysis, wrote manuscript. 3) Alistair Evans: 10%. Guided data analysis, wrote manuscript.	No
6	Ultrasonic hearing and echolocation in the earliest toothed whales	Published	80%. Conceived the study, data processing & analysis, wrote manuscript.	1) Erich Fitzgerald: 10%. Conceived the study, specimen photography, guided data analysis, wrote manuscript. 2) Alistair Evans: 10%. Guided data analysis, wrote manuscript.	No

I have renumbered sections of submitted or published papers in order to generate a consistent presentation within the thesis.

This thesis also includes two chapters which have not been submitted for publication. In the case of chapters four and five my contribution to the work involved the following:

Thesis Chapter	Publication Title	Status (Not submitted, published, in press, accepted or returned for revision)	Nature and % of student contribution	Co-author name(s) Nature and % of Co-author's contribution*	Co-author(s), Monash student Y/N*
4	Predatory basilosaurids to filter-feeding giants: transformation of the basicranium and the evolution of hearing in baleen whales	Not submitted	85%. Conceived the study, data processing & analysis, wrote manuscript.	1) Erich Fitzgerald: 15%. Guided data analysis, feedback on manuscript.	No
5	Shape Analysis of Odontocete Mandibles: Correlations between morphology and hearing abilities	Not submitted	80%. Conceived the study, data processing & analysis, wrote manuscript.	1) Erich Fitzgerald: 10%. Feedback on manuscript 2) Alistair Evans: 10%. Guided data analysis, feedback on manuscript.	No

Student signature: ███████   **Date:** 24/06/2017
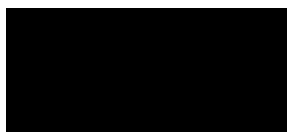
The undersigned hereby certify that the above declaration correctly reflects the nature and extent of the student's and co-authors' contributions to this work. In instances where I am not the responsible author I have consulted with the responsible author to agree on the respective contributions of the authors.

Main Supervisor signature: ███████   **Date:** 24/06/2017

Acknowledgements

Since I began this thesis in 2013, my life has changed in many ways. Most notably, I have become both a husband and a father; and it is my wife Heather and son Lenox who are my greatest respective sources of support and inspiration. I love you both very much and could not have done this without you. To my parents, I thank you for instilling in me the curiosity about the world and its past that drives me as a scientist. To my Mother and Father in-law, I thank you for giving me the freedom to pursue my dream to become a scientist. I'd also like to give a special mention to Poppy, Presto and Belle for being my furry little study-buddies at various times during my PhD.

I'd like to think that I have also become a better scientist over the past four years. If true, the two primary reasons for this are my supervisors, Dr. Alistair Evans and Dr. Erich Fitzgerald. I'd like to thank you both for your guidance and endless patience during the PhD process. I hope that we continue to collaborate together for many years to come.

Also key to my academic development have been my peers. I'd like to extend my sincere gratitude to Matthew McCurry, Felix Marx, David Hocking, Lap Chieu, Qamariya Nasrullah and Alana Sharp. I very rarely fail to come out of a discussion about science with any of you without feeling inspired and bursting with new enthusiasm. Thanks are also extended to the rest of the members of the Evans EvoMorph Lab, both past and present.

I'd also like to thank everyone at Museums Victoria for all their help and support especially David Pickering, Lisa Nink, and Tim Ziegler. David, in particular, always went out of his way to help me if I needed it. Thank you, you will be dearly missed. Thanks also to Richard Reina, Justin Adams and Anne Peters for being on my thesis committee and to Fiona Hibbert for assistance with the administrative side of the PhD. Thanks are also due to everyone who provided access to their respective museum collections during the course of my candidature. I am also indebted to Jorge Vélez-Juarbe, Jim Mead and Diane Nyhoff for offering up their homes to me during my research travels.

I also wish to gratefully acknowledge the financial support I have received during the course of this PhD, which would have not been possible to complete if not given. This came from an Australian Postgraduate Award, a Museums Victoria 1854 Scholarship, a Monash University Postgraduate Travel Grant, an Australian Geographic Seed Grant and a University of California Berkeley Welles Fund Travel Grant.

Thank you all.

"The sea is murky. Sight and smell, which work well for mammals on the land, are not of much use in the depths of the ocean. Those ancestors of the whales who relied on these senses to locate a mate or a baby or a predator did not leave many offspring. So another method was perfected by evolution; it works superbly well and is central to any understanding of the whales: the sense of sound."

Carl Sagan, Cosmos (1980)

Is it not curious, that so vast a being as the whale should see the world through so small an eye, and hear the thunder through an ear which is smaller than a hare's?"

Herman Melville, Moby Dick (1851)

"In all cetaceans the sense of hearing is the most important of the special senses."

Fraser& Purves (1960)

Contents

1. Introduction

Our senses connect us to the world. Complex, precise and dynamic systems, sensitive enough to detect a single photon or molecule from a bewildering array of competing stimuli, they allow animals to perceive their surroundings, detect prey and avoid predators. Studying the underlying evolutionary patterns and mechanisms of sensory systems sheds light on some of the most fundamental events in the evolution of life, such as the secondary adaptation of tetrapods to water.

A stunning example of sensory evolution is found within the cetaceans (whales and dolphins). These enigmatic marine mammals have adapted their original terrestrial sensory bauplan to function in a medium 800 times denser than air. Modern cetaceans comprise the toothed whales (odontocetes) and baleen whales (mysticetes). Both groups use auditory cues as the primary method of interpreting and interacting with their surroundings, with their olfactory abilities being the poorest of any mammal group (Pihlström 2008) and vision being limited due to low light levels in water at depth. The two modern groups of cetaceans also display a clear dichotomy in their acoustic biology, with odontocetes capable of hearing and producing ultrasonic signals (>20,000 Hz) for echolocation, and mysticetes possessing low frequency or infrasonic (<20 Hz) hearing and vocalisations (Ketten 2000; Cummings & Thompson 1971). However, the timing, rate and the processes involved in establishing this dichotomy remains uncertain, with critical data on the earliest members of the two living groups (especially the mysticetes) lacking.

1.1 Hearing in mammals

The auditory system in mammals is morphologically unique, with the quadrate, articular and angular of the early synapsid compound jaw being co-opted as the incus, malleus and tympanic bones respectively in the mammalian middle ear (Allin & Hopson 1992). The inner ear also changed dramatically, with the cochlear canal lengthening, enhancing frequency

discrimination (Vater et al. 2004) and eventually becoming coiled in therian mammals (Manley 2012).

In the terrestrial mammal auditory pathway, sound enters the ear via the pinna (external ear) and an air-filled external auditory meatus to the tympanic membrane, where the differential pressures cause it to vibrate and pass the sound onto the three middle ear ossicles: the malleus, incus, and stapes (Fig 1.1). This chain of tiny bones serves to amplify the sound pressure by decreasing the area through which the sound is passed (Nummela et al. 2007). At the internal end of the ossicular chain, the stapes transmits the sound to the fluid-filled cochlea via a piston-like action (Nummela et al. 2004) (Fig 1.1A). Within the cochlea, this action causes the displacement of fluid in the scala vestibuli (Fig 1.1B). This displacement travels apically along the scala vestibuli as well as being passed into the scala media where the movement of the fluid sets the basilar membrane into motion. The region of the basilar membrane that experiences peak displacement is determined by the frequency of the acoustic stimulus. High frequency sounds will cause maximum displacement near the base of the cochlea, where the basilar membrane is stiffest, whereas low frequency sounds will cause maximum displacement at the apex of the cochlea where the basilar membrane is more flexible. At this point the sound is transduced into a nerve signal by specialised hair cells in the organ of Corti and sent to the brain via the cochlear nerve (Fig 1.1B) (Echteler et al. 1994).
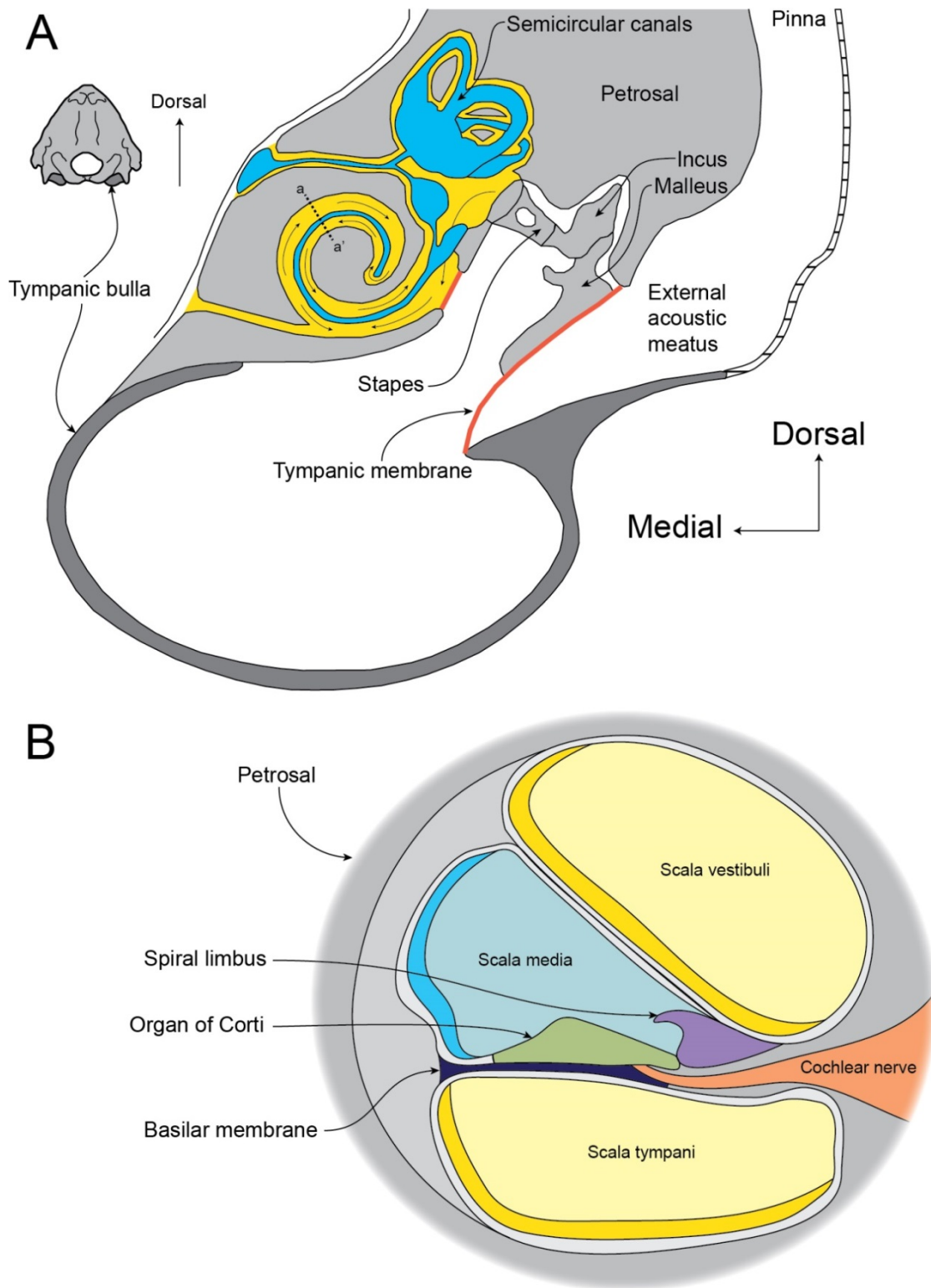
Fig 1.1. A, Cross-section through the head of a domestic dog (*Canis familiaris*) showing structures of outer, middle, and inner ears. Arrows in the cochlea show direction that vibrations travel. Dashed line a–a' indicates position of slice in section B. Modified from Evans (1993) and Ekdale (2016). B, Cross section of the cochlear canal showing distribution of structures and scalae.

This pathway is not effective underwater, however, as the external auditory meatus becomes filled with water, reducing the pressure differential at the tympanic membrane and therefore greatly diminishing its ability to transmit sounds to the middle ear bones. Furthermore, when underwater, the similar density of animal tissue to water means that sounds will simply travel through the soft tissues and bones, a phenomenon known as bone conduction (Denny 1993; Nummela et al. 2007). However, this will mean that sounds reach both ears at the same time, preventing the animal from using the interaural (between ears) difference to distinguish which direction the sound originally came from. This terrestrial auditory pathway would have been the plesiomorphic morphology possessed by the ancestor of all cetaceans; therefore, extensive changes were required for effective underwater hearing.

1.2 Cetacean evolution: a brief primer

Cetaceans are first found in the fossil record in the Early Eocene of Pakistan; these animals were semiaquatic "walking whales" belonging to the Pakicetidae and Ambulocetidae (Gingerich et al. 1983; Thewissen et al. 1996; Madar 2007). They still retained the ability to move around on land although their skeleton was denser than their wholly terrestrial relatives (Madar 2007). By the Middle Eocene, the Remingtonocetidae and Protocetidae had appeared (Kumar & Sahni 1986; Hulbert Jr 1998a; Gingerich et al. 2001,2009; Bajpai et al. 2011) and evolved into nearshore marine (Gingerich et al. 1995; Clementz et al. 2006) animals that possessed a crocodile-like morphology, with long bodies, short limbs and a narrow, elongated rostrum (Thewissen & Bajpai 2009). The protocetids rapidly diversified and spread across the globe, reaching as far as North and South America (Hulbert et al. 1998b; Uhen et al. 2011). The transition to an obligately aquatic lifestyle was completed with the appearance of the basilosaurids in the late Middle Eocene. Their remains are known from every continent except for Australia (Uhen 2009). The basilosaurids (and especially the Dorudontinae) are

thought to have given rise to Neoceti (the group comprised of Mysticeti and Odontoceti) (Uhen 2004).

1.3 Hearing in archaeocete cetaceans

As cetaceans evolved from wholly terrestrial into obligately marine mammals during the course of the Eocene (52-34 million years ago), their entire anatomy underwent major restructuring and modification. Perhaps no other organ system underwent as profound and wholesale a series of changes as that of the ear region which had to evolve the ability to detect sound in a much denser medium (Fig 1.2).

The earliest whales, the pakicetids, displayed very few adaptations for underwater hearing. They possessed ossicles that had partly rotated and become pachyostotic (thickened) and a thickened tympanic bone (the involucrum) that lacked a rostromedial connection to the periotic, allowing the tympanic to vibrate independently of the periotic (Nummela et al. 2004,2006). This enhanced their ability to use bone conduction, which would have been the method by which sound was transmitted when underwater, although directional hearing underwater would still have been poor (Thewissen & Hussain 1993; Luo 1998; Luo & Gingerich, 1999; Nummela et al. 2004,2007). The mandibular foramen was small and had a relatively thick lateral mandibular wall, indicating the lack of the mandibular fat pad seen in later cetaceans. This feature first appears in ambulocetids, where the first integration of the mandible into the auditory pathway and development of the tympanic plate (Fleischer 1975,1978) for use in a sound conduction pathway is seen. These animals possessed a large mandibular foramen, which would have housed a mandibular fat pad consisting of fats whose structure provides an acoustically favourable pathway to the middle ear. Uniquely, ambulocetids also possessed a jaw joint that had expanded in such a way that the tympanic bulla and the mandibular condyle actually share a bony contact (Thewissen et al. 1996). Because of this, it has been hypothesised that *Ambulocetus* may have used bone conduction

5

on land by placing its lower jaw to the ground and hearing the vibrations, in a similar manner to some extant crocodiles or mole rats (Rado et al. 1989; Thewissen et al. 1996).

The remingtonocetids and protocetids also possessed large mandibular foramina, but the lateral wall of the mandible is thinner than that seen in ambulocetids, meaning that the sensitivity of their underwater hearing had increased. A functional fibrocartilaginous external auditory meatus is still present, based on the morphology of the tympanic ring (Nummela et al. 2007), indicating that these animals could also still hear in air, albeit poorly. The contact between the tympanic and periotic is also further reduced and the middle ear ossicles are enlarged, fully rotated and beginning to approach the morphology of modern cetaceans (Thewissen 2014). The tympanic plate has further thinned and enlarged. In protocetids, the periotic had become more detached from the skull via the development of the peribullary sinus (the posterior sinus would have been incipient if at present (Luo & Gingerich 1999)), allowing for improved directional underwater hearing (Nummela et al. 2007). However, the tympanic bulla and the periotic still contacted the basioccipital (Luo & Gingerich 1999), limiting the extent to which directional underwater hearing could be effective.

In basilosaurids, the ear was functionally the same as modern cetaceans, with the lateral wall of the mandible almost as thin as that in odontocetes and the tympano-periotic complex was acoustically isolated via air sinuses, implying that underwater hearing was now the primary function of the ear. Debate remains over whether basilosaurids were adapted to hear high (Fahlke et al. 2011; Churchill et al. 2016) or low (Uhen 2004; Nummela et al. 2007; Ekdale & Racicot 2015) frequencies. Overall, this transition from an exclusively terrestrial hearing system to a sensitive underwater hearing system took place in less than 10 million years (Nummela et al. 2004).
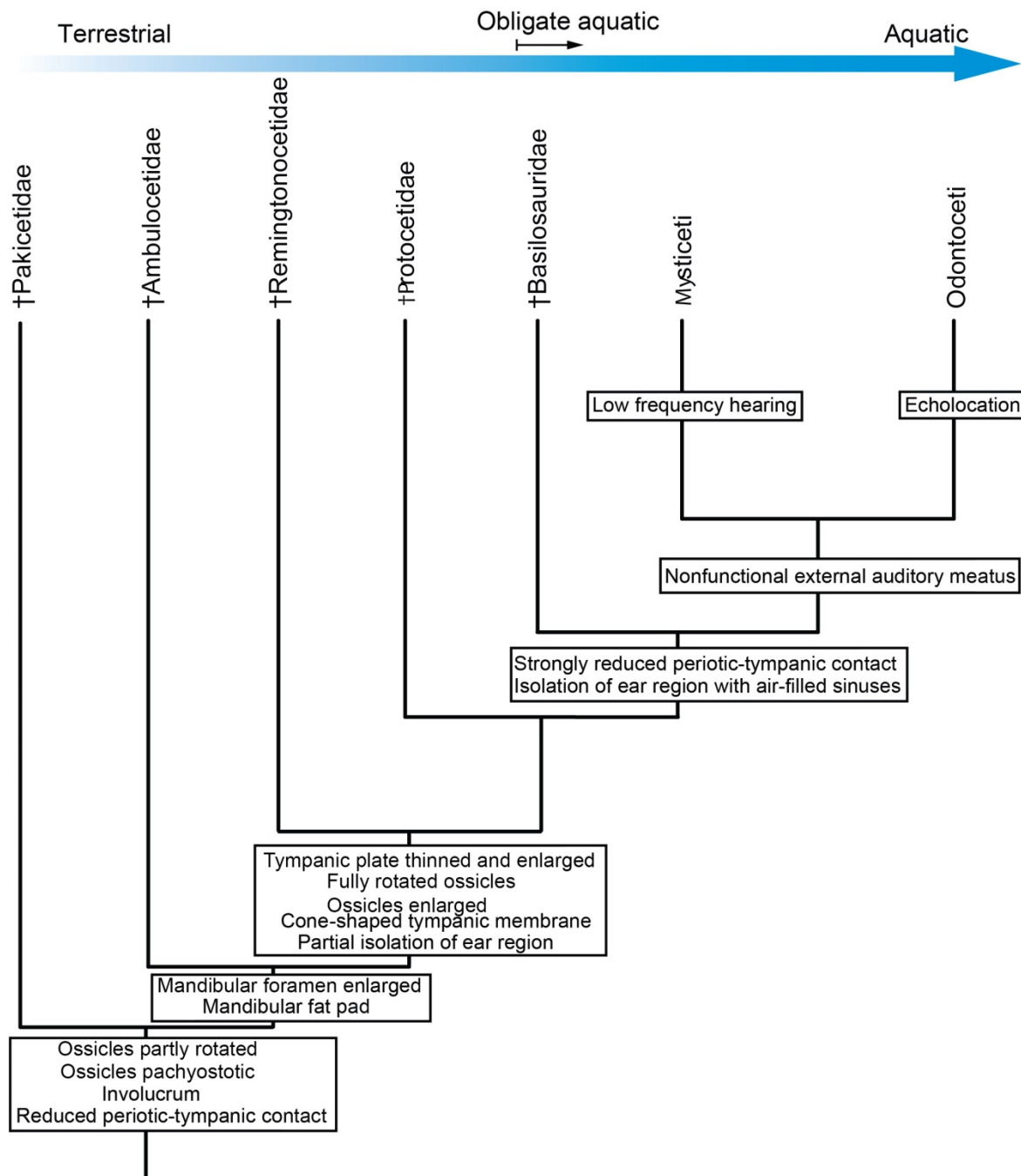
Fig 1.2. Cladogram showing evolution of features related to hearing in cetaceans. Data sources: Nummela et al. (2004,2007); Thewissen (2014); Marx et al. (2016a).

1.4 Hearing in Neoceti

By the time Neoceti had diverged from basilosaurids in the late Eocene (Marx & Fordyce 2015), the mandibular fat pad had completely replaced the external auditory meatus as the entry point of the auditory pathway. For early odontocetes and mysticetes, this means that the

auditory pathway was composed of three functional modules: the mandible; the basicranium/middle ear; and the inner ear.

As noted above, living odontocetes and mysticetes have distinctly different hearing abilities. Odontocetes specialise in hearing extremely high frequencies, up to 200 kHz in some species (Wang et al. 1992). Their ear bones have become even more isolated from the rest of the skull, being attached only via ligaments in some species (Kellogg 1928) and the surrounding air sinuses have become greatly enlarged. The high frequency hearing of odontocetes is tied with their signature innovation, echolocation. Firstly, high frequency sounds are produced using the phonic lips and air sacs of the nasal passage. These sounds are then emitted though the fatty melon in the forehead which acts as an acoustic lens (Varansi 1975). The sounds reflect off the surrounding environment, travel back to the animal, enter through the fat pad in the mandible and pass through the middle ear and eventually into the inner ear (Fig 1.3).

Despite the existence of the mandibular fat pad being known since the 1800s it was not associated with the auditory system until Norris (1964) proposed it may provide a low impedance pathway to the ears. The idea was initially met with scepticism but was validated by a number of studies in the following years (Bullock et al. 1968; Norris & Harvey 1974; Brill et al. 1988).

More recent developments have seen non-invasive visualisation techniques to study the in situ auditory anatomy of odontocetes and model the auditory pathway in odontocete heads (e.g. Ketten & Wartzok 1990; Ketten 1994, 1997, 2000; Aroyan 2001; Cranford et al. 2008,2010). The skulls of fossil odontocetes suggest that they too possessed the ability to echolocate, although whether or not the inner ears of these early taxa could actually detect high frequencies has until now been uncertain (see Chapter 6; Churchill et al. 2016). Whilst

much remains to be determined, the hearing abilities of modern odontocetes are relatively

well known.
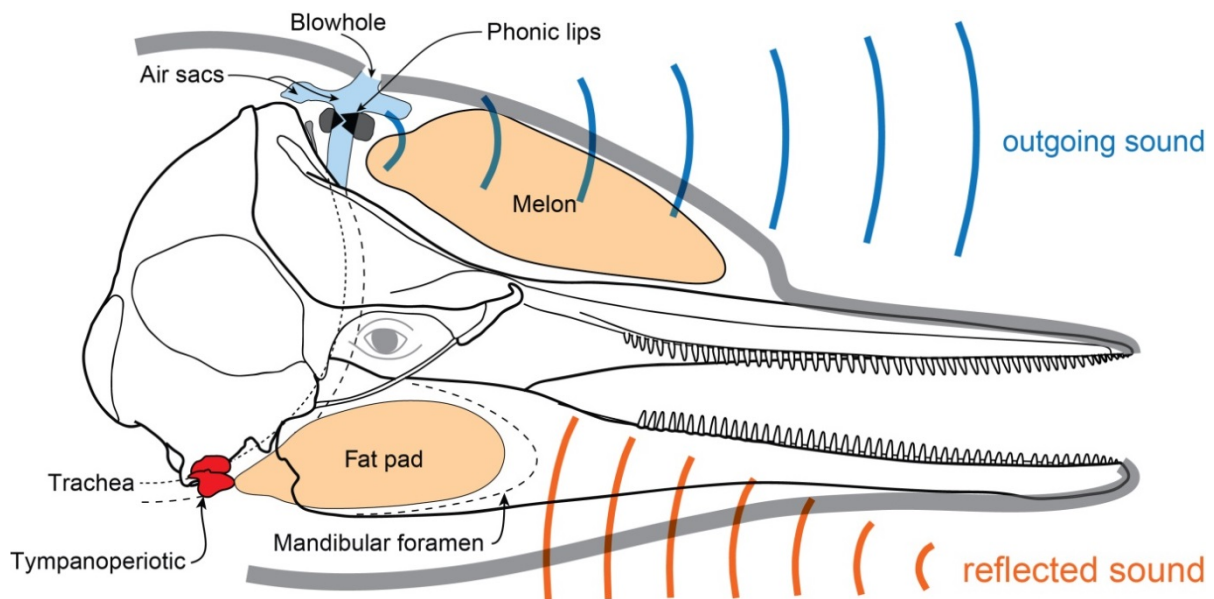
Fig 1.3. Schematic right lateral view of the odontocete auditory pathway. Based on Cranford et al. (1996) and Marx et al (2016a).

On the other hand, the same cannot be said for our knowledge of mysticete hearing.

Some species are known to produce infrasonic (<20 Hz) frequencies (Cummings &

Thompson 1971). The ear bones are also tightly attached to the skull (Fig 1.4), unlike the

loose attachment seen in most odontocetes, suggesting that mysticetes hear in a different way.

Exactly how mysticetes hear sounds is still unknown. The sheer magnitude of mysticete body

size means it is extremely difficult to keep the animals in captivity and to train them to

perform experiments. Similarly, their large size prevents most species from being put in CT

scanning machines to visualise their internal anatomy (Mooney et al. 2012). Only in the last

few years has the technology become available to accommodate larger specimens, with

recent studies revealing two potential (but not mutually exclusive) auditory pathways.

Yamato et al. (2012) proposed a potential sound reception pathway via the fat body that

contacts the tympano-periotic complex laterally in the minke whale (*Balaenoptera*

acutorostrata). Cranford and Krysl (2015) used finite element analysis (FEA) on a juvenile

fin whale (*Balaenoptera physalus*) to determine that mysticetes may use bone conduction to pass sound to the ears. Other research has examined the inner ear of mysticetes, confirming their ability to hear low frequency sounds (Ekdale & Racicot 2015).
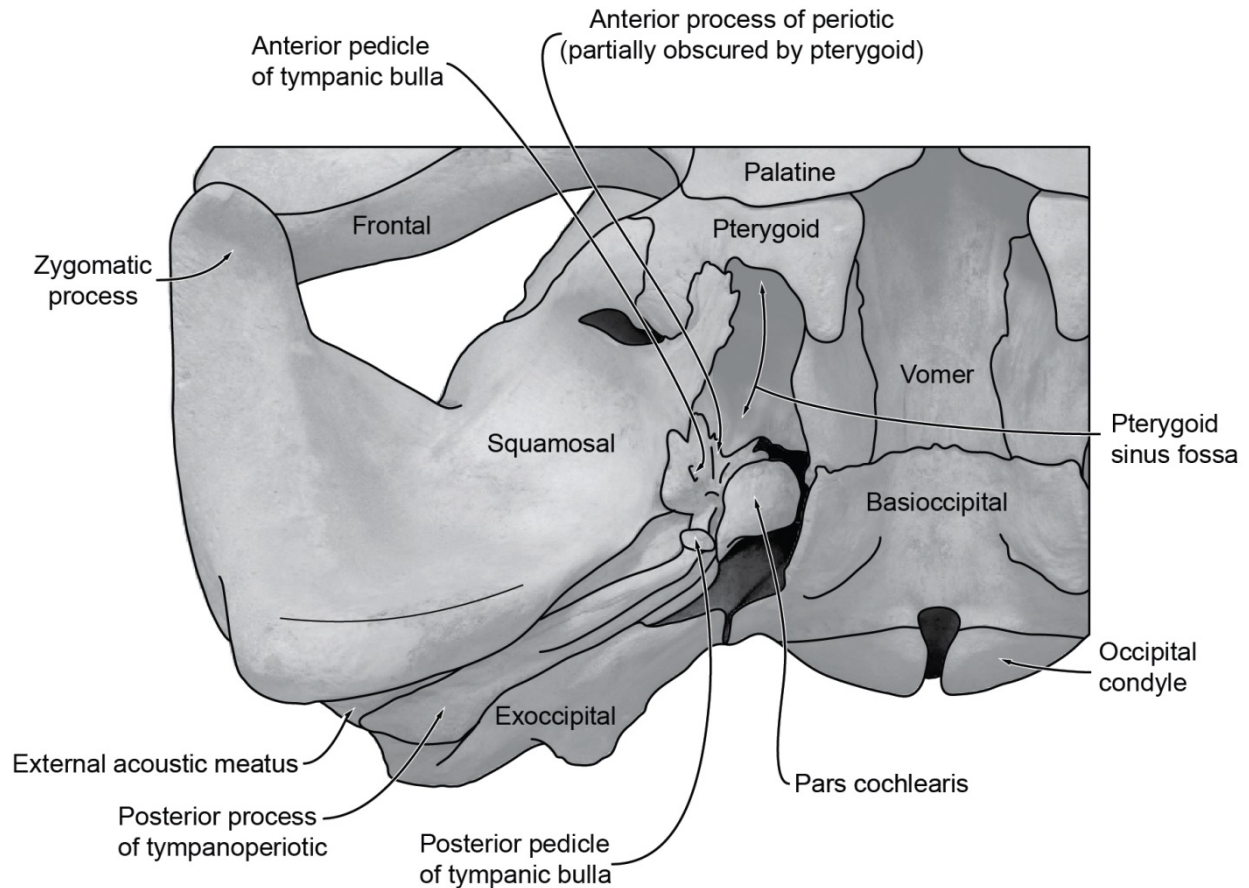
Fig 1.4. Right basicranium of a mysticete, showing high degree of contact of periotic with skull. Image courtesy of Felix Marx, used with permission.

1.5 Early mysticetes: the great unknown of cetacean hearing

The importance of hearing to cetaceans has ensured that much time and effort has been devoted to investigating how it has evolved in archaeocetes and how it works in living species. As a result, the key morphological changes associated with hearing in cetaceans as they shifted from a terrestrial to an increasingly aquatic lifestyle are relatively well understood. Nevertheless, unanswered questions remain.

Perhaps the biggest unknown in the field of cetacean hearing is the hearing abilities of the earliest mysticetes. These archaic animals did not yet possess baleen (Marx et al. 2016a,b; but see Deméré & Berta 2008) but still retained teeth. Did these small-bodied animals also have low frequency hearing like that in modern mysticetes or did they instead have high frequency hearing which was then lost? Toothed mysticetes also possessed an enlarged mandibular foramen similar to basilosaurids and odontocetes, whereas modern mysticetes have lost this feature. What does this imply for their auditory pathway?

Determining the hearing abilities of toothed mysticetes can also inform broader questions on the evolution of the group and even Neoceti as a whole. Were the hearing abilities of mysticetes established from the very beginning of their lineage or were there changes in hearing abilities that occurred with other key functional acquisitions, such as baleen or giant body size? When was the dichotomy between the hearing abilities of odontocetes and mysticetes first established?

1.6 Research objectives

The lack of knowledge regarding the hearing abilities of toothed mysticetes is the catalyst for this thesis. It is perhaps the greatest gap in our knowledge of the evolution of cetacean hearing. However, there are several other gaps in our knowledge of cetacean hearing that, if tackled, will give us the best context within which to understand the evolution of mysticete hearing.

One such gap is whether the earliest odontocetes were capable of detecting high frequency sounds. Skullsof stem taxa possess premaillary sac fossae, suggesting they had the air sacs required to produce high frequency sounds (Uhen 2008; Geisler et al. 2014), but it has never been confirmed whether their cochleae was capable of detecting the high frequencies required to echolocate. Establishing this allows comparisons to be made

concerning when the acoustic dichotomy between odontocetes and mysticetes was first established.

Another gap in knowledge is the extent of sampling of inner ear data in modern mysticetes. Previous studies have detailed the cochleae of all living mysticete families except one, the Cetotheriidae (or Neobalaenidae). By describing the inner ear of the single living representative of this lineage, *Caperea marginata*, every modern mysticete family will be represented and a more accurate picture of variation in mysticete cochleae will be obtained.

Additionally, how sounds reach the inner ears is not adequately explored. Therefore, understanding the evolution of the basicranium and the mandible in mysticetes is important for interpreting change sin acoustics between archaeocetes and chaeomysticetes.

Finally, the relationship between the shape of the mandible and what frequencies a cetacean can hear is yet to be investigated. If a relationship were found in modern odontocetes who have published frequency ranges, then these data could theoretically be used to estimate the frequency ranges in fossil taxa, including toothed mysticetes.

1.7 Thesis structure

This thesis examines hearing in Neoceti with a focus on the toothed mysticetes. In order to so the auditory pathway has been split into three functional modules: the mandible; the basicranium/middle ear; and the inner ear (the cochlea). Each chapter deals with either a particular functional module of the toothed mysticete auditory pathway, or addresses one of the gaps in knowledge required to better understand toothed mysticete hearing. The thesis is structured as follows:

- **Chapter 2:** This chapter provides the first detailed descriptions of toothed mysticete cochleae and compares them to modern mysticetes, odontocetes and basilosaurid cochleae. This has important implications for determining what sounds toothed mysticetes could hear. This chapter was published in the

journal *Proceedings of the Royal Society B: Biological Sciences* in February 2017.

- **Chapter 3:** This chapter uses the same techniques as Chapter 2 to describe the cochlea of the enigmatic living mysticete species *Caperea marginata* and compare it to other living and fossil mysticetes. This chapter has been submitted doe publication in the Journal of Morphology.

- **Chapter 4:** This chapter describes the basicrania of a representative of every toothed mysticete family and compares them to other fossil mysticetes, modern mysticetes and basilosaurids in the context of the degree of isolation of the ear bones from the skull and development of the air sinuses. This is then tied in with recent research on the auditory pathway in modern mysticetes to synthesise the first model of the evolution of hearing in Mysticeti.

- **Chapter 5:** This chapter explores whether there is a relationship between mandible shape and the frequencies heard in a range of modern odontocetes that have published frequency ranges. This is done using the quantitative analytical technique of 3D geometric morphometrics. Implications for interpreting the functional significance of mandible morphology in stem mysticetes are discussed

- **Chapter 6:** This chapter determines whether or not one of the earliest odontocete lineages, the Xenorophidae, possessed the cochlear morphology required to detect the high frequencies used in echolocation. This is important for determining when the acoustic dichotomy of Neoceti first became established. This chapter was published in the journal *Biology Letters* in April 2016.

- **Chapter 7:** This chapter presents the discussion and future directions that stem from this thesis.

- **Chapter 8:** This final chapter presents the conclusions of this thesis.

References

Allin EF, Hopson JA. 1992. Evolution of the Auditory System in Synapsida ("Mammal-Like Reptiles" and Primitive Mammals) as Seen in the Fossil Record. In Webster DB, Fay RR, Popper AN, eds, The Evolutionary Biology of Hearing. Springer-Verlag, New York, pp. 587–614.

Aroyan JL. 2001. Three-dimensional modelling of hearing in *Delphinus delphis*. The Journal of the Acoustical Society of America 110, 3305–3318.

Bajpai S, Thewissen JGM, Conley RW. 2011. Cranial Anatomy of Middle Eocene *Remingtonocetus* (Cetacea, Mammalia) from Kutch, India. Journal of Paleontology 85, 703–718.

Berta A, Sumich JL, Kovacs KM. 2015. Marine Mammals Evolutionary Biology (3rd ed). Academic Press, London, 726 p.

Brill RL, Sevenich ML, Sullivan TJ, Sustman JD, Witt RE. 1988. Behavioral evidence for hearing through the lower jaw by an echolocating dolphin (*Tursiops truncatus*). Marine Mammal Science 4, 223–230.

Bullock TH, Grinnell AD, Ikezono F, Kameda K, Katsuki Y, Nomoto M, Sato O, Suga N, Yanagisava K. 1968. Electrophysiological studies of the central auditory mechanisms in cetaceans. Zeitschrift für Vergleichende Physiologie 59, 117–156.

Churchill M, Martínez-Cáceres M, de Muizon C, Mnieckowski J, Geisler JH. 2016. The Origin of High-Frequency Hearing in Whales. Current Biology http://dx.doi.org/10.1016/j.cub.2016.06.004.

Clementz MT, Goswami A, Gingerich PD, Koch PL. 2006. Isotopic records from early whales and sea cows: contrasting patterns of ecological transition. Journal of Vertebrate Paleontology 26, 355–70.

Cranford TW, Krysl P. 2015. Fin Whale Sound Reception Mechanisms: Skull Vibration
Enables Low-Frequency Hearing. PLoS ONE 10, e0116222.

Cranford TW, Amundin M, Norris KS. 1996. Functional morphology and homology in the
odontocete nasal complex: Implications for sound generation. Journal of Morphology
228, 223–285.

Cranford TW, Krysl P, Hildebrand JA. 2008. Acoustic pathways revealed: Simulated sound
transmission and reception in Cuvier's beaked whale (*Ziphius cavirostris*).
Bioinspiration & Biomimetics 3, 1–10.

Cranford TW, Krysl P, Amundin M. 2010. A new acoustic portal into the odontocete ear and
vibrational analysis of the tympanoperiotic complex. PLoS ONE 5, e11927.

Cummings WC, Thompson PO. 1971. Underwater sounds from the blue whale, *Balaenoptera
musculus*. The Journal of the Acoustical Society of America 50, 1193–1198.

Denny MW. 1993. Air and water: the biology and physics of life's media. Princeton
University Press, New Jersey, 341 p.

Deméré TA, Berta A. 2008. Skull anatomy of the Oligocene toothed mysticete *Aetiocetus
weltoni* (Mammalia; Cetacea): implications for mysticete evolution and functional
anatomy. Zoological Journal of the Linnean Society of London 154, 302–352.

Echteler SM, Fay RR, Popper AN. 1994. Structure of the Mammalian Cochlea. In Fay RR,
Popper AN, eds, Comparative Hearing: Mammals. Springer-Verlag, New York, pp.
134–171.

Ekdale EG. 2016. Form and function of the mammalian inner ear. Journal of anatomy. 228,
324–337.

Ekdale EG, Racicot RA. 2015. Anatomical evidence for low frequency sensitivity in an archaeocete whale: comparison of the inner ear of *Zygorhiza kochii* with that of crown Mysticeti. Journal of Anatomy 226, 22–39.

Evans, HE. 1993. The ear. In Evans HE, ed, Miller's Anatomy of the Dog, (3rd ed). Saunders, Philadelphia, pp. 988–1008.

Fahlke J, Gingerich PD, Welsh RC, Wood AR. 2011. Cranial asymmetry in Eocene archaeocete whales and the evolution of directional hearing in water. Proceedings of the National Academy of Sciences 108, 14545–14548.

Fleischer G. 1975. Über das spezialisierte Gehörorgan von Kogia breviceps (Odontoceti). Zeitschrift für Säugetierkunde, 40, 89–102.

Fleischer G. 1978. Evolutionary Principles of the Mammalian Middle Ear. Advances in Anatomy, Embryology, and Cell Biology, 55, 1–70.

Geisler JH, Colbert MW, Carew JL. 2014. A new fossil species supports an early origin for toothed whale echolocation. Nature 508, 383–386.

Gingerich, PD, Wells N, Russell D, Shah SM. 1983. Origin of whales in epicontinental remnant seas: new evidence from the early Eocene of Pakistan. Science 220, 403–406.

Gingerich PD, Arif M, Clyde WC. 1995. New archaeocetes (Mammalia, Cetacea) from the middle Eocene Domanda Formation of the Sulaiman Range, Punjab (Pakistan). Contributions of the Museum of Paleontology of the University of Michigan 29, 291–330.

Gingerich PD, Haq MU, Zalmout IS, Khan IH, Malakani MS. 2001. Origin of whales from early artiodactyls: hands and feet of Eocene Protocetidae from Pakistan. Science 293, 2239–2242.

Gingerich PD, ul-Haq M, von Koenigswald W, Sanders WJ, Smith BH, Zalmout ES. 2009.

    New protocetid whale from the middle Eocene of Pakistan: birth on land, precocial

    development, and sexual dimorphism. PLoS One 4, e4366.

Hulbert Jr RC 1998a. Postcranial osteology of the North American middle Eocene protocetid

    Georgiacetus. In Thewissen JGM, ed, The Emergence of Whales, Evolutionary

    Patterns in the Origin of Cetacea. Plenum Press, New York, pp. 235–267.

Hulbert Jr RC, Petkewich RM, Bishop GA, Bukry D, Aleshire DP, 1998b. A new middle

    Eocene protocetid whale (Mammalia: Cetacea: Archaeoceti) and associated biota

    from Georgia. Journal of Paleontology 72, 907–27.

Kumar K, Sahni A. 1986. *Remingtonocetus harudiensis*, new combination, a middle Eocene

    archaeocete (Mammalia, Cetacea) from western Kutch, India. Journal of Vertebrate

    Paleontology 6, 326–349.

Kellogg R. 1928. The history of whales—Their adaptation to life in the water (concluded).

    The Quarterly Review of Biology 3, 174–208.

Ketten DR. 1994. Functional analyses of whale ears: Adaptations for underwater hearing.

    IEEE Proceedings in Underwater Acoustics 1, 264–270.

Ketten DR. 1997. Structure and function in whale ears. Bioacoustics 8, 103–135.

Ketten DR, 2000. Cetacean ears. In Au WWL, Popper AN, Fay RR, eds, Hearing by whales

    and dolphins. Springer-Verlag, New York, pp. 43–108.

Ketten DR, Wartzok D. 1990. Three dimensional reconstructions of the dolphin ear. In

    Thomas JA, Kastelein RA, eds, Sensory abilities of Cetaceans. Plenum Press, New

    York, pp. 81–105.

Luo ZX. 1998. Homology and transformation of cetacean ectotympanic structures. In

    Thewissen JGM, ed, The emergence of whales: evolutionary patterns in the origin of

    Cetacea. Kluwer Academic/Plenum, New York, pp. 269–301.

Luo ZX, Gingerich PD. 1999. Terrestrial Mesonychia to aquatic Cetacea: transformation of the basicranium and evolution of hearing in whales. University of Michigan Papers on Paleontology 31, 1–98.

Madar SI. 2007. The postcranial skeleton of early Eocene pakicetid cetaceans. Journal of Paleontology 81, 176–200.

Manley GA. 2012. Evolutionary Paths to Mammalian Cochleae. Journal of the Association for Research in Otarlaryngology 13, 733–743.

Marx FG, Fordyce RE. 2015. Baleen boom and bust: a synthesis of mysticete phylogeny, diversity and disparity. Royal Society Open Science 2, 140434.

Marx FG, Lambert O, Uhen MD. 2016a. Cetacean Paleobiology. John Wiley & Sons, Chichester, 345 p.

Marx FG, Hocking DP, Park T, Ziegler T, Evans AR, Fitzgerald EMG. 2016b. Suction feeding preceded filtering in baleen whale evolution. Memoirs of Museum Victoria 75: 71–82.

Mooney TA, Yamato M, Branstetter BK. 2012. Hearing in Cetaceans: From Natural History to Experimental Biology. Advances in Marine Biology 63, 197–246.

Norris KS. 1964. Some problems of echolocation in cetaceans. In Tavolga WN, ed, Marine Bioacoustics. Pergamon, New York, pp. 316–336.

Norris KS, Harvey GW. 1974. Sound transmission in the porpoise head. The Journal of the Acoustical Society of America 56, 659–664.

Nummela S, Thewissen JGM, Bajpai S, Hussain ST, Kumar K. 2004. Eocene evolution of whale hearing. Nature 430, 776–778.

Nummela S, Hussain ST, Thewissen JGM. 2006. Cranial anatomy of Pakicetidae (Cetacea, Mammalia). Journal of Vertebrate Paleontology 26, 746–759.

Nummela S, Thewissen JGM, Bajpai S, Hussain T, Kumar K. 2007. Sound transmission in archaic and modern whales: anatomical adaptations for underwater hearing. Anatomical Record 290, 716–733.

Pihlström H. 2008. Comparative anatomy and physiology of chemical senses in aquatic mammals. In Thewissen JGM, Nummela S, eds, Sensory Evolution on the Threshold: Adaptations in secondarily aquatic vertebrates. University of California Press, Berkeley, 95–109.

Rado R, Himelfarb M, Arensburg B, Terkel J, Wollberg Z. 1989. Are seismic communication signals transmitted by bone conduction in the blind mole rat? Hearing Research 41, 23–30.

Thewissen JGM. 2014. The Walking Whales. From Land to Water in Eight Million Years. University of California Press, Oakland, 256 p.

Thewissen JGM, Hussain ST. 1993. Origin of underwater hearing in whales. Nature 361, 444–445.

Thewissen JGM, Bajpai S, 2009. New skeletal material of *Andrewsiphius* and *Kutchicetus*, two Eocene cetaceans from India. Journal of Paleontology 83, 635–63.

Thewissen JGM, Madar SI, Hussain ST. 1996. *Ambulocetus natans*, an Eocene cetacean (Mammalia) from Pakistan. Courier Forschungsinstitut Senckenberg 191, 1–86.

Uhen MD. 2004. Form, function, and anatomy of *Dorudon atrox* (Mammalia, Cetacea): an archaeocete from the middle to late Eocene of Egypt. University of Michigan Papers in Paleontology 34, 1–222.

Uhen MD. 2008. A new *Xenorophus*-like odontocete cetacean from the Oligocene of North Carolina and a discussion of the basal odontocete radiation. Journal of Systematic Palaeontology 6, 433–452.

Uhen MD, Pyenson ND, Devries TJ, Urbina M, Renne PR. 2011. New Middle Eocene whales from the Pisco Basin of Peru. Journal of Paleontology 85, 955–969.

Varansi U, Feldman HR, Malins, DC. 1975. Molecular basis for formation of lipid sound lens in echolocating cetaceans. Nature 255, 340–343.

Vater M, Meng J, Fox RC. 2004. Hearing Organ Evolution and Specialization: Early and Later Mammals. In Manley GA, Popper AN, Fay RR, eds, Evolution of the Vertebrate Auditory System. Springer-Verlag, New York, pp. 256–288.

Wang D, Wang K, Ziao Y, Sheng G. 1992. Auditory sensitivity of a Chinese river dolphin (*Lipotes vexillifer*). In Thomas JA, Kastelein RA, Supin AY, eds, Marine Mammal Sensory Systems. Plenum Press, New York, pp. 213–221.

Yamato M, Ketten DR, Arruda J, Cramer S, Moore K. 2012. The auditory anatomy of the minke whale (*Balaenoptera acutorostrata*): a potential fatty sound reception pathway in a baleen whale. Anatomical Record 295, 991–998.

2. Low frequency hearing preceded the evolution of giant body size and filter feeding in baleen whales

Travis Park[1,2], Alistair R. Evans[1,2], Stephen J. Gallagher[3] and Erich M. G. Fitzgerald[2,4,5]

[1]School of Biological Sciences, Monash University, Melbourne, Australia.

[2]Geosciences, Museums Victoria, Melbourne, Australia.

[3]School of Earth Sciences, University of Melbourne, Melbourne, Australia.

[4]Department of Vertebrate Zoology, National Museum of Natural History, Smithsonian Institution, Washington, DC, USA.

[5]Department of Life Sciences, Natural History Museum, London, UK.

Abstract

Living baleen whales (mysticetes) produce and hear the lowest frequency (infrasonic) sounds among mammals. There is currently debate over whether the ancestor of crown cetaceans (Neoceti) was able to detect low frequencies. However, the lack of information on the most archaic fossil mysticetes has prevented us from determining the earliest evolution of their extreme acoustic biology. Here I report the first anatomical analyses and frequency range estimation of the inner ear in Oligocene (34–23 Ma) fossils of archaic toothed mysticetes from Australia and the USA. The cochlear anatomy of these small fossil mysticetes resembles the basilosaurid archaeocete examined, but is also similar to that of today's baleen whales, indicating that even the earliest mysticetes detected low frequency sounds, and lacked ultrasonic hearing and echolocation. This suggests that, in contrast to recent research, the plesiomorphic hearing condition for Neoceti was low frequency, which was retained by toothed mysticetes, and the high frequency hearing of odontocetes is derived. Therefore, the low frequency hearing of baleen whales has remained relatively unchanged over the last ~34

million years, being present before the evolution of other signature mysticete traits including filter feeding, baleen and giant body size.

2.1. Introduction

The monophyletic living cetacean groups Odontoceti (toothed whales and dolphins) and Mysticeti (baleen whales) display a clear dichotomy in their acoustic biology, with odontocetes hearing and producing ultrasonic signals (>20,000 Hz) for echolocation, and mysticetes possessing low frequency or infrasonic (<20 Hz) hearing and vocalisations (Ketten 2000; Cummings & Thompson 1971).

Although it is debated whether the earliest cetaceans (archaeocetes) were low or high frequency specialists (Ekdale & Racicot 2015; Ekdale 2016; Churchill et al. 2016), archaic odontocetes have been shown to use high frequency echolocation (Churchill et al. 2016; Park et al. 2016; Geisler et al. 2014). However, no descriptions of the cochlear anatomy of early mysticetes have been published, which included the critical transition from predation using teeth to filtering with baleen (Marx et al. 2015). Because of this, it has not been possible to establish whether the earliest mysticetes retained the primitive low frequency hearing of archaeocetes, or initially evolved high frequency hearing like odontocetes, which was then subsequently lost. The latter has been suggested by studies based on the presence of a large mandibular foramen, asymmetry in basilosaurid skulls, analyses of basilosaurid cochlear morphology and ancestral state reconstructions from molecular phylogenies (Ketten 1993; Milinkovitch 2005; Fahlke et al. 2011; Churchill et al. 2016). For the first time, I describe the cochlear anatomy of toothed archaic mysticetes using micro-computed tomography (microCT) of periotic bones representing Mammalodontidae (Museums Victoria NMV P173220, P199986) and Aetiocetidae (NMV P229119), early-diverging clades pivotal to

understanding the origin of baleen whales (Fordyce & Muizon 2001; Fitzgerald 2006,2010; Deméré et al. 2008; Uhen, 2010).

2.2 Materials and Methods

Three toothed mysticete periotics were scanned using the Zeiss Xradia 520Versa microCT at the Monash University X-ray Microscope Facility for Imaging Geomaterials (XMFIG). The raw data from these scans were used to create three-dimensional digital models of the periotics using the visualisation software package Avizo (Version 9.0.1 Standard) (Visualisation Sciences Group – a FEI Company 2013). From these models digital endocasts of the cochleae were segmented using Avizo. The same process was carried out for a comparative sample of one extant odontocete species, five extant mysticete species and one species of basilosaurid archaeocete (*Zygorhiza kochii*) (table 2.1), the same specimen that was studied in Ekdale & Racicot (2015). The sample size for each species was n=1. Due to their larger size, the five extant mysticete specimens were scanned using a Siemens 128-slice PET-CT scanner at the Melbourne Brain Centre Imaging Unit. All specimens examined are considered to be adult with the exception of the aetiocetid and *B. acutorostrata*. Multiple linear morphometrics were measured, with several ratios calculated from them e.g. basal ratio (cochlear height divided by cochlear width), axial pitch (cochlear height divided by number of turns) and radii ratio (basal cochlear radius divided by apical cochlear radius). Both maximum and minimum frequency limits were estimated. Estimates of the low frequency hearing limit for the toothed mysticetes were calculated from the linear regression of low frequency hearing limit and radii ratio for other mammals performed by Manoussaki et al. (2008). Estimates of the maximum frequency limit for the toothed mysticetes (except NMV P229119) and other fossil cetaceans were made using the a new equation derived in this study from a linear regression of basal basilar membrane width and maximum frequency limit for a

14 species of terrestrial mammal and 14 species of cetacean. Basilar membrane width was either taken from previously published measurements or estimated from laminar gap width measurements, corrected for the overestimate reported in Ketten (2000), using the slice tool in Avizo. Detailed methods can be found in Appendix 1.

Another feature associated with low frequency hearing is the presence of the "tympanal recess", a radial expansion of the scala tympani (Fleischer 1976). Whilst all cetaceans appear to have a slight expansion of the scala tympani at the basal most point of the basal turn, in most taxa it disappears by the first quarter of the basal turn. Several mysticete taxa as well as *Physeter* and ziphiids (Park et al. 2016) however possess a much greater radial expansion of the scala tympani, of which the function remains unknown. I follow the definition of the tympanal recess where any radial expansion of the scala tympani that exceeds the basal quarter turn is classed as a tympanal recess.

Table 2.1. Key measurements of cetaceans sampled and estimated low frequency limits. AP, axial pitch; BR, basal ratio; CBA, cannot be ascertained; CL, canal length; Estd. LFL, estimated low frequency limit; RR, radii ratio; S#, specimen number; Sl., slope; #T, number of turns; SSL, secondary spiral lamina; Vol., volume.

Taxon	S#	#T	CL (mm)	RR	% SSL	BR	AP	Sl.	Vol. (mm^3)	Estd. LFL (Hz)
Odontoceti										
Steno bredanensis	NMV C36961	1.5	30.32	3.39	74.18	0.50	3.47	0.11	154.85	378.31
Mysticeti										
Balaenoptera acutorostrata	NMV C24936	2.25	42.78	8.24	44.17	0.53	3.00	0.07	412.34	22.88
Balaenoptera borealis	NMV P166415	2.25	69.56	7.33	32.86	0.47	3.56	0.05	790.72	38.75
Balaenoptera edeni	NMV P171502	2	70.74	7.33	31.15	0.51	4.22	0.06	797.40	38.80
Eubalaena australis	NMV C27879	2.25	52.01	7.22	22.53	0.64	4.28	0.08	748.64	41.42
Megaptera novaeangliae	NMV C28892	2	56.35	7.10	38.40	0.50	4.39	0.08	804.95	44.29
Aetiocetidae indet.	NMV P229119	2.5	15.18	7.47	39.09	0.60	1.31	0.09	CBA	35.90
Mammalodon colliveri	NMV P199986	2.25	33.15	6.77	33.29	0.55	2.57	0.08	145.57	53.81
Mammalodontidae indet.	NMV P173220	2.5	29.26	6.44	42.41	0.58	2.23	0.08	162.13	65.07
Archaeoceti										
Zygorhiza kochii	USNM 214433	2.5	32.83	9.63	41.72	0.67	3.02	0.09	259.14	10.26

2.3. Descriptions of cochlear anatomy

(a) Mammalodontidae

The description of mammalodontid cochlear morphology is based on *Mammalodon colliveri* (NMV P199986: figure 1) and a mammalodontid of indeterminate species (NMV P173220: Fig 2.1), with values for the former specimen given first and the latter given in parentheses where different. The cochlea completes approximately 2.25 turns (2.5 turns). The scala tympani is inflated radially along the first quarter turn only, lacking a distinct tympanal recess like that seen in some mysticetes and odontocetes (Fleischer 1976; Geisler & Luo 1996; Ekdale 2013,2016; Ekdale & Racicot 2015; Park et al. 2016; Churchill et al. 2016). The cochlear canal retains its width for the first turn, before tapering in the second turn, becoming narrowest at the apex. The fenestra cochleae is large and opens posteriorly to the cochlear canal, with the canaliculus cochleae for the membranous perilymphatic duct (only the base of which is shown) extending dorsomedially (dorsally), dorsal to the fenestra cochleae.

In vestibular view the first quarter of the basal turn of the cochlea is separated from the apical turns, similar to *Zygorhiza kochii*. The apical turns are, however, tightly coiled, with a small open space enclosed by the apical turn (apex essentially completely closed). There is a high degree of overlap of the turns, with well over half of the apical-most turn overlapping the section of the cochlear canal below it. The basal ratio is 0.55 (0.58), indicating that the cochlea is approximately twice as wide as it is high. The axial pitch and slope values are 2.57 (2.23) and 0.08 respectively. The radii ratio of the cochlea is 6.77 (6.44), a value within the range of those calculated for living mysticetes previously (Ekdale & Racicot 2015). In cross section, the bone separating the basal turn from the apical turn is thin, similar to living mysticetes.
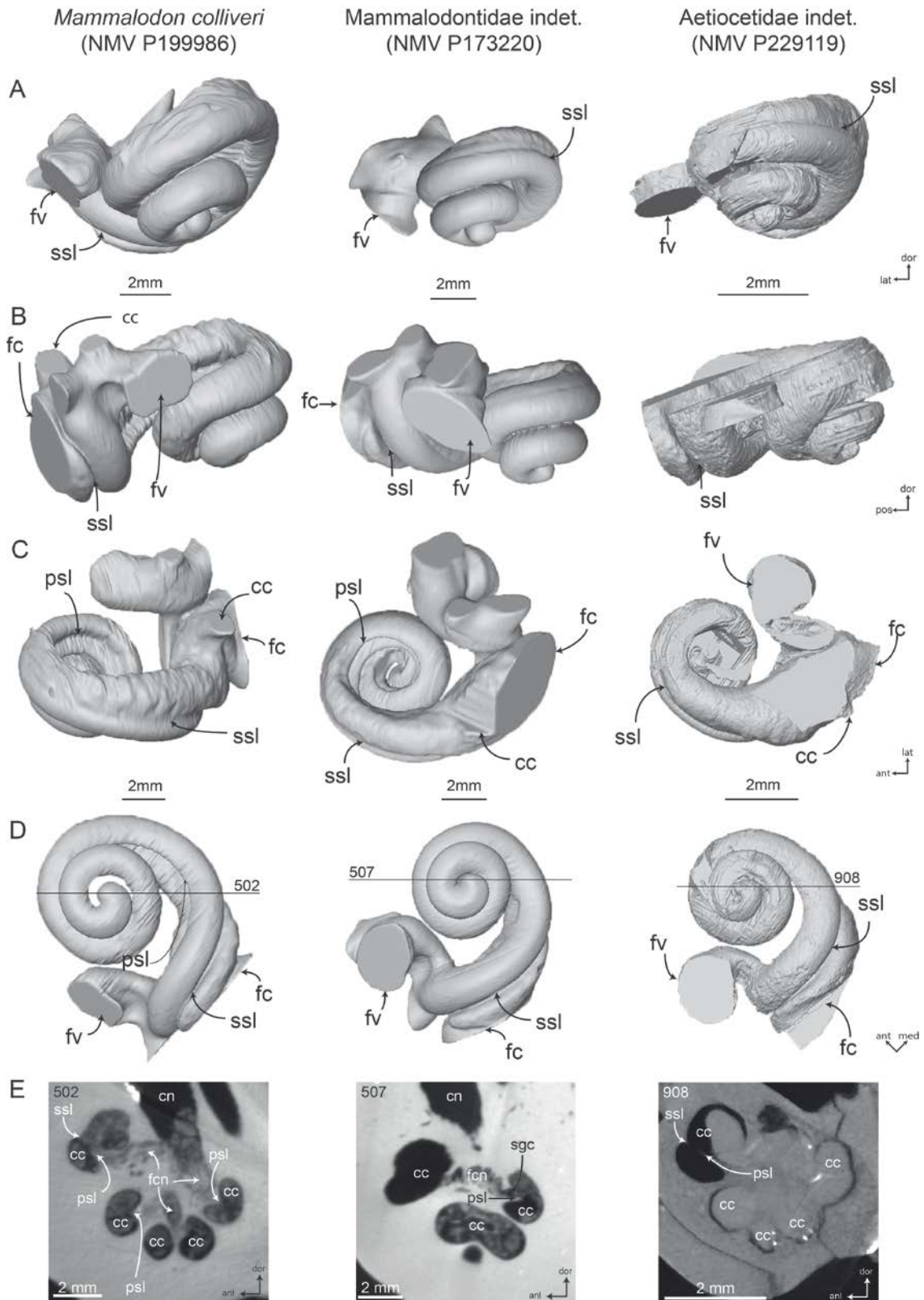
Fig 2.1. Digital endocasts of cochleae of *Mammalodon colliveri* (NMV P19986), Mammalodontidae indet. (NMV P173220) and Aetiocetidae indet. (NMV P229119) reconstructed from microCT data in (A) anterior, (B) lateral, (C) dorsal, (D) vestibular views. (E) shows microCT cross-sectional slices through periotics, location of slice indicated by line through cochleae in (D). All specimens are shown as right cochlea with NMV P173220 reversed. ant, anterior; cc, cochlear canal; cn, cranial neve VIII; dor, dorsal; fc, fenestra cochleae; fcn, foramina for cranial nerve VIII; fv, fenestra vestibuli; lat, lateral; med, medial; pos, posterior; psl, primary spiral lamina; ssl, secondary spiral lamina; vc, vestibular curve.

The spiral laminae are represented on these digital endocast models as grooves. The primary spiral lamina extends for almost the entire length of the cochlea, being widest at the base. The secondary spiral lamina extends along the radial wall of the cochlear canal for less than half of the basal turn (approximately 33% (42%) of the total length of the cochlear canal), a value similar to extant mysticetes. Using the equation from Manoussaki et al. (2008), the estimated low frequency hearing limits are 53.81 Hz (65.07 Hz). The basal basilar membrane width (*bmw*) was related to the maximum frequency limit (f_{max}) as: $\log(f_{max}) = -1.3090\log(bmw) + 4.1316$, with an R^2 of 0.78. Using this equation, the estimated maximum frequency limits are 17.37 kHz (4.59 kHz). The sizeable difference between the maximum frequency estimates of the two specimens is most likely due to the fact that the tips of the laminae in NMV P173220 are damaged, giving an artificially large laminar gap width.

(b) Aetiocetidae

The aetiocetid represented by periotic NMV P229119 (Fig 2.1) probably represents a juvenile individual (see Appendix 1 for further details) and is smaller in absolute size compared to the other toothed mysticetes in this study (table 2.1). The cochlea completes 2.5 turns. This cochlea is not as well preserved as the others, with matrix infilling much of the cochlear canal and destroying most of the more delicate structures. Similar to mammalodontids, the scala tympani is inflated radially along the first quarter turn only, lacking a distinct tympanal recess. The cochlear canal retains its width for the first turn, before tapering in the second turn, becoming narrowest at the apex. The fenestra cochleae is large and opens posteriorly. The canaliculus cochleae for the membranous perilymphatic duct extends dorsally from the cochlear canal. The apical turns are tightly coiled with minor, if any, open space enclosed by the apical turn. The apical-most turn overlaps the section of the cochlear canal below it. The basal ratio is 0.60 and the axial pitch and slope values are 1.31 and 0.09 respectively. The radii ratio of the cochlea is 7.47, a value within the range of living mysticetes. The spiral

laminae are poorly preserved so their full extent cannot be estimated; however the secondary spiral lamina extends for at least half a turn, a value similar to the other toothed mysticetes examined. Using the equation of Manoussaki et al. (2008) the estimated low frequency limit of NMV P229119 is 35.90 Hz. The maximum frequency limit could not be calculated for the aetiocetid due to internal damage of the cochlea.

2.4. Discussion

(a) Comparisons

Overall, there are no clear differences between aetiocetid and mammalodontid cochleae. Both groups share the same basilosaurid-like cochlear morphology and have very similar measurements, with the only source of variation being the absolutely smaller size of the juvenile aetiocetid periotic. The cochleae of the archaeocete and mysticetes examined in this study have numbers of turns ranging from 2–2.5. This falls within the range of archaeocete and mysticete cochleae examined in other studies which have 2–3 turns (table 2.1) (Fleischer 1976; Geisler & Luo 1996; Ekdale 2013,2016; Ekdale & Racicot 2015; Ketten et al. 2016; Park et al. 2016; Churchill et al. 2016). The fenestra cochleae is large in all toothed mysticetes examined, similar to that of archaeocetes and extant mysticetes (Fig A1.4). The fenestra cochleae and the bony canaliculus cochleae are enclosed in separate passages, which appears to be the normal condition for all cetaceans except for *Eschrichtius*, which possesses an undivided perilymphatic foramen (Ekdale & Racicot 2015). In all toothed mysticete specimens examined, there is a high degree of overlap of the basal turn(s) by the apical turns (Fig 2.1). This is again similar to the condition found in archaeocetes and extant mysticetes. The degree of overlap is reflected in the thin walls of bone between the basal and apical turns (Fig 2.1;A1.2; table 2.1). In contrast, toothed mysticetes and *Eubalaena* have either a closed apex of the cochlea or a small open space whereas the apex of the cochlea in balaenopteroids

is more open (Fig A1.4). None of the toothed mysticete specimens possessed an expanded tympanal recess (Fig 2.1), although Ekdale (2016) reported the presence of this feature in an indeterminate toothed mysticete taxon (ChM PV5720). Like the specimens described by Ekdale & Racicot (2015), I found that extant balaenopterids possess a tympanal recess and balaenids do not. The expansion of the scala tympani only marginally extends past the basal-most quarter turn in *Zygorhiza* and the toothed mysticete specimen examined by Ekdale (2016). However, as it tapers off very rapidly past this point unlike the expansions seen in balaenopteroids, *Physeter* and ziphiids, I do not consider this to be a definitive tympanal recess, as explained in Appendix 1.

The basal ratio, axial pitch and slope values for the toothed mysticetes in this study are consistent with those from the archaeocetes and extant mysticetes in this study (table 2.1). The cochlear volumes of the toothed mysticetes are smaller than those for *Z. kochii* (259.14–341.65 mm^3) and the extant mysticete taxa examined in all studies to date (412.34–974.00 mm^3) (Ekdale & Racicot 2015). As the sampled toothed mysticetes were probably smaller in body size than both *Z. kochii* and living mysticetes (Marino et al. 2000; Pyenson et al. 2011), smaller cochlear volumes are to be expected. The radii ratio values of the toothed mysticetes examined in this study range from 6.44–7.47, similar to living mysticetes (7.10–8.24). The radii ratio value of *Zygorhiza kochii*, however, is higher than any other taxon in this study (9.63). Ekdale and Racicot (2015) found a similar value for *Zygorhiza* in their study (10.0). The extent of the secondary spiral lamina in toothed mysticetes is short, like that of extant mysticetes. In the mammalodontids examined in this study, it does not extend more than 43% of the total cochlear length. This is similar to the values obtained for *Z. kochii* (42%) and living mysticetes in this study, except for *Eubalaena australis* (23%).

(b) Hearing across the archaeocete-mysticete transition

A prominent point of debate in the study of cetacean acoustics is the ancestral condition of hearing in Neoceti. Arguments for possessing both high frequency (Ketten 1993; Milinkovitch 2005; Fahlke et al. 2011; Churchill et al. 2016) and low frequency (Uhen 2004; Park et al. 2016; Churchill et al. 2016) hearing have been advanced. Most recently, a principal component analysis of cochlear measurements by Churchill et al. (2016) suggested that basilosaurids show greater capabilities for hearing higher frequencies than living mysticetes. Their position in the morphospace is largely driven by: (1) the length of the secondary spiral lamina; and (2) the radius of the spiral ganglion canal. I re-ran their analysis (Fig 2.2), adding the corresponding measurements from the toothed mysticete cochleae in our sample. Like basilosaurids, toothed mysticetes plot in a region of morphospace intermediate to mysticetes and odontocetes (Fig 2.2), potentially showing that they too can hear high frequencies. Nonetheless, there are several lines of evidence suggesting that this is not be the case and that *Zygorhiza* and toothed mysticetes were low frequency sound specialists. Firstly, *Zygorhiza* (42–45% of cochlear length) and toothed mysticetes (39–42% of cochlear length) have secondary spiral laminae that extend a similar length of the cochlear canal as that of extant mysticetes (22–44% of cochlear length) (table 2.1) (Fleischer 1976; Ketten 2000). Secondly, high radii ratio values (not calculated by Churchill et al. (2016)), which strongly correlate to low frequency hearing (Manoussaki et al. 2008), are also highly congruent in *Zygorhiza* and mysticetes (table 2.1). Low frequency limit estimates for *Zygorhiza* and toothed mysticetes calculated using the equation of Manoussaki et al. (2008) were also all very low frequencies (<54 Hz), contrasting to a considerably higher low frequency limit of 378.31 Hz for the odontocete *Steno* (table 1). These low frequency limit estimates cannot yet be verified as no audiograms of mysticetes have been constructed. A simulated mysticete audiogram was generated by Cranford & Krysl (2015) which estimated that the lowest frequency detected for a juvenile fin whale was 10 Hz, slightly lower but still consistent with

the estimated low frequency limits of the extant mysticetes examined in this study. The estimated maximum frequencies for the mammalodontids and *Zygorhiza* are also within the limits of modern mysticetes, but are notably much lower than odontocetes, including the xenorophid inner ear described by Park et al. (2016), which I calculate here to have an estimated maximum frequency limit similar to some modern species (~ 86 kHz), but not as high as more specialised taxa (Fig 2.2; table A1.5). Further indicative of low frequency hearing are the higher number of turns in archaeocete and toothed mysticete cochleae (>2), as well as the large amount of overlap of the basal turn by the apical turn(s). Additionally, preliminary results of a quantitative shape analysis of cetacean cochleae by Ekdale (2016) indicates that *Zygorhiza* and an indeterminate species of toothed mysticete (ChM PV5720) plots within the cochlear morphospace of mysticetes. A final point to note is that virtually all studies to-date (Fleischer 1976; Ketten 1993; Geisler & Luo 1996; Ekdale 2013,2016; Ekdale & Racicot 2015; Ketten et al. 2016; Park et al. 2016; Churchill et al. 2016) on the diversity/evolution of cetacean inner ear anatomy have sampled different taxa/specimens for scanning/analyses under differing protocols. This has resulted in datasets that may not overlap taxonomically or analytically, which hampers comparison of results across multiple studies. It is possible that recent disagreement in the interpretation of cetacean acoustic evolution may reflect this limited degree of comparability in datasets.
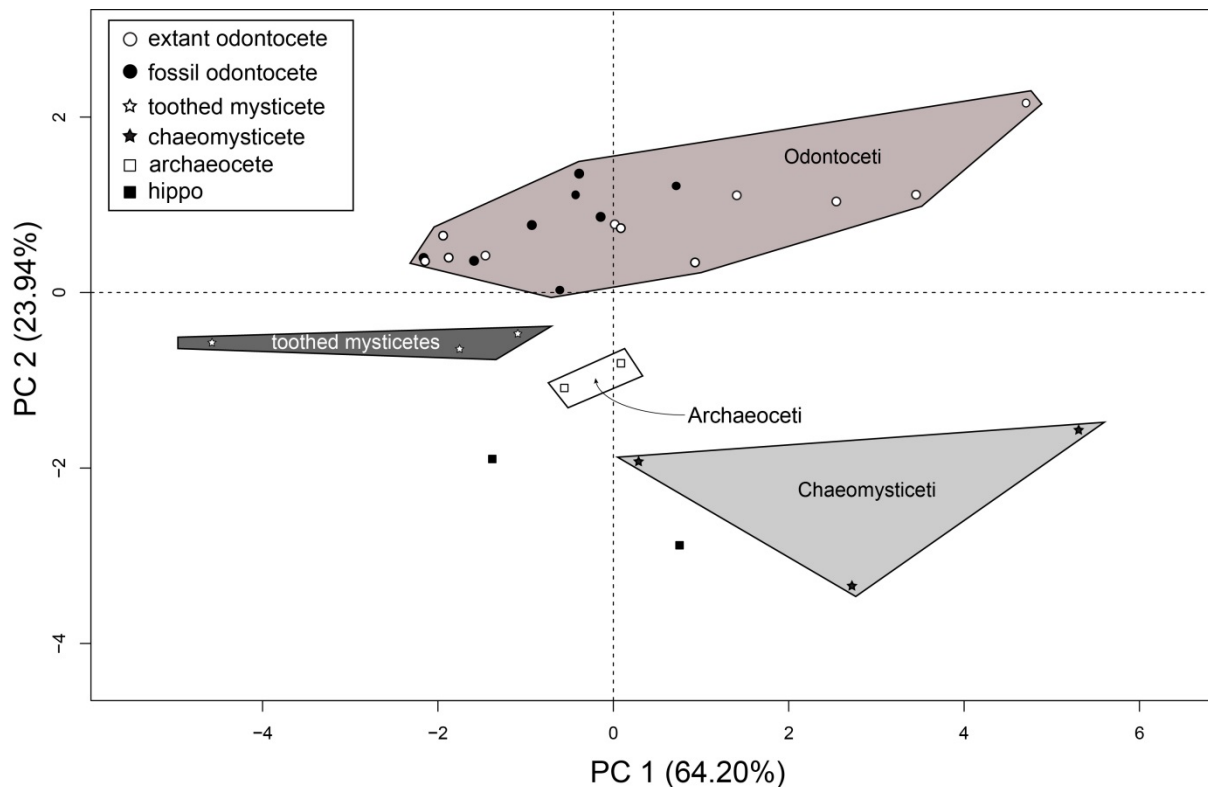
Figure 2.2. Principal component analysis (PCA) of linear cochlear measurements following the protocols of Churchill et al. (2016), with the toothed mysticetes from this study added to the analysis. PC 1 mainly represents variation in body size, while PC 2 mainly represents variation in morphological features. See Churchill et al. (2016) for discussion of principle components and table S4 for PC weightings.

Toothed mysticetes could therefore be said to possess the "Type M" cochlear morphology of Ketten & Wartzok (1990) and Ketten (1992), although the range of axial pitch values, cochlear height and cochlear volume values on the other hand are more like that of "Type II" odontocete cochleae (lower-range ultrasonics) (table 2.1). However, these differences in toothed mysticete cochleae do not indicate that they could hear high frequencies like odontocetes as the features do not affect the stiffness of the basilar membrane, which is critical in determining the frequencies that an animal can detect (Echteler 1994). They can instead be explained by the smaller body size of toothed mysticetes relative to their living counterparts, with mammalodontids and aetiocetids estimated to have been between 2.94–3.25 m and 2.10–3.50 m total length, respectively (Jefferson et al. 2008; Marx et al. 2015), smaller than living mysticetes, which range from 5.5–33 m (Pyenson & Sponberg 2011). Additionally, it is noteworthy that despite the juvenile

age and diminutive size (e.g. estimated bizygomatic width = 192 mm) of the aetiocetid it is still estimated to have detected low frequency sounds, corroborating the presence of precocial development of the auditory system in early Neoceti (Lancaster et al. 2015). Although toothed mysticetes may not have been capable of detecting infrasonic frequencies (<20 Hz) as has been demonstrated in living species (Ketten & Wartzok 1990), I contend that *Zygorhiza*, mammalodontids and aetiocetids were still specialised for hearing low frequencies (<1000 Hz) and were almost certainly incapable of detecting high frequency sounds approximating the capabilities of odontocetes (>30,000 Hz).

(c) Evolution of the extreme biology of baleen whales

The finding that mammalodontid and aetiocetid toothed mysticetes retained the plesiomorphic low frequency hearing of the basilosaurid archaeocete *Zygorhiza* has significant implications for our understanding of mysticete evolution in a phylogenetic and geochronologic context. First, the specialised high frequency hearing of odontocetes is confirmed as the derived condition within Neoceti (Ekdale & Racicot 2015), contra (Ketten 1993; Milinkovitch 2005; Fahlke et al. 2011; Churchill et al. 2016) who hypothesised high frequency hearing in the common ancestor of Neoceti. Second, low frequency hearing did not evolve in mysticetes as a result of their evolving extremely large body size. Ketten (1992,1993,2000) speculated that the low frequency cochlea in mysticetes was a consequence of isometric scaling of cochlear dimensions with the evolution of increasingly larger body size. However, the earliest diverging toothed mysticetes (Mammalodontidae + Aetiocetidae (Marx & Fordyce 2015)), were relatively small-bodied animals up to about 4 m in length (Pyenson & Sponberg, 2011; Tsai & Kohno 2016) (but see Tsai & Kohno (2016) and Tsai & Ando (2016)) and already possessed low frequency-adapted cochleae (Fig 2.3). The estimated maximum body length of the vast majority of mysticetes was <7 m until the middle Miocene (Lambert et al. 2010), and a body length of <7 m was likely for the primitive

Chaeomysticeti (Tsai & Kohno 2016). Large-bodied mysticetes (>10 m total length) first

occur in the middle Miocene (Lambert et al. 2010) and gigantic mysticetes (>15 m total

length) first evolved within the last 5 million years (Lambert et al. 2010; Pyenson & Vermeij

2016), all of which is well after the appearance of low frequency hearing in Mysticeti (Fig
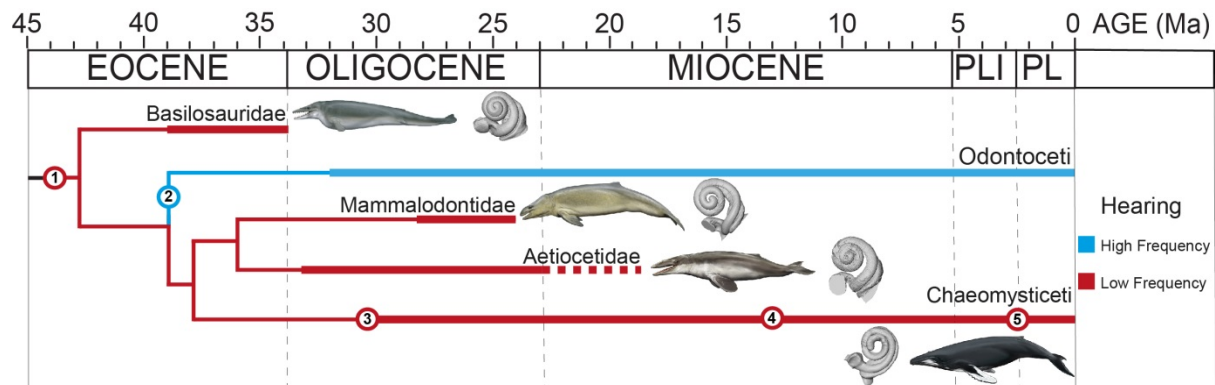
2.3).

Figure 2.3. Evolution of mysticete hearing based on the phylogeny of Marx & Fordyce (2015) in relation to other key mysticete features, illustrating how low frequency hearing evolved prior to the evolution of filter feeding and large body size in mysticetes. Cochlea renderings are of *Zygorhiza kochii* (USNM 214433), *Steno bredanensis* (NMV C36961), *Mammalodon colliveri* (NMV P199986), Aetiocetidae indet. (NMV P229119) and *Megaptera novaeangliae* (NMV C28892). Thickened bars indicate stratigraphic ranges of cetacean clades, following Marx & Fordyce (2015).1, evolution of low frequency hearing in Cetacea; 2, evolution of high frequency hearing in Odontoceti; 3, appearance of obligate filter feeding using baleen; 4, acquisition of large body size (>10 m); 5, acquisition of giant body size (>15 m). Dates for events in mysticete body size evolution from Lambert et al. (2010) and Tsai et al. (2016). PL, Pleistocene; PLI, Pliocene. Illustrations by Carl Buell, used with permission.

Third, low frequency hearing in mysticetes did not evolve as a result of the

ecomorphological shift to bulk filter feeding and/or the appearance of baleen. It has been

implied that mysticetes were initially sensitive to high frequencies (Ketten 1993), but as they

evolved bulk filter feeding, baleen and migration to high latitude feeding grounds there was

reduced selection pressure for maintaining high frequency hearing (Ketten 1992,1993).

Irrespective of whether *Aetiocetus weltoni* possessed an incipient form of baleen, as has been

suggested by Deméré et al. (2008), the presence of low frequency cochleae in

mammalodontids, aetiocetids and basilosaurids suggests that the common ancestor of

mammalodontids and aetiocetids also had low frequency hearing. Crucially, this stem

mysticete would have probably lacked baleen, therefore refuting this hypothesis (Marx et al.

35

2016b). Finally, the low frequency-adapted cochleae of toothed archaic mysticetes, coupled with their lack of nasofacial osteological correlates of soft tissues (i.e. the premaxillary sac fossae and related bony structures) that generate or modify outgoing signals (as supported by character optimisation (Geisler et al. 2014)), suggest the earliest mysticetes were not capable of echolocation (Fitzgerald 2006).

The signature innovations of mysticetes (baleen) and odontocetes (echolocation) were acquired at different stages in their evolutionary history: anatomical specialisations for bulk filter feeding were not present in the earliest stem mysticetes (Fitzgerald 2006,2010; Marx et al. 2015), contrasting with the presence of echolocation in basal odontocete lineages (Geisler et al. 2014; Park et al. 2016; Churchill et al. 2016). Nevertheless, our findings show that the characteristic low frequency mysticete cochlear morphology was present in the earliest members of the group, having been retained from their archaeocete ancestors.

Acknowledgements

References

Churchill M, Martínez-Cáceres M, de Muizon C, Mnieckowski J, Geisler JH. 2016. The origin of high-frequency hearing in whales. Current Biology http://dx.doi.org/10.1016/j.cub.2016.06.004.

Cranford TW, Krysl P. 2015. Fin whale sound reception mechanisms: skull vibration enables low-frequency hearing. PLoS ONE. 10, e0116222.

Cummings WC, Thompson PO. 1971. Underwater sounds from the blue whale, *Balaenoptera musculus*. Journal of the Acoustical Society of America 50, 1193–1198.

Deméré TA, McGowen MR, Berta A, Gatesy J. 2008. Morphological and molecular evidence for a stepwise evolutionary transition from teeth to baleen in mysticete whales. Systematic Biology 57, 15–37.

Echteler SM, Fay RR, Popper AN. 1994. Structure of the mammalian cochlea. In Fay RR, Popper AN, eds, Comparative Hearing: Mammals. Springer-Verlag, New York, pp. 134–171.

Ekdale EG. 2013. Comparative anatomy of the bony labyrinth (inner ear) of placental mammals. PLoS ONE 8, e66624.

Ekdale EG. 2016. Morphological diversity among the inner ears of extinct and extant baleen whales (Cetacea: Mysticeti). Journal of Morphology 277, 1599–1615.

Ekdale EG, Racicot RA. 2015. Anatomical evidence for low frequency sensitivity in an archaeocete whale: comparison of the inner ear of *Zygorhiza kochii* with that of crown Mysticeti. Journal of Anatomy 226, 22–39.

Fahlke J, Gingerich PD, Welsh RC, Wood AR. 2011. Cranial asymmetry in Eocene archaeocete whales and the evolution of directional hearing in water. Proceedings of the National Academy of Sciences 108, 14545–14548.

Fitzgerald EMG. 2006. A bizarre new toothed mysticete (Cetacea) from Australia and the early evolution of baleen whales. Proceedings of the Royal Society B: Biological Sciences 273, 2955–2963.

Fitzgerald EMG. 2010. The morphology and systematics of *Mammalodon colliveri* (Cetacea: Mysticeti), a toothed mysticete from the Oligocene of Australia. Zoological Journal of the Linnean Society 158, 367–476.

Fleischer G. 1976. Hearing in extinct cetaceans as determined by cochlear structure. Journal of Paleontology 50, 133–152.

Fordyce RE, de Muizon C. 2001. Evolutionary history of cetaceans: a review. In Mazin JM, Buffrénil, eds, Secondary Adaptation of Tetrapods to Life in Water. Verlag Dr. Fredrich Pfeil, Munich, pp. 169–233.

Geisler JH, Colbert MW, Carew JL. 2014. A new fossil species supports an early origin for toothed whale echolocation. Nature 508, 383–386.

Geisler JH, Luo ZX. 1996. The petrosal and inner ear of *Herpetocetus* sp. (Mammalia: Cetacea) and their implications for the phylogeny of hearing of archaic mysticetes. Journal of Paleontology 70, 1045–1066.

Jefferson TA, Webber MA, Pitman RL. 2008. Marine mammals of the world: A comprehensive guide to their identification. Academic Press, San Diego, 592 p.

Ketten DR. 1992. The marine mammal ear: specializations for aquatic audition and echolocation. In Webster DB, Fay RR, Popper AN, eds, The Evolutionary Biology of Hearing. Springer-Verlag, New York pp. 717–750.

Ketten DR. 1993. The cetacean ear: Form frequency and evolution. In Thomas JA, Kastelein RA, Supin AY, eds, Marine Mammal Sensory Systems. Springer Science & Business Media, New York, pp. 53–75.

Ketten DR. 2000. Cetacean ears. In, Au WWL, Popper AN, Fay RR, eds, Hearing by whales and dolphins. Springer-Verlag, New York, pp. 43–108.

Ketten DR, Wartzok D. 1990. Three dimensional reconstructions of the dolphin ear. In Thomas JA, Kastelein RA, eds, Sensory abilities of Cetaceans. Plenum Press, New York, pp. 81–105.

Ketten DR, Arruda J, Cramer S, Yamato M. 2016. Great ears: Low-frequency sensitivity correlates in land and marine leviathans. In Popper AN, Hawkins A, eds, The Effects of Noise on Aquatic Life II. Springer Science & Business Media, New York, pp. 529–538.

Lambert O, Bianucci G, Post K, de Muizon C, Salas-Gismondi R, Urbina M, Reumer J. 2010. The giant bite of a new raptorial sperm whale from the Miocene epoch of Peru. Nature 466, 105–108.

Lancaster WC, Ary WJ, Krysl P, Cranford TW. 2015. Precocial development within the tympanoperiotic complex in cetaceans. Marine Mammal Science 31, 369–75.

Manoussaki D, Chadwick RS, Ketten DR, Arruda J, Dimitriadis EK, O'Malley JT. 2008. The influence of cochlear shape on low-frequency hearing. Proceedings of the National Academy of Sciences 105, 6162–6166.

Marino L, Uhen MD, Frohlich B, Aldag JM, Blane C, Bohaska D, Whitmore Jr FC. 2000. Endocranial volume of mid-late Eocene archaeocetes (Order: Cetacea) revealed by computed tomography: implications for cetacean brain evolution. Journal of Mammalian Evolution 7, 81–94.

Marx FG, Fordyce RE. 2015. Baleen boom and bust: a synthesis of mysticete phylogeny, diversity and disparity. Royal Society Open Science 2, 140434.

Marx FG, Tsai C-H, Fordyce RE. 2015. A new Early Oligocene toothed 'baleen' whale (Mysticeti: Aetiocetidae) from western North America: one of the oldest and the smallest. Royal Society Open Science 2, 150476.

Milinkovitch MC. 2005. Molecular phylogeny of cetaceans prompts revision of morphological transformations. Trends in Ecology and Evolution 10, 328–334.

Park T, Fitzgerald EMG, Evans AR. 2016. Ultrasonic hearing and echolocation in the earliest toothed whales. Biology Letters 12, 20160060.

Pyenson ND, Sponberg SN. 2011. Reconstructing body size in extinct crown Cetacea (Neoceti) using allometry, phylogenetic methods and tests from the fossil record. Journal of Mammalian Evolution 18, 269–288.

Pyenson ND, Vermeij GJ. 2016. The rise of ocean giants: maximum body size in Cainozoic marine mammals as an indicator for productivity in the Pacific and Atlantic Oceans. Biology Letters 12, 20160186.

Tsai CH, Ando T. 2016. Niche partitioning in Oligocene toothed mysticetes (Mysticeti: Aetiocetidae). Journal of Mammalian Evolution 23, 33–41.

Tsai CH, Kohno N. 2016. Multiple origins of gigantism in stem baleen whales. Science and Nature 103, 89.

Uhen MD. 2004. Form, function, and anatomy of *Dorudon atrox* (Mammalia, Cetacea): an archaeocete from the middle to late Eocene of Egypt. University of Michigan Papers in Paleontology 34, 1–222.

Uhen MD. 2010. The origin(s) of whales. Annual Review of Earth and Planetary Sciences 38, 189–219.

Visualization Sciences Group – a FEI Company. 2013. Avizo: 3D Analysis Software for Scientific and Industrial Data, Standard Edition 8.0.0. Berlin: Konrad-Zuse-Zentrum für Informationstechnik.

3. The cochlea of the enigmatic pygmy right whale *Caperea marginata* informs mysticete phylogeny

Travis Park[1,2], Felix G. Marx[1-3] , Erich M.G. Fitzgerald[2,4,5], Alistair R. Evans[1,2]

[1]School of Biological Sciences, Monash University, Melbourne, Victoria, Australia

[2]Geosciences, Museums Victoria, Melbourne, Victoria, Australia

[3] Directorate of Earth and History of Life, Royal Belgian Institute of Natural Sciences, Brussels, Belgium

[4] National Museum of Natural History, Smithsonian Institution, Washington, DC, USA

[5]Department of Life Sciences, Natural History Museum, London, UK

Abstract

The pygmy right whale, *Caperea marginata*, is the least understood extant baleen whale (Cetacea, Mysticeti). Knowledge on its basic anatomy, ecology and fossil record is limited, even though its singular position outside both balaenids (right whales) and balaenopteroids (rorquals + grey whales) gives *Caperea* a pivotal role in mysticete evolution. Recent investigations of the cetacean organ of hearing – the cochlea – have provided new insights into sensory capabilities and phylogeny. Here, I extend this advance to *Caperea* by describing, for the first time, the inner ear of this enigmatic species. The cochlea is large and appears to be sensitive to low-frequency sounds, but its hearing limit is relatively high. The presence of a well-developed tympanal recess links *Caperea* with cetotheriids and balaenopteroids, rather than balaenids, contrary to the traditional morphological view of a close *Caperea*-balaenid relationship. Nevertheless, a broader sample of the cetotheriid *Herpetocetus* demonstrates that the presence of a tympanal recess can be variable at the specific and possibly even the intraspecific level.

3.1. Introduction

The pygmy right whale, *Caperea marginata* (Gray 1846), is the most bizarre and least known of all extant baleen whales. Its basic anatomy and ecology are poorly understood, with limited data on distribution and behaviour (Kemper 2009; 2014; Kemper et al. 2012; Ross et al. 1975; Sekiguchi et al. 1992). The phylogenetic position of *Caperea* is the most contentious problem in mysticete systematics, with morphological analyses traditionally advocating a close relationship with right whales (Balaenidae) (Bisconti 2015; Churchill et al. 2012; Steeman 2007), whereas molecular data routinely place *Caperea* as sister to rorquals and grey whales (Balaenopteroidea) (Deméré et al. 2008; McGowen et al. 2009; Steeman et al. 2009). A third hypothesis, also consistent with the molecular data, groups *Caperea* with the otherwise extinct family Cetotheriidae (Fordyce & Marx 2013; Gol'din & Steeman 2015; Marx & Fordyce 2016), but remains a matter of ongoing debate among morphologists (Berta et al. 2016; Bisconti 2015; El Adli et al. 2014).

Much of the uncertainty about the ecology and evolution of the pygmy right whale stems from a lack of data on its disparate morphology, which combines a right whale-like, arched rostrum with traits more typical of cetotheriids and/or balaenopteroids, such as a narrow, tetradactyl flipper, an elongate scapula, the presence of a squamosal cleft, and an enlarged posterior process of the tympanoperiotic (Kemper 2009; Marx & Fordyce 2016). Even more strikingly, *Caperea* stands out for a range of unique features, such as the partial detachment of the anterior process from the remainder of the periotic, as little as one or two lumbar vertebrae, and its armour-like, supernumerary and partially overlapping ribs (Beddard 1901; Buchholtz 2011).

New insights might arise from further studies on functional morphology (e.g. swimming style) and sensory capabilities. In particular, considerable progress has been made in recording the anatomy of the cetacean cochlea, which is one of the few sensory structures

whose detailed shape can be studied in both extant and extinct species (Ekdale 2016; Ekdale & Racicot 2015; Fleischer 1976; Geisler & Luo, 1996; Luo & Eastman 1995; Luo & Marsh 1996; Park et al. 2016; Park et al. 2017). However, the inner ear anatomy of the pygmy right whale is currently undocumented. Here, I describe for the first time, the cochlea of *Caperea marginata* and compare it to that of other modern and fossil mysticetes.

3.2. Materials and methods

(a) Specimens examined

I scanned the right cochlea of *Caperea marginata* (NMV C28531), previously figured by Ekdale et al. (2011: Fig. 11), as well as four isolated and hitherto undescribed periotics of the cetotheriid *Herpetocetus*, one of its putative fossil relatives (Fordyce & Marx 2013).The specimens were scanned by two of the authors (TP & ARE) and Rob Williams at the Melbourne Brain Centre Imaging Unit All four specimens clearly represent *Herpetocetus* based on the presence of (i) a shelf-like, anteriorly projected lateral tuberosity; (ii) a well-developed ridge for the attachment of the tensor tympani on the anterior process; (iii) a medially projecting anteromedial corner of the pars cochlearis; and (iv), in IRSNB V00377, a distally enlarged compound posterior process with a deep facial sulcus bordered by well-developed anterior and posterior ridges (Fordyce & Marx 2013; Geisler & Luo 1996; Whitmore & Barnes, 2008) (Fig. A2.1).

Two of the *Herpetocetus* periotics (IRSNB V00372 and V00373) come from the Lee Creek Mine exposure of the Yorktown Formation (Aurora, North Carolina, USA; Early Pliocene) (Browning et al. 2009), whereas the remainder (IRSNB V00376, V00377) are from the Kattendijk Formation as exposed in the Deurganckdok of Antwerp, Belgium (Early Pliocene) (De Schepper et al. 2009). The species-level taxonomy of *Herpetocetus* remains problematic, owing to the lack of mature, well-preserved type specimens for most species. Nevertheless, IRSNB V00372 and V00373 come from the same locality and, presumably,

horizon as *H. transatlanticus*, and furthermore resemble this species in having a triangular

(rather than rounded) lateral tuberosity. I therefore here tentatively refer the North American

specimens to *H*. cf. *transatlanticus.* For detailed comparisons, only IRNSB V00372 and

V00377 were segmented and measured. Additional comparative data for other cetotheriid

species were taken from Geisler & Luo (1996), Churchill et al. (2016) and Ekdale (2016).

(b) Scanning technique

The periotics were scanned using either the Zeiss Xradia 520 Versa at the Monash University

X-ray Microscopy Facility for Imaging Geo-materials (XMFIG) or, in the case of the extant

mysticetes, the Siemens 128-slice PET-CT scanner at the Melbourne Brain Centre Imaging

Unit (see table 1 for scan parameters). The raw CT data were then compiled into three-

dimensional models, and digital endocasts of the cochleae were segmented using the

visualisation software package Avizo (Version 9.1.0 Standard) (FEI).

Table 3.1. Parameters of CT scans of cetacean periotics in this study. kV, kilovolt; µm, micrometres

Taxon	Specimen number	Scan power (kV)	No of slices	Section thickness (µm)	Voxel/Pixel size (µm)
Caperea marginata	NMV C28531	140	1831	100	236
Herpetocetus cf. *transatlanticus*	IRNSV 00372	140	1601	58.77	58.77
Herpetocetus cf. *transatlanticus*	IRNSB V 00373	140	1601	37.17	37.17
Herpetocetus sp.	IRNSB V00376	140	1601	37.17	37.17
Herpetocetus sp.	IRNSB V00377	140	1601	37.17	37.17

(c) Cochlear measurements

Basic measurements of the internal structures of the cochlea were taken using the Measure,

Slice and Spline Probe tools in Avizo, following the protocols of Park et al. (2016). These

measurements include: (i) cochlear height; (ii) cochlear width; (iii) number of turns; (iv)

cochlear canal length (measured along the midline); (v) extent of the secondary spiral lamina;

(vi) cochlear volume; (vii) basal radius; and (viii) apical radius (Fig. 3.1). The extent of the

spiral laminae is a proxy for the stiffness of the basilar membrane (Ekdale and Racicot,

2015), which supports the organ of Corti. The extension (%) of the secondary spiral lamina

(SSL) was measured by dividing the length of the cochlear canal at the apical-most point of

the SSL by the total length of the cochlear canal, then multiplying by 100. Our approach

slightly differs from that of Ekdale & Racicot (2015), who instead measured the length of the

SSL directly along the outer edge of the cochlea. I amended their method because the outer

edge of the cochlea follows an inherently larger spiral than the midline of the cochlear canal

(where the length of the canal is measured), leading to an overestimate of relative SSL

extension.
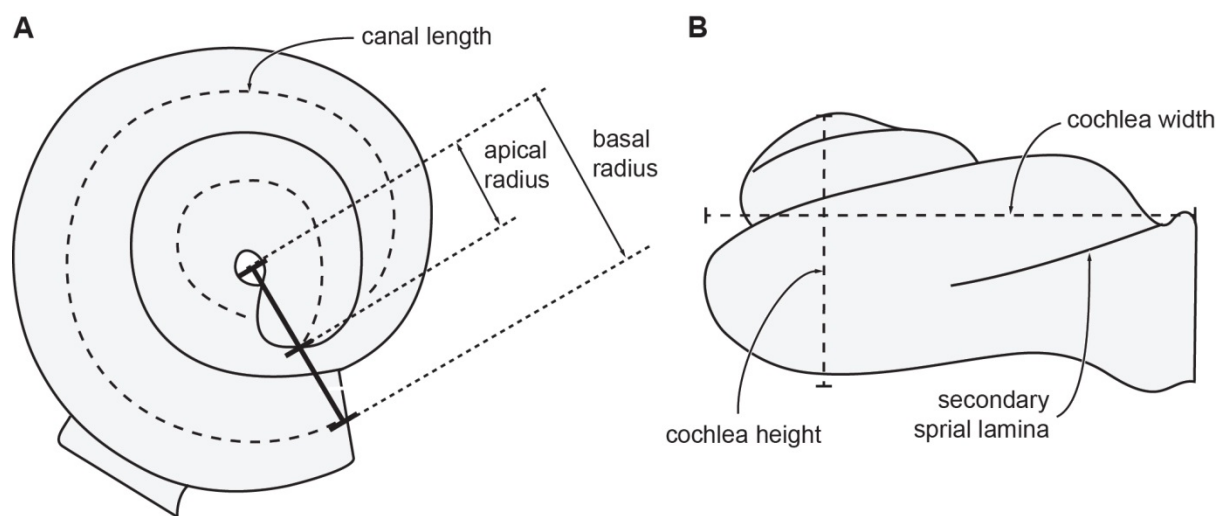
Fig. 3.1. Line drawing of a cochlea in (A) vestibular and (B) posterior view, illustrating key measurements. Redrawn from Ekdale (2013), under a CC-BY licence.

From our initial measurements, I calculated several previously established ratios,

which together form a quantitative description of cochlear morphology (Ketten & Wartzok

1990). First, the axial pitch, which is the height of the cochlea divided by the number of turns

and, in odontocetes, is negatively proportional to frequency (Ketten & Wartzok 1990);

secondly, the basal ratio, which is the height of the cochlea divided by its basal diameter, here

measured following the method of Ekdale (2013) (Fig. 3.1), and is negatively proportional to

frequency (Ketten & Wartzok 1990); thirdly, the cochlear slope, which is the height of the

cochlea divided by the length of the cochlear canal divided by the number of turns (Ketten &

Wartzok 1990); and, finally, the radii ratio, or graded curvature, is the radius of the cochlea at

its base divided by the radius at its apex, and is strongly correlated with low frequency hearing limits (Manoussaki et al. 2008). For the radii ratio, radius measurements were taken using the Slice tool in Avizo, with the apical radius measured to the outer wall of the cochlea (as in Ekdale & Racicot 2015), rather than the midpoint of the basilar membrane (as in Ketten et al. 2016).

Finally, I estimated the low frequency hearing limit for all specimens following Manoussaki et al. (2008):

$$f = 1507\exp(-0.578[\rho-1])$$

where f = low frequency hearing limit at 60 dB re 20 μPa in air and 120 dB re 1 μPa in water, and ρ = radii ratio value. However, this equation was derived mainly from terrestrial mammals in air, and should therefore be considered tentative until audiograms of mysticetes become available (Ekdale and Racicot 2015).

In addition to quantitative measurements, I scored the presence of a radial expansion of the scala tympani, or tympanal recess (Fleischer 1976). An incipient expansion occurs in all cetaceans, but usually disappears by the first quarter of the basal turn. By contrast, the expansion is much more pronounced in several mysticetes, as well as *Physeter* and ziphiids (Ekdale 2016; Ekdale & Racicot 2015; Park et al. 2016). To reflect this situation, I therefore here redefine the tympanal recess as a radial inflation of the scala tympani extending beyond the basal quarter turn of the cochlea in vestibular (or ventral) view.

(d) Institutional abbreviations

IRSNB, Institut Royal des Sciences Naturelles de Belgique, Brussels, Belgium; NMV, Museum Victoria, Melbourne, Australia; USNM, National Museum of Natural History, Smithsonian Institution, Washington DC, USA.

3.3. Results

***Caperea marginata*, NMV C28531:** The cochlea completes approximately 2 turns (Fig. 3.2A). There is a distinct tympanal recess, with the scala tympani being inflated radially along the first half turn and the greatest point of inflation being located at the half turn mark. In vestibular view, the first quarter of the basal turn and the apical turns are close to each other, as in other modern mysticetes and fossil cetotheriids. The apical turn is tightly coiled and encloses a small open space, rather than being fully closed like in more primitive taxa (e.g. *Zygorhiza*). Approximately three quarters of the apical turn overlap the section of the cochlear canal immediately below. In cross section, the bone separating the basal turn from the apical turn is thin, as in other modern mysticetes (Fig. 3.3).

The cochlea is large in absolute terms, with a height of 10.41 mm, a width of 18.7 mm, a volume of 874.38 mm^3 and a cochlear canal length of 60.97 mm (table 2). The secondary spiral lamina extends along the radial wall of the cochlear canal for approximately half of the basal turn (approximately 37% of the total length of the cochlear canal). The basal ratio of *Caperea* is 0.56, indicating that the cochlea is approximately twice as wide as it is high. The axial pitch, cochlear slope and radii ratio values are 5.20, 0.085 and 6.43, respectively, resulting in an estimated low frequency hearing limit of 65 Hz.
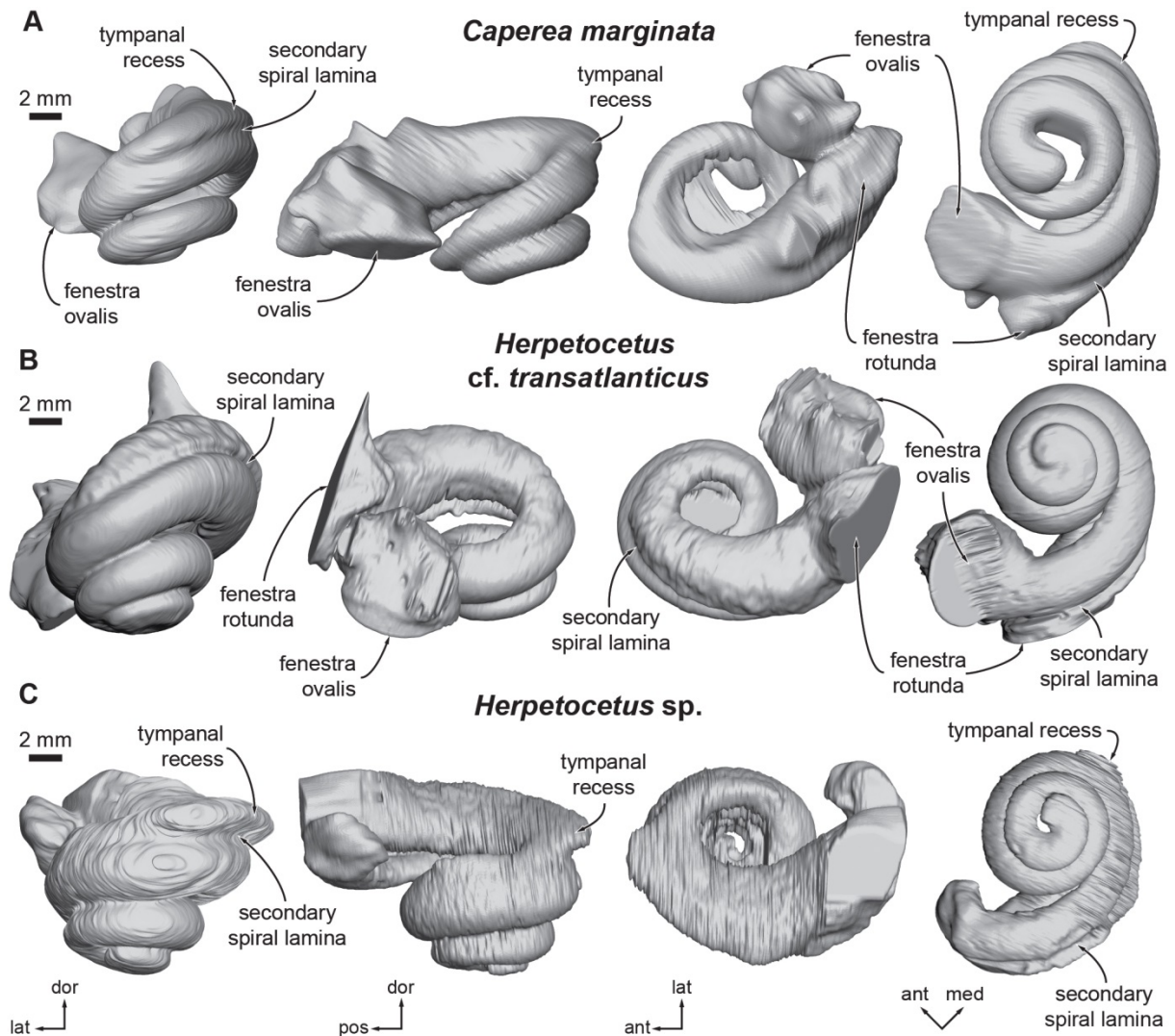
Fig. 3.2. Digital endocasts of the cochlea of (A) *Caperea marginata*, NMV C28531, (B) *Herpetocetus* cf. *transatlanticus*, IRNSB V00372, and (C) *Herpetocetus* sp., IRSNB V00377. Starting from the left, specimens are shown in anterior, lateral, dorsal, and vestibular views. All specimens are shown as right cochlea with specimens from the left side reversed. Abbreviations: ant, anterior; dor, dorsal; med, medial; pos, posterior.

***Herpetocetus* cf. *transatlanticus*, IRSNB V00372:** The cochlea completes approximately 2.75 turns (Fig. 3.2B), slightly fewer than in the indeterminate *Herpetocetus* specimen examined by Geisler & Luo (3 turns; 1996) and *Herpetocetus morrowi* (3.3 turns; Ekdale 2016). There is a small amount of radial inflation in the first quarter of the basal turn, similar to most cetaceans, but no distinct tympanal recess. The apical turn is tightly coiled and encloses a small open space. The entire apical turn overlaps the section of the cochlear canal immediately below.

48

The cochlea has a height of 7.97 mm, a width of 10.88 mm, a volume of 274.99 mm^3 and a cochlear canal length of 35.08 mm (Table 2). This is smaller than in all extant mysticetes, but comparable to several small-sized fossil species (Ekdale 2016), and may hence – at least in part – reflect the relatively small body size of cetotheriids. The secondary spiral lamina extends along the radial wall of the cochlear canal for approximately half of the basal turn (approximately 42% of the total length of the cochlear canal). The basal ratio of IRNSB V00372 is 0.73. The axial pitch, cochlear slope and radii ratio values are 2.90, 0.082 and 6.43, respectively, resulting in an estimated low frequency hearing limit of 65 Hz.

Herpetocetus **sp., IRSNB V00377:** The cochlea completes approximately 2.5 turns (Fig. 3.2C), slightly fewer than in IRSNB V00372. There is a distinct tympanal recess resembling that of *Caperea*. The apical turn is tightly coiled and encloses a small open space. The entire apical turn overlaps the section of the cochlear canal immediately below. The cochlea has a height of 8.17 mm, a width of 12.45 mm, a volume of 279.64 mm^3 and a cochlear canal length of 42.20 mm, similar to IRNSB V00372 (table 2). The secondary spiral lamina extends along the radial wall of the cochlear canal for approximately half of the basal turn (approximately 40% of the total length of the cochlear canal). The basal ratio of IRNSB V00377 is 0.64. The axial pitch, cochlear slope and radii ratio values are 3.27, 0.077 and 6.70, respectively, resulting in an estimated low frequency hearing limit of 56 Hz.
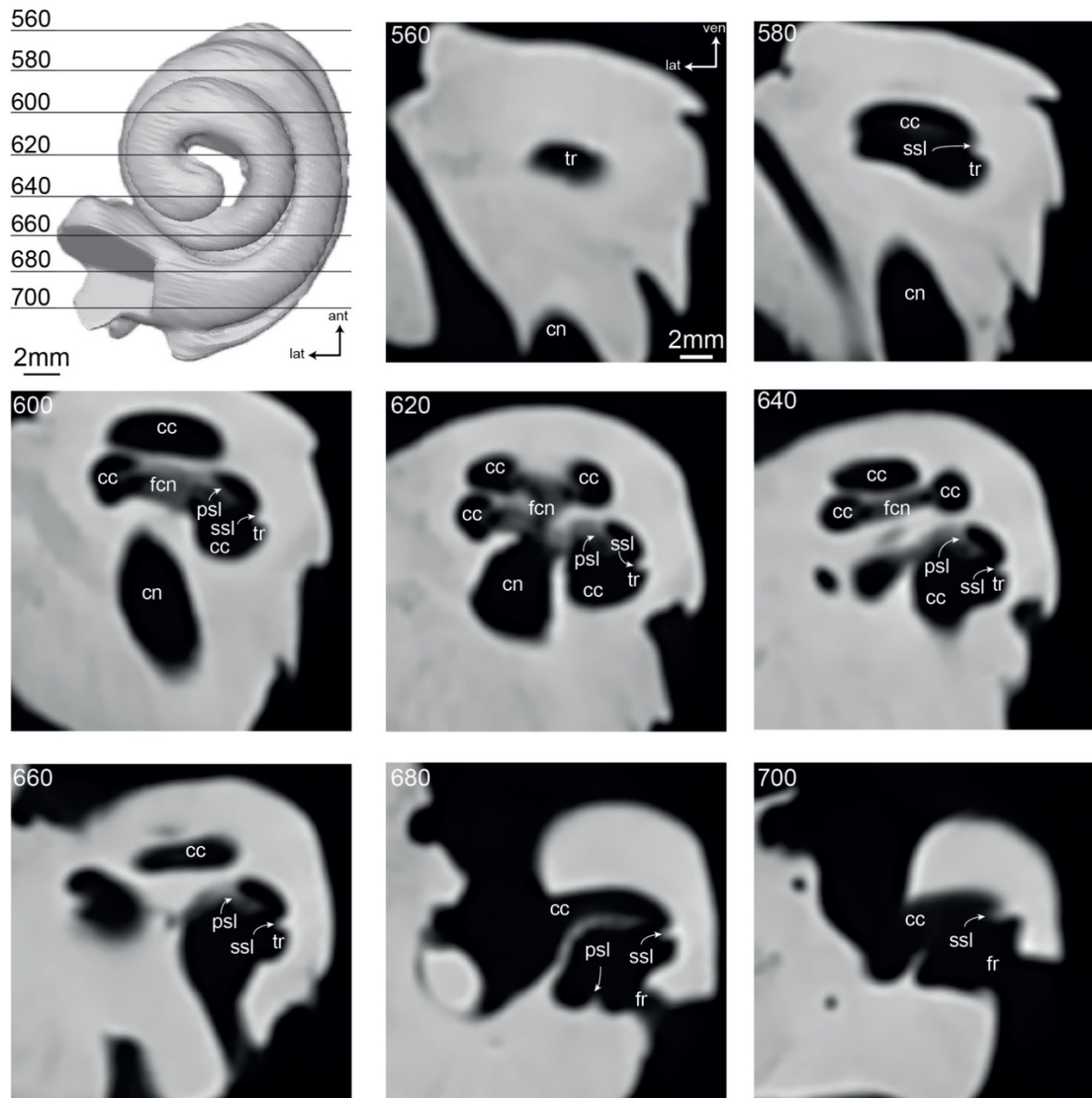
Fig. 3.3. Raw CT slices through right inner ear of NMVC28531. Slice number is indicated in the top left corner. Abbreviations: ant, anterior; cc, cochlear canal; cn, canal for cranial nerve VIII (auditory nerve); fcn, foramina for the cochlear nerves; fr fenestra rotunda; lat, lateral; psl, primary spiral lamina; ssl, secondary spiral lamina; tr, tympanal recess; ven, ventral.

3.4. Discussion

(a) Possible effects of ontogeny

All of the scanned specimens represent juveniles at various stages of development, with

NMV C28531 (*Caperea*) representing a 3.30 m long individual with open skull sutures.

Nevertheless, its periotic resembles that of adults in having an elongate compound posterior

process, a sharply defined promontorial groove, a cranially elongated anterior portion of the

pars cochlearis, and a relatively massive bone surface texture (see photos in Ekdale et al.

2011: Fig. 11). The age of the fossils is harder to gauge. Of the North American specimens, IRSNB V00372 is likely the older given its larger size, better defined attachment for the tensor tympani, and larger and more anteriorly positioned lateral tuberosity. The periotics from Belgium are comparable in size, but IRSNB V00376 appears to older based on its larger, more anteriorly projected lateral tuberosity and the pronounced hypertrophy of its suprameatal area. In mysticetes, a certain degree of ontogenetic change affects the tympanoperiotic (Bisconti 2001), and could hence plausibly also influence cochlear shape. Observations on other mammals, however, suggest that the cochlea remains relatively stable after initial ossification, enabling comparisons that are largely independent of age class (Ekdale 2010; Hoyte 1961; Jeffery & Spoor, 2004).

Table 3.2. Measurements for the cochleae of *Caperea* and *Herpetocetus*. AP, axial pitch; BR, basal ratio; CL, canal length; Est. LFL, estimated low frequency limit; Hz, hertz (rounded to the nearest integer); RR, radii ratio #T, number of turns; SSL, secondary spiral lamina; Vol, volume.

Taxon	Specimen No	#T	CL (mm)	RR	SSL length (mm)	% extent of OSL	BR	AP	Slope	Vol (mm³)	Estd. LFL (Hz)
Caperea marginata	NMV C28531	2.00	60.97	6.43	22.74	37.29	0.56	5.21	0.085	952.06	65
Herpetocetus cf. *transatlanticus*	IRNSB V00372	2.75	35.08	6.43	14.75	42.06	0.73	2.90	0.082	274.99	65
Herpetocetus sp.	IRNSB V00377	2.50	42.20	6.70	16.69	39.55	0.64	3.27	0.077	279.64	56

(b) Comparisons of *Caperea* with other taxa

The two turns completed by the cochlea of *Caperea* fall at the lower end of values reported for other mysticetes (Ekdale 2016; Ekdale & Racicot 2015; Fleischer 1976; Geisler & Luo 1996) (table 2). The fenestra rotunda is large and separated from the cochlear aqueduct, as in archaeocetes and the majority of modern mysticetes. The extension of the secondary spiral lamina (~37% of cochlear canal length) falls into the range of other living and fossil mysticetes (15%–69%), but is considerably shorter than in odontocetes (Ekdale 2016; Park et al. 2016).

The high degree of overlap of the basal and apical turns also resembles the condition found in archaeocetes and modern mysticetes, but not odontocetes (Ekdale 2016; Ekdale &

Racicot 2015). In mysticetes, the apical turn is shifted posteriorly towards the fenestra rotunda, whereas in odontocetes and archaeocetes it tends to be located further anteriorly. The tightness of apical coiling in *Caperea* is most similar to that of fossil cetotheriids and balaenids, and contrasts with the much more loosely coiled apices of balaenopterids (Yamada & Yoshizaki 1959).

Caperea shares with nearly all other members of Plicogulae – balaenopterids and cetotheriids – the presence of a tympanal recess (Churchill et al. 2016: Fig. 3; Ekdale 2016; Ekdale & Racicot 2015). Among cetotheriids, a similar structure is present in one of the *Herpetocetus* specimens examined here (IRSNB V00377), as well as *Herpetocetus morrowi*, *Metopocetus durinasus*, *Piscobalaena nana* and, to a lesser extent, *Cephalotropis coronatus* (Churchill et al. 2016: Fig. 3; Ekdale 2016). IRSNB V00377 furthermore shares with *Caperea* and an undescribed fossil balaenopterid (Ekdale & Racicot 2015: Fig. 6H) a similar morphology of the tympanal recess, with a distinct distal expansion forming a blunt point (Fig. 2). Strikingly, however, a tympanal recess is entirely absent in the other three *Herpetocetus* cochleae examined here (e.g. IRSNB V00372; Fig. 3.2).

A lack of data on total body size (e.g. for *Herpetocetus*) currently prevents comparisons of relative cochlear size. Nevertheless, at 952 mm^3, *Caperea* has one of the largest reported cochlear volumes of any cetacean, surpassing *Balaena mysticetus* (618 mm^3), *Eubalaena glacialis* (559 mm^3) and *Eschrichtius robustus* (783 mm^3), and exceeded only by an indeterminate species of extinct balaenopterid (974 mm^3) (Ekdale 2016: table S2). Likewise, its cochlear height and width are within the upper range of values for mysticetes (Ekdale 2016: table S2), notwithstanding the status of *Caperea* as the smallest extant mysticete (Kemper 2009).

A basal ratio of 0.56 is comparable with that of balaenopterids, but below that of balaenids and extinct cetotheriids (Table 2) (Ekdale 2016). The radii ratio of *Caperea* is also

comparatively low, with only *Herpetocetus* (Table 2), *Cephalotropis coronatus*, *Cophocetus oregonensis* and *Balaena mysticetus* reaching similar or lower values (Ekdale 2016). By contrast, its axial pitch (5.20) and slope (0.085) are among the highest of any mysticete studied so far (table 2) (Ekdale 2016).

(c) Hearing abilities of *Caperea*

The cochlea of *Caperea* is unambiguously of the mysticete type or "Type M" of Ketten & Wartzok (1990), and thus specialised for detecting low frequency sounds. Nevertheless, its low radii ratio give *Caperea* one the highest low frequency hearing limits (65 Hz) of any mysticete, apparently matched or exceeded only by one of the specimens of *Herpetocetus* (IRSNB V00372; 65 Hz), *Balaena mysticetus* (106 Hz) and *Cophocetus oregonensis* (112 Hz) (table 2) (Ekdale 2016). Notably, the hearing limit of *Caperea* approximately corresponds to the lowest frequency sound (ca 60 Hz) previously recorded from a juvenile individual of the same species (Dawbin & Cato 1992). The functional implications of the large size of the *Caperea* cochlea currently remain unclear. Nevertheless, our findings add to the impression that *Caperea* stands out from other mysticetes not only in terms of its external and skeletal morphology, but also in its sensory capabilities (Bischoff et al. 2012; Meredith et al. 2013).

(d) Phylogenetic implications

Besides its large size, one the most striking features of the cochlea of *Caperea* is the presence of a well-developed tympanal recess. The same structure occurs in a variety of other mysticetes, including most balaenopteroids and cetotheriids, but is absent in balaenids and stem mysticetes, as well as the archaic balaenopterid *'Megaptera' miocaena* and some individuals of *Herpetocetus* (Fig. 3.2) (Churchill et al. 2016; Ekdale 2016; Ekdale & Racicot

2015; Park et al. 2017). *Herpetocetus* in particular demonstrates that the tympanal recess can be variable with a single genus and, potentially, even within a single species. Further, much broader sampling of neocete species is required to assess the prevalence of this phenomenon. Nevertheless, the frequent occurrence of the tympanal recess among the more than 20 species of living and fossil mysticete sampled so far appears to follow a pattern, which suggests the existence of a phylogenetic signal irrespective of intraspecific variation.

Specifically, ancestral state reconstruction recovers the presence of a tympanal recess as a synapomorphy of the clade uniting *Caperea* with cetotheriids and balaenopteroids (3 steps; Fig. 3.4), as supported by molecular and recent morphological evidence (Marx & Fordyce 2016; McGowen et al. 2009). By contrast, placing *Caperea* as sister to balaenids, the traditional position suggested by several morphological studies (e.g. Bisconti 2015; El Adli et al. 2014), increases the number of steps to four (Fig. 4). Thus, the tympanic recess offers strong, independent morphological support for the monophyly of Plicogulae.

Apart from suggesting a placement inside Plicogulae, the cochlear anatomy of *Caperea* does not provide specific evidence for or against a close relationship with cetotheriids. While the similar shape of the tympanal recess in *Caperea* and IRSNB V00377 is striking, the cochlea of *Herpetocetus* in general appears more archaic. One exception to this is the large number of turns (≥ 2.75) shown by it and certain other cetotheriids, which appears to be a derived feature and may point to specialised hearing abilities (Ekdale 2016; Geisler & Luo 1996). These differences in morphology either imply that *Caperea* and balaenopteroids show a certain degree of convergent evolution (e.g. via a secondary reduction of the number of turns in *Caperea*), or that *Caperea* is not as deeply nested within Cetotheriidae as previously suggested.
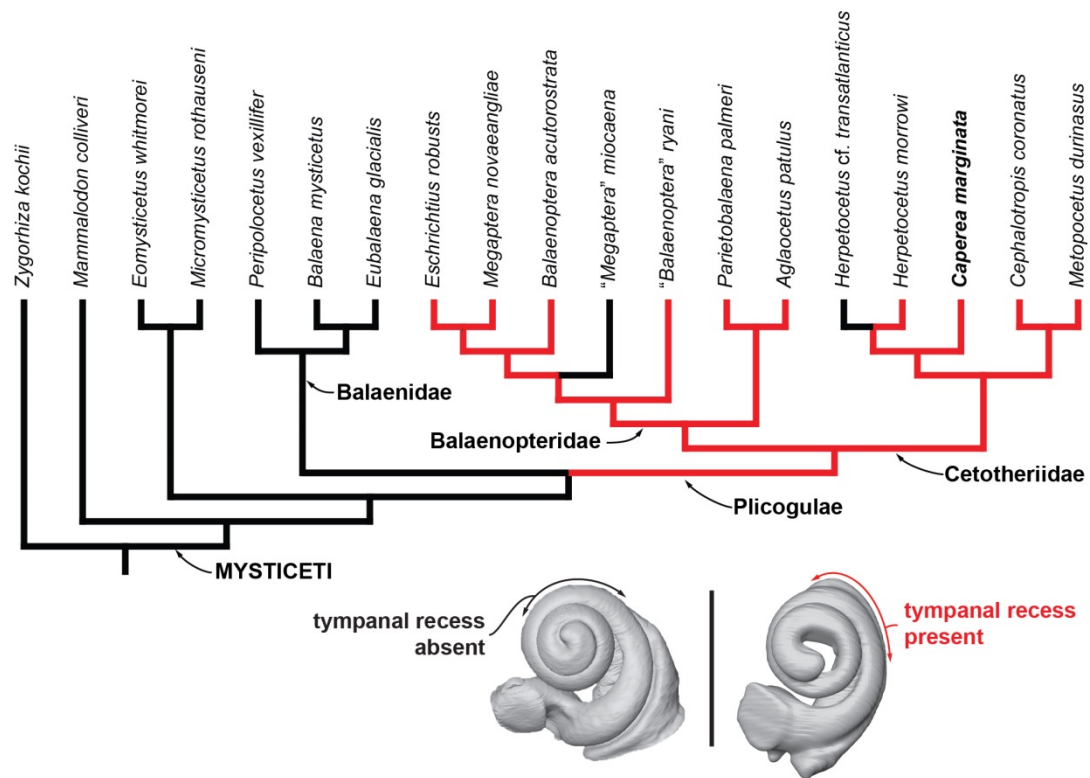
Fig. 3.4. Mysticete phylogeny showing the distribution of the tympanal recess. Topology based on Marx & Fordyce (2016: Fig. S2). Ancestral states were reconstructed using parsimony. Red and black indicate the presence and absence of a tympanal recess, respectively. The current topology requires three steps: acquisition of a tympanal recess at the base of Plicogulae, followed by losses in *Herpetocetus* cf. *transatlanticus* and "*Megaptera*" *miocaena*. Placing *Caperea* as sister to balaenids, as traditionally advocated by morphological studies, increases the number of steps to four.

Acknowledgements

References

Bischoff N, Nickle B, Cronin TW, Velasquez S, Fasick JI. 2012. Deep-sea and pelagic rod visual pigments identified in the mysticete whales. Visual Neuroscience 29, 95–103.

Bisconti M. 2015. Anatomy of a new cetotheriid genus and species from the Miocene of Herentals, Belgium, and the phylogenetic and palaeobiogeographical relationships of Cetotheriidae s.s. (Mammalia, Cetacea, Mysticeti). Journal of Systematic Palaeontology 13, 377–395.

Bisconti M, Bosselaers M. 2016. *Fragilicetus velponi*: a new mysticete genus and species and its implications for the origin of Balaenopteridae (Mammalia, Cetacea, Mysticeti). Zoological Journal of the Linnean Society London 177, 450–474.

Buchholtz EA. 2011. Vertebral and rib anatomy in *Caperea marginata*: implications for evolutionary patterning of the mammalian vertebral column. Marine Mammal Science 27, 382–397.

Churchill M, Berta A, Deméré TA. 2012. The systematics of right whales (Mysticeti: Balaenidae). Marine Mammal Science 28, 497-521.

Churchill M, Martínez-Cáceres M, de Muizon C, Mnieckowski J, Geisler JH. 2016. The Origin of High-Frequency Hearing in Whales. Current Biology 26, 1–6.

Deméré TA, McGowen MR, Berta A, Gatesy J. 2008. Morphological and molecular evidence for a stepwise evolutionary transition from teeth to baleen in mysticete whales. Systematic Biology 57, 15–37.

Ekdale EG. 2013. Comparative anatomy of the bony labyrinth (inner ear) of placental mammals. PLoS ONE 8, e66624.

Ekdale EG. 2016. Morphological variation among the inner ears of extinct and extant baleen whales (Cetacea: Mysticeti). Journal of Morphology 277, 1599–1615.

Ekdale EG, Racicot RA. 2015. Anatomical evidence for low frequency sensitivity in an archaeocete whale: comparison of the inner ear of *Zygorhiza kochii* with that of crown Mysticeti. Journal of Anatomy 226, 22–39.

Ekdale EG, Berta A, Demere TA. 2011. The Comparative Osteology of the Petrotympanic Complex (Ear Region) of Extant Baleen Whales (Cetacea: Mysticeti). PLoS ONE 6, e21311.

El Adli JJ, Deméré TA, Boessenecker RW. 2014. *Herpetocetus morrowi* (Cetacea: Mysticeti), a new species of diminutive baleen whale from the Upper Pliocene (Piacenzian) of California, USA, with observations on the evolution and relationships of the Cetotheriidae. Zoological Journal of the Linnean Society London 170, 400–466.

Fitzgerald EMG. 2012 Possible neobalaenid from the Miocene of Australia implies a long evolutionary history for the pygmy right whale *Caperea marginata* (Cetacea, Mysticeti). Journal Vertebrate Paleontology 32, 976–980.

Fleischer G. 1976. Hearing in extinct cetaceans as determined by cochlear structure. Journal of Paleontology 50, 133–152.

Fordyce RE, Marx FG. 2013. The pygmy right whale *Caperea marginata*: the last of the cetotheres. Proceedings of the Royal Society London B: Biological Sciences 280, 20122645.

Geisler JH, Luo Z. 1996 The petrosal and inner ear of *Herpetocetus* sp. (Mammalia; Cetacea) and their implications for the phylogeny and hearing of archaic mysticetes. Journal of Paleontology 70, 1045–1066.

Gol'din P, and Steeman ME. 2015. From problem taxa to problem solver: a new Miocene family, Tranatocetidae, brings perspective on baleen whale evolution. PLoS ONE 10, e0135500.

Kemper CM. 2009. Pygmy right whale *Caperea marginata*. In: Perrin WF, Würsig B, Thewissen JGM, eds, Encyclopedia of Marine Mammals, (2nd ed). Academic Press, Burlington, pp. 939–941.

Kemper CM, Middleton JF, van Ruth PD. 2012. Association between pygmy right whales (*Caperea marginata*) and areas of high marine productivity off Australia and New Zealand. New Zealand Journal of Zoology 40, 102–128.

Ketten DR, Wartzok D. 1990. Three dimensional reconstructions of the dolphin ear. In Thomas JA, Kastelein RA, eds, Sensory abilities of Cetaceans. Plenum Press, New York, pp. 81–105.

Ketten DR, Arruda J, Cramer S, Yamato M. 2016. Great ears: Low-frequency sensitivity correlates in land and marine leviathans. In Popper AN, Hawkins A, eds, The Effects of Noise on Aquatic Life II. Springer Science & Business Media, New York, pp. 529–538.

Manoussaki D, Chadwick RS, Ketten DR, Arruda J, Dimitriadis EK, O'Malley JT. 2008. The influence of cochlear shape on low-frequency hearing. Proceedings of the National Academy of Sciences 105, 6162–6166.

Marx FG, Fordyce RE. 2015. Baleen boom and bust: a synthesis of mysticete phylogeny, diversity and disparity. Royal Society Open Science 2, 140434.

Marx FG, Fordyce RE. 2016. A link no longer missing: New evidence for the cetotheriid affinities of *Caperea*. PLoS ONE 11, e0164059.

McGowen MR, Spaulding M, Gatesy J. 2009. Divergence date estimation and a comprehensive molecular tree of extant cetaceans. Molecular Phylogenetics and Evolution 53, 891–906.

Meredith RW, Gatesy J, Emerling CA, York VM, Springer MS. 2013. Rod monochromacy and the coevolution of cetacean retinal opsins. PLoS Genetics 9, e1003432.

Park T, Fitzgerald EMG, Evans AR. 2016. Ultrasonic hearing and echolocation in the earliest toothed whales. Biology Letters 12, 20160060.

Ross GJB, Best PB, Donnelly BG. 1975. New records of the pygmy right whale (*Caperea marginata*) from South Africa, with comments on distribution, migration, appearance, and behavior. Journal of the Fisheries Research Board of Canada 32, 1005–1017.

Sekiguchi K, Best PB, Kaczmaruk BZ. 1992. New information on the feeding habits and baleen morphology of the pygmy right whale *Caperea marginata*. Marine Mammal Science 8, 288–293.

Steeman ME. 2007. Cladistic analysis and a revised classification of fossil and recent mysticetes. Zoological Journal of the Linnean Society 150, 875–894.

Steeman ME, Hebsgaard MB, Fordyce RE, Ho SYW, Rabosky DL, Nielsen R, Rahbek C, Glenner H, Sørensen MV, Willerslev E. 2009. Radiation of extant cetaceans driven by restructuring of the oceans. Systematic Biology 58, 573–585.

Visualization Sciences Group – a FEI Company. 2013. Avizo: 3D Analysis Software for Scientific and Industrial Data, Standard Edition 8.0.0. Berlin: Konrad-Zuse-Zentrum für Informationstechnik.

Whitmore FC, Barnes LG. 2008. The Herpetocetinae, a new subfamily of extinct baleen whales (Mammalia, Cetacea, Cetotheriidae). Virgina Museum of Natural History Special Publication 14, 141–180.

Yamada M, Yoshizaki F. 1959. Osseous labyrinth of Cetacea. Scientific Reports of the Whales Research Institute 14, 291–304.

4. Predatory basilosaurids to filter-feeding giants: transformation of the basicranium and the evolution of hearing in baleen whales

Travis Park[1,2], Erich M. G. Fitzgerald[2-4]

[1]School of Biological Sciences, Monash University, Australia.

[2]Geosciences, Museums Victoria, Melbourne, Australia.

[3]Department of Vertebrate Zoology, National Museum of Natural History, Smithsonian Institution, Washington, DC, USA.

[4]Department of Life Sciences, Natural History Museum, London, UK.

Abstract

Living baleen whales are creatures of superlatives, their bodies pushing the limits of biology. Among their extreme characteristics is the ability to make and detect the lowest frequency sounds of any mammal. Whilst other studies have shown that the inner ear of mysticetes has remained relatively unchanged compared to their basilosaurid ancestors, the timing and extent of the changes that occurred in the mysticete basicranium as they became the giants of today is yet to be documented. This analysis describes and compares the basicrania of a range of fossil mysticetes from key clades with those of basilosaurid archaeocetes and modern mysticetes. Toothed mysticetes and eomysticetids retain the plesiomorphic basicranial morphology seen in basilosaurids and therefore shared the same auditory pathway of mandible–basicranium–inner ear. In contrast, modern mysticetes display substantial changes in their basicranial morphology that are indicative of a switch to using bone conduction as the primary method of directing sounds to the middle and inner ear.

4.1. Introduction

In the spectrum of placental mammal radiation, baleen whales have evolved some of the most extreme adaptations, including: the largest ever body sizes, an elaborate filter-feeding apparatus (baleen) and specialised low frequency vocalisation and hearing. Modern mysticetes are thought to be able to detect these low frequency sounds by using their skulls to transmit vibrations to the inner ear (cochlea) (Cranford & Krysl 2015), which is located inside the periotic bone. Similarly, archaic mysticetes are also thought to have possessed low frequency hearing, based on strong similarities in inner ear morphology with living Mysticeti (see Chapter 2). However, the periotic is situated within the basicranium, and sounds must first pass through this region of the cranium to reach the inner ear. Hence the basicranium also influences what sounds are eventually heard.

The mysticete basicranium is well adapted for directional underwater hearing, having developed features such as pachyostosis (thickening of bone), osteosclerosis (increased bone density) and pneumatic sinuses. The extent of these features, as well as the relationship between the basicranium and the tympanoperiotic, determine what sounds a cetacean can hear. Early researchers laid the foundations for studying the cetacean basicranium (Fraas 1904; Lille 1910; Pompeckj 1922; Ridewood 1922; Kellogg 1928, 1936), with a clearer understanding of the morphological basis of cetacean hearing and the role of the basicranium in this process not being realised until several decades later (Fraser and Purves 1960; Norris 1968; Kasuya 1973; Fleischer 1976). A key study by Luo and Gingerich (1999) detailed the transformation of the cetacean basicranium, linked to increasing specialisation towards underwater hearing, as they evolved from a terrestrial to an aquatic lifestyle. Crucially, all of these studies only included living mysticetes and did not address the extent of changes required and the timing of the appearance of modern mysticete basicranial apomorphies as they evolved from small, toothed predators to the giant, filter-feeding species alive today.

Here, I describe and compare the basicrania of a range of fossil mysticetes from key stem clades with those of basilosaurid archaeocetes and modern mysticetes. This study enables us to determine when the auditory specialisations seen in the basicrania of modern mysticetes first evolved, filling a critical gap in our understanding of the evolution of cetacean hearing.

4.2. Materials and Methods

Taxa included in this study are listed in table 4.1 and Fig 4.1. For outgroup comparisons, I examined two species of basilosaurid archaeocete (*Cynthiacetus peruvianus* and *Zygorhiza* sp.). Basilosauridae are generally thought to be near the common ancestry of Neoceti (Luo & Gingerich 1999, Geisler & Sanders 2003, Uhen 2004; Fordyce 2009). These were compared to six fossil mysticete taxa representing at least three families (Aetiocetidae, Mammalodontidae and Eomysticetidae). The fossil taxa were also compared with a modern balaenid, balaenopterid and the cetotheriid *Caperea marginata*. I therefore follow the taxonomy of Mysticeti proposed by Marx & Fordyce (2015) where *Caperea marginata* is considered as Cetotheriidae. Each specimen was studied by direct observation and/or high resolution photography. The cameras used were a Sony α7 with a Minolta AF DT 18–70 mm lens and a Nikon D90 digital SLR camera with a Nikon Nikkor 60 mm micro lens. Anatomical terminology used here follows that of Mead & Fordyce (2009) unless indicated otherwise.

Table 4.1. Specimens included in this study.

Taxon	Specimen(s)	Key reference(s)
Cynthiacetus peruvianus	MNHN.F.PRU 10	Martínez-Cáceres & Muizon (2011)
Zygorhiza sp.	NMV P231828 (cast of OU 22100)	Köhler & Fordyce (1994)
Janjucetus hunderi	NMV P216929	Fitzgerald (2006)
Mammalodontidae indet.	NMV P48794	Fitzgerald (2010)
Aetiocetus weltoni	UCMP122900	Deméré & Berta (2008)
Fucaia goedertorum	LACM 131146	Barnes et al. (1994)
Micromysticetus rothauseni	ChM PV4844	Sanders & Barnes (2002)
Yamatocetus canaliculatus	KMNH VP 000,017	Okazaki (2012)
Eubalaena australis	NMNZ MM002239	N/A
Caperea marginata	OM VT227	N/A
Balaenoptera acutorostrata	NMNS M42450	N/A

Institutional abbreviations –Charleston Museum Vertebrate Palaeontology Collection, Charleston, South Carolina, USA (ChM PV); Kitakyushu Museum of Natural and Human History, Kitakyushu, Kyushu, Japan (KMNH); Natural History Museum of Los Angeles County, Los Angeles, California (LACM); Muséum National d'Histoire Naturelle (MNHN); National Museum of Nature and Science, Tokyo/Tsukuba, Japan (NMNS); Museums Victoria Palaeontology Collection, Melbourne, Victoria (NMV P); Marine Mammal Collection, Museum of New Zealand Te Papa Tongarewa, Wellington, New Zealand (NMNZ MM); Otago Museum, Dunedin, New Zealand (OM VT); Geology Museum, University of Otago, Dunedin, New Zealand (OU); University of California Berkeley Museum of Paleontology (UCMP); National Museum of Natural History, Smithsonian Institution, Washington D.C. (USNM).
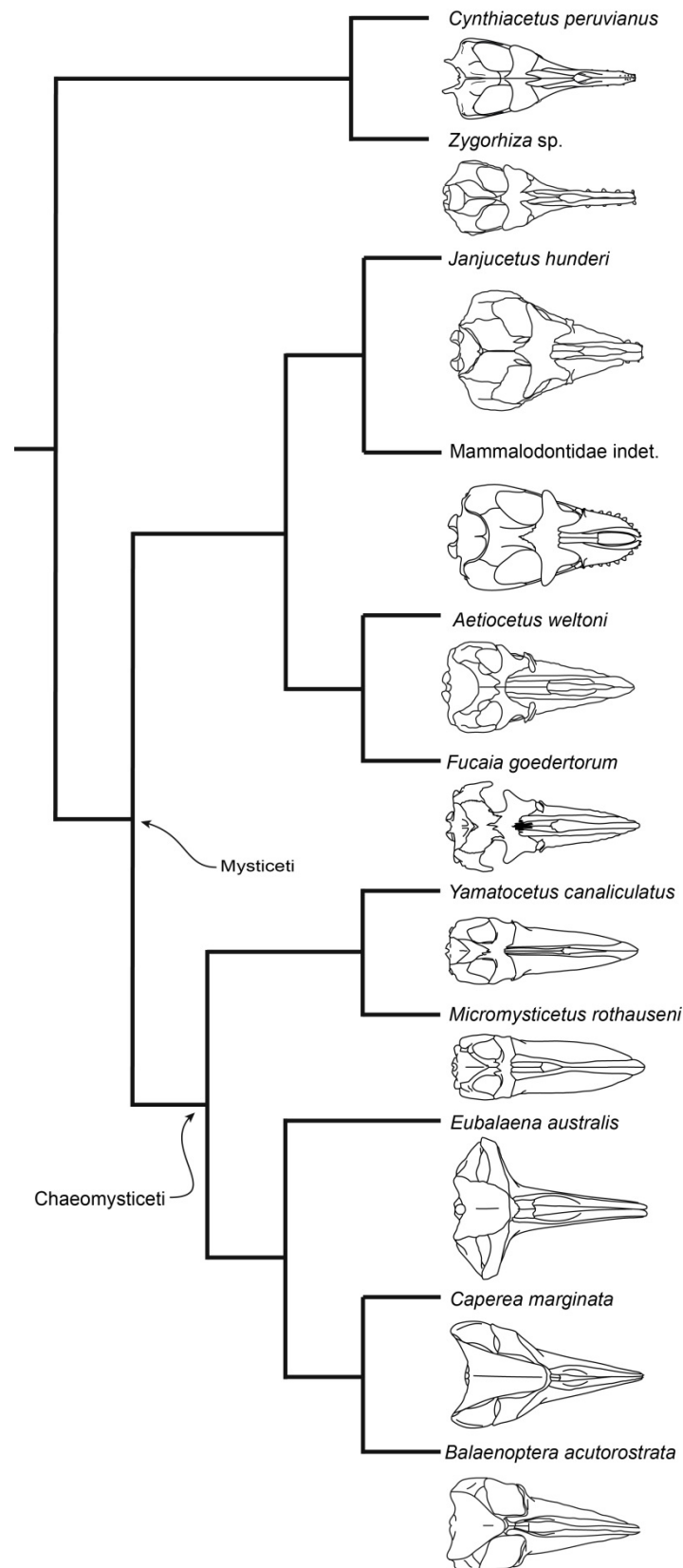
Figure 4.1. Phylogeny (based on that of Marx & Fordyce 2015) of the taxa sampled in this study. Skull drawing of *Cynthiacetus* based on figure 2a of Martínez-Cáceres and Muizon (2011), with rostrum torsion corrected. Skull drawings of *Janjucetus*, *Aetiocetus* and *Balaenoptera* modified from Marx (2010). Skull drawings of *Zygorhiza*, *Mammalodon*, *Fucaia*, *Eubalaena* and *Caperea* modified from Uhen (2010). Skull drawing of *Yamatocetus canaliculatus* and *Micromysticetus rothauseni* modified from Boessenecker & Fordyce (2016). Drawings not to scale.

4.3. Descriptions

The basicranium is one of the most altered regions of the cetacean skeleton, with the necessity of good underwater hearing causing large-scale departures from the standard terrestrial mammal basicranial bauplan. The periotic and tympanic bulla have joined together to form the tympanoperiotic. In terrestrial mammals these two elements contribute to the floor of the braincase, but in cetaceans the tympanoperiotic has become partially isolated from the rest of the skull, with an opening known as the cranial hiatus occurring between the tympanoperiotic and the basioccipital (Mead & Fordyce 2009). In living mysticetes, other parts of the basicranium have instead seen an increased degree of contact with the anterior and posterior processes of the tympanoperiotic. The basicranium has also been greatly shaped by the development of a sinus complex which has excavated fossae of varying extent into the pterygoid and paroccipital. This extension of the Eustachian tube has led to a series of air sinuses that further isolate the auditory region from other tissues. Additionally, parts of the basicranium have become denser relative to surrounding tissues.

Basilosauridae

Cynthiacetus peruvianus

This taxon is represented in this study by a complete, well-preserved skull (MNHN.F.PRU 10). The specimen is from the late Eocene to early Oligocene of Paracas Bay, Peru (Martínez-Cáceres & Muizon 2011) (Figure 4.2).
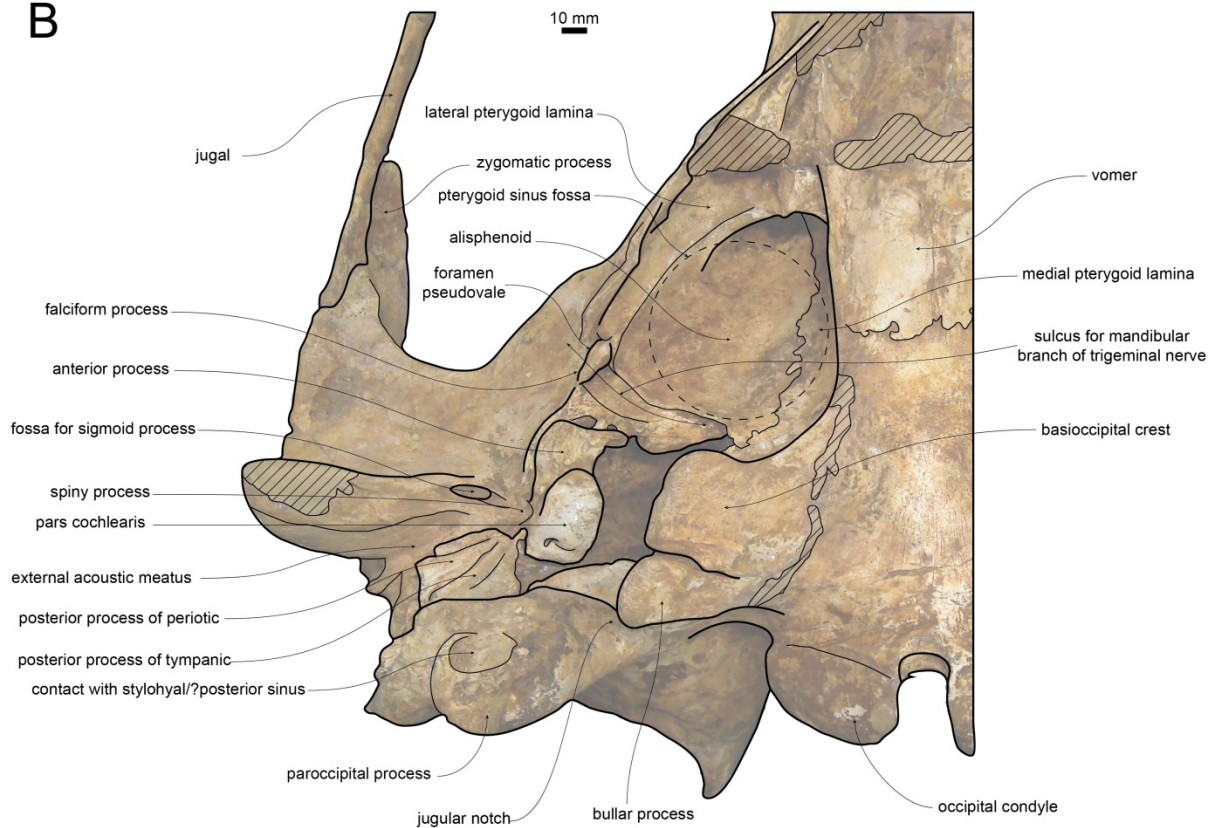
Figure 4.2. Right half of basicranium (including periotic) of the basilosaurid *Cynthiacetus peruvianus* (MNHN.F.PRU 10) in ventral view: A, photograph; and B, line drawing (modified from Martínez-Cáceres & Muizon (2011)). Diagonal hatching indicates breakage. Scale bar = 10 mm.

In *C. peruvianus* the pterygoid is strongly excavated by the sinus fossa and completely exposed, with the level of the dorsal lamina of the pterygoid well dorsal to the level of the basisphenoid. The pterygoid sinus fossa is bound by the lateral and medial laminae of the pterygoid, which is a synapomorphy of Basilosauridae and Neoceti (Fraser & Purves 1960; Mead & Fordyce 2009). It extends anterior to the level of the foramen pseudovale (= external opening of the foramen ovale in Fraser and Purves (1960) and Luo and Gingerich (1999)). The lateral lamina of the pterygoid extends posteriorly to a point slightly anterior of the foramen pseudovale. The pterygoid-squamosal suture is serrate in form. The medial lamina of the pterygoid partially covers the basisphenoid on its lateral extremities, extending to a point just anterior of the bulbous basioccipital crests. Martínez-Cáceres & Muizon (2011) state that the dorsal lamina is not present in this specimen, with the pterygoid sinus fossa being roofed by the alisphenoid and the squamosal. However, the dorsal lamina is present in other basilosaurids (Kellogg, 1936; Luo & Gingerich, 1999).

The sulcus for the mandibular branch of the trigeminal nerve runs at an oblique angle posterior to the pterygoid sinus fossa, extending medially almost to the basioccipital. Portions of the alisphenoid continue past this point posteriorly and appear to contact the anterior process of the periotic. The foramen pseudovale (= external foramen ovale of Fraser & Purves (1960) and Mead & Fordyce (2009)) appears to lie within the squamosal albeit on the anteriormost portion. The falciform process is plate-like with an anteroposteriorly wide base. It projects anteroventrally from the main body of the squamosal and articulates with the lateral lamina of the pterygoid anteriorly, the anterior process of the periotic medially and the tympanic bulla posteroventrally. The spiny process of the squamosal (= squamosal wing of Luo & Gingerich (1999)) is present but damaged. Lateral to the spiny process of the squamosal is a transverse fossa that receives the sigmoid process of the tympanic bulla. The external auditory meatus is anteroposteriorly wide and deeply incised, widens laterally and is

bounded posteriorly by the posterior meatal crest. The anterior meatal crest does not appear to be present.

The basioccipital crests of *C. peruvianus* are wide and bulbous, in contrast to the transversely narrow basioccipital crests of *Zygorhiza.* The crests diverge posteriorly. There is a large cranial hiatus (= basicapsular fissure of Luo & Gingerich (1999)) between the basioccipital crests and the periotic, which would have housed the peribullary sinus.

The paroccipital process of the exoccipital in *C. peruvianus* possesses an excavated ventral surface that may have hosted the posterior sinus (=posterior pterygoid sinus of Luo & Gingerich (1999)), but is more likely to have been the point of contact for the stylohyoid. However, Mead & Fordyce (2009) noted that the often-large presumed paroccipital fossa for posterior sinus may be for a lobe of peribullary sinus. If an elliptical foramen is present, then there may have been a sinus. Whilst there is an anterior fossa, the ventral surface of the paroccipital process lacks an excavation for the posterior sinus like that seen in some toothed mysticetes. The bullar process is also bulbous, similar to the basioccipital crest, leaving a wide jugular notch posterolateral to it.

The periotic tightly articulates with the squamosal via the short anterior process and the superior process (tegmen tympani of Martínez-Cáceres & Muizon (2011)) in addition to the posterior process of the periotic also contacting the exoccipital. The anterior process of the periotic is short, with the apex turning medially, similar to other dorudontine basilosaurids. The posterior process of the periotic is elongate, situated between the external auditory meatus and the exoccipital.

Martínez-Cáceres & Muizon (2011) wrote that the anterior pedicle of the tympanic bulla contacts the pars cochlearis, rather than the anterior process of the periotic as seen in other archaeocete and early neocete taxa. The tympanic bulla (not figured) also contacts the

falciform process of the squamosal laterally and the basioccipital crest medially (Martínez-Cáceres & Muizon 2011).

Zygorhiza sp.

This genus is represented by a largely complete braincase broken at the anterior end of the intertemporal region (OU 22100), from the Middle Eocene of Waihao Greensand of New Zealand. Sutures on the skull suggest the individual was a subadult or an adult (Perrin 1975) (Fig 4.3). The specimen was originally described by Köhler and Fordyce (1997). A cast (NMV P231828) of the original specimen was examined for this study.

The alisphenoid is broken in the centre of the pterygoid sinus fossa, which has excavated the skull to a point well dorsal to the level of the basisphenoid, as seen in *Cynthiacetus*. The fossa extends anteriorly past the foramen pseudovale, which is situated entirely within the squamosal. There is also a posterolateral extension of the alisphenoid that passes dorsal to the foramen pseudovale (forming part of the sulcus for the mandibular branch of the trigeminal nerve) and is tightly appressed to the falciform process of the squamosal and the anterior process of the periotic. The sulcus for the mandibular branch of the trigeminal nerve runs at an oblique angle just posterior to the pterygoid sinus fossa and runs into the posterior lacerate foramen. The ventral extent of the falciform process is obscured as it is broken. The external auditory meatus is anteroposteriorly wide and widens laterally. Anterior to the external auditory meatus is the groove for the sigmoid process of the tympanic bulla. Posterior to this is the spiny process of the squamosal.

The basioccipital crests are less bulbous than in *Cynthiacetus* and diverge slightly posteriorly, meaning that there is a large cranial hiatus. On the medial face of the basioccipital crests are two deep grooves bounded by crests, which may represent an excavation made by the peribullary sinus. Köhler and Fordyce (1997) speculated that the

anterior-most crest may represent the anterior border of the path for the acoustic nerve, VIII, from the inner ear to the brain.

The paroccipital process is thick and rounded, with a deep, rugose concavity laterally for the contact with the stylohyal or possibly also the posterior sinus, although there does not appear to be a separate fossa for the posterior sinus itself. The bullar process of the exoccipital projects posterolaterally and appears to share a suture with the basioccipital crest. Lateral to this process, the jugular notch is wide and deep.

The periotic closely approximates the falciform process of the squamosal, but the edges appear to be free of it. The anterior process of the periotic is laterally compressed, forming a keel, and appears to contact the posterolateral extension of the alisphenoid, increasing its articulation with the rest of the skull. Articulation is also increased by the superior process. It also possesses a deep notch that forms the medial border of the opening of the anteroexternal sulcus. Posterior to this notch is a large, shallow depression for the head of the malleus which is bounded anteriorly and laterally by a crest. The posterior processes of the periotic and the tympanic bulla are tightly appressed and are wedged between the exoccipital and squamosal. On the ventral surface of the posterior process of the tympanic bulla is the broken posterior pedicle of tympanic bulla.

A

B

basisphenoid

narial passsage
pterygoid sinus fossa

alisphenoid

lateral pterygoid lamina
sulcus for mandibular branch of trigeminal nerve
foramen pseudovale
posterolateral extension of alisphenoid
falciform process
anterior process

medial pterygoid
lamina

pars cochlearis
ventral opening for anteroexternal sulcus
mallear fossa

basioccipital crest

zygomatic process
(broken)

fossa for sigmoid process

excavations of
basioccipital
crest

stapes
spiny process

external acoustic meatus

posterior pedicle

posterior process of tympanic bulla

occipital condyle

contact with stylohyal/?posterior sinus

10 mm

bullar process

jugular notch

paroccipital process

Figure 4.3. Cast of the basicranium (including periotic) of the basilosaurid *Zygorhiza* sp. (NMV P231828) in ventral view. Original specimen is OU 22100: A, photograph; and B, line drawing. Diagonal hatching indicates breakage. Scale bar = 10 mm.

Mammalodontidae

Janjucetus hunderi

This species is represented by a virtually complete skull (NMV P216929) from the late Oligocene of Jan Juc, Victoria, Australia (Fitzgerald 2006) (Fig 4.4). All skull sutures are closed or at least closely approximated, indicating that this individual was either a subadult or adult.

The pterygoid of *Janjucetus* is completely exposed ventrally. The pterygoid sinus fossa is bounded by the lateral, medial and dorsal laminae of the pterygoid, in addition to the alisphenoid in the posterior portion of the pterygoid sinus fossa. The fossa extends anteriorly past the foramen pseudovale. The fossa is excavated dorsally to a point approximately level with the basioccipital medial to it, similar to aetiocetids (see below), but differing from basilosaurids. It is uncertain whether the foramen pseudovale is entirely within the squamosal or is located between the squamosal and the pterygoid, but is most likely the latter. The Eustachian notch is prominently displayed anteroventrally to the pterygoid sinus fossa and is smooth and rounded, forming the anterior border of the pterygoid sinus fossa. The sulcus for the mandibular branch of the trigeminal nerve appears to have been oriented laterally on the alisphenoid, just posterior to the dorsal lamina of the pterygoid.
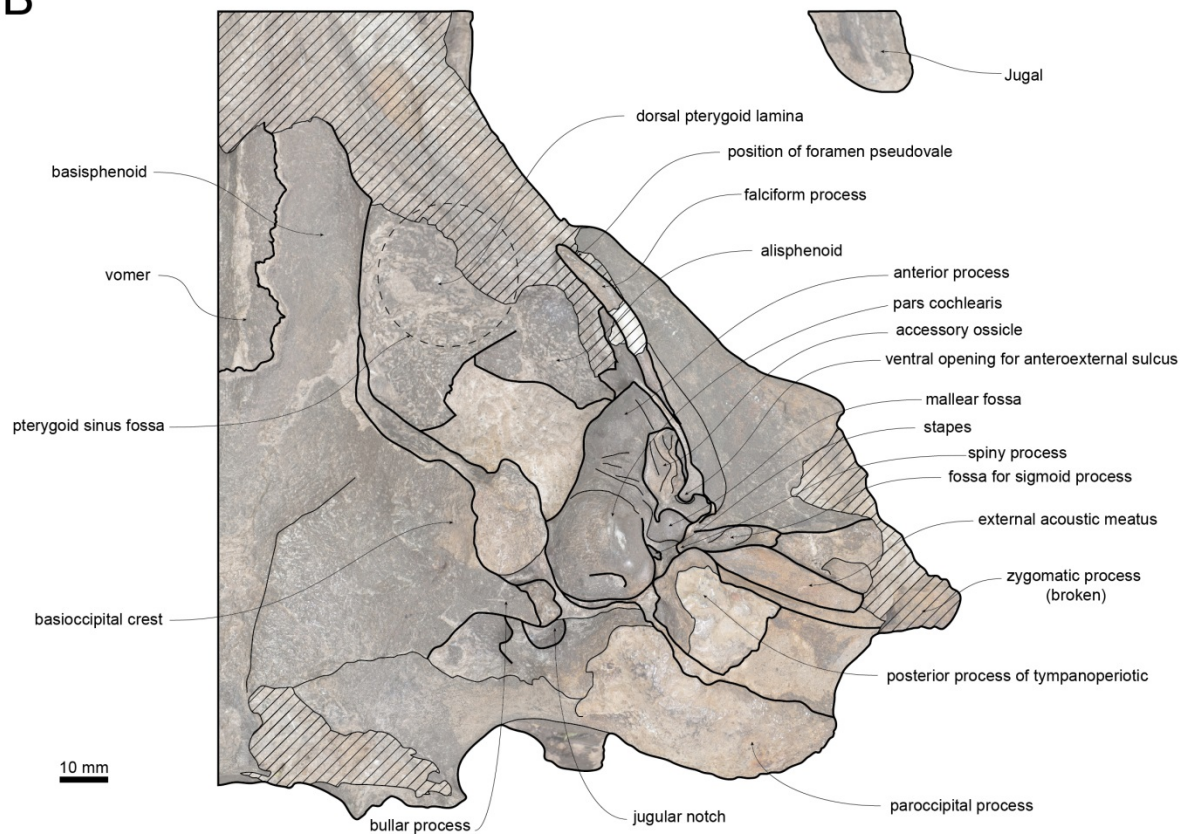
Figure 4.4. Left half of basicranium (including periotic) of the mammalodontid *Janjucetus hunderi* (NMV P216929) in ventral view: A, photograph; and B, line drawing. Diagonal hatching indicates breakage. Scale bar = 10 mm.

The squamosal of *Janjucetus* has a thin, plate-like falciform process with a broad base. The foramen pseudovale is not situated more ventrally than the rest of the squamosal, similar to basilosaurids and other toothed mysticetes. There is a distinct fossa for the sigmoid process of the tympanic bulla. The periotics in *Janjucetus* are *in situ* so the periotic fossa is not visible. The spiny process of the squamosal is present, similar to basilosaurids. The external acoustic meatus is wide and deeply incised. *Janjucetus* has a broad basioccipital with transversely expanded basioccipital crests. The basioccipital crests diverge posteriorly. The cranial hiatus between the basioccipital crest and the periotic is relatively small, indicating that the peribullary sinus was also small relative to that seen in other toothed mysticetes. There do not appear to be any excavations for the peribullary sinus on the lateral sides of the basioccipital crests, but these regions are poorly preserved so they may still be present. Both exoccipitals are quite damaged in *Janjucetus*. The jugular notch is roughly equal in height and width.

The right periotic has been slightly dislodged from its *in vivo* position. The following is based on the left periotic, which remains in its *in vivo* position. The body of the periotic appears to be tightly appressed to the squamosal and the exoccipital, but the lateral edge of the periotic is free from the falciform process. The posterior process of the periotic is tightly sutured to the posterior process of the tympanic bulla. There is a relatively large accessory ossicle that provides a substantial attachment to the tympanic, with the dorsal surface of the accessory ossicle fused to the anterior wall of the mallear fossa. Only the right tympanic bulla is still articulated with the cranium (Fig 4.5). Overall, the morphology of the tympanic bulla is basilosaurid-like and closely approximates the falciform process of the squamosal. However, there is no clear articulation facet on the squamosal for the tympanic bulla like that seen in basilosaurids. The outer lip of the bulla is fused to the anterior process of the periotic. There

is a shallow excavation on the medial side of the tympanic bulla that may have housed part of the peribullary sinus.
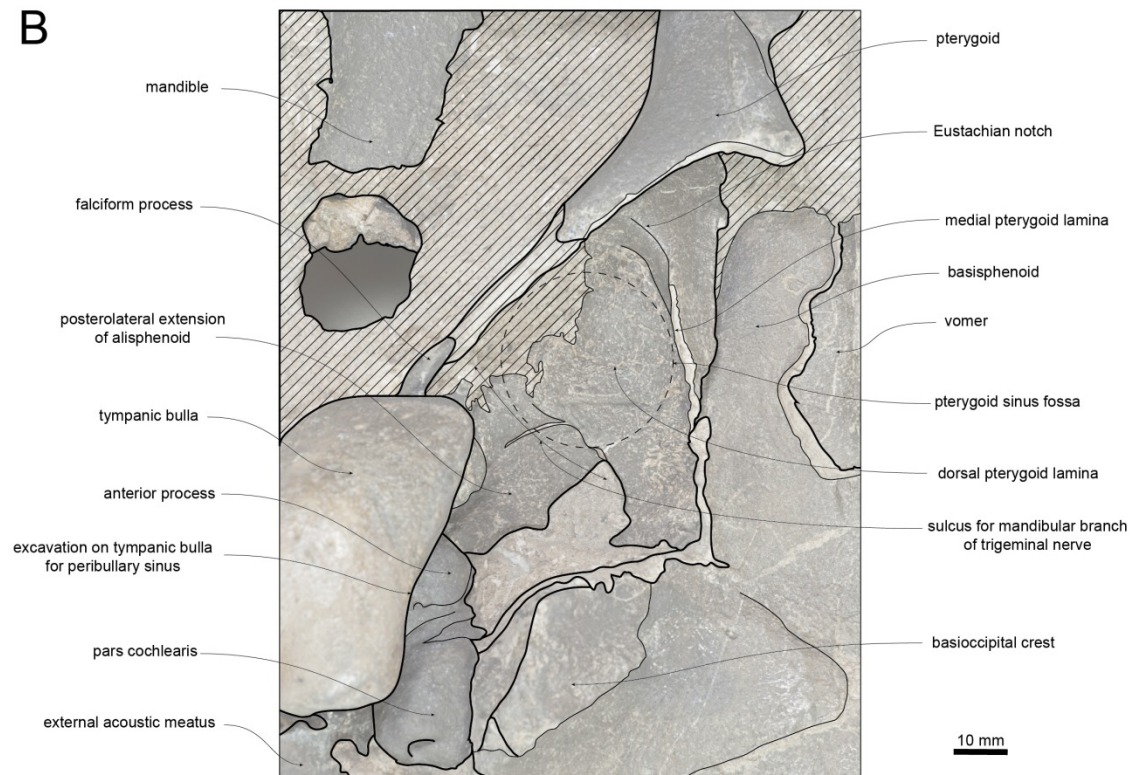
Figure 4.5. Close-up of the right half of basicranium (including periotic & tympanic bulla) of the mammalodontid *Janjucetus hunderi* (NMV P216929) in ventral view, showing pterygoid sinus fossa in detail: A, photograph; and B, line drawing. Diagonal hatching indicates breakage. Scale bar = 10 mm.

Mammalodontidae indet.

This specimen (NMV P48794) is an incomplete cranium with the left periotic in situ (Fig 4.6). It was figured in Fitzgerald (2010) and used to supplement the description of the basicranium of *Mammalodon colliveri*.

The pterygoid is not preserved in this specimen, with the alisphenoid exposed ventrally. The sulcus for the mandibular branch of the trigeminal nerve is oriented obliquely. The squamosal has a thin falciform process which has lost its ventral-most tip. The fossa for the sigmoid process of the tympanic bulla is distinct, with the spiny process of the squamosal posteromedial to it. The external acoustic meatus is wide and deeply incised, bounded by the anterior and posterior meatal crests.

The periotic in NMV P48794 closely approximates the squamosal and exoccipital. However, the edges of the periotic are free from the squamosal. As seen in *Janjucetus* the ventral opening of the anteroexternal sulcus is present and is laterally exposed. Directly medial to this is the broken base of the anterior pedicle of the tympanic bulla. The anterior process is short but extends medially, increasing contact area with the squamosal. The short posterior process is tightly wedged between the squamosal and exoccipital and is not exposed on the external wall of the braincase.
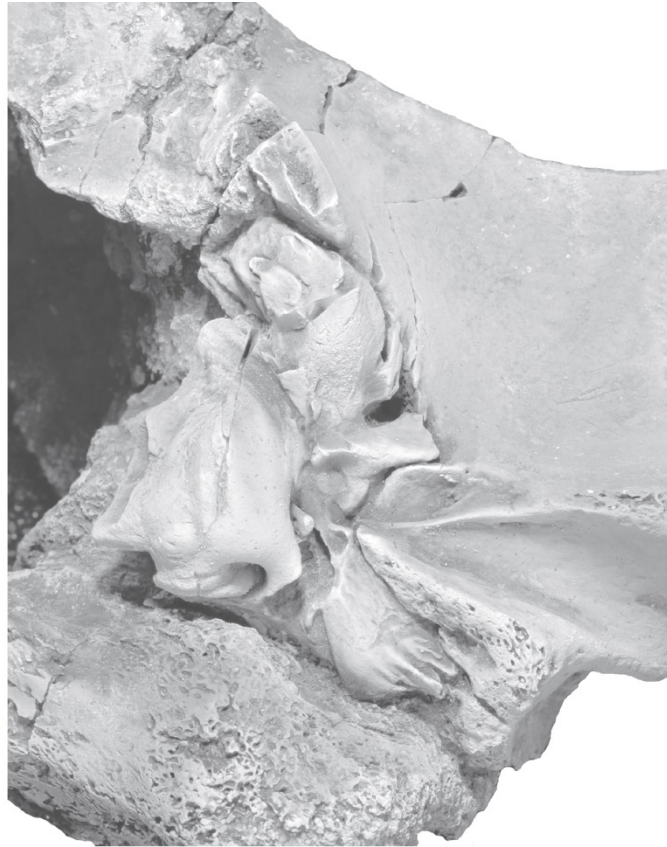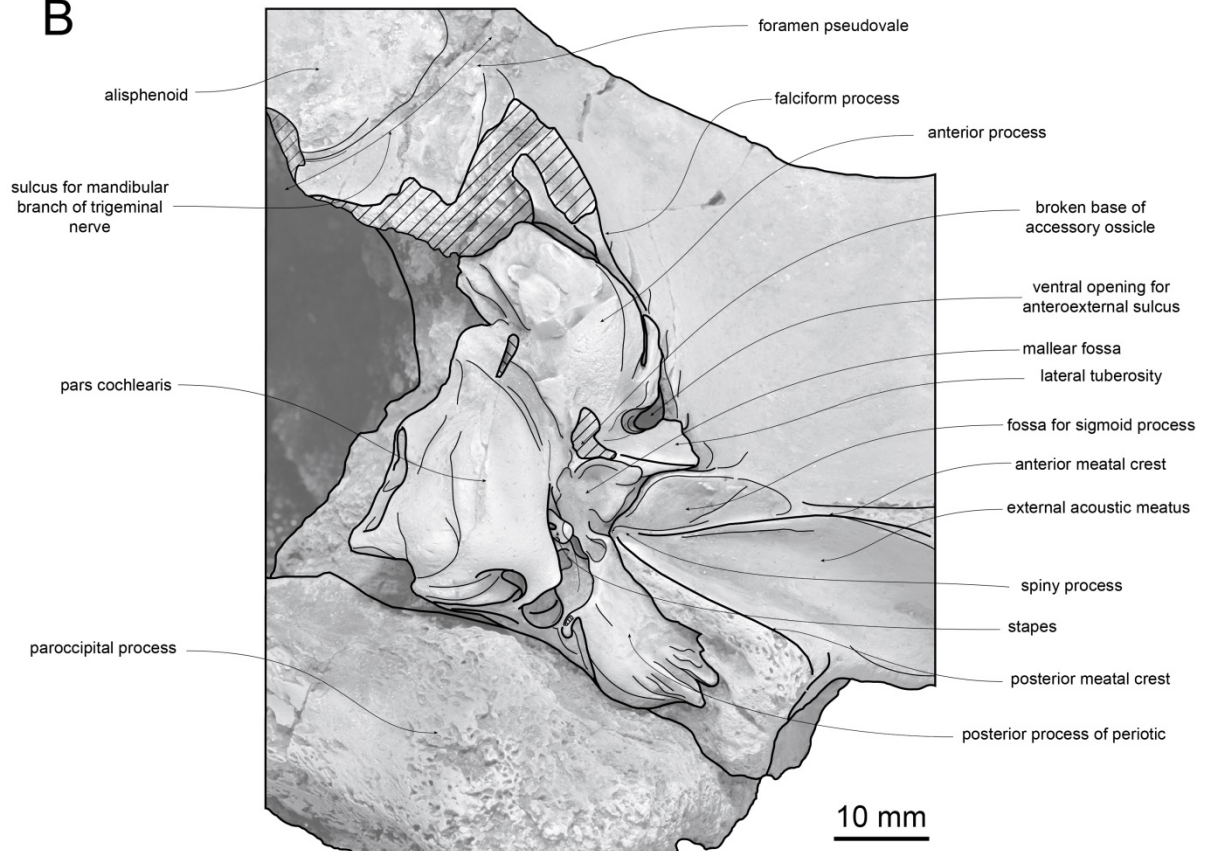
Figure 4.6. Partial left basicranium (including periotic) of an indeterminate mammalodontid (NMV P48794) in ventral view: A, photograph; and B, line drawing. Diagonal hatching indicates breakage. Scale bar = 10 mm.

Aetiocetidae

Aetiocetus weltoni

This taxon is represented by UCMP122900, which includes a nearly complete skull (missing most of the supraoccipital) from the late Oligocene of Oregon, USA (Fig 4.7). Based on the degree of fusion seen in the cranial sutures, this individual was most likely a subadult (Deméré and Berta 2008).

Ventrally, the pterygoid is completely exposed, like archaeocetes and other toothed mysticetes. The pterygoid sinus fossa is deeply excavated, similar to other aetiocetids, but differing from mammalodontids. It extends anteriorly past the foramen pseudovale, which is located entirely within the squamosal. The fossa is bounded by dorsal, lateral and medial laminae of the pterygoid as well as the falciform process of the squamosal, which extends anteriorly so that it is situated lateral to the lateral lamina. As noted by Deméré and Berta (2008), the dorsal lamina possesses a rugose surface texture. The sulcus for the mandibular branch of the trigeminal nerve, like *Cynthiacetus peruvianus*, is on the alisphenoid rather than being on the dorsal lamina of the pterygoid as indicated by Deméré & Berta (2008). It is oriented obliquely and may represent the posterior border of the dorsal lamina and pterygoid sinus fossa. Like *Cynthiacetus* and *Zygorhiza*, *Aetiocetus* has a section of alisphenoid that extends posterolaterally and makes contact with the anterior process of the periotic. However, in *Aetiocetus* this section of the alisphenoid appears to have been excavated by the pterygoid sinus. Alternatively, this morphology may result from breakage of the dorsal pterygoid lamina where it would have continued over the groove, flooring the sulcus, technically creating a foramen.
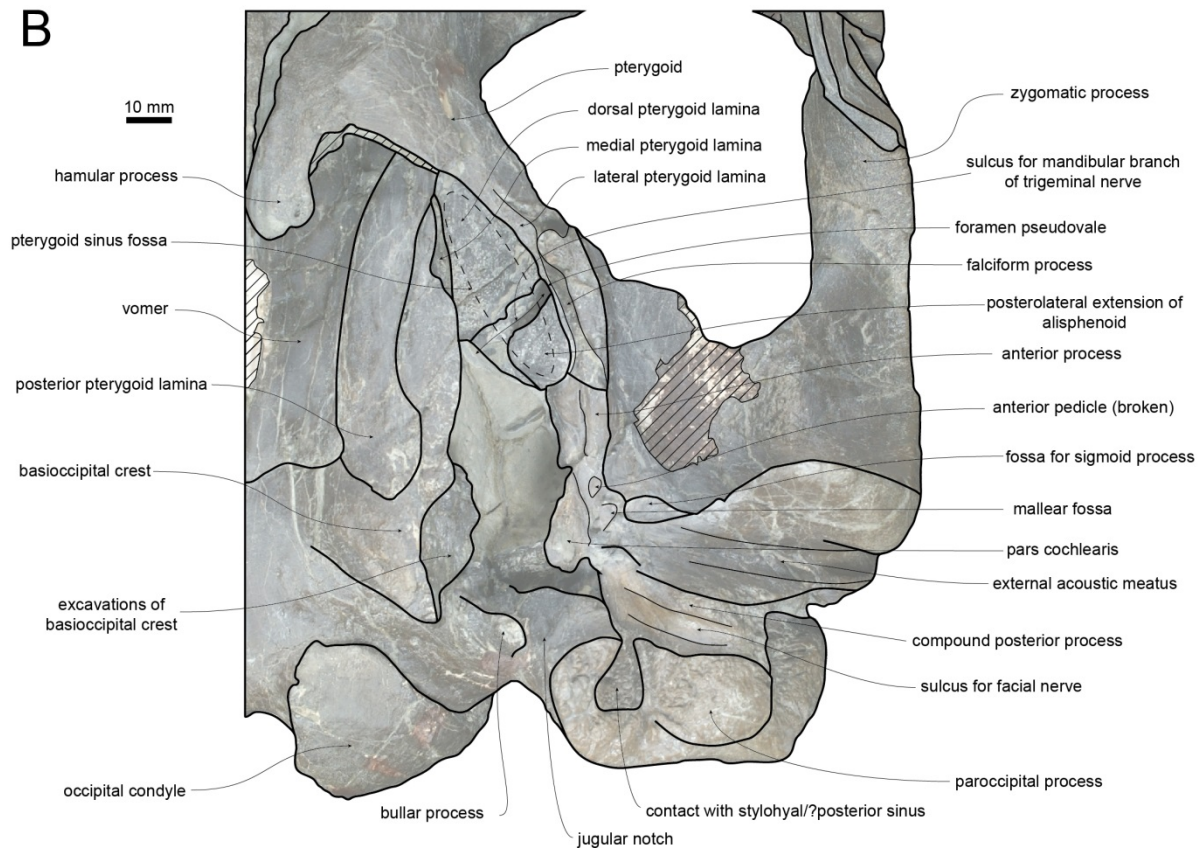
Figure 4.7. Left half of basicranium (including periotic) of the aetiocetid *Aetiocetus weltoni* (UCMP122900) in ventral view: A, photograph; and B, line drawing. Diagonal hatching indicates breakage. Scale bar = 10 mm.

The falciform process is plate-like with an anteroposteriorly wide base. Posterolaterally, a fossa for the sigmoid process of the tympanic bulla is present, similar to basilosaurids, other toothed mysticetes and even protocetids (Geisler and Sanders, 2003). The foramen pseudovale is entirely within the squamosal, unlike some modern taxa (e.g. *Megaptera*) where it is located between the squamosal and the pterygoid. The external auditory meatus is wide and deeply incised and widens laterally.

The posterior lamina of the pterygoid extends posteriorly on the ventral surface of the basisphenoid and basioccipital, obscuring the suture between the two. The ventral edge of the basioccipital crests is essentially parallel to the sagittal plane. They project laterally, slightly obscuring the posterior lacerate foramen and pterygoid sinus fossa in ventral view. The cranial hiatus is large, with a wide space between the basioccipital crest and the periotic. The lateral surface of the basioccipital has a shallow excavation which would have partially housed a large peribullary sinus.

There appears to be a posterior sinus present, as evidenced by the deeply excavated section of the paroccipital process posteromedial to the well-defined sulcus for the facial nerve. This sinus would most likely have been confluent with the peribullary sinus (Deméré & Berta 2008). This excavation forms a crescent-shaped margin when viewed ventrally. The jugular notch is situated lateral to an elongate, finger-like bullar process of the exoccipital and is relatively narrow, being much deeper than it is wide.

Both periotics are in place in *A. weltoni*; however, only the left is visible as the right is obscured ventrally by the articulated tympanic bulla. Additionally, the left periotic is incompletely preserved, but remains *in situ*. It is tightly articulated with the squamosal along its length. There is a small piece of the anterior pedicle of the tympanic bulla situated at the posteroventral margin of the anterior process of the periotic. However, the posterior processes of the periotic and the tympanic bulla are most likely not fused (F. Marx pers. comm.), contra

Deméré and Berta (2008). The posterior process is at a right angle relative to the anterior process, extending laterally in the skull.

The right tympanic bulla remains articulated with the skull of *A. weltoni* (Fig 4.8). The anterior tip of the tympanic bulla slightly contacts the falciform process of the squamosal, but not the basioccipital crests, where there is a slender gap between the two elements. However, there is no clear articulation facet for the tympanic bulla like that seen in basilosaurids. The posterior process of the bulla is tightly articulated with the skull and the posterior process of the periotic. Additionally, the sigmoid process of the bulla articulates with its fossa on the squamosal.

Figure 4.8. Right half of basicranium of the aetiocetid *Aetiocetus weltoni* (UCMP122900) in ventral view showing tympanic bulla in articulation.

Fucaia goedertorum

This taxon is represented by a partial skull (LACM 131146) from the upper Oligocene Pysht Formation in Washington, USA (Fig 4.9). The species was originally named as *Chonecetus goedertorum* by Barnes et al. (1994), but was placed in the new combination *F. goedertorum* by Marx et al. (2015).

The pterygoid sinus fossa is excavated to a point well dorsal of the level of the basisphenoid. It extends anteriorly past the foramen pseudovale, which is located entirely within the squamosal. The pterygoid laminae are badly worn but remnants of the medial and dorsal laminae are present. The dorsal lamina is restricted to the anteromedial corner of the pterygoid sinus fossa, similar to the preservation in *Aetiocetus* and *Janjucetus*. Posterior to the pterygoid sinus fossa, the sulcus for the mandibular branch of the trigeminal nerve runs laterally at an oblique angle on the alisphenoid. *Fucaia* appears to lack the posterolateral extension of the alisphenoid that contacts the anterior process of the periotic seen in basilosaurids, mammalodontids and *Aetiocetus*.

The fossa for the sigmoid process of the tympanic bulla is present, just anterior to the external auditory meatus. Similar to *Aetiocetus* and basilosaurids, the spiny process of the squamosal is present. The basioccipital crests diverge posteriorly and are similar to those of *Aetiocetus*. The cranial hiatus between the basioccipital crest and the periotic is large. The exoccipitals are damaged so the extent of the fossa for the stylohyal contact and/or the posterior process is uncertain. The bullar processes are not well preserved and the jugular notch is deeper than it is wide.

A

B
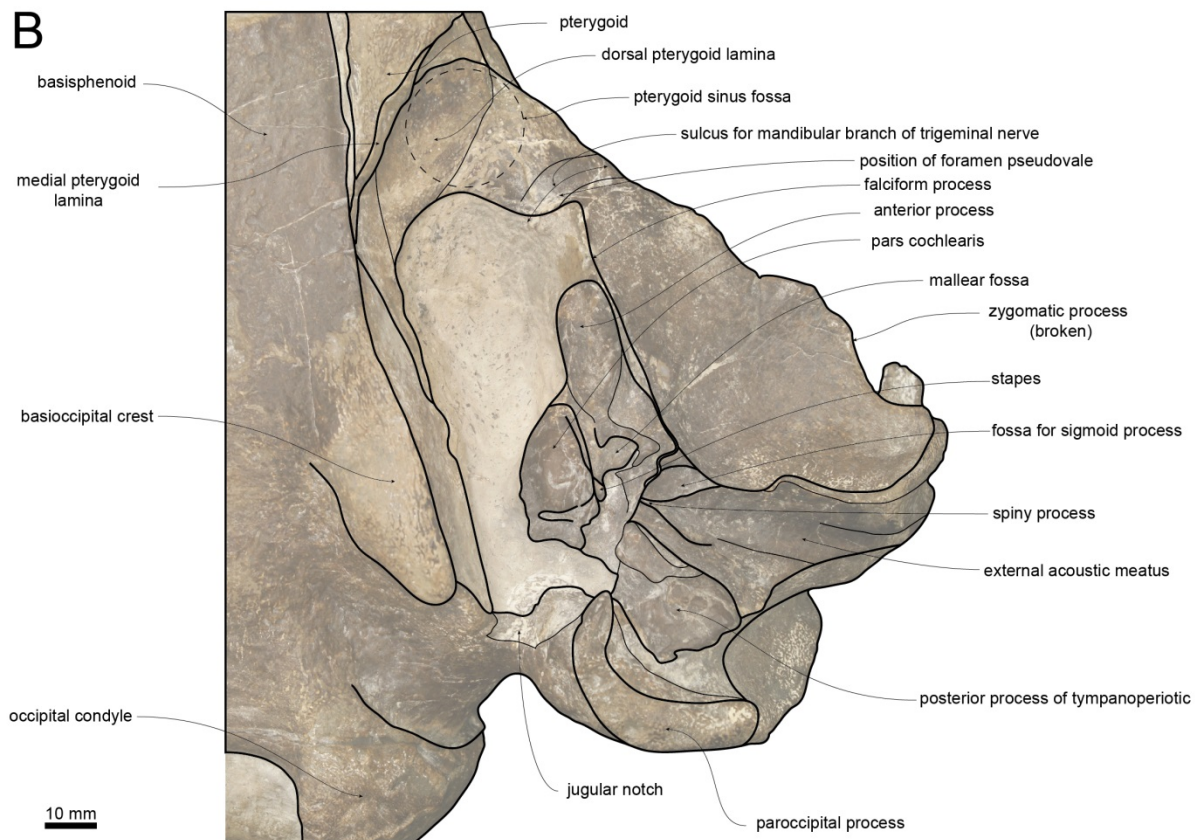
Figure 4.9. Left half of basicranium (including periotic) of the aetiocetid *Fucaia goedertorum* (LACM 131146) in ventral view: A, photograph; and B, line drawing. Diagonal hatching indicates breakage. Scale bar = 10 mm.

The left periotic of *Fucaia goedertorum* is relatively well preserved, although the body of the periotic has suffered some damage. The lateral edges of the periotic are free from the squamosal. The anterior process is longer than in mammalodontids. The posterior processes of the tympanic bulla and the periotic are closely sutured and the process is triangular in ventral view, being tightly wedged between the squamosal and exoccipital.

Eomysticetidae

As there is no single eomysticetid taxon that has a sufficiently well-preserved basicranium to act as an exemplar, the following basicranial description is a composite. Figured are two of the best preserved examples, *Yamatocetus canaliculatus* and *Micromysticetus rothauseni*. The holotype of *Yamatocetus* (KMNH VP 000,017) is a complete cranium with both dentaries, in addition to postcranial material from the early Oligocene of Wakamatsu Ward, Japan (Okazaki 2012; Marx & Fordyce 2015) (Fig 4.10). *Micromysticetus rothauseni* (ChM PV4844) is a partial cranium from the late Oligocene of South Carolina, USA (Sanders & Barnes 2002a) (Fig 4.11). Additional information is also taken from Boessenecker and Fordyce (2014).

A

B

zygomatic process

pterygoid

lateral pterygoid lamina

hamular process

falciform process

tympanic bulla

medial pterygoid lamina

basisphenoid

external acoustic meatus

basioccipital crest

paraoccipial cavity

paroccipital process

jugular notch

occipital condyle

50 mm
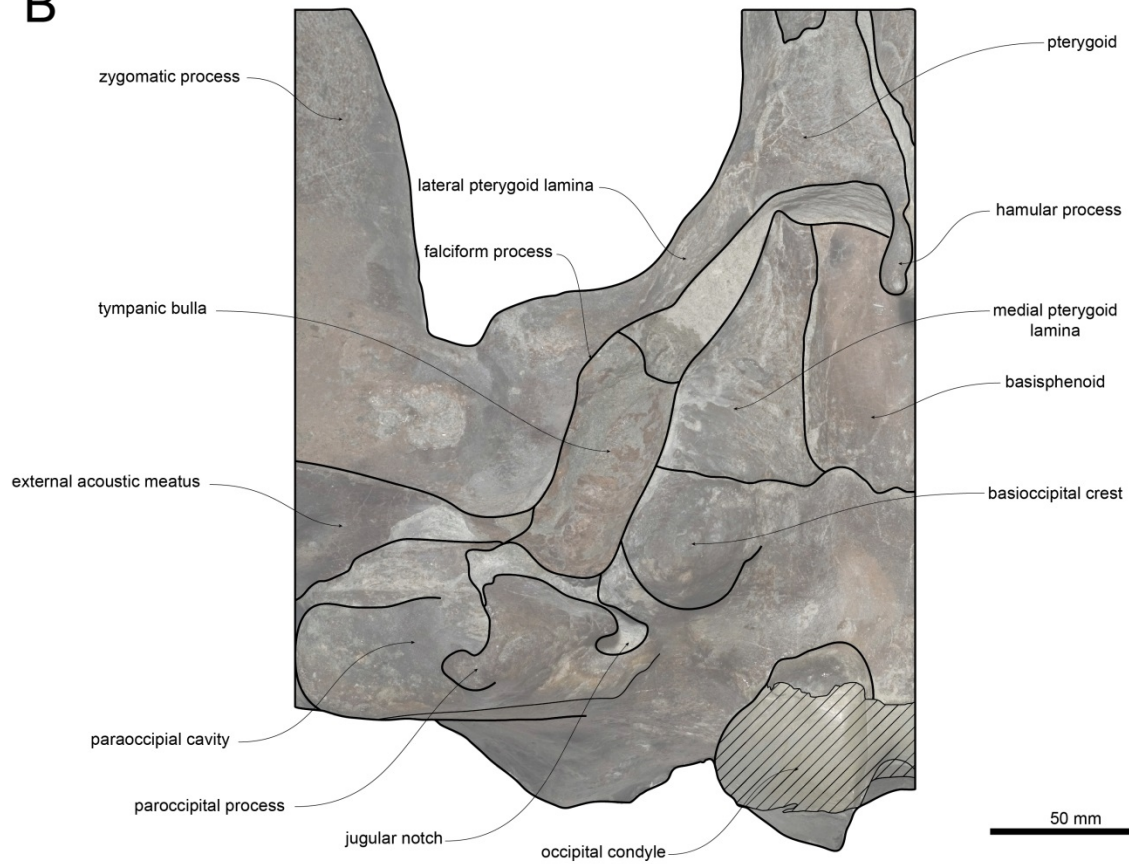
Figure 4.10. Right half of basicranium of the eomysticetid *Yamatocetus canaliculatus* (KMNH VP 000,017) in ventral view: A, photograph; and B, line drawing. Diagonal hatching indicates breakage. Scale bar = 10 mm

Based on *Yamatocetus*, eomysticetid pterygoids are more similar to those of modern mysticetes than to toothed mysticetes or basilosaurids. The pterygoid laminae are very well developed and extend well posterior to the foramen pseudovale. In particular the medial lamina has become extremely well developed, extending posteriorly as far as the basisphenoid-basioccipital suture and also reducing the transverse width of the basisphenoid. The presence of the dorsal lamina is uncertain due to unprepared matrix in the fossa. Unlike modern mysticetes, the ventral lamina of the pterygoid is absent as the fossa is almost completely visible. Most other eomysticetids do not preserve the pterygoid, making it uncertain how representative these morphological features are of eomysticetid pterygoids.

The foramen pseudovale is located entirely within the squamosal. The falciform process is plate-like and extends as far anteriorly as the foramen pseudovale. The fossa for the sigmoid process of the tympanic bulla is triangular in shape, but appears to be less well-developed compared to toothed mysticetes and basilosaurids. In contrast, the spiny process of the squamosal is exceptionally well-developed, extending further medially. It is present in *Eomysticetus* and *Micromysticetus* (Sanders & Barnes 2002a,b) as well as *Tohoraata raekohao*. (Boessenecker & Fordyce 2014). The sulcus for the mandibular branch of the trigeminal nerve runs transversely at an oblique angle posterior to the pterygoid sinus fossa (Sanders & Barnes 2002a). The external auditory meatus is wide and deeply incised and widens anteroposteriorly towards it lateral end.

A

B

sulcus for mandibular branch of trigeminal nerve

anterior process

falciform process

ventral opening for anteroexternal sulcus

zygomatic process
(broken)

mallear
fossa

fossa for
sigmoid
process

spiny
process

stapes

anterior meatal crest

external acoustic meatus

pars cochlearis

posterior meatal crest

posterior process of periotic

paroccipital cavity

paroccipital process

jugular notch

bullar process

pterygoid sinus
fossa

basisphenoid

basioccipital
crest

excavations of
basioccipital
crest

occipital condyle

50 mm

Figure 4.11. Right half of basicranium of the eomysticetid *Micromysticetus rothauseni* (ChM PV4844) in ventral view: A, photograph; and B, line drawing. Scale bar = 10 mm.

The basioccipital crests are wide and bulbous and are oriented almost parallel to the midline of the skull. The cranial hiatus is large. Interestingly, in *Micromysticetus rothauseni* there are deep circular excavations on the dorsolateral portions of the basioccipital crests, which may represent extensions of the peribullary sinus. The exoccipitals display a large, flat paroccipital concavity, similar to that of *Metopocetus* and *Eschrichtius*, suggesting that a large contact for the stylohyal and/or a posterior sinus was present (Marx et al. 2016). The bullar processes are greatly reduced compared to those seen in toothed mysticetes and basilosaurids. The jugular notch is approximately the same width and depth, although there is a constriction at its ventral extent.

The periotic in eomysticetids possesses a relatively elongate anterior process compared to toothed mysticetes and basilosaurids. The process is extremely compressed transversely and broadly expanded dorsoventrally. The lateral edge of the periotic is free from the squamosal, with a well-developed opening for the anteroexternal sulcus. The mallear fossa is present, just medial to the fossa for the sigmoid process. Boessenecker and Fordyce (2015) noted that when the periotic and tympanic bulla are placed in articulation the orientation differs from that of both toothed mysticetes and basilosaurids, being rotated dorsomedially.

Balaenidae

Eubalaena australis

This taxon is represented by a juvenile skull (NMNZ MM002239) from the collections at Museum of New Zealand Te Papa Tongarewa, Wellington, New Zealand (Fig 4.12). The extreme dorsoventral arching of the rostrum has resulted in the zygomatic process extending laterally and the basicranium itself facing posteroventrally rather than ventrally. Therefore the figure itself is in posteroventral view rather than ventral view.

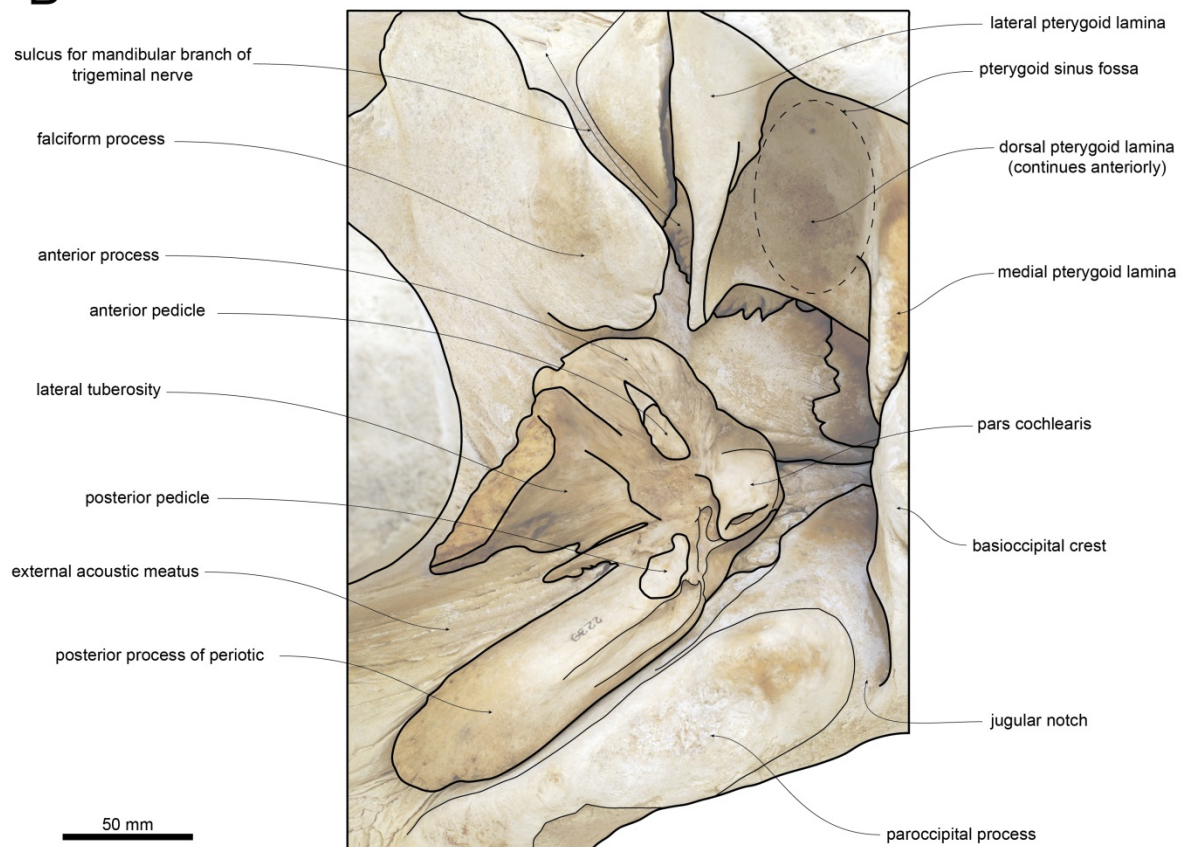Figure 4.12. Right half of basicranium (including periotic) of the southern right whale *Eubalaena australis* (NMNZ MM002239) in posteroventral view: A, photograph; and B, line drawing. Scale bar = 10 mm. Image provided by R. Ewan Fordyce.

The pterygoid in *Eubalaena* is completely covered ventrally by the palatine (Fig 4.13). The pterygoid sinus fossa is much larger than in toothed mysticetes or basilosaurids, both in anterior and dorsoventral extent. The fossa is also floored by the ventral lamina of the pterygoid and potentially also partially by the pterygoid hamuli which are expanded into a dorsoventrally flattened plate, a feature not seen in fossil mysticetes and basilosaurids. The foramen pseudovale: is between the squamosal and pterygoid; is situated much more ventrally than the tympanoperiotic; opens posteriorly; and lacks a posterior edge. This again is different to fossil mysticetes and basilosaurids. The falciform process is anteroposteriorly short and is situated entirely anterior to the anterior process of the periotic. The fossa for the sigmoid process of the tympanic bulla, the ventral opening for the anteroexternal sulcus and the spiny process are not present. The sulcus for the mandibular branch of the trigeminal nerve runs laterally across the alisphenoid posterior and lateral to the pterygoid sinus fossa, being partially floored by it. The external auditory meatus is wide and deep. The basioccipital crests diverge posteriorly and appear to be confluent with the bullar process. The jugular notch is wide and deep.

The periotic of balaenids is very different to that of fossil mysticetes and basilosaurids. It appears to be even more intricately and tightly sutured to the squamosal than in fossil taxa. The anterior process and lateral tuberosity are hypertrophied, forming a large area of contact between the periotic and the squamosal. The thick composite posterior process of the tympanoperiotic (only the posterior process of the periotic is figured) is also greatly elongated relative to toothed mysticetes and basilosaurids. It is, however, less elongate that in *Caperea* and *Balaenoptera* (Ekdale 2011). The anterior bullar facet is absent, and the anterior process is fused to the bulla via the large anterior pedicle. The tympanic bulla (Fig 4.13) is box-shaped and diverges posteriorly when in articulation (Ekdale 2011). They are also larger relative to body size than other mysticete bullae.
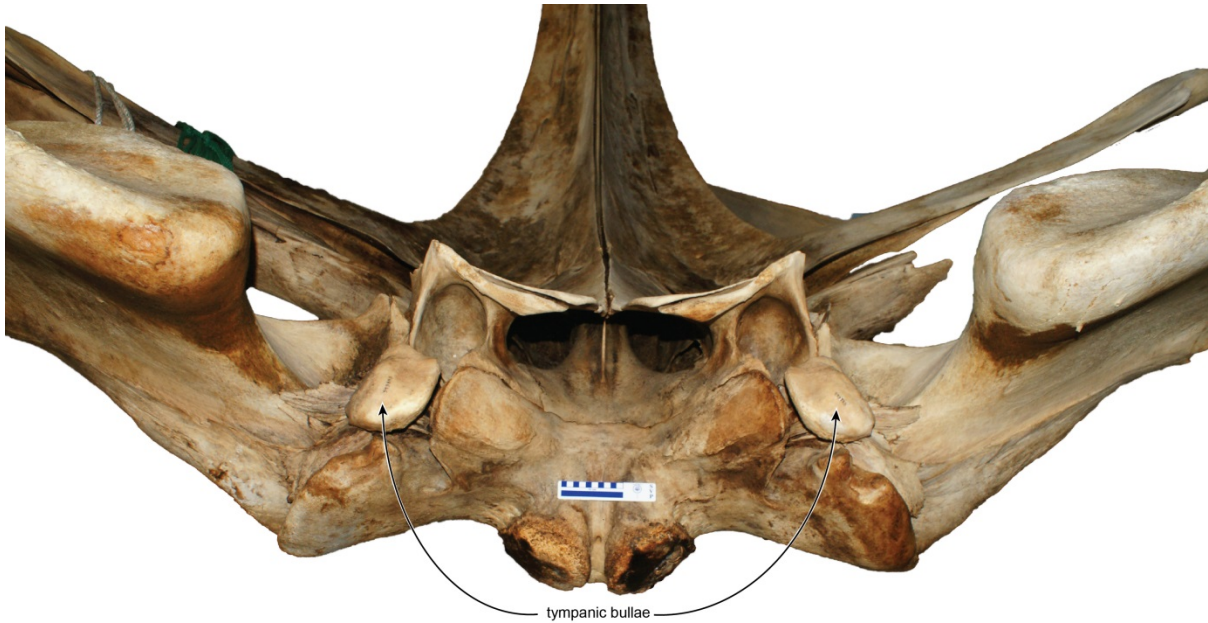
Figure 4.13. Basicranium of the north Atlantic right whale *Eubalaena glacialis* (USNM 593893) in posteroventral view, showing the large articulated tympanic bulla: A, photograph; and B, line drawing. Scale bar = 100 mm.

Cetotheriidae

Caperea marginata

This enigmatic species, which is the last surviving cetothere (Fordyce & Marx 2013; Marx & Fordyce 2016) is represented by an essentially adult skull (OM VT227) from the collections of the Otago Museum, Dunedin, New Zealand (Fig 4.15).
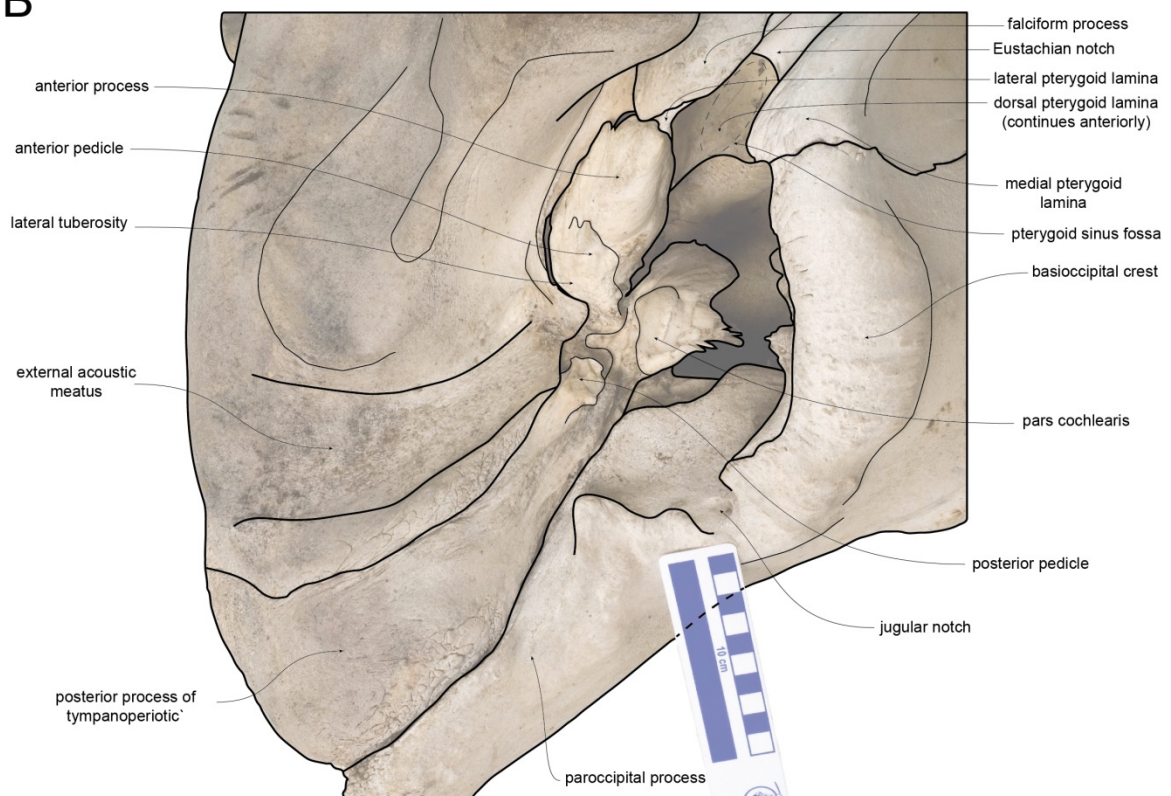
Figure 4.14. Right half of basicranium (including periotic) of the pygmy right whale *Caperea marginata* (OM VT227) in posteroventral view: A, photograph; and B, line drawing. Scale bar = 100 mm.

The pterygoid in *Caperea* differs from other mysticetes in that it has a large ventral exposure rather than being covered by the palatine. It also uniquely entirely surrounds the foramen pseudovale (Fig 4.15). The pterygoid sinus fossa is less voluminous than in *Eubalaena* or *Balaenoptera* but is still larger than in fossil mysticetes and basilosaurids. It is also floored by the ventral lamina of the pterygoid, although the posterior extent of this lamina is restricted by the path of the Eustachian notch. The lateral lamina of the pterygoid extends onto the anterior process of the periotic. The falciform process is anteroposteriorly short and is situated entirely anterior to the anterior process of the periotic, posterolateral to the foramen pseudovale. There is no ventral opening for the anteroexternal sulcus, fossa for the sigmoid process or spiny process of the squamosal, although the squamosal does appear to extend medially onto the lateral tuberosity of the periotic. Similar to *Aetiocetus*, eomysticetids and balaenopterids, the basioccipital crests do not diverge posteriorly, but instead run parallel to the long axis of the skull. The jugular notch is approximately as wide as it is deep, and is much smaller than in *Eubalaena*. There is no distinct paroccipital concavity on the exoccipital.
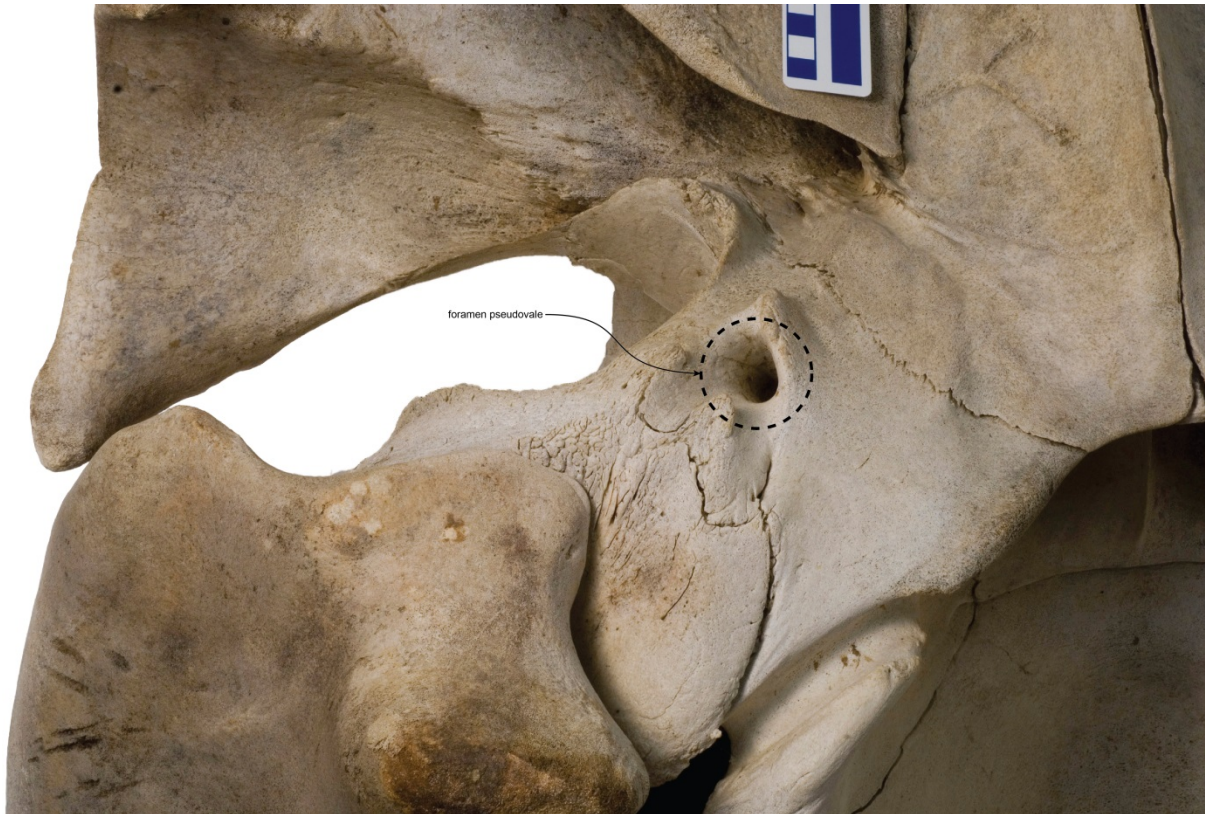
Figure 4.15. Right side of skull of the pygmy right whale *Caperea marginata* (OM VT227) in ventral view, showing foramen pseudovale entirely in the pterygoid. Scale bar = 10 mm.

The periotic in *Caperea* is firmly appressed to the squamosal. The anterior process of the periotic differs from other mysticetes and basilosaurids in being almost completely detached from the body of the periotic and being l-shaped (Fordyce & Marx 2013; Marx & Fordyce 2016). Additionally, the lateral tuberosity is hypertrophied, extending along the anterior process as a broad shelf. The compound posterior process of the tympanoperiotic is extremely expanded both anteroposteriorly and dorsoventrally, and widely exposed on the lateral skull wall. The anterior bullar facet is absent, and the anterior process is fused to the bulla via the large anterior pedicle. The tympanic bulla is dorsoventrally flattened and is oriented parallel to the long axis of the skull, similar to *Balaenoptera* (Fig 4.16).

Figure 4.16. Basicranium of the pygmy right whale *Caperea marginata* (NMNZ MM002235) in posteroventral view, showing articulated tympanic bullae. Scale bar = 100 mm.

Balaenopteridae

Balaenoptera acutorostrata

Rorquals are represented in this study by an adult specimen of *Balaenoptera acutorostrata* (NMNS M42450) from the National Museum of Nature and Science, Tokyo/Tsukuba, Japan (Fig 4.17).
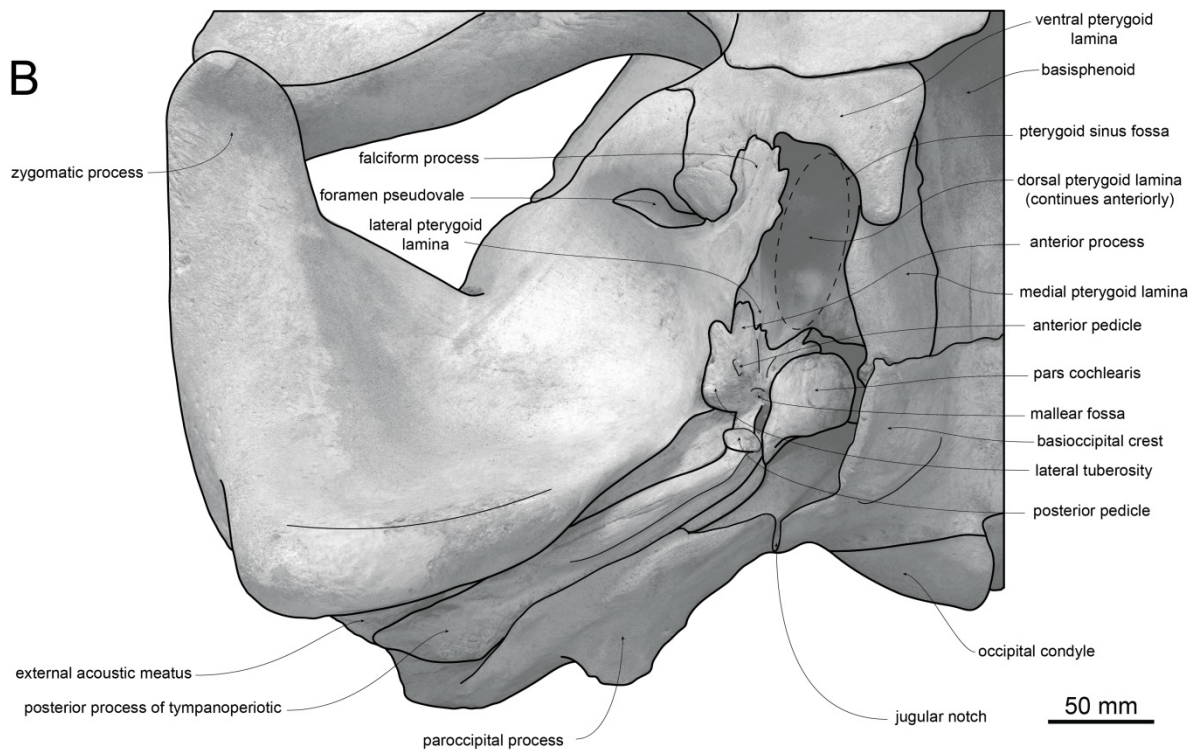
Figure 4.17. Right half of basicranium (including periotic) of the minke whale *Balaenoptera acutorostrata* (NMNS M42450) in ventral view: A, photograph; and B, line drawing.

The pterygoid in *Balaenoptera* is only partially covered by the palatine, which has a wide transverse contact/overlap with the pterygoid. The dorsal lamina completely covers the alisphenoid ventrally. There is also a short ventral lamina of the pterygoid flooring the

anteriormost edge of the pterygoid sinus fossa, a feature only found in crown mysticetes. Similar to *Eubalaena* and *Caperea*, the excavation of the pterygoid sinus fossa itself is much greater than in fossil mysticetes, suggesting a much larger pterygoid sinus.

The foramen pseudovale is situated entirely within the squamosal. It is also situated much more ventrally than the tympanoperiotic, a feature only seen in modern mysticetes. The falciform process is thin and forms the medial border of the foramen pseudovale and its medial surface is sutured to the lateral lamina. The fossa for the sigmoid process of the tympanic bulla is not present and appears to be lost in crown mysticetes. There is no ventral opening for the anteroexternal sulcus. The sulcus for the mandibular branch of the trigeminal nerve is obscured in ventral view, being floored by the dorsal lamina of the pterygoid and runs laterally across the alisphenoid. Similar to all other mysticetes and basilosaurids the external auditory meatus is wide and deep.

The basiocciptial crests in *Balaenoptera* are wide and bulbous, similar to all mysticetes. They differ from toothed mysticetes and basilosaurids, however, in that the basioccipital crests do not diverge posteriorly, but rather are oriented essentially parallel to the sagittal plane of the skull, a morphology shared with eomysticetids and *Caperea*. The lateral wall of the basioccipital is relatively smooth and does not possess any excavations like that seen in *Micromysticetus*. There appears to be no distinct paroccipital concavity present, suggesting that if a posterior sinus was present it was relatively poorly developed. The jugular notch is deep and thin.

Like all mysticetes and basilosaurids, the periotic in *Balaenoptera* is firmly appressed to the squamosal. The anterior process of the periotic is more elongated than the pars cochlearis and is overlapped by the lateral lamina of the pterygoid, similar to *Aetiocetus*. The anterior bullar facet is absent, and the anterior process is fused to the bulla, as in all

mysticetes. The composite posterior process of the tympanoperiotic is extremely elongated and is situated between the exoccipital and the squamosal.

4.4. Basicranial Evolution

Plesiomorphy or specialisation?

As shown in Chapter 2, toothed mysticete cochleae are extremely similar in shape and structure to both those of basilosaurids (but see Churchill et al. 2016) and modern mysticetes. This indicates that the plesiomorphic morphology of basilosaurid cochleae has been retained by mysticetes. This chapter has set out to investigate whether the same pattern is repeated in the basicranium. By establishing the degree of specialisation for underwater hearing in the basicranium of stem mysticetes, it can be determined when in both mysticete phylogeny and geological time the modern pattern of the mysticete basicranium and therefore acoustic abilities arose.

Basilosaurids to toothed mysticetes and eomysticetids

Just like their cochleae, the basicrania of toothed mysticetes are extremely similar to those of basilosaurids. The basicrania of eomysticetids also do not depart from the same overall morphology and it is expected that their cochleae would also possess a comparable structure, as indicated by the specimens included in the cochlear shape analysis of Ekdale (2016). One clear difference is the degree of articulation of the tympanic bulla with the rest of the skull. In basilosaurids the tympanic bulla contacts the falciform process, the sigmoid fossa, and the anterior and posterior processes of the periotic (Luo & Gingerich, 1999). In toothed mysticetes and eomysticetids this contact is reduced by one articulation point, the articulation facet on the falciform process (Deméré & Berta, 2008). This could reflect increasing isolation of the tympanoperiotic complex from the rest of the skull. A more variable difference is the reduction of the superior process of the periotic. Overall, the trend has been for this feature to

diminish (Marx et al. 2015), but some extant mysticetes possess a well-developed superior process (Ekdale et al. 2011).

Excluding these differences, size and some minor interspecific variation, e.g. extent of the dorsal lamina of the pterygoid or which element forms the foramen pseudovale, the overall morphology of the basicranium in toothed mysticetes and eomysticetids is essentially identical to that of basilosaurids. This implies that the sinuses surrounding the tympanoperiotic complex were also of the same extent, with the pterygoid sinus excavating the pterygoid; the peribullary sinus (situated between the basioccipital crest, paroccipital process, tympanic bulla and periotic) and the posterior sinus, if present being poorly developed. Given that the mandibles of stem mysticetes and basilosaurids also possess an enlarged mandibular foramen like that of odontocetes (see below), it is highly likely that basilosaurids, toothed mysticetes and eomysticetids also received sound in the same manner as odontocetes, i.e. sound entering through the acoustic fat pad in the enlarged mandibular foramen and travelling to the inner ear via the middle ear auditory ossicles. The plesiomorphic condition in the mysticete basicranium is: 1) pterygoid sinus fossa reasonably well excavated; 2) pterygoid sinus fossa bound by dorsal, medial and lateral laminae and/or alisphenoid; 3) bullar processes clearly separate from basioccipital crest; 4) short anterior and posterior processes of the tympanoperiotic; 5) lateral edges of periotic free from/ make minor contact with squamosal; 6) ventral opening of the anteroexternal sulcus present; 7) foramen pseudovale at same level as tympanoperiotic. This condition was retained in mysticetes until the evolution of crown Mysticeti.

Toothed mysticetes and eomysticetids to modern mysticetes

In contrast to the generalised morphology seen in toothed mysticete and eomysticetid basicrania, a greater number of changes in the basicranium have occurred following the divergence of crown mysticetes (Fig 4.18). Although some changes are more likely related to

changes in feeding ecology, e.g. the pterygoid hamuli becoming widely separated, most

changes in the basicranium appear to be related to hearing. These hearing related changes can

be seen to have two main effects: (1) to cause the pterygoid sinus to become more enclosed

by bone; and (2) to increase the degree of contact of the tympanoperiotic bones with each

other and the rest of the skull. The first effect is driven by the anterior expansion of the

pterygoid sinus within the pterygoid and the development of an inferior lamina of the

pterygoid. In mammalodontids and aetiocetids, the pterygoid sinus fossa accounts for a

relatively small proportion of the pterygoid. In living mysticetes, essentially the entire

pterygoid has been excavated by the pterygoid sinus fossa, expanding both anteriorly and

dorsoventrally, with the most extreme state seen in balaenopterids (Fraser & Purves, 1960).

The sinus is also floored to some extent by an inferior lamina of the pterygoid or a

broadening of the pterygoid hamuli expanded into a dorsoventrally flattened plate flooring

the pterygoid sinus fossa as seen in balaenids. Functionally, the increased amount of bone

around the pterygoid sinus provides a 'buttress' that allows changes in the volume of the gas

filled sinus to be compensated for by corresponding changes in the adjacent soft tissues with

an incursion of blood (Fraser & Purves, 1960; Costidis & Rommel, 2012). This adaptation

could influence what range of frequencies can reach the tympanoperiotic complex and

therefore be heard. This idea is corroborated by Cranford & Krysl (2015) who state that the

most important function for sinuses around the tympanoperiotic complex may be to maintain

sufficient air volume in the tympanic cavity around the ossicular chain to allow the ossicles to

vibrate free of damping or interference by nearby soft tissues.
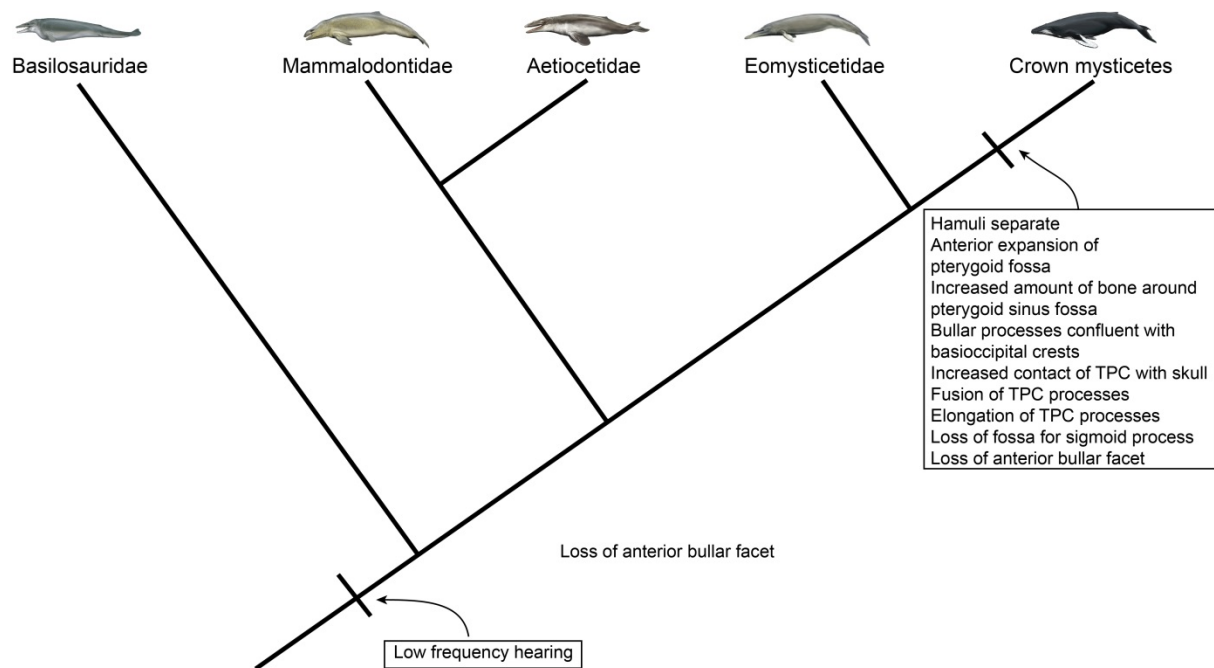
Figure 4.18. Cladogram showing where features relevant to hearing in mysticetes first appeared. Note high degree of changes in crown mysticete relative to stem mysticetes.

In contrast, the increased contact between the tympanic bulla, periotic and the rest of the skull is driven by fusion and elongation of elements. The posterior processes of the periotic and tympanic bulla are completely fused in adult modern mysticetes (Geisler & Luo, 1996; Luo 1998), whereas in toothed mysticetes and eomysticetids these two processes are tightly sutured instead (Marx & Fordyce 2015). This fusion is accompanied by an extreme elongation of the compound posterior process, wedging tightly between the squamosal and exoccipital, something not seen in the relatively short posterior processes of toothed mysticetes and eomysticetids. Similarly, the anterior processes of the periotic and tympanic bulla are fused in modern mysticetes via the anterior pedicle, between the squamosal and the pterygoid. These processes also show elongation relative to those of toothed mysticetes and eomysticetids but it is not as pronounced as that of the compound posterior process. Modern mysticetes have lost the articulation point between the sigmoid process of the tympanic bulla and the squamosal. This may have been a necessary prerequisite for the rotation of the tympanic bullae seen in rorquals, which has been hypothesised to have been a result of their

lunge-feeding behaviour (Yamato & Pyenson 2015). However, what degree of contact existed i.e. whether there was direct bone-to-bone contact, ligamentous contact or just soft tissue between the two is unclear. Nevertheless the increase in contact via the anterior process, lateral tuberosity and especially the posterior process is greater than any loss in contact between the tympanoperiotic and the skull due to the loss of the fossa for the sigmoid process.

These data are suggestive of a change in how sound reaches the inner ear of mysticetes. The ancestral pathway using acoustic fats requires the earbones to be acoustically isolated from the rest of the basicranium, a trend that is reversed in mysticete evolution. Alternative pathways for sounds to reach the inner ear are discussed in the proceeding sections.

4.5. Bone conduction and the auditory pathway in mysticetes

The exact path by which sound reaches the inner ear in mysticetes remains uncertain (Mooney *et al.*, 2012; Yamato & Pyenson, 2015). Recent research by Yamato *et al.* (2012) identified a large body of fat in the minke whale (*Balaenoptera acutorostrata*) that inserts into the tympanoperiotic complex and hypothesised it to be a lateral sound reception pathway. Preliminary investigations also indicate that these fats are also present in humpback and fin whales (Yamato *et al.*, 2012) and Yamada (1953) reported similar tissues in blue, sei and fin whales, indicating that they are likely present in all balaenopterids.

An alternative pathway was presented by Cranford & Krysl (2015), where finite element analysis (FEA) of a small fin whale head revealed that the predominant mechanism by which the tympanoperiotic complex is excited is skull-vibration-enabled bone conduction. Mysticetes that use this mechanism are able to use their skulls to pass the vibrations from soundwaves of much longer wavelength (i.e. lower frequency) sounds to the tympanoperiotic complex than would be possible if they were using a smaller detecting structure, such as an

acoustic fat pad in the mandible. Further evidence for this mechanism comes from the internal morphology of the fin whale skull. They found a series of dense bony ossifications within the squamosal that appear to fan out from the junction with the adjacent periotic portion of each tympanoperiotic complex. These may function to anchor or extend and reinforce the connection between the tympanoperiotic complex and the rest of the skull (Cranford & Krysl, 2015: Fig 2 & Fig 3), creating a preferential pathway for skull vibrations to travel into the inner ear.

The patterns of mysticete basicranial evolution I described in the preceding section add weight to this hypothesis. The enlarged pterygoid sinus seen in modern mysticetes could prevent interference of vibration of the middle ear bones by nearby tissues. Additionally, both Lillie (1915) and Yamato et al. (2012) have described a thick layer of collagenous padding around much of the tympanic bulla which would also aid in prevention of interference. Fleischer (1976) also discussed the impedance mismatch barrier of bone and soft tissue. The fusion seen in the tympanoperiotic complex and the extremely enlarged processes wedged tightly to the skull next to the dense bony anchors are ubiquitous across all modern mysticetes (Lillie 2010; Nummela et al. 2007) highlighting their importance in modern mysticete hearing and would favour conduction of sound to the inner ear. Exactly when bone conduction was first exploited by mysticetes remains an open question, but a potential method of shedding light on this would be to CT scan other modern and fossil mysticete squamosals to check for the presence of the bony anchors found in the fin whale. It should also be noted that although bone conduction appears to be the primary means of detecting sound in modern mysticetes, a secondary pathway using the lateral ear fats described by Yamato et al. (2012) is also in use (i.e. the 'pressure mechanism' of Cranford & Krysl (2015)). This secondary pathway is speculated to be used for higher frequencies (Yamato & Pyenson 2015).

4.6. The Role of the Mandible in Mysticete Hearing

Another aspect of mysticete hearing that requires discussion in light of the findings presented here is how the role of the mandible, or more precisely the acoustic fat pad located in the mandibular foramen, has changed over time. Recent mysticetes possess a greatly reduced mandibular foramen (Marx *et al*., 2016) (Fig 4.19), whereas basilosaurids, toothed mysticetes and eomysticetids retained an enlarged foramen that presumably housed a substantial mandibular fat pad (Fitzgerald 2006; Martínez-Cáceres & Muizon, 2011; Okazkai 2012).

This would suggest that in the latter fossil taxa, sounds reached the inner ear by travelling through these acoustic fats, as occurs in living odontocetes (Cranford *et al.*, 2008), and did not use bone conduction. However, there are both cetotheriids (Bisconti 2006) and stem-balaenopteroids (Lydekker 1894; Kellogg 1924,1968,1969; Roth 1978; Kimura et al. 1998; Yoshida et al. 2003; Otsuka & Ota 2008; Steeman 2009; Bisconti et al. 2013) that also possess an enlarged mandibular foramen, indicating that reduction of the mandibular foramen has occurred convergently in crown mysticete evolution. If the reduction of the mandibular foramen was a direct correlate of bone conduction then it could imply that bone conduction has also evolved on several occasions within Mysticeti. Yet, this seems unlikely because modern mysticetes have both bone and acoustic fat conduction pathways that are employed simultaneously (Cranford & Krysl, 2015). Instead, I consider it more parsimonious that the reduction of the mandibular foramen represents the point in those mysticete lineages that bone conduction became the dominant auditory pathway, and potentially when those clades became capable of detecting infrasonic frequencies.
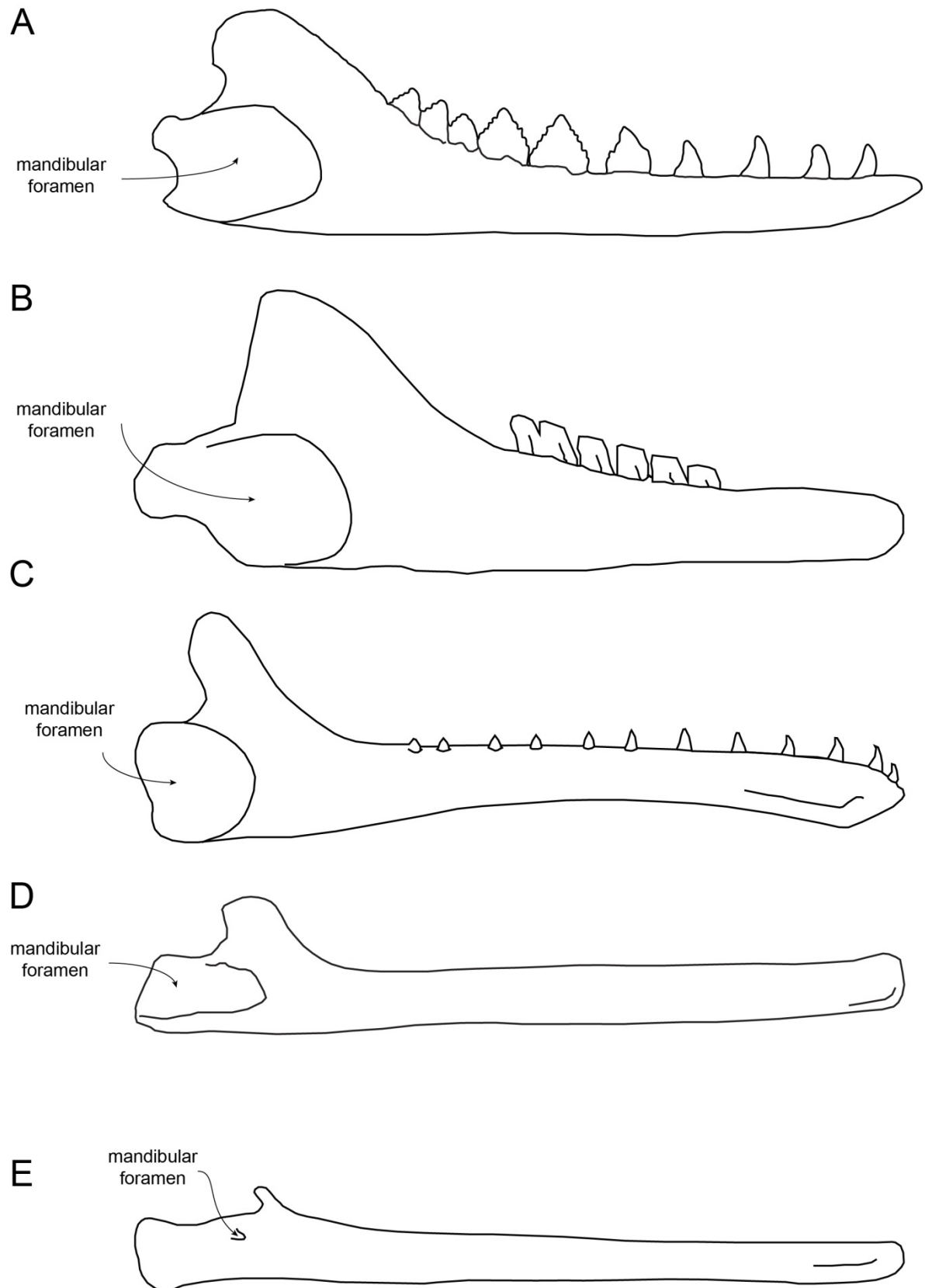
Figure 4.19. Reconstructed mandibles of a basilosaurid, basal mysticetes and a modern mysticete in left medial view, showing changes in shape during mysticete evolution. Mandibles are scaled to the same length. Where necessary, right mandibles have been reflected to aid comparison. A, *Cynthiacetus peruvianus* (modified from Martínez-Cáceres & Muizon (2011); B, *Mammalodon colliveri* (modified from Fitzgerald (2010)); C, *Aetiocetus weltoni* (modified from Deméré & Berta (2008)); D, *Yamatocetus canaliculatus*; E, *Balaenoptera bonaerensis*.

4.7. Conclusions

There appear to be three functional complexes within the basicranium that inform understanding of underwater hearing specialization in mysticetes: (1) degree of bony contact between tympanoperiotic and the surrounding basicranium; (2) development of the pterygoid sinus system; and (3) aspects of the zygomatic process of squamosal and glenoid region (i.e. bone conduction versus acoustic lipid conduction).

Description and comparison of the basicrania of representative species of basilosaurid, aetiocetid, mammalodontid, eomysticetids, balaenids, cetotheriid and balaenopterid reveals that toothed mysticetes and eomysticetids retain the plesiomorphic basicranial morphology seen in basilosaurids, consistent with similarities between the cochleae of basilosaurids and stem mysticetes (Ekdale & Racicot, 2015; Park et al. 2017). Toothed mysticetes and eomysticetids therefore shared the same auditory pathway as basilosaurids, where sounds entered through the gular region (Cranford et al. 2008) and were transmitted to the middle and inner ear via the acoustic fat pad in the enlarged mandibular foramen. Modern mysticetes on the other hand display substantial changes in their basicranial morphology that are indicative of a switch to using bone conduction as the primary method of directing sounds to the middle and inner ear, although a secondary pathway incorporating acoustic fats is also employed.

The switch to bone conduction enabled mysticetes to detect even lower frequencies than was previously possible. This would have rendered the mandibular fat pad redundant and could have driven the convergent reduction of the mandibular foramen seen in all living lineages of mysticete. Bone conduction could potentially be the evolutionary innovation that enabled mysticetes to detect infrasonic frequencies.

Future work should aim to identify in finer temporal and phylogenetic resolution when the key morphological changes associated with bone conduction (e.g. extreme

elongation of tympanoperiotic processes) first occurred and if these changes have evolved once or in multiple lineages. Potential drivers of the switch to bone conduction should also be explored, such as did the need for long distance communication in migrating species of mysticete play a role?

Acknowledgements

References

Bisconti M. 2006. *Titanocetus*, a new baleen whale from the Middle Miocene of northern Italy (Mammalia, Cetacea, Mysticeti). Journal of Vertebrate Paleontology 26, 344–354.

Bisconti M, Lambert O, Bosselaers M. 2013. Taxonomic revision of *Isocetus depauwi* (Mammalia, Cetacea, Mysticeti) and the phylogenetic relationships of archaic cetothere mysticetes. Palaeontology 56, 95–127.

Boessenecker RW, Fordyce RE. 2015. Anatomy, feeding ecology, and ontogeny of a transitional baleen whale: a new genus and species of Eomysticetidae (Mammalia: Cetacea) from the Oligocene of New Zealand. PeerJ 3, e1129.

Boessenecker RW, Fordyce RE. 2016. A new eomysticetid from the Oligocene Kokoamu Greensand of New Zealand and a review of the Eomysticetidae (Mammalia, Cetacea). Journal of Systematic Palaeontology http://dx.doi.org/10.1080/14772019.2016.1191045.

Churchill M, Martínez-Cáceres M, de Muizon C, Mnieckowski J, Geisler JH. 2016. The Origin of High-Frequency Hearing in Whales. Current Biology http://dx.doi.org/10.1016/j.cub.2016.06.004.

Costidis A, Rommel SA. 2012. Vascularization of Air Sinuses and Fat Bodies in the Head of the Bottlenose Dolphin (*Tursiops truncatus*): Morphological Implications on Physiology. Frontiers in Physiology 3, 243.

Cranford TW, Krysl P, Hildebrand JA. 2008. Acoustic pathways revealed: simulated sound transmission and reception in Cuvier's beaked whale (*Ziphius cavirostris*). Bioinspiration & biomimetics 3, 016001.

Cranford TW, Krysl P. 2015. Fin Whale Sound Reception Mechanisms: Skull Vibration Enables Low-Frequency Hearing. PLoS ONE 10, e0116222.

Deméré TA, Berta A. 2008. Skull anatomy of the Oligocene toothed mysticete *Aetiocetus weltoni* (Mammalia; Cetacea): implications for mysticete evolution and functional anatomy. Zoological Journal of the Linnean Society 154, 308–352.

Ekdale EG. 2016. Morphological diversity among the inner ears of extinct and extant baleen whales (Cetacea: Mysticeti). Journal of Morphology 277, 1599–1615.

Ekdale EG, Racicot RA. 2015. Anatomical evidence for low frequency sensitivity in an archaeocete whale: comparison of the inner ear of *Zygorhiza kochii* with that of crown Mysticeti. Journal of Anatomy 226, 22–39.

Ekdale EG, Berta A, Deméré TA. 2011. The Comparative Osteology of the Petrotympanic Complex (Ear Region) of Extant Baleen Whales (Cetacea: Mysticeti). PLoS ONE 6, e21311.

Evans, HE. 1993. The ear. In Evans HE, ed, Miller's Anatomy of the Dog, (3rd ed). Saunders, Philadelphia, pp. 988–1008.

Fitzgerald EMG. 2006. A bizarre new toothed mysticete (Cetacea) from Australia and the early evolution of baleen whales. Proceedings of the Royal Society B: Biological Sciences 273, 2955–2963.

Fitzgerald EMG. 2010. The morphology and systematics of *Mammalodon colliveri* (Cetacea: Mysticeti), a toothed mysticete from the Oligocene of Australia. Zoological Journal of the Linnean Society 158, 572–367.

Fleischer G. 1976. Hearing in extinct cetaceans as determined by cochlear structure. Journal of Paleontology 50, 133–152.

Fleischer G. 1976. Über Beziehungen zwischen Hörvermögen und Schädelbau bei Walen. Säugetierkundliche Mitteilungen 24, 48–59.

Fordyce RE. 1994. *Waipatia maerewhenua*, new genus and new species (Waipatiidae, new Family), an archaic Late Oligocene dolphin (Cetacea: Odontoceti: Platanistoidea)

from New Zealand. In Berta A, Deméré TA, eds, Contributions in marine mammal paleontology honoring Frank C. Whitmore, Jr. Proceedings of the San Diego Society of Natural History 29, 147–176.

Fordyce RE. 2009. Neoceti. In Perrin WF, Wursig B, eds, Encyclopaedia of Marine Mammals (2nd ed), Academic Press, London, pp. 758–763.

Fordyce RE, Marx FG. 2013. The pygmy right whale *Caperea marginata*: the last of the cetotheres. Proceedings of the Royal Society London B: Biological Sciences 280, 20122645.

Fraas E. 1904. Neue Zeuglodonten aus dem unteren Mitteleociin vom Mokattam bei Cairo. Geologische und Palaontologische Abhandlungen, Jena, Neue Folge, 6, 197– 220.

Fraser FC, Purves PE. 1960. Hearing in cetaceans: Evolution of the accessory air sacs and the structure of the outer and middle ear in Recent cetaceans. Bulletin of the British Museum (Natural History), Zoology 7, 1–140.

Geisler JH, Sanders AE. 2003. Morphological evidence for the phylogeny of Cetacea. Journal of Mammalian Evolution 10, 23–129.

Geisler JH, Godfrey SJ, Lambert O. 2012. A new genus and species of late Miocene inioid (Cetacea, Odontoceti) from the Meherrin River, North Carolina, USA. Journal of Vertebrate Paleontology 32, 198–211.

Heyning JE. 1989. Comparative facial anatomy of beaked whales (Ziphiidae) and a systematic revision among the families of extant Odontoceti. Contributions in Science, Natural History Museum of Los Angeles County 405, 1–64.

Hooker SK. 2009. Toothed Whales, Overview. In Perrin WF, Wursig B, eds, Encyclopaedia of Marine Mammals (2nd ed), Academic Press, London, pp. 1173–1179.

Kasuya T. 1973. Systematic consideration of recent toothed whales based on morphology of tympanoperiotic bone. Scientific Reports of the Whale Research Institute, Tokyo, 25, 1–103.

Kellogg AR. 1924. Description of a new genus and species of whalebone whale from the Calvert Cliffs, Maryland. Proceedings of the United States National Museum 63, 1–14.

Kellogg R. 1928. The history of whales—Their adaptation to life in the water (concluded). The Quarterly Review of Biology 3, 174–208.

Kellogg AR. 1936. A review of the Archaeoceti. Carnegie Institution of Washington Publication 482, 1–366.

Kellogg AR. 1968. Fossil marine mammals from the Miocene Calvert Formation of Maryland and Virginia: Part 6. A hitherto unrecognized Calvert cetothere. United States National Museum Bulletin 247, 133–161.

Kellogg AR. 1969. Cetothere skeletons from the Miocene Choptank Formation of Maryland and Virginia. United States National Museum Bulletin 294, 1–40.

Kimura T, Sakamoto O, Hasegawa Y. 1998. A cetothere from the Miocene Chichibumachi Group, Saitama Prefecture, Japan. Bulletin of Saitama Museum of Natural History 16, 1–13.

Lillie DG. 1910. Observations on the anatomy and general biology of some members of the larger Cetacea. Proceedings of the Zoological Society of London 1910, 769–792.

Lillie DG. 1915. Cetacea. In, British Antarctic ("Terra Nova") Expedition, 1910. Natural History Report Zoology British Museum (Natural History), London 3, 85–124.

Lilljeborg W. 1861. Hvalben funna i jorden på Gräsön I Roslagen i Sverige. Forhandlinger ved de Skandinaviske Naturforskeres, Ottende Møde 8, 599–616.

Luo Z. 1998. Homology and transformation of cetacean ectotympanic structures. In, Thewissen JGM, ed. The emergence of whales. New York, Plenum Press, 269–301.

Luo Z, Gingerich PD. 1999. Terrestrial Mesonychia to aquatic Cetacea: transformations of the basicranium and evolution of hearing in whales. University of Michigan Papers on Paleontology 31, 1–98.

Lydekker R. 1894. Cetacean skulls from Patagonia. Anales del Museo de la Plata 2, 1–13.

MacPhee RD. 1981. Auditory regions of primates and eutherian insectivores. Contributions to Paleobiology 18, 1–282.

Martínez-Cáceres M, de Muizon C. 2011. A new basilosaurid (Cetacea, Pelagiceti) from the late Eocene to early Oligocene Otuma Formation of Peru. Comptes Rendus Palevol 10, 517–26.

Marx FG, Fordyce RE. 2015. Baleen boom and bust: a synthesis of mysticete phylogeny, diversity and disparity. Royal Society Open Science 2, 140434.

Marx FG, Fordyce RE. 2016. A link no longer missing: New evidence for the cetotheriid affinities of *Caperea*. PLoS ONE 11, e0164059.

Marx FG, Tsai C-H, Fordyce RE. 2015. A new Early Oligocene toothed 'baleen' whale (Mysticeti: Aetiocetidae) from western North America: one of the oldest and the smallest. Royal Society Open Science 2, 150476.

Marx FG, Bosselaers MEJ, Louwye S. 2016. A new species of *Metopocetus* (Cetacea, Mysticeti, Cetotheriidae) from the Late Miocene of the Netherlands. PeerJ 4, e1572.

Mead JG, Fordyce RE. 2009. The therian skull: a lexicon with emphasis on the odontocetes. Smithsonian Contributions to Zoology 627, 1–248.

Miller GS Jr. 1923. The telescoping of the cetacean skull. Smithsonian Miscellaneous Collections 76, 1–70.

Mooney TA, Yamato M, Branstetter BK. 2012. Hearing in cetaceans: from natural history to experimental biology. Advances in Marine Biology 63, 197–246.

Muller, J. 1954. Observations on the orbital region of the skull of the Mystacoceti. Zoologische Mededelingen (Leiden) 32, 279–290.

Norris KS. 1968. The evolution of acoustic mechanisms in odontocete cetaceans. In Drake ET, ed, Evolution and environment, Yale University Press, New Haven, pp. 297–324.

Nummela S, Thewissen JG, Bajpai S, Hussain ST, Kumar K. 2004. Eocene evolution of whale hearing. Nature 430, 776–8.

Nummela S, Hussain ST, Thewissen JG. 2006. Cranial anatomy of Pakicetidae (Cetacea, Mammalia). Journal of Vertebrate Paleontology 26, 746–59.

Nummela S, Thewissen JG, Bajpai S, Hussain T, Kumar K. 2007. Sound transmission in archaic and modern whales: anatomical adaptations for underwater hearing. The Anatomical Record 290, 716–33.

Okazaki Y. 2012. A new mysticete from the upper Oligocene Ashiya Group, Kyushu, Japan and its significance to mysticete evolution. Bulletin of the Kitakyushu Museum of Natural History and Human History Series A: Natural History 10, 129–152.

Otsuka H, Ota Y. 2008. Cetotheres from the early Middle Miocene Bihoku Group in Shobara District, Hiroshima Prefecture, West Japan. Miscellaneous Reports of Hiwa Museum of Natural History 49, 1–66.

Park T, Fitzgerald EMG, Gallagher SJ, Evans AR. 2017. Low frequency hearing preceded the evolution of giant body size and filter feeding in baleen whales. Proceedings of the Royal Society B: Biological Sciences 284, 20162528.

Perrin WE. 1975. Variation of spotted and spinner porpoise (genus *Stenella*) in the eastern tropical Pacific and Hawaii. Bulletin of the Scripps Institution of Oceanography 21, 1–206.

Pompeckj JF. 1922. Das Ohrskelett von Zeuglodon. Senckenbergiana, 4, 44–100.

Ridewood WG. 1922. Observations on the skull in foetal specimens of whales of the genera *Megaptera* and *Balaenoptera*. Philosophical Transactions of the Royal Society of London. Series B, Containing Papers of a Biological Character 211, 209–272.

Roth F. 1978. *Mesocetus argillarius* sp.n. (Cetacea, Mysticeti) from Upper Miocene of Denmark, with Remarks on the Lower Jaw and t,he Echolocation System in Whale Phylogeny.

Sanders AE, Barnes LG. 2002a. Paleontology of the Late Oligocene Ashley and Chandler Bridge Formations of South Carolina, 3: Eomysticetidae, a new family of primitive mysticetes (Mammalia: Cetacea). In Emry RJ, ed, Cenozoic mammals of land and sea: tributes to the career of Clayton E. Ray. Smithsonian Contributions to Paleobiology 93, 313–356.

Sanders AE, Barnes LG. 2002b. Paleontology of the Late Oligocene Ashley and Chandler Bridge Formations of South Carolina, 2: *Micromysticetus rothauseni*, a primitive cetotheriid mysticete (Mammalia: Cetacea). In Emry RJ, ed. Cenozoic mammals of land and sea: tributes to the career of Clayton E. Ray. Smithsonian Contributions to Paleobiology 93, 271–293.

Steeman ME. 2009. A new baleen whale from the Late Miocene of Denmark and early mysticete hearing. Palaeontology 52, 1169–1190.

Uhen MD. 2004. Form, function, and anatomy of *Dorudon atrox* (Mammalia, Cetacea): an archaeocete from the Middle to Late Eocene of Egypt. University of Michigan Papers on Paleontology 34, 1–222.

Uhen MD. 2010. The origin(s) of whales. Annual Review of Earth and Planetary Sciences 38, 189–219.

Van Kampen PN. 1905. Die Tympanalgegend des Säugetierschädels. Morphologisches Jahrbuch 34, 1–6.

Wartzok D, Ketten DR. 1999. Marine mammal sensory systems. In, Reynolds JE, Rommel SE, eds, Biology of marine mammals. Washington, D.C, Smithsonian Institution Press, 117–175.

Yamato M, Pyenson ND. 2015. Early development and orientation of the acoustic funnel provides insight into the evolution of sound reception pathways in cetaceans. PLoS ONE 10, e0118582.

Yamada MU. 1953. Contribution to the anatomy of the organ of hearing of whales. Scientific Reports of the Whales Research Institute 8, 1–79.

Yamato M, Ketten DR, Arruda J, Cramer S, Moore K. The auditory anatomy of the minke whale (*Balaenoptera acutorostrata*): a potential fatty sound reception pathway in a baleen whale. The Anatomical Record 295, 991–8.

Yoshida K, Kimura T, Hasegawa Y. 2003. New cetothere (Cetacea: Mysticeti) from the Miocene Chichibumachi Group, Japan. Bulletin of Saitama Museum of Natural History 20-21, 1–10.

5. Shape Analysis of Odontocete Mandibles: Correlations between morphology and hearing abilities

Travis Park[1,2], Alistair R. Evans[1,2], and Erich M. G. Fitzgerald[2,3,4]

[1]School of Biological Sciences, Monash University, Australia.

[2]Geosciences, Museums Victoria, Melbourne, Australia.

[3] Department of Vertebrate Zoology, National Museum of Natural History, Smithsonian Institution, Washington, DC, USA.

[4]Department of Life Sciences, Natural History Museum, London, UK.

Abstract

Odontocetes possess mandibles that play a crucial role in both feeding and hearing. Although the influence of feeding on mandibular shape has been quantified, the influence of different species' sensitivity to specific sound frequencies has yet to be determined. Here I use 3D geometric morphometrics to quantify mandibular shape of a sample of odontocete mandibles from 12 different species. The results of this analysis were then correlated with published frequency ranges for sampled species. The frequencies an odontocete species can hear were found to have only a minor relationship to mandible shape, primarily affecting the size and shape of the mandibular foramen, which houses the acoustically-linked mandibular fat pad. Additional odontocete audiograms and analyses that incorporate the effects of absolute size are required to further expand on the findings presented here.

5.1. Introduction

The mandibles of the two living cetacean groups, the baleen whales (mysticetes) and the toothed whales (odontocetes) are distinctly different. Mysticetes lack teeth in their jaws, instead using their signature innovation, baleen, to filter large amounts of small prey from the

water. Toothed whales, on the other, hand possess teeth in their jaws. However, the mandible of toothed stem mysticetes was more similar to living odontocetes than crown mysticetes, possessing features such as teeth and an expanded mandibular foramen. Given these striking similarities, a better understanding of how the morphology of the odontocete mandible reflects competing demands of acoustic/feeding function may provide a basis for interpreting functional significance of evolutionary transformation in the mysticete mandible.

Uniquely amongst mammals, odontocetes initially receive incoming sounds via a specialised fat pad that is housed in the massively expanded mandibular foramen at the posterior end of the jaw (Nummela et al. 2007). Competing (but not necessarily mutually exclusive) theories debate whether sound reaches this fat pad through the thin lateral mandibular wall i.e. the acoustic window hypothesis (Norris 1968) or through the gular region (Cranford et al. 2008). The dual function of the odontocete jaw in both hearing and feeding signifies there are competing demands shaping its overall anatomy. The feeding styles of odontocetes produce clear differences in their mandibles; for example, odontocetes that are specialist suction feeders tend to be edentulous/ have reduced dentition and possess wider, more bluntly shaped mandibles, whereas raptorial taxa tend to have a well-developed dentition and narrow jaws (Werth 2006).

The fact that sound first enters the auditory pathway via the mandible in odontocetes suggests that hearing adaptations may also influence mandibular morphology. It has been suggested that odontocetes with particular acoustic abilities have particular morphologies of the pars cochlearis (Gutstein et al. 2014). Do other parts of the odontocete auditory pathway (e.g. the mandible) also reflect what frequencies that animal is sensitive to? In this study I employ quantitative analytical techniques and statistical methods to investigate whether the shape of the mandible in odontocetes is influenced by their hearing abilities. If a relationship were found in modern odontocetes who have published frequency ranges, then these data

could theoretically be used to estimate the frequency ranges in fossil taxa, including toothed mysticetes.

5.2. Materials and Methods

Data collection – A total of 12 species representing six families were used in this study. To ensure correlations between mandible shape and frequency ranges were as unambiguous as possible only taxa that have previously established audiograms were used (table 5.1). Mandibles were examined from four museums: Museums Victoria, Melbourne (NMV); Australian Museum, Sydney (AM); Smithsonian Institution National Museum of Natural History, Washington DC (USNM). Three-dimensional shape data was gathered by scanning the mandibles using X-ray computed tomography (CT). Raw data from these scans were then used to create three-dimensional models of the mandibles using AVIZO (v. 9.1.0 Standard) (Visualisation Sciences Group – a FEI Company, 2013) (Fig 5.1).

Table 5.1. Taxa and specimens used in this study, measurements and frequency data. BCW, mandibular bicondylar width; MF, mandibular foramen; ML, mandible length; S#, specimen number SL, symphysis length; Vol., volume.

Taxon	S#	ML (mm)	SL (mm)	BCW	MF Area (mm^2)	Vol. (mm^3)	Min freq (kHz)	Max freq (kHz)	Mean freq (kHz)	Freq range (kHz)	Frequency source data
Delphinapterus leucas	USNM 291204	464	67	277	7878	162905	8	128	68	120	Klishin et al. (2000)
Feresa attenuata	USNM 593894	264	28	188	2196	34993	5	120	63	115	Montie et al. (2011)
Grampus griseus	NMVC 10924	418	62	318	8535	181237	4	150	77	146	Nachtigall et al. (2005)
Inia geoffrensis	USNM 395614	355	181	18	2719	19893	1	105	53	104	Jacobs & Hall (1972)
Lagenorhynchus obliquidens	USNM 290642	313	25	154	2350	29650	0.3	140	70	140	Ketten (2000)
Lipotes vexillifer	USNM 218293	466	226	191	4524	42606	1	200	101	199	Wang et al. (1992)
Mesoplodon densirostris	NMVC 36362	692	195	299	9948	281372	5.6	160	83	154	Pacini et al. (2011)
Orcinus orca	AMM 22839	528	127	337	11422	338514	4	100	52	96	Szymanski et al. (1999)
Phocoena phocoena	NMVC 24749	208	23	121	2090	17821	1	150	76	149	Andersen (1970)
Pseudorca crassidens	AMM 33594	462	84	340	9298	174114	4	45	25	41	Yuen et al. (2005)
Steno bredanensis	NMVC 25028	428	121	207	4281	49483	10	120	65	110	Mann et al. (2010)
Tursiops truncatus	AMM 28255	439	53	170	6717	89239	10	150	80	140	Houser & Finneran (2006)
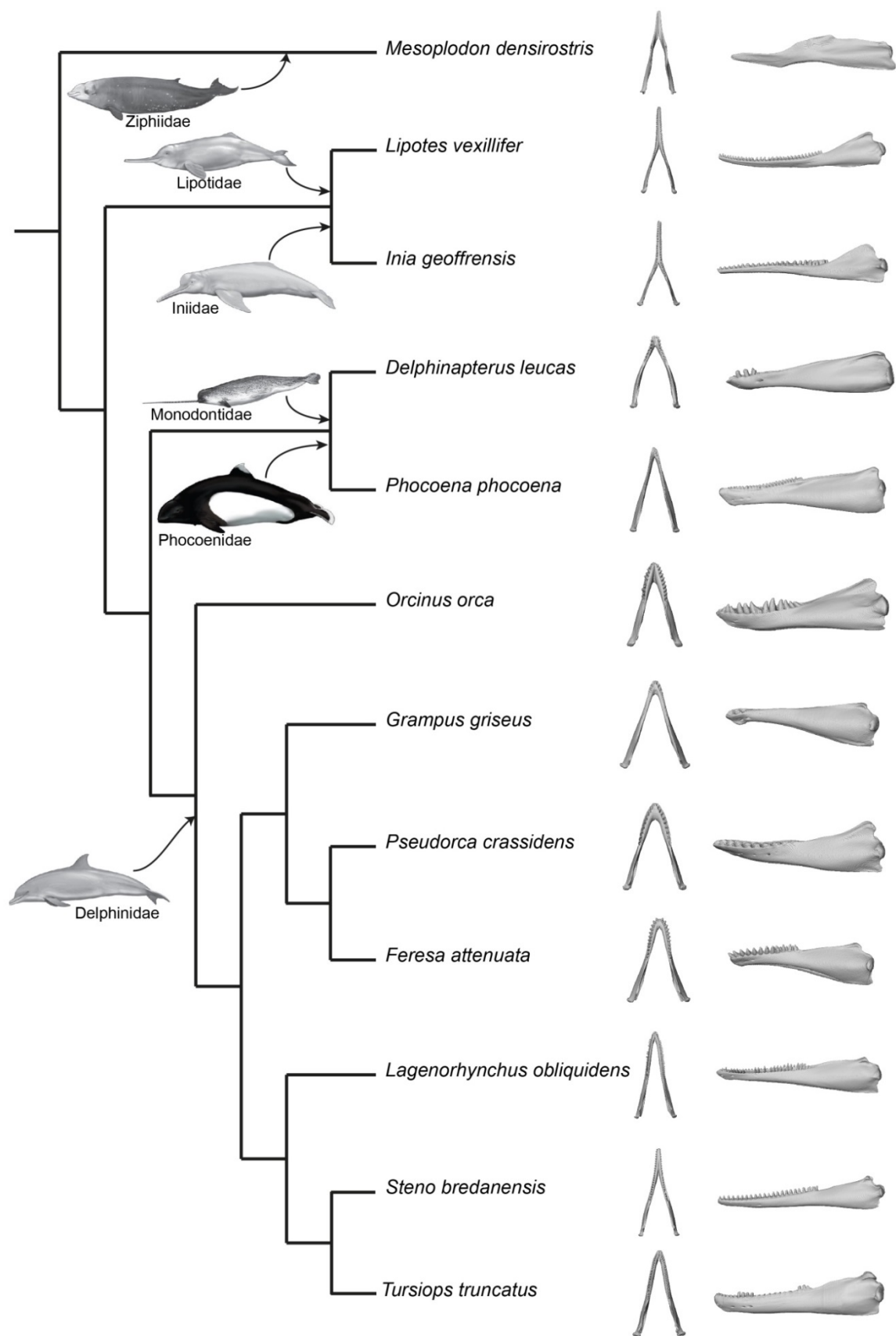
Fig 5.1. Phylogenetic position of specimens used in this study, according to the phylogeny of Steeman et al. (2009) and the 3D models of their mandibles in dorsal and lateral views. Illustrations are by Carl Buell, used with permission.

119

Geometric morphometric analysis – A total of 82 landmarks were identified for each

specimen and the three-dimensional coordinates (x, y and z) were recorded. 42 of the

landmarks were fixed in addition to 2 curves each containing 20 landmarks. The curves were

placed along the outline of the mandibular foramen beginning and ending at a point equal to

90% of the total length of the mandible (see table 2 and Fig 5.2 for landmark locations).

Landmarks were placed in the 3D CAD software package Rhino (Robert McNeel &

Associates 2015). The landmark coordinates were exported as a points file, then manually

reformatted as a morphologika file (O'Higgins & Jones 2006). The statistical programming

language and environment R (R Core Team 2015) was used to perform Procrustes

superimposition and principle component analysis, via the geomorph package version 3.0.1

(Adams et al. 2016). Three separate geometric morphometric analyses were run using subsets

of these landmarks: (1) both mandibles; (2) an isolated mandible only (digitally separated);

and (3) the mandibular foramen only.
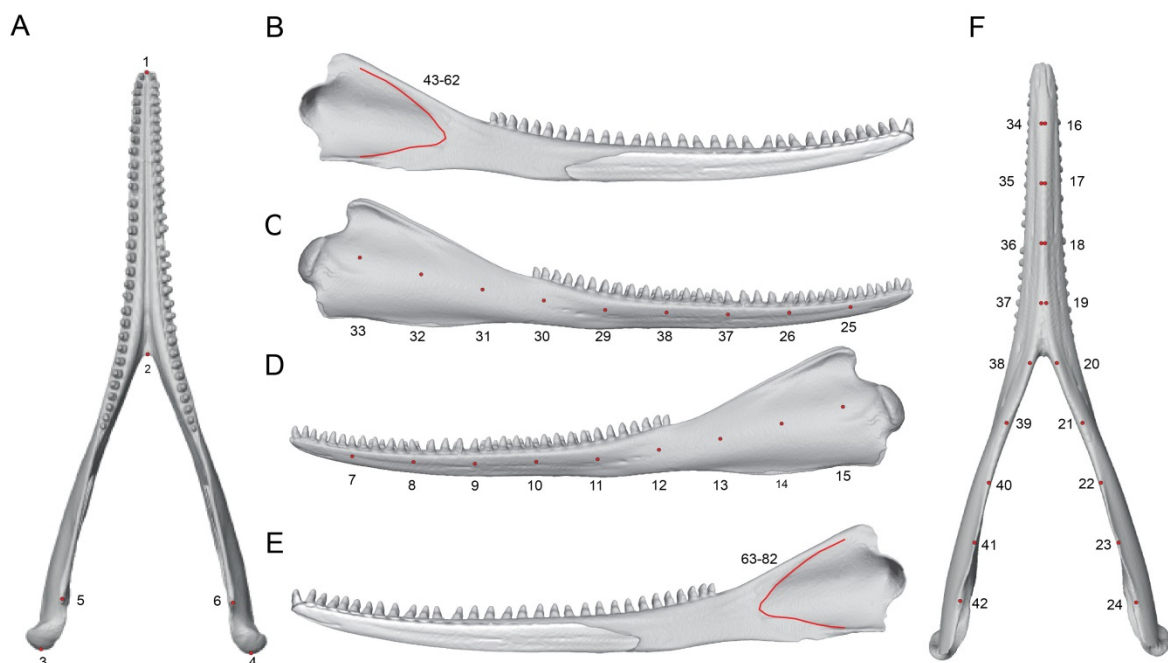
Fig 5.2. Positions of the landmarks used in this study. A, dorsal view; B, medial view; C, lateral view; D, ventral view. Schematic drawings based on outputs from the geomorph package and showing extremes in mandibular features of that principal component.

Statistical analysis – Regressions were performed to test for a relationship between the results of the shape analysis and the frequency ranges the animals could hear. To account for the fact that species data points are non-independent as a result of shared ancestry (Symonds & Blomberg 2014), the phylogenetic comparative method of phylogenetic generalised least squares (PGLS) (Grafen 1989; Martins & Hansen 1997; Pagel 1997,1999; Rohlf 2001) was used. The R package caper version 0.5.2 (Orme et al. 2013) was used for all PGLS analyses, regressing the first five principal components, mandible length, symphysis length, bicondylar width, mandibular foramen area and minimum mandibular foramen volume against maximum, minimum and mean frequency values for each species. PGLS requires a phylogenetic tree; the supermatrix of Steeman et al. (2009) was chosen as the phylogenetic tree for the PGLS as it contained all taxa analysed in this study. Due to the small sample size, the value of the scaling parameter lambda (λ) was changed to one and then compared with the results of the same analysis when the maximum likelihood ratio was used for λ. Frequency was considered to have significant effect on mandible shape if the value of the overall model was significant at a level of <0.05. To enhance visualisation of the relationship between the variables, the PC data were log transformed prior to the PGLS regressions being performed.

Table 5.2. Landmarks for the analysis of both mandibles. SSL, sliding semi-landmark.

Landmark no.	Landmark	Landmark no.	Landmark
1	Anterior point of mandibular symphysis	42	90% total length ventral (right)
2	Posterior point of mandibular symphysis	43	Left SSL 1
3	Posterior point of left mandibular condyle	44	Left SSL 2
4	Posterior point of right mandibular condyle	45	Left SSL 3
5	Dorsal point of left coronoid process	46	Left SSL 4
6	Dorsal point of right coronoid process	47	Left SSL 5
7	10% total length 50% height medial (left)	48	Left SSL 6
8	20% total length 50% height medial (left)	49	Left SSL 7
9	30% total length 50% height medial (left)	50	Left SSL 8
10	40% total length 50% height medial (left)	51	Left SSL 9
11	50% total length 50% height medial (left)	52	Left SSL 10
12	60% total length 50% height medial (left)	53	Left SSL 11
13	70% total length 50% height medial (left)	54	Left SSL 12
14	80% total length 50% height medial (left)	55	Left SSL 13
15	90% total length 50% height medial (left)	56	Left SSL 14
16	10% total length ventral (left)	57	Left SSL 15
17	20% total length ventral (left)	58	Left SSL 16
18	30% total length ventral (left)	59	Left SSL 17
19	40% total length ventral (left)	60	Left SSL 18
20	50% total length ventral (left)	61	Left SSL 19
21	60% total length ventral (left)	62	Left SSL 20
22	70% total length ventral (left)	63	Right SSL 1
23	80% total length ventral (left)	64	Right SSL 2
24	90% total length ventral (left)	65	Right SSL 3
25	10% total length 50% height medial (right)	66	Right SSL 4
26	20% total length 50% height medial (right)	67	Right SSL 5
27	30% total length 50% height medial (right)	68	Right SSL 6
28	40% total length 50% height medial (right)	69	Right SSL 7
29	50% total length 50% height medial (right)	70	Right SSL 8
30	60% total length 50% height medial (right)	71	Right SSL 9
31	70% total length 50% height medial (right)	72	Right SSL 10
32	80% total length 50% height medial (right)	73	Right SSL 11
33	90% total length 50% height medial (right)	74	Right SSL 12
34	10% total length ventral (right)	75	Right SSL 13
35	20% total length ventral (right)	76	Right SSL 14
36	30% total length ventral (right)	77	Right SSL 15
37	40% total length ventral (right)	78	Right SSL 16
38	50% total length ventral (right)	79	Right SSL 17
39	60% total length ventral (right)	80	Right SSL 18
40	70% total length ventral (right)	81	Right SSL 19
41	80% total length ventral (right	82	Right SSL 20

5.3. Results

Both mandibles – Principal Component (PC) 1 – PC4 cumulatively explain 93.50% of the

variance in shape (Appendix 3). PC1 (77.04% of shape variance) describes a change in flare

of the mandibles (as described by Barroso et al. 2012), in addition to changes in symphysis

length (Fig 5.3). PC2 (9.78% of shape variance) describes symphysis length and is the

relative movement of the two symphyseal landmarks (landmarks 1 and 2) (Fig 5.3). The two

river dolphins (*Inia* and *Lipotes*) clustered together in the top right of the mandible PC1-PC2

morphospace, whereas *Delphinapterus*, *Grampus* and *Pseudorca* clustered towards the left of

the mandible morphospace (Fig 5.3). These regions of morphospace are associated with

narrow mandibles with elongate symphyses and wide mandibles with relatively shorter

symphyses respectively.

PC3 (3.49% of shape variance) was composed of differences in the anterior extent of

the mandibular foramen and the profile of the ventral surface of the mandibles (Fig 5.3). PC4

(3.20% of shape variance) was composed of the ventral extent of the anterodorsal edge of the

mandibular foramen and the anterior extent of the mandibular foramen (fig 3). *Feresa* and

Inia cluster together in the middle of the top left quadrant of the mandible PC3-PC4

morphospace, whereas *Mesoplodon* is out by itself at the middle of the bottom of this

mandible morphospace. These regions of morphospace are associated with mandibles that

have a more concave profile of the ventral edge in lateral view and rounded anterior edge of

the mandibular foramen and mandibles with a slightly more convex profile of the ventral

edge and a strongly ventral anterodorsal edge of the mandibular foramen respectively (Fig

5.3).

One of the PGLS regressions was found to be significant (PC3 vs. frequency range) (p

= 0.0412) (Fig 5.4). Other strong (but not significant) relationships were found between: PC3

and maximum frequency (p = 0.05308); and PC3 and mean frequency (p = 0.06856). Based

on Based on comparing values of branch length transformations with differing λ values (see

methods) there appears to have been no effect of phylogeny on these results.

Fig 5.3. PCA plot of the analysis of both mandibles. A, PC1 vs PC2; B, PC3 vs PC4. Schematic drawings based on outputs from the geomorph package and showing extremes in mandibular features of that PC.

Figure 5.4. Plots showing the statistically significant relationships for: A, the analysis of both mandibles; B, the analysis of the left mandible; C, the analysis of the mandibular foramen. Schematic drawings based on outputs from the geomorph package and showing extremes in mandibular features of that PC.

Isolated mandible only – PC1 – PC4 cumulatively explain 91.33% of the variance in shape. PC1 (67.37% of shape variance) is composed of symphysis length and the height of the mandibular foramen (Fig 5.5). PC2 (12.18% of shape variance) is composed of the anterior extent of the mandibular foramen, the height of the coronoid process and the symphysis length (Fig 5.5). The two river dolphins (*Inia* and *Lipotes*) clustered together in the far right of the isolated mandible PC1-PC4 morphospace, a region of morphospace associated with mandibles that have elongate mandibular symphyses, shorter mandibular foramens that are less anteriorly expanded and have shorter coronoid processes. *Lagenorhynchus* and *Tursiops* clustered towards the top left, a region of morphospace associated with short mandibular symphyses and a tall anteriorly expanded mandibular foramen (Fig 5.5). *Mesoplodon* and *Steno* also cluster together towards the top right of the mandible morphospace, a region of morphospace associated with slightly elongate mandibular symphyses and a tall anteriorly expanded mandibular foramen.

PC3 (6.78% of shape variance) describes the degree of medial bowing of the mandible (Fig 5.5). PC4 (5.01% of shape variance) describes the ventral extent of the antero-dorsal edge of the mandibular foramen (Fig 5.4). Many species occupy their own region of morphospace. *Tursiops* is in the top middle of the top left quadrant of the mandible morphospace, a region of morphospace associated with mandibles that have more medially bowed mandible with a round anterior edge of the mandibular foramen. *Delphinapterus* is in the bottom middle of the bottom left quadrant of morphospace, a region of morphospace associated with a more medially bowed mandible with a strongly ventral anterodorsal edge of the mandibular foramen. *Mesoplodon* is in the bottom middle of the bottom right quadrant of the mandible morphospace, a region of morphospace associated with a straighter mandible with a dorsoventrally compressed anterior edge of the mandibular foramen (Fig 5.5).

One of the PGLS regressions was found to be significant (PC3 vs. frequency range) (p = 0.03721) (Fig 5.4). Based on comparing values of branch length transformations with differing λ values (see methods) there appears to have been no effect of phylogeny on these results.

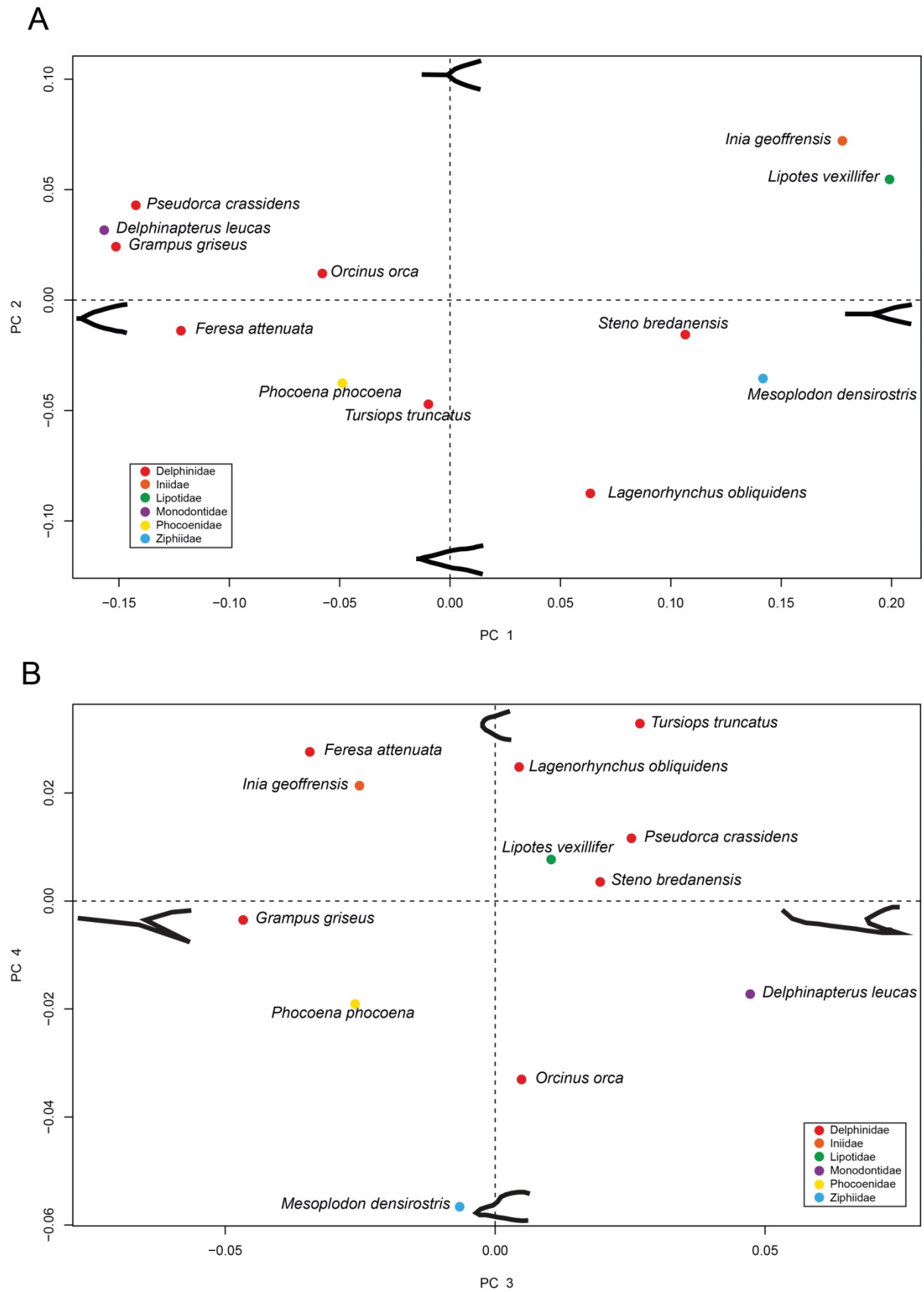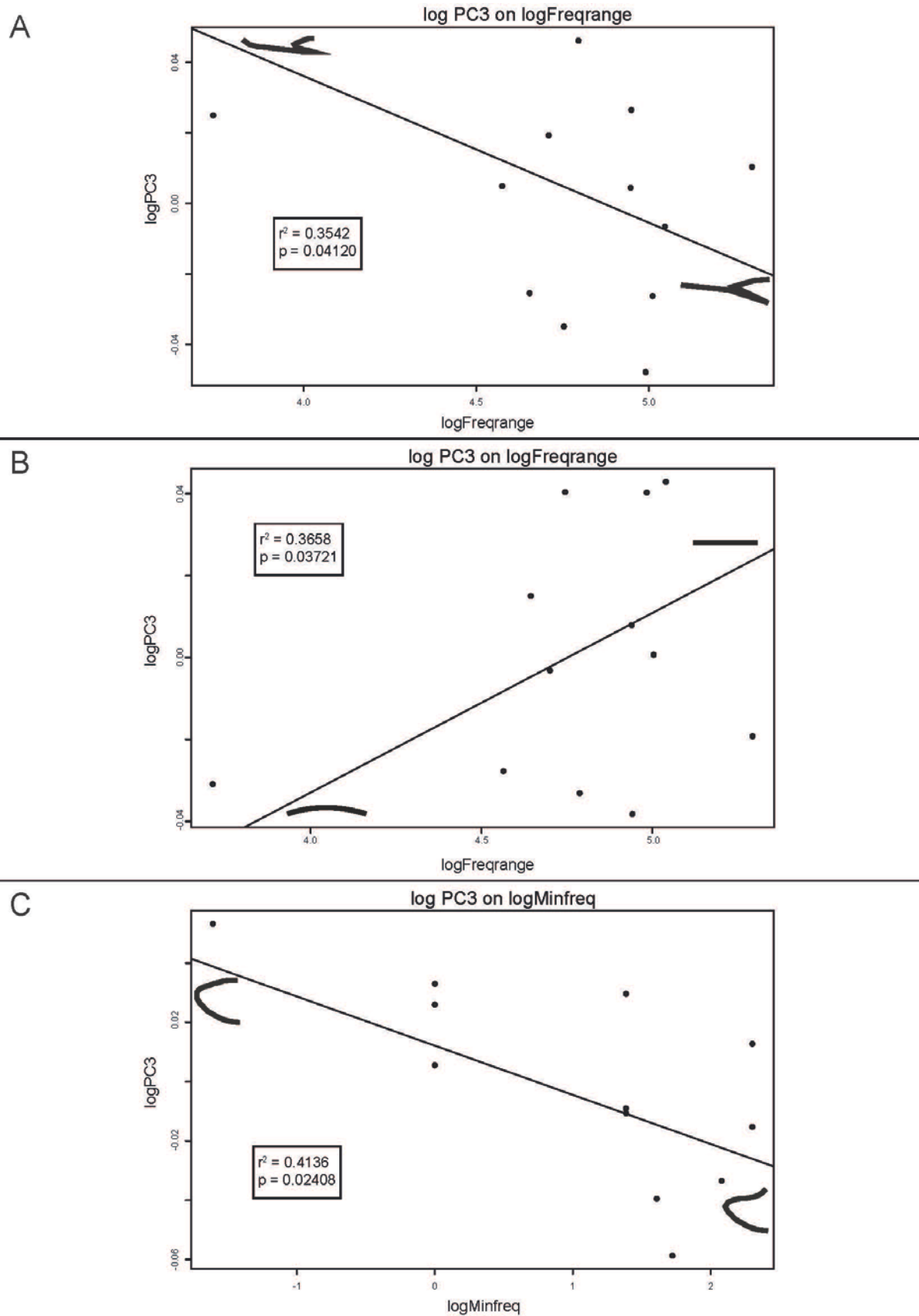Fig 5.5. PCA plot of the analysis of the left mandible. A, PC1 vs PC2; B, PC3 vs PC4. Schematic drawings based on outputs from the geomorph package and showing extremes in mandibular features of that PC.
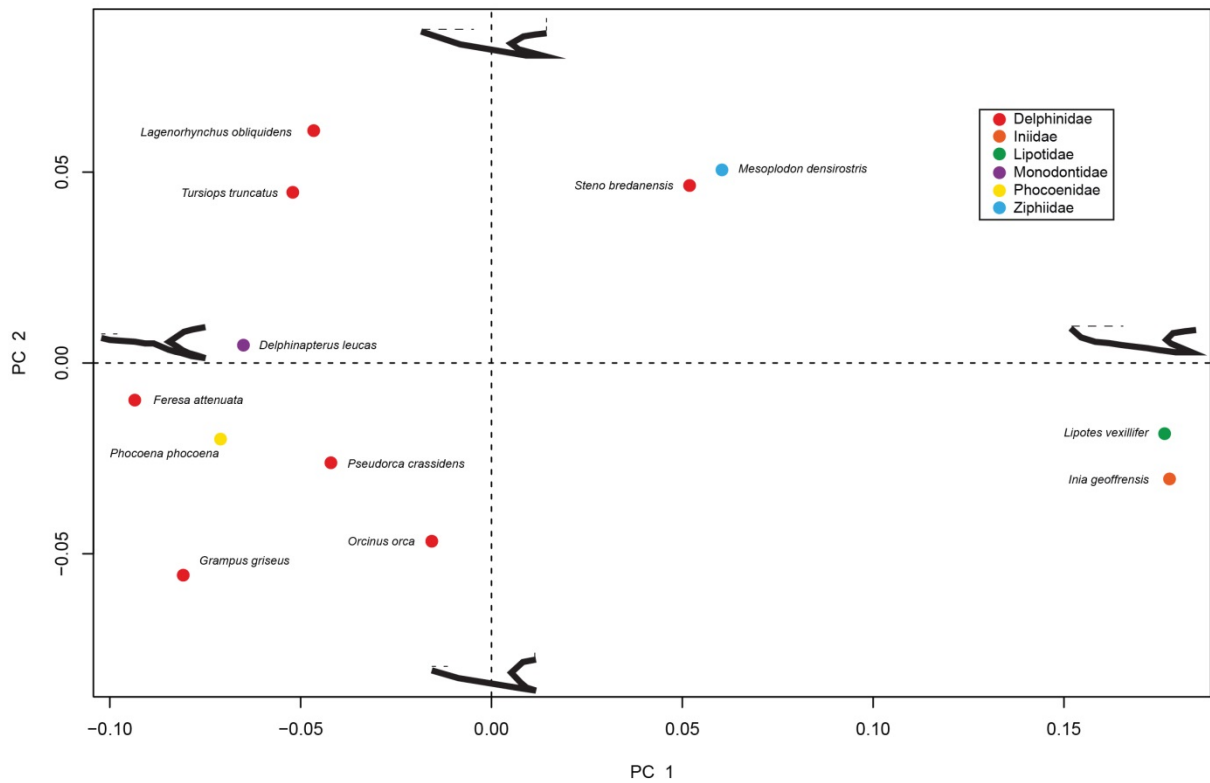
Mandibular foramen only – PC1 – PC4 cumulatively explain 91.97% of the variance in shape. PC1 (43.97% of shape variance) describes the ventral extent of the anterodorsal edge of the mandibular foramen (Fig 5.6). PC2 (28.89% of shape variance) describes the position of the anterior most point of the mandibular foramen (Fig 5.6). *Mesoplodon* is isolated in the far left of the mandible morphospace (Fig 5.6). *Tursiops* is isolated at the bottom right of the mandible morphospace. These regions of morphospace are associated with mandibles that have a ventrally extending anterodorsal edge of the mandibular foramen with a centrally situated anterior-most point and those that have a parabolic anterior edge of the mandibular foramen and a more ventral anterior-most point respectively.

PC3 (11.36% of shape variance) describes the degree of medial bowing of the mandible (Fig 5.6). PC4 (7.75% of shape variance) describes the dorsoventral compression of the anterior edge of the mandibular foramen (Fig 5.6). *Inia* is isolated in the top middle of the top left quadrant of the mandible morphospace and *Mesoplodon* is isolated in the bottom of the mandible morphospace (Fig 5.6). These regions of morphospace are associated with mandibles that have a more dorsally convex and rounded anterior edge of the mandibular foramen and those that have a more dorsally concave and dorsoventrally compressed anterior edge of the mandibular foramen respectively.

One of the PGLS regressions was found to be significant (PC3 vs. minimum frequency) (p = 0.02408) (Fig 5.4). Another strong (but not significant) relationship was found between bicondylar width and frequency range (p = 0.1064). Based on comparing values of branch length transformations with differing λ values (see methods) there appears to have been no effect of phylogeny on these results.
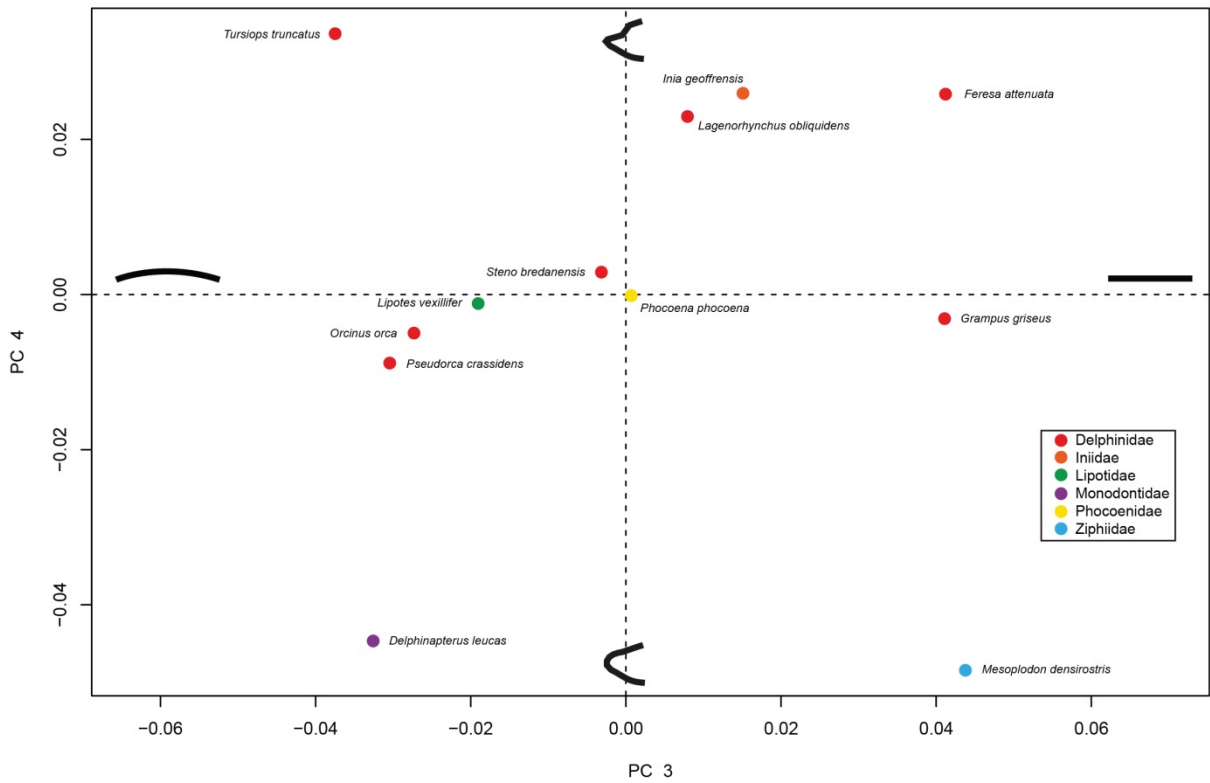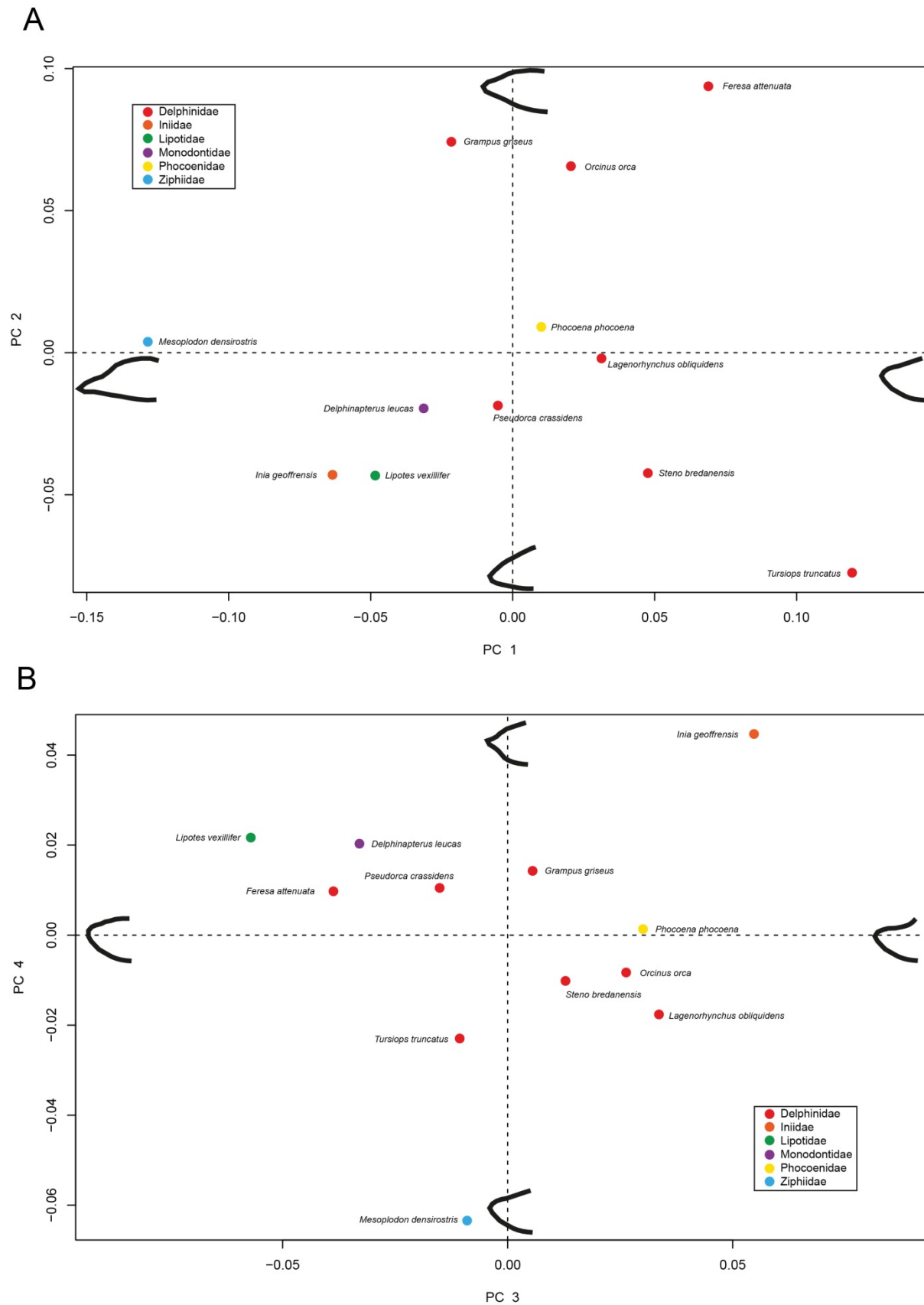
Fig 5.6. PCA plot of the analysis of the mandibular foramen. A, PC1 vs PC2; B, PC3 vs PC4. Schematic drawings based on outputs from the geomorph package and showing extremes in mandibular features of that PC.

5.4. Discussion

This study aimed to investigate the relationship between mandibular shape and the hearing abilities of odontocetes that have published audiograms. There were statistically significant relationships between PC3 (both mandibles and isolated mandible analyses) and frequency range and also between PC3 (mandibular foramen analysis) and minimum frequency. The results of the analysis of both mandibles show that a species with a more anteriorly expanded mandibular foramen and a convex ventral surface of the mandible is sensitive to a greater sound frequency range. In the analysis of the isolated mandible only a species with a straighter mandible can hear a greater range of frequencies than that of a species with a medially bowed mandible. The analysis of only the mandibular foramen on the other hand, showed that species with a more convex dorsal margin of the mandibular foramen can hear lower frequencies than those with a more concave dorsal margin of the mandibular foramen. Overall, frequency sensitivity appears to have a relatively minor effect on the shape of odontocete mandibles. Other features, such as jaw flare and symphysis length explain a far greater proportion of mandible shape variance (86.82% in the analysis of both mandibles). These are features which are clearly linked to feeding ecology (Barroso et al. 2012) rather than sound detection. The morphological factors that do have a significant effect on mandible shape appear to be linked to the physical properties of sound waves themselves. In the analysis of both mandibles those animals that had a more anteriorly expanded mandibular foramen could hear a greater range of frequencies. A larger mandibular foramen may indicate the presence of an enlarged mandibular fat pad, used to direct sound to the middle and inner ear. A larger fat pad is capable of detecting lower frequency sound waves, as they possess longer wavelengths and could not be detected by a shorter fat pad in a smaller mandibular foramen (Barroso et al. 2012; Ekdale & Racicot 2015). The significant relationship in the mandibular foramen only analysis between a convex dorsal edge of the mandibular foramen

and lower frequencies is also likely related to a more anteriorly expanded mandibular foramen and the presence of a larger fat pad. I argue that greater convexity of the dorsal margin of the mandibular foramen in taxa that can hear lower frequencies is the result of a biomechanical trade-off between expanding the mandibular foramen and maintaining the structural integrity of the mandible itself. Another way of increasing the size of the mandibular foramen (and therefore the mandibular fat pad) could be to curve the mandibles, allowing for a longer fat pad in a mandible of the same length. This could potentially explain the significant relationship between animals that can detect a greater range of frequencies and those that have more medially bowed mandibles that was detected in the isolated mandible only analysis.

Study limitations – This research represents a preliminary exploration of the relationship between mandible shape and the sounds that odontocetes can detect. The preliminary nature of the study is caused by several limitations. One such limitation is the small number of odontocete taxa that currently have a recorded audiogram. At present only 17 taxa have audiograms (approximately 23% of all odontocetes), of which 12 were included in this study. Greater numbers of audiograms of odontocetes are necessary for gaining a clear understanding of differences in hearing abilities and any potential influences on mandible shape.

The methods by which audiograms were obtained also varied, with some studies using behavioural methods to determine what sounds an animal is responsive to (e.g. Jacobs & Hall 1972; Wang et al. 1992), whereas other studies have used an electrophysiological method known as the auditory evoked potential method (e.g. Klishin et al. 2000; Montie et al. 2011). Ideally, all audiograms would be obtained using consistent methods across all taxa. The small sample size also limited the ability of the PGLS to detect a phylogenetic effect. PGLS usually needs 20-30 data points to detect a signal (Freckleton et al. 2002). This was

remedied in this study by making λ =1 and comparing it to the results of the same analysis

when the maximum likelihood ratio is used for λ. As the results were not significantly

different the results of the analyses of this study are those for when λ = 1.

A further limitation is that this study, using a generalised Procrustes analysis to

remove size effects from the data prior to the principal components analysis, does not take

into effect how body size influences the morphometrics of acoustically-linked features. For

example, an orca will have an absolutely larger mandibular fat pad than a porpoise and by

virtue of this may be able to detect lower frequencies with longer wavelengths. A solution to

this issue would be to use a type of an approach known as size and shape space or

conformation space (Klingenberg 2016) that involves a superimposition of the landmark

configurations without standardizing to unit centroid size (e.g. Goswami 2006). This issue

will be addressed in future work.

Other limitations include the fact that the ontogenetic age and sex are not specified for

audiogram subject animals and that the sample size for each species in the geometric

morphometric analysis was n=1.

Palaeobiological implications – As noted above, toothed mysticete mandibles are very

similar to those of living odontocetes. The results of this study caution against being able to

predict frequency ranges for stem mysticetes using mandibular foramen shape, although there

are potential methods using cochlear features (Ekdale & Racicot 2015). The mandibular

foramen in mysticetes has become greatly reduced over time, meaning that as mysticetes

continued to hear low frequencies (as indicated by their cochleae and basicrania), the entry

point of the mandibular foramen was no longer used and an alternative pathway evolved,

possibly via bone conduction (see Chapters 2 & 4).

5.5. Conclusions

This study identifies that the frequencies that odontocetes can detect have a minor influence on the overall shape of the mandible, with the strongest influences on shape being feeding. The main influence that hearing abilities have on mandible shape are confined to the size and shape of the mandibular foramen, which houses the mandibular fat pad. A higher proportion of odontocetes with recorded audiograms and analyses that incorporate the effects of absolute size are required to further expand on the findings presented here. Toothed mysticete frequency ranges cannot be predicted via this method.

References

Adams DC, Otarola-Castillo E. 2016. geomorph: an R package for the collection and analysis of geometric morphometric shape data. Methods in Ecology and Evolution 4, 393-399.

Andersen S. 1970. The auditory sensitivity of the harbor porpoise, *Phocoena phocoena*. In Pilleri G, ed, Investigations on Cetacea, Berne-Bumpliz, Berne, pp. 255–259.

Au WWL. 2009. Echolocation. In Perrin WF, Wursig B. eds, Encyclopaedia of Marine Mammals (2nd ed), Academic Press, London, pp. 348–357.

Barroso C, Cranford TW, Berta A. 2012. Shape analysis of odontocete mandibles: functional and evolutionary implications. Journal of Morphology 273, 1021–1030.

Cranford TW, Krysl P, Hildebrand JA. 2008. Acoustic pathways revealed: Simulated sound transmission and reception in Cuvier's beaked whale (*Ziphius cavirostris*). Bioinspiration & Biomimetics 3, 1–10.

Ekdale EG, Racicot RA. 2015. Anatomical evidence for low frequency sensitivity in an archaeocete whale: comparison of the inner ear of *Zygorhiza kochii* with that of crown Mysticeti. Journal of Anatomy 226, 22–39.

Freckleton RP, Harvey PH, Pagel M. 2002. Phylogenetic analysis and comparative data: a test and review of evidence. American Naturalist 160, 712–726.

Grafen A. 1989. The phylogenetic regression. Philosophical Transactions of the Royal Society B: Biological Sciences 326, 119–157.

Goswami A. 2006. Cranial modularity shifts during mammalian evolution. American Naturalist 168, 270–280.

Gutstein CS, Figueroa-Bravo CP, Pyenson ND, Yury-Yañez RE, Cozzuol MA, Canals M. 2014. High frequency echolocation, ear morphology, and the marine–freshwater

transition: A comparative study of extant and extinct toothed whales. Palaeogeography, Palaeoclimatology, Palaeoecology 400, 62–74.

Hooker SK. 2009. Toothed Whales, Overview. In Perrin WF, Wursig B, eds, Encyclopaedia of Marine Mammals (2nd ed), Academic Press, London, pp. 1173–1179.

Houser DS, Finneran JJ. 2006. A comparison of underwater hearing sensitivity in bottlenosed dolphins (*Tursiops truncatus*) determined by electrophysiological and behavioural methods. The Journal of the Acoustical Society of America 120, 1713–1722.

Jacobs DW, Hall JD. 1972. Auditory thresholds of a freshwater dolphin, *Inia geoffrensis* Blainville. The Journal of the Acoustical Society of America 51, 530–533.

Ketten DR. 2000. Cetacean ears. In, Au WWL, Popper AN, Fay RR, eds, Hearing by whales and dolphins. Springer-Verlag, New York, pp. 43–108.

Klingenberg CP. 2016. Size, shape, and form: concepts of allometry in geometric morphometrics. Development Genes and Evolution 226, 113–137.

Klishin VO, Popov VV, Supin AY. 2000. Hearing capabilities of a beluga whale, *Delphinapterus leucas*. Aquatic Mammals 26, 212–228.

Mann D, Hill-Cook M, Manire C, Greenhow D, Montie E, Powell J, Wells R, Bauer G, Cunningham-Smith P, Lingenfelser R, DiGiovanni R, Stone A, Brodsky M, Stevens R, Kieffer G, Hoetjes P. 2010. Hearing loss in stranded odontocete dolphins and whales. PLoS ONE 5, e13824.

Martins EP, Hansen TF. 1997. Phylogenies and the comparative method: a general approach to incorporating phylogenetic information into the analysis of interspecific data. American Naturalist 149, 646–667.

Montie EW, Manire CA, Mann DA. 2011. Live CT imaging of sound reception anatomy and hearing measurements in the pygmy killer whale, *Feresa attenuata*. The Journal of Experimental Biology 214, 945–955.

Nachtigall PE, Yuen MML, Mooney TA, Taylor KA. 2005. Hearing measurements from a

stranded infant Risso's dolphin, *Grampus griseus*. The Journal of Experimental

Biology 208, 4181–4188.

Norris KS. 1968. The evolution of acoustic mechanisms in odontocete cetaceans. In Drake

ET, ed, Evolution and environment, Yale University Press, New Haven, pp. 297–324.

Nummela S, Thewissen JGM, Bajpai S, Hussain T, Kumar K. 2007. Sound transmission in

archaic and modern whales: anatomical adaptations for underwater hearing.

Anatomical Record 290, 716–733.

O'Higgins P, Jones N. 2006. Morphologika 2, v. 2.4. Hull York Medical School, York.

Orme D, Freckleton R, Thomas G, Petzoldt T, Fritz S, Isaac N, Pearse W. 2013. caper:

Comparative Analyses of Phylogenetics and Evolution in R. R package version 0.5.2.

http://CRAN.R-project.org/package=caper.

Pacini AF, Nachtigall PE, Quintos CT, Schofield TD, Look DA, Levine GA, Turner JP.

2011. Audiogram of a stranded Blainville's beaked whale (*Mesoplodon densirostris*)

measured using auditory evoked potentials. The Journal of Experimental Biology

214, 2409–2415.

Pagel M. 1997. Inferring evolutionary processes from phylogenies. Zoologica Scripta 26,

331–348.

Pagel M. 1999. Inferring the historical patterns of biological evolution. Nature 401, 877–884.

R Core Team. 2015. R: A language and Environment for Statistical Computing. R

Foundation for Statistical Computing, Vienna.

Robert McNeel & Associates. 2015. Rhinoceros 3D, Version 5.0. Robert McNeel &

Associates, Seattle, USA.

Rohlf FJ. 2001. Comparative methods for the analysis of continuous variables: geometric

interpretations. Evolution 55, 2143–2160.

Steeman ME, Hebsgaard MB, Fordyce RE, Ho SYW, Rabosky DL, Nielsen R, Rahbek C, Glenner H, Sørensen MV, Willerslev E. 2009. Radiation of extant cetaceans driven by restructuring of the oceans. Systematic Biology 58, 573–585.

Symonds MRE, Blomberg SP. 2014. In Garamszegi LZ ed, Modern phylogenetic comparative methods and their application in evolutionary biology. Concepts and Practice. Springer, London, pp. 105–130.

Szymanski MD, Bain DE, Kiehl K, Pennington S, Wong S, Henry KR. 1999. Killer whale (*Orcinus orca*) hearing: Auditory brainstem response and behavioural audiograms. The Journal of the Acoustical Society of America 106, 1134–1141.

Visualization Sciences Group – a FEI Company. 2013. Avizo: 3D Analysis Software for Scientific and Industrial Data, Standard Edition 8.0.0. Berlin: Konrad-Zuse-Zentrum für Informationstechnik.

Wang D, Wang K, Ziao Y, Sheng G. 1992. Auditory sensitivity of a Chinese river dolphin (*Lipotes vexillifer*). In Thomas JA, Kastelein RA, Supin AY, eds, Marine Mammal Sensory Systems. Plenum Press, New York, pp. 213–221.

Werth AJ. 2006. Mandibular and dental variation and the evolution of suction feeding in Odontoceti. Journal of Mammalogy 87, 579–88.

Yuen MML, Nachtigall PE, Breese M, Supin AY. 2005. Behavioral and auditory evoked potential audiograms of a false killer whale (*Pseudorca crassidens*). The Journal of the Acoustical Society of America 118, 2688–2695.

6. Ultrasonic hearing and echolocation in the earliest toothed whales

Travis Park[1,2], Erich M. G. Fitzgerald[2,3], Alistair R. Evans[1,2]

[1]School of Biological Sciences, Monash University, Melbourne, Australia.

[2]Geosciences, Museums Victoria, Melbourne, Australia.

[3]Department of Paleobiology, National Museum of Natural History, Smithsonian Institution, Washington DC, USA.

Abstract

The evolution of biosonar (production of high frequency sound and reception of its echo) was a key innovation of toothed whales and dolphins (Odontoceti) that facilitated phylogenetic diversification and rise to ecological predominance. Yet exactly when high frequency hearing first evolved in odontocete history remains a fundamental question in cetacean biology. Here I show that archaic odontocetes had a cochlea specialized for sensing high frequency sound, as exemplified by an Oligocene xenorophid from the late Oligocene of North Carolina, one of the earliest-diverging stem groups. This specialization is not as extreme as that seen in the crown clade. Paired with anatomical correlates for high frequency signal production in Xenorophidae, this is strong evidence that the most archaic toothed whales possessed a functional biosonar system, and that this signature adaptation of odontocetes was acquired at or soon after their origin.

6.1. Introduction

Living odontocete whales possess a complex echolocation system for sensing their prey and environment. High frequency sounds are produced in the nasal passages, transmitted through air sinuses and the fatty melon (Cranford et al. 1996). The reflected signal reaches the inner

ear through acoustic fat pads surrounding the posterior end of the mandible and middle ear (Nummela et al. 2007). The advent of echolocation is thought to be a key innovation that supported exploitation of a vast pelagic biomass—vertically-migrating organisms, especially cephalopods—and explosive diversification of odontocetes (Lindberg & Pyenson 2007; Steeman et al. 2009). Bony correlates of nasofacial tissues linked to ultrasonic signal production have been identified in archaic fossil odontocetes (Fordyce 2002; Geisler et al 2014), but until now we have lacked anatomical evidence from their inner ear to test for high frequency hearing, and verify functional echolocation (Montgomery et al. 2013; Geisler et al. 2014; Sanders & Geisler 2015). Here I describe the cochlear anatomy in a member of the Oligocene Xenorophidae, one of the earliest diverging odontocete clades (Geisler et al. 2014; Sanders & Geisler 2015), showing that the most archaic odontocetes could detect high frequency sound, although probably not in the upper range of some living odontocetes and retain greater sensitivity to lower frequencies. In addition, a functional echolocation system was probably a hallmark of odontocetes from their earliest divergence.

6.2. Material and Methods

United States National Museum of Natural History, Washington, DC (USNM) specimen 534010, an isolated right periotic (Fig A4.1) from the Upper Oligocene Belgrade Formation at Onslow Beach, Camp Lejeune Marine Base, Onslow County, North Carolina, USA. Strontium isotope analysis yielded a date of 26.5 Ma which falls in the NP25 calcareous nannoplnkton zone (Vandenberghe et al. 2012).

USNM 534010 was microCT scanned using a Zeiss Xradia 520Versa at the Monash University X-ray Microscopy Facility for Imaging Geo-materials (XMFIG). Raw data from these scans (Fig A4.2) were then used to create a three-dimensional model of the periotic using Avizo (Version 8.1.0 Standard) (Fig 6.1) (Visualisation Sciences Group – a FEI Company 2013). From this model an endocast of the cochlea was digitally segmented using

Avizo (Fig 6.1; Figure A4.3). This process was also carried out on a comparative sample of seven modern odontocete taxa and one modern mysticete taxon (Fig A4.4). An estimate of the low frequency hearing limit for the xenorophid was calculated from the linear regression of low frequency hearing limit and radii ratio for other mammals performed by Manoussaki et al. (2008).

The internal structures of the cochlea, especially the secondary spiral lamina (SSL), are very delicate and as a result are often broken in fossil specimens. Fortunately the base of the SSL is more robust and can be used to determine the extent of the secondary spiral lamina along the length of the cochlea, even if the length of the lamina itself is unable to be measured. The extent of the spiral laminae can be used as a proxy for the stiffness of the basilar membrane, the structure which supports the organ of hearing, known as the organ of Corti. Detailed methods can be found in the supplementary material (Appendix 4).

6.3. Results

USNM 534010 possesses a combination of characters unique to the periotic of xenorophid odontocetes (Fig A4.1): (1) transversely thin, blade-like anterior process (apomorphic); (2) indistinct anterior bullar facet; (3) indistinct or absent fovea epitubaria; (4) elongate lateral tuberosity (apomorphic) (Fordyce 2002); (5) wide pars cochlearis with a trapezoid outline in ventral view; (6) salient dorsal crest; (7) dorsal crest with a dorsally concave profile in lateral view; (8) well developed suprameatal fossa; and (9) in dorsal view, thick pars cochlearis medial and anterior to the internal acoustic meatus. I could not identify any potential autapomorphies of USNM 534010 shared with a particular xenorophid species (see Appendix 4), hence I refer USNM 534010 to Xenorophidae, gen. et sp. indet. A phylogenetic analysis was not performed as the specimen is an isolated element (but see Tsai & Fordyce (2016) and Tanaka & Fordyce (2016)).
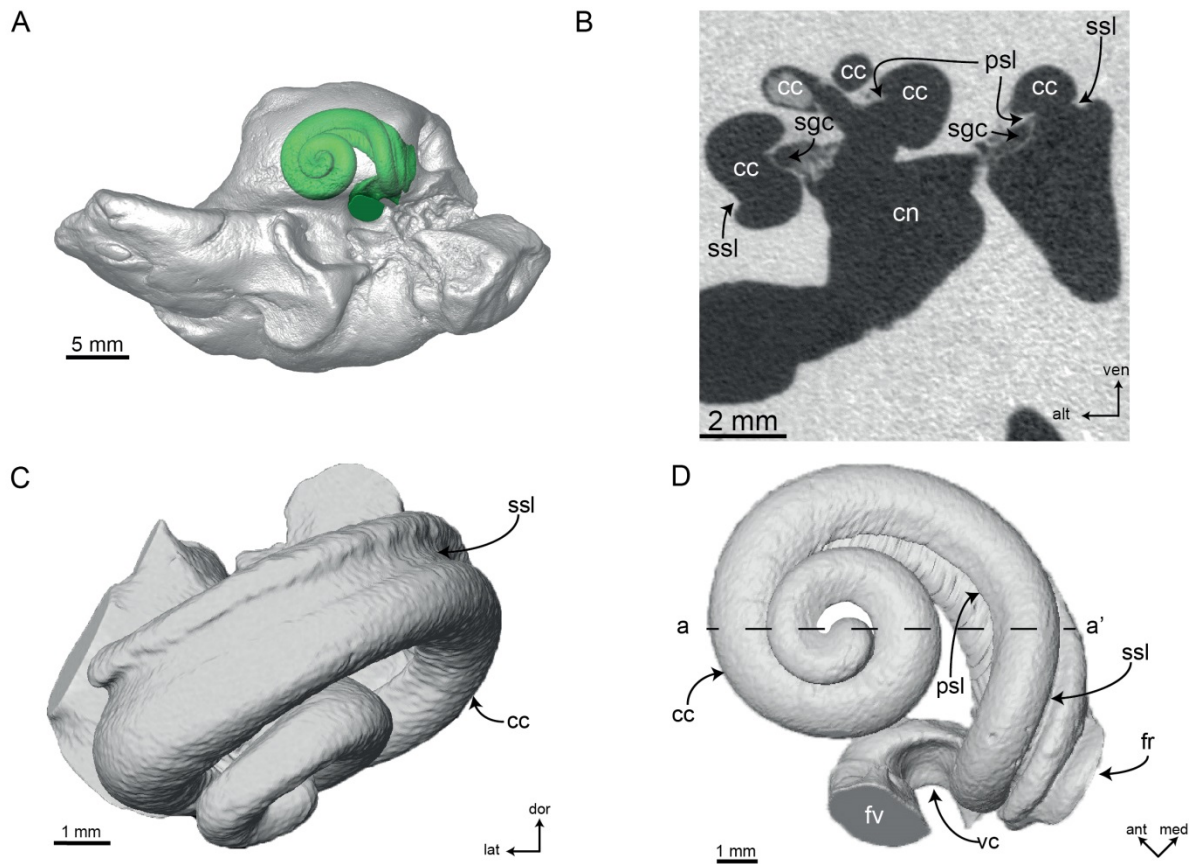
Fig 6.1. (A) USNM534010, right periotic, digital model reconstructed from microCT data in ventral view. Outer surface has made transparent to show position of the cochlea (green). (B) microCT cross sectional slice through cochlea of USNM534010. (C,D) Digital endocast of right cochlea of USNM534010 reconstructed from microCT data in anterior and vestibular views. Dashed line a–a' indicates position of slice in section (B). alt, anterolateral; ant, anterior; cc, cochlear canal; cn, canal for cranial nerve VIII (auditory nerve); fr, fenestra rotunda; fv, fenestra vestibuli; psl, primary spiral lamina; sgc, spiral ganglion canal; ssl, secondary spiral lamina; vc, vestibular curve; ven, ventral.

The cochlea completes two turns, a number within the range of modern odontocetes (Ketten 2000). The fenestra rotunda is small and is located posterior to the first quarter of the basal turn (Fig 6.1D). This portion of the cochlea is not recurved towards the fenestra rotunda, a feature known as the 'cochlear hook', that is present in some more crownward odontocetes, especially delphinids (Yamada & Yoshizaki 1959; Luo & Eastman 1995; Luo & Marsh 1996; Ekdale 2013). The cochlear canal retains its width for the first turn, tapering in the second turn, becoming narrowest at the apex. The cochlear aqueduct is long and sub-circular in cross section, extending dorsomedially from the basal turn just medial to the fenestra rotunda to the outer surface of the periotic.

In vestibular view (Fig A4.3D) the first quarter of the basal turn is more loosely coiled than the remaining 1.75 turns. The apical-most half turn slightly overlaps the basal turn. The basal ratio is 0.48, meaning that the cochlea is approximately twice as wide as it is tall. The axial pitch is 2.41 and the slope is 0.08 (table 6.1). The radii ratio is 5.04, a value that is slightly higher than those calculated for the modern odontocetes in this study (except for ziphiids, values for which are unusually high for odontocetes (table A4.1)). In cross section, the bone separating the basal turn from the apical turn is thick, similar to modern odontocetes (Fig 6.1).

Table 6.1. Key measurements of USNM534010 and estimated low frequency limit (LFL). CL, canal length; Hz, hertz; mm, millimetres; mm^3, millimetres cubed; #T, number of turns; SSL, secondary spiral lamina.

Taxon	Specimen number	#T	CL (mm)	RR	% SSL	BR	AP	Vol. (mm^3)	Slope	Estd. LFL (Hz)
Xenorophidae indet.	USNM534010	2	28.83	5.04	50	0.48	2.41	122.29	0.08	145.91

The primary spiral lamina extends almost the entire length of the cochlea, being widest at the base. The secondary spiral lamina extends along the radial wall of the cochlear canal for one turn (approximately 50% of the total length of the cochlear canal) (Fig 6.1), a value slightly lower than those calculated for the modern odontocetes in this study but patently longer than *Balaenoptera acutorostrata* (table A4.1). The laminar gap is narrowest at the base. For additional comparisons see Appendix 4.

6.4. Discussion

Recent analyses of early odontocetes show that even the most archaic stem taxa possessed cranial morphology functionally linked to generation of high frequency signals and therefore the potential to echolocate (Fordyce 2002; Montgomery et al. 2013; Sanders & Geisler 2015). The xenorophid inner ear described here corroborates the latter, demonstrating that early-diverging stem odontocetes had cochleae sensitive to high frequency sounds pivotal in echolocation. Specifically, the cochlea of USNM 534010 possesses several adaptations to high frequency hearing: reduced number of turns; shorter cochlear length; an extended

secondary spiral lamina (relative to mysticetes); a low radii ratio value; and reduced

overlapping of turns (Fig 6.2). These features are absent in the low frequency-sensitive

cochleae of archaeocetes and extant mysticetes (Ekdale & Racicot 2105). The xenorophid

represented by USNM 534010 would have therefore possessed a relatively stiff basilar

membrane capable of detecting the echo of high frequency sounds produced in its nasal

passages.
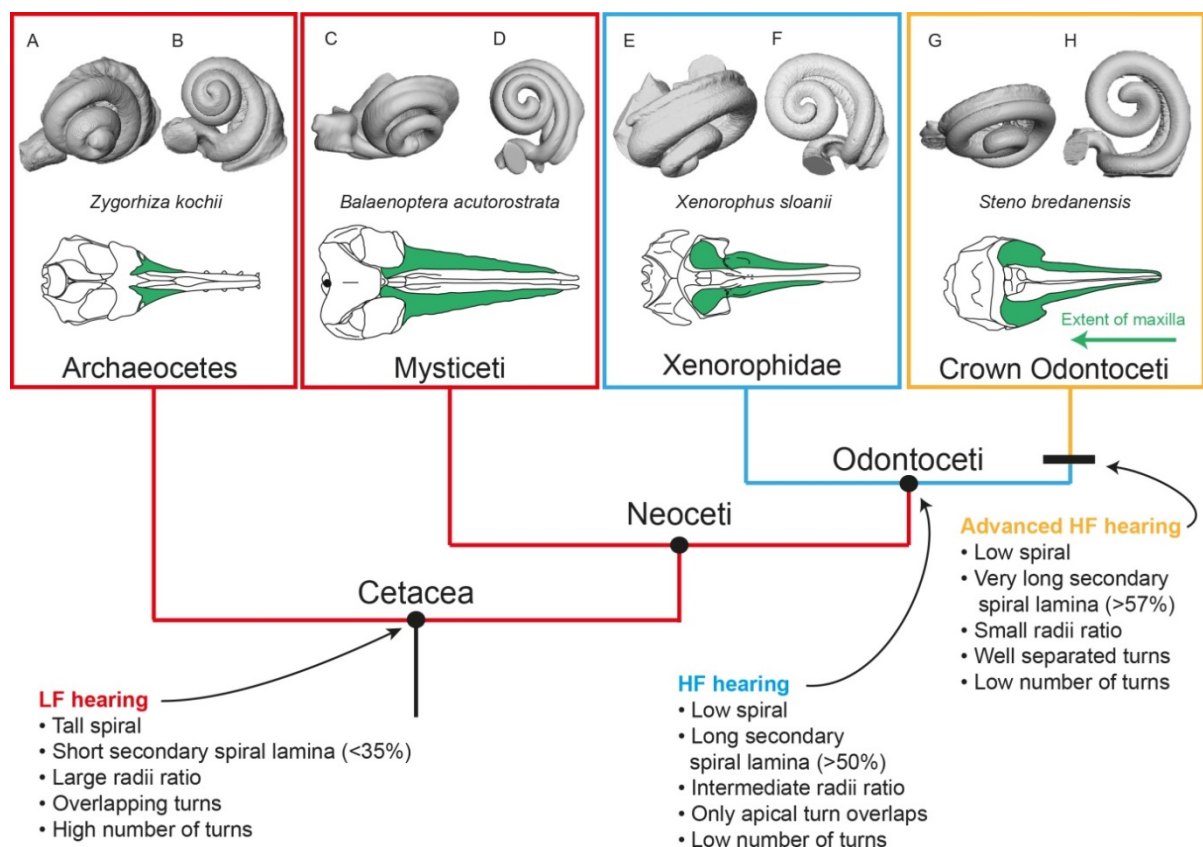
Fig 6.2. Evolution of odontocete hearing, based on the phylogeny of Geisler et al. (2014), showing how the cochlea (in (A,C,E,G) anterior and (B,D,F,H) vestibular views) has become progressively more specialised towards high frequency hearing. The line drawing of *Xenorophus sloani* is adapted by permission from Macmillan Publishers Ltd: Nature, copyright (2014). LF, low frequency; HF, high frequency.

Despite the cochlea of USNM 534010 being specialised to detect high frequencies,

several features illustrate its intermediate condition relative to basilosaurid archaeocetes and

crown odontocetes: an intermediate extension of the secondary spiral lamina (and therefore a

less stiff basilar membrane) relative to mysticetes and modern odontocetes; its radii ratio

value (indicating a greater sensitivity to low frequency sounds than crown odontocetes, with

an estimated low frequency hearing limit of 145.91 Hz, lower than any modern odontocete excepting the aberrant ziphiids); and intermediate overlapping of turns. USNM 534010 lacks derived features seen in modern odontocetes, such as: a longer extension of the secondary spiral lamina; a small radii ratio; and no overlapping turns. Whilst xenorophids could clearly detect high frequency sounds, they were not as specialised as modern odontocete taxa (Fig 6.2).

At least three of the synapomorphies identified for Odontoceti are nasofacial osteological correlates for echolocation (Sanders & Geisler 2015), hinting at the importance of this sensory behaviour in the divergence and initial diversification of the clade. These are: 1) expansion of ascending process of maxilla; 2) premaxillary foramen; and 3) premaxillary sac fossa (and possibly the maxillary foramen) (Sanders & Geisler 2015). Thus, the ability to detect high frequency sounds in one of the most basal odontocete lineages (Xenorophidae), as demonstrated by USNM 534010, is strong corroborating evidence that a functional echolocation system was likely present in the most recent common ancestor of xenorophids and all other odontocetes (Fig 6.2). Within Xenorophidae, the posterior migration of the maxillae evolved independently of a convergent change in craniofacial morphology (and perhaps elaboration of high frequency signal generation) along the stem leading to crown odontocetes (Geisler et al. 2014). This raises the possibility that there was equivalent parallel evolution towards high frequency sensitivity in the cochleae of xenorophids and crown odontocetes. That USNM 534010 has cochlear specializations for high frequency hearing intermediate between basilosaurid archaeocetes and crown odontocetes suggests two intriguing alternative hypotheses: (1) the 'intermediate' inner ear anatomy and degree of high frequency sensitivity of USNM 534010 is typical for all Xenorophidae; or (2) USNM 534010 represents a basal xenorophid and hence its cochlear anatomy is plesiomorphic, while later-diverging xenorophids (like *Cotylocara*) possess cochlear specialization for ultrasonic

hearing approaching that of the crown odontocetes with which they (convergently) share an advanced state of posterior migration of rostral bones. A comparison between the cochlear canal from a *Cotylocara*-grade xenorophid and that of a more basal xenorophid is required to evaluate these hypotheses. High frequency hearing was present in archaic odontocetes and echolocation appears to have been an important factor in their evolutionary success. It remains to be determined however, whether the ability to hear high frequency sounds preceded the ability to produce them as seen in bats (Carter & Adams 2016), or vice versa.

Acknowledgements

References

Carter RT, Adams RA. 2016. Integrating ontogeny of echolocation and locomotion gives unique insights into the origin of bats. Journal of Mammalian Evolution.

Cranford TW, Amundin M, Norris KS. 1996. Functional morphology and homology in the odontocete nasal complex: Implications for sound generation. Journal of Morphology 228, 223–285.

Ekdale EG. 2013. Comparative anatomy of the bony labyrinth (inner ear) of placental mammals. PLoS ONE 8, e66624.

Ekdale EG, Racicot RA. 2015. Anatomical evidence for low frequency sensitivity in an archaeocete whale: comparison of the inner ear of *Zygorhiza kochii* with that of crown Mysticeti. Journal of Anatomy 226, 22–39.

Fordyce RE. 2002. *Simocetus rayi* (Odontoceti: Simocetidae, New Family): A bizarre new archaic Oligocene dolphin from the eastern Pacific. In Emry RE, ed, Cenozoic Mammals of Land and Sea, Tributes to the Career of Clayton E. Ray. Smithsonian Contributions to Paleobiology 93, 185–222.

Geisler JH, Colbert MW, Carew JL. 2014. A new fossil species supports an early origin for toothed whale echolocation. Nature 508, 383–386.

Ketten DR, 2000. Cetacean ears. In Au WWL, Popper AN, Fay RR, eds, Hearing by whales and dolphins. Springer-Verlag, New York, pp. 43–108.

Lindberg DR, Pyenson ND. 2007. Things that go bump in the night: Evolutionary interactions between cephalopods and cetaceans in the Tertiary. Lethaia 40, 335–343.

Luo ZX, Eastman ER. 1995. Petrosal and inner ear of a squalodontoid whale: implications for evolution of hearing in odontocetes. Journal of Vertebrate Paleontology 15, 431–442.

Luo ZX, Marsh K. 1996. Petrosal (periotic) and inner ear of a Pliocene kogiine whale (Kogiinae, Odontoceti): Implications on relationships and hearing evolution of toothed whales. Journal of Vertebrate Paleontology 16, 328–348.

Manoussaki D, Chadwick RS, Ketten DR, Arruda J, Dimitriadis EK, O'Malley JT. 2008. The influence of cochlear shape on low-frequency hearing. Proceedings of the National Academy of Sciences 105, 6162–6166.

Montgomery SH, Geisler JH, McGowen MR, Fox C, Marino L, Gatesy J. 2013. The evolutionary history of cetacean brain and body size. Evolution 67, 3339–3353.

Nummela S, Thewissen JGM, Bajpai S, Hussain T, Kumar K. 2007. Sound transmission in archaic and modern whales: anatomical adaptations for underwater hearing. Anatomical Record 290, 716–733.

Sanders AE, Geisler JH. 2015. A new basal odontocete from the Upper Rupelian of South Carolina, U.S.A., with contributions to the systematics of *Xenorophus* and *Mirocetus* (Mammalia, Cetacea). Journal of Vertebrate Paleontology 35, e890107.

Steeman ME, Hebsgaard MB, Fordyce RE, Ho SYW, Rabosky DL, Nielsen R, Rahbek C, Glenner H, Sørensen MV, Willerslev E. 2009. Radiation of extant cetaceans driven by restructuring of the oceans. Systematic Biology 58, 573–585.

Tanaka Y, Fordyce RE 2016. Awamokoa tokarahi, a new basal dolphin in the Platanistoidea (late Oligocene, New Zealand). Journal of Systematic Palaeontology http://dx.doi.org/10.1080/03036758.2016.1156552.

Tsai CH, Fordyce RE. 2016. Archaic baleen whale from the Kokoamu Greensand: earbones distinguish a new late Oligocene mysticete (Cetacea: Mysticeti) from New Zealand. Journal of the Royal Society of New Zealand http://dx.doi.org/10.1080/14772019.2016.1202339.

Uhen MD. 2008. A new *Xenorophus*-like odontocete cetacean from the Oligocene of North

    Carolina and a discussion of the basal odontocete radiation. Journal of Systematic

    Palaeontology 6, 433–452.

Vandenberghe N, Hilgen FJ, Speijer RP, Ogg JG, Gradstein FM, Hamer, Hollis CJ, Hooker

    JJ.. 2012. Chapter 28 - The Paleogene Period. In Gradstein FM, Ogg JG, Schmitz

    MD, Ogg GM, eds, The Geologic Time Scale. Elsevier, Boston, pp. 855–921.

Visualization Sciences Group – a FEI Company. 2013. Avizo: 3D Analysis Software for

    Scientific and Industrial Data, Standard Edition 8.0.0. Berlin: Konrad-Zuse-Zentrum

    für Informationstechnik.

Yamada M, Yoshizaki F. 1959. Osseous labyrinth of Cetacea. Scientific Reports of the

    Whales Research Institute 14, 291–304.

7. Discussion

7.1. Evolution of the mysticete auditory pathway

This thesis has examined the auditory pathway of mysticetes by examining it as three functional modules: the mandible, the basicranium and the inner ear. The analyses of previous chapters have revealed that there are differences in the degree to which they have changed over the past 34 million years.

The cochlea has changed the least, with basilosaurid and toothed mysticete cochleae essentially identical to one another. Further along the mysticete lineage, there do appear to be some differences. Absolute size of the cochlea has increased, most likely as a result of the overall increase in body size in modern mysticetes. Apical coiling increased in cetotheriids, who have the highest number of turns and the most extreme coiling of any mysticete, hinting at specialised hearing abilities within that group. The tympanal recess (discussed in more detail below) appears to have evolved only within Plicogulae in mysticetes. Balaenids also possess greatly reduced secondary spiral laminae, also potentially reflecting further auditory specialisation. On the whole, however, mysticete cochleae are very alike in the majority of features and are also similar to basilosaurid cochleae. This indicates that toothed mysticetes retained the plesiomorphic condition in their cochleae, having low frequency hearing prior to the evolution of other signature mysticete characteristics including filter feeding, baleen and giant body size. Based on cochlear morphology alone, the similarity of archaic and modern mysticetes may signify that toothed mysticetes were capable of hearing infrasonic frequencies. However, as explained below, the other functional modules of the mysticete auditory pathway determine what frequencies actually reach the cochlea and likely restricted toothed mysticetes to low, but not necessarily infrasonic, frequencies.

The mysticete basicranium, unlike the cochlea, has undergone substantial transformation. Interestingly, this transformation only seems to have commenced in crown

Mysticeti, with the basicrania of eomysticetids and toothed mysticetes remaining essentially the same as that of basilosaurids. The changes that do occur in crown Mysticeti, namely the increased degree of ossification around the pterygoid sinuses and the increased contact of the tympanoperiotic bones with the rest of the skull (see Chapter 4 for more detail), are highly indicative of a change in how sounds are transmitted to the inner ear. The derived morphology suggests that bone conduction has become the primary method by which sounds reach the cochlea, although the presence of lateral fat pads in balaenopterids (Yamato et al. 2012) suggests that there may be more than one pathway in use in mysticetes, with the lateral fat pathway facilitating the transmission of higher frequency sounds to the tympanoperiotic complex (Yamato & Pyenson 2015) (Fig 7.1). Similarly, the mysticete mandible has changed significantly, with the major structural changes occurring only within crown Mysticeti. The eventual loss of the enlarged mandibular foramen in all crown mysticete clades means that the mandible no longer possesses the fat pad which provided a preferential pathway for sounds to reach the middle ear that was present in eomysticetids and toothed mysticetes. Similar to the results of the study on odontocetes in Chapter 6, this indicates that the primary driver of mandible morphology is feeding rather than hearing, adding further evidence that some other means of sound conduction is being used in crown mysticetes.
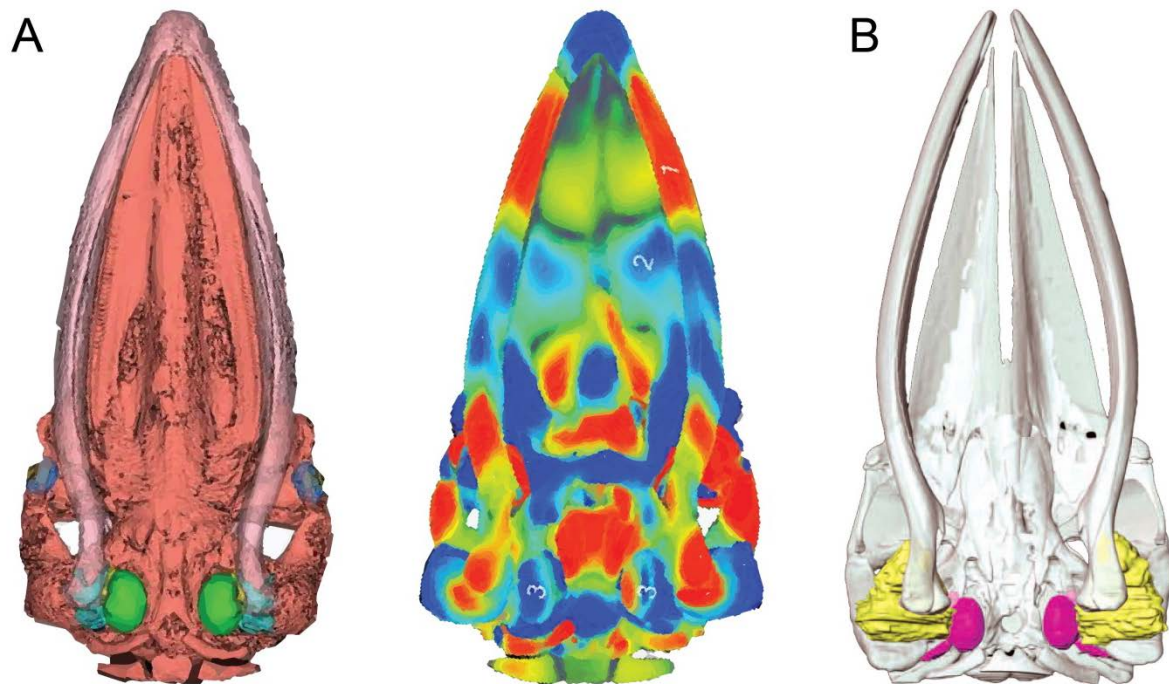
Fig 7.1. Possible auditory pathways in modern mysticetes. A, bone conduction: 3D model of a neonate skull of *Balaenoptera physalus* (left & middle) and the deformation pattern as the skull bones interact with an incoming 3 kHz underwater acoustic pressure wave (right). Images from Cranford & Krysl (2015). B, Acoustic fats: Skull of *B. acutorostrata* showing the ear fats (yellow) and the tympano-periotic complex (pink). Image from Yamato et al. (2012). Images used under a CC-BY license from PLoS ONE and Wiley respectively.

Taking the above into consideration, it is therefore unlikely that toothed mysticetes could hear infrasonic frequencies. The long wavelength of infrasonic soundwaves and relatively small size of toothed mysticete skulls and mandibular fat pads coupled with the lack of adaptations listed above seen in more derived mysticetes would have made it unlikely that toothed mysticetes were capable of detecting infrasonic sounds. Their cochlear morphology, on the other hand, suggests that had they somehow been able to intercept the infrasonic soundwaves and transmit them to the inner ear, they would have been capable of hearing infrasonic sounds. The physical properties of soundwaves suggest that mysticetes may require a skull of a minimum size in order to detect infrasonic frequencies, although this idea needs to be explicitly tested. Although low frequency hearing was present in small-bodied toothed mysticetes, infrasonic hearing may only have evolved after mysticetes evolved the much larger body sizes seen in crown taxa.

7.2. Evolution of odontocete hearing

The ancestral condition of hearing for Neoceti is low frequency. Early mysticetes retained this plesiomorphic condition (see Chapter 2) but odontocetes evolved extremely derived high frequency hearing used for echolocation. The exact timing and sequence of this process remains to be determined, but the cranial morphology of described fossil odontocetes suggest that they had at least an incipient form of the air sacs required to produce high frequency sounds necessary for echolocation. In Chapter 5 of this thesis I confirm for the first time that the Xenorophidae, one of the most basal lineages of odontocete, possess cochlear adaptations for detecting high frequency sounds. This finding coupled with the presence of premaxillary sac fossae for housing the epicranial air sinuses makes it highly likely that they were capable of echolocation.

The rapid adaptation of the odontocete cochlea is mirrored by the rest of their anatomy, with even the earliest odontocetes possessing most odontocete synapomorphies. Stem odontocetes do, however, show remarkable diversity and disparity, displaying various degrees of cranial telescoping, polydonty, homodonty and development of the pterygoid sinus system. Future work should aim to determine if there are also differences in the cochlear morphology of these taxa and establish whether there is a functional relationship between cochlear shape and these other anatomical features, which could indicate different auditory regimes. An initial step toward this would be to look at modern odontocetes and establish whether there is a functional relationship between cochlear shape and particular cranial adaptations and hearing abilities, forming the basis for comparisons in fossil taxa. There have been some studies that have correlated aspects of cochlear morphology (e.g. length of secondary spiral lamina, cochlea height, number of turns) with peak frequency and even habitat preference (Ketten 1992,2000; Gutstein et al. 2014). However, the three-dimensional

shape of the cochlea and its relationship to these and multiple other factors (e.g. diet, dive depth, cranial anatomy) are yet to be explored.

Further attention should also be given to the hearing abilities of xenorophids. Geisler et al. (2014) demonstrated that the posterior migration of the frontals, maxillae and premaxillae in xenorophids occurred in parallel to that of the stem Odontoceti (Fig 7.2). It may be hypothesised that their cochleae will also display similar convergent evolution towards specialised high frequency hearing. The only named xenorophid whose cochlear anatomy has been described is *Echovenator sandersi* (Churchill et al. 2016). In order to test this hypothesis the cochleae of both more derived (e.g. *Cotylocara*) and more basal (*Xenorophus*) taxa should be described and compared.

A final point of speculation is the acoustic biology of odontocete lineages that are more basal than xenorophids. Recent phylogenetic studies have indicated that the Ashleycetidae and potentially even the Mirocetidae are more basal than xenorophids (Sanders & Geisler 2015; Godfrey et al. 2016). There are also reports of extremely archaic odontocetes from the Northwest Pacific region (Barnes et al. 2001). Given their proximity to a low frequency ancestor, it is possible that the cochleae of these earliest odontocetes may display fewer (or even no) adaptations for high frequency hearing compared to xenorophids and other more crownward taxa. Determining this will require the description of ashleycetid and mirocetid cochleae, as well as additional primitive odontocete taxa to be studied and named.
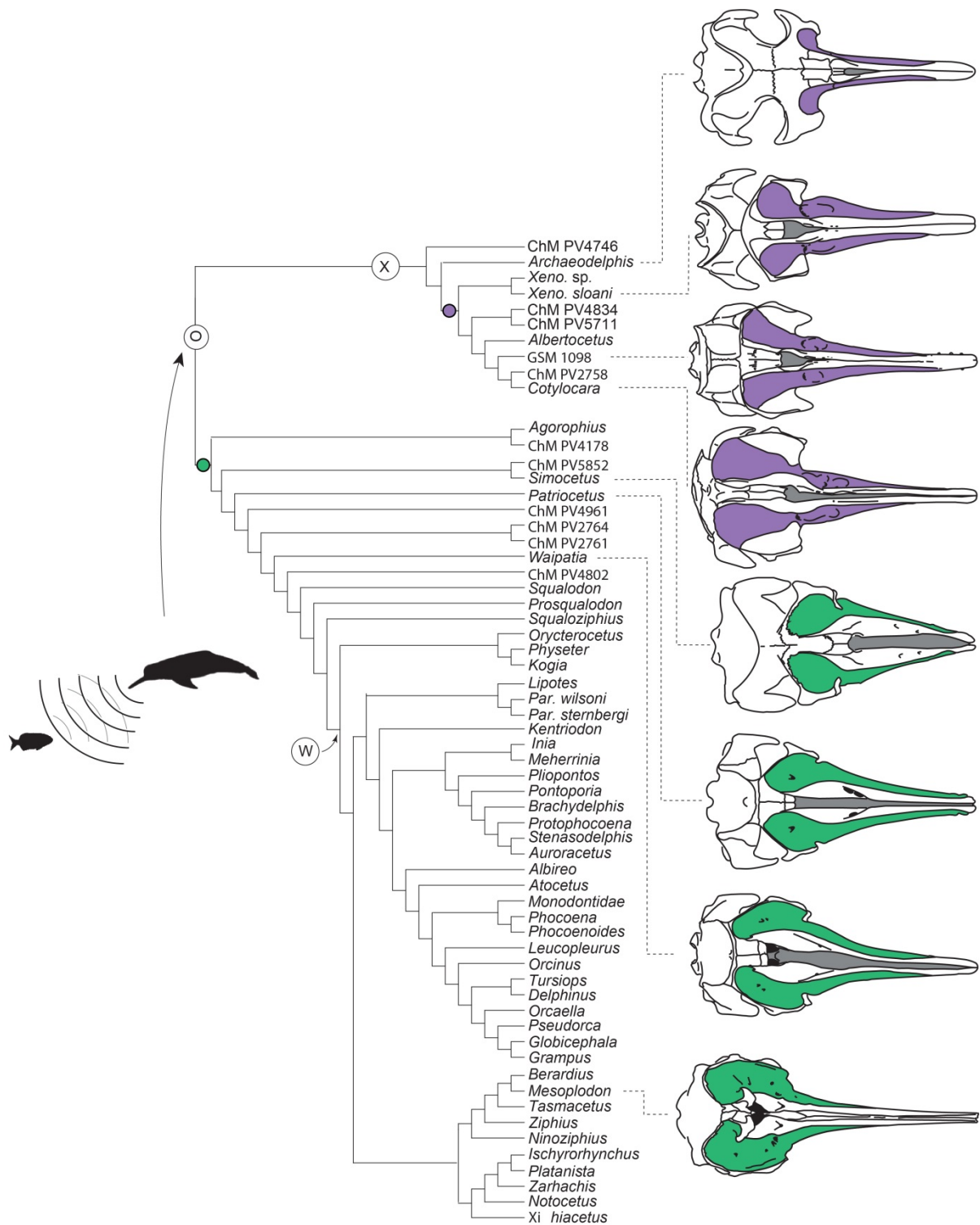
Fig 7.2. Phylogeny and skull drawings illustrating the convergent evolution of the craniofacial region in xenorophids and other odontocetes. Purple indicates elaboration of maxillae in xenorophids and green represents convergent elaboration of maxillae in crown-lineage odontocetes. O, Odontoceti; W, crown Odontoceti; X, Xenorophidae. Image adapted from Geisler et al. (2014).

7.3. Evolution of the tympanal recess

The radial expansion of the scala tympani, also known as the tympanal recess, appears to be an apomorphy of Neoceti. Despite Fleischer (1976) reporting a substantial tympanal recess in *Physeter macrocephalus*, Ekdale (2013) and Ekdale & Racicot (2015) state that the feature is only present in balaenopteroids (balaenopterids + eschrichtiids) and the extinct cetotheriid *Herpetocetus*. More recent research has also identified the feature in *Metopocetus*, *Piscobalaena* and *Cephalotropis* as well as an indeterminate early odontocete and toothed mysticete (Churchill et al. 2016; Ekdale 2016). However, following the definition of the tympanal recess given in Chapter 2, where any radial expansion of the scala tympani that exceeds the basal quarter turn is classed as a tympanal recess, I do not consider there to be a tympanal recess in the toothed mysticete cochlea figured by Ekdale (2016: Fig 3) (ChM P5720).This thesis has further shown a distinct tympanal recess not only occurs in the taxa mentioned above, but also *Caperea marginata* and in several odontocetes (*Physeter* and ziphiids). This scattered distribution across Neoceti confounds potential functional explanations of its evolution. Below I discuss several hypotheses that could have driven the evolution of the tympanal recess.

Body size: it may be possible that the tympanal recess is a result of the evolution of the extreme body size seen in most modern mysticetes, with the scala tympani disproportionately expanding in size as the animals became larger. Whilst this could account for the evolution of the feature in balaenopteroids and physeterids which reach lengths of 33 m and 16 m respectively (Berta et al. 2015), it does not explain the development of a tympanal recess in the much smaller *C. marginata*, *Mesoplodon grayi* and *Tasmacetus shepherdi*. Size does not appear to be the driving factor, unless these relatively small extant taxa have inherited and retained a tympanal recess from larger-bodied ancestors.

Dive depth: an expanded scala tympani could be an adaptation that allows the cochlea to function at extreme depth, which in physeterids and ziphiids can be 2000 m and 3000 m respectively (Watkins et al., 1993; Schorr et al., 2014). This, however, does not explain the presence of the tympanal recess in baleen whales, which do not dive further than 350 m (Curry & Brownell Jr 2014). Furthermore, some odontocete taxa such as *Kogia breviceps* dive deeper (up to 1200 m (McAlpine 2014)) than mysticete taxa that possess a tympanal recess, yet do not possess a tympanal recess themselves.

Reduction of hydrodynamic distortion: Fleischer (1976) hypothesised that an expanded scala tympani reduces hydrodynamic distortion at high sound intensities in the cochlear fluid. Whilst this could help explain how cetacean ears can handle the extremes in wavelengths and intensities that they have become specialised for, it does not account for the fact that some taxa lack a tympanal recess and yet also encounter the same intensities in hearing (Au & Hastings 2008).

Feeding ecology: could the manner in which a cetacean feeds influence cochlear morphology and drive the evolution of the tympanal recess? Another part of the auditory pathway has been previously linked with specialisations in feeding ecology. Yamato & Pyenson (2015) found that balaenopteroids possess laterally facing acoustic funnels and parallel tympanic bullae, linking this morphology to the specialised lunge-feeding seen in rorquals. Interestingly, a common feature of the feeding of taxa that possess a tympanal recess is a rapid opening of the mouth, with balaenopterids being lunge feeders (Lambertsen et al. 2005; Goldbogen et al. 2006,2007) and eschrichtiids, physeterids and ziphiids being suction feeders. All taxa with a tympanal recess have some form of throat grooves thought to increase the capacity of the oral cavity. Crucially, in odontocetes, only sperm whales and beaked whales possess this feature (Norris 1968; Mead 2009). Exactly what the link between possessing throat grooves and rapidly opening your mouth and having tympanal recess

remains unclear, although it may be related to any sudden change in pressure level within the cochlear fluid of these animals as they rapidly open their mouths. The exception to this hypothesis, however, is *Caperea marginata*. Although it does possess throat grooves like all other tympanal recess-possessing taxa, it skim-feeds like balaenids, a method that does not employ a rapid opening of the oral cavity or generation of suction. It may be the case, however, that the tympanal recess in *C. marginata* is a result of phylogenetic constraint. Evidence for this comes from the fact that other cetotheriids, which possessed a tympanal recess (e.g. *Herpetocetus*), were also thought to have employed lateral suction feeding in a manner analogous to eschrichtiids (El Adli et al. 2014; Ekdale 2016) and that its disparate feeding ecology relative to other cetotheriids allowed it to survive when the rest of the lineage went extinct (Fordyce & Marx 2013).

Focusing acoustic energy: an earlier paper (Manoussaki et al. 2008) showed there is a strong relationship between low frequency hearing and the graded curvature of the cochlea, where the ratio of the radii of curvature from the basal and apical turns of the cochlear spiral is inversely proportional to the low frequency limit. Increasing the basal radius of the cochlea will therefore increase the value this ratio, allowing the animal to detect lower frequencies. It might appear, therefore, that this increase in the basal radius could theoretically be achieved by an expansion of the scala tympani (i.e. a tympanal recess). Whilst this appears to make sense, the physical pathway that an incoming sound takes in the inner ear makes this impossible. Sound travels to the apex of the cochlea via the scala vestibuli, passes through the helicotrema and then back down the cochlear spiral along the scala tympani (see introduction chapter for details on the scalae of the cochlea). Therefore, expanding the scala tympani will not help to focus acoustic energy towards the top of the cochlea as the vibrations are travelling in the wrong direction.

Vibroacoustic duct mechanism: A hypothetical solution to the previous issue is a novel route of cochlear stimulation known as the vibroacoustic duct mechanism, which was proposed by March et al. (2015). Rather than sounds reaching the cochlea via the middle ear bones in the traditional manner, the vibroacoustic duct mechanism instead transmits acoustic energy to the cochlea via the perilymphatic duct, entering the cochlea through the canaliculus cochleae (Fig 7.3). Vibrations will therefore travel to the cochlea apex via the scala tympani rather than the scala vestibuli, meaning that having a tympanal recess would be useful for focusing acoustic energy towards the apex. Whilst not all mysticete clades possess a tympanal recess, it is interesting to note that those that do not (i.e. balaenids) have more loosely coiled cochlear apices (Ekdale, 2016), perhaps using this morphology to achieve a similar effect as that of the tympanal recess. This mechanism therefore presents an alternative pathway for low frequency sounds to reach the cochlea, especially given that low frequency sounds are not sufficiently strong as an excitation mechanism on the tympanoperiotic complex for wavelengths longer than the body of the animal (Cranford & Krysl 2015). For example, for an animal 5 m in length, any sounds with a frequency lower than 320 Hz will not have an effect on the tympanoperiotic complex. In mysticetes in particular, the vibroacoustic duct mechanism would complement hypotheses of bone conduction, where acoustic energy is transmitted to the tympanoperiotic complex by vibration of the skull itself.
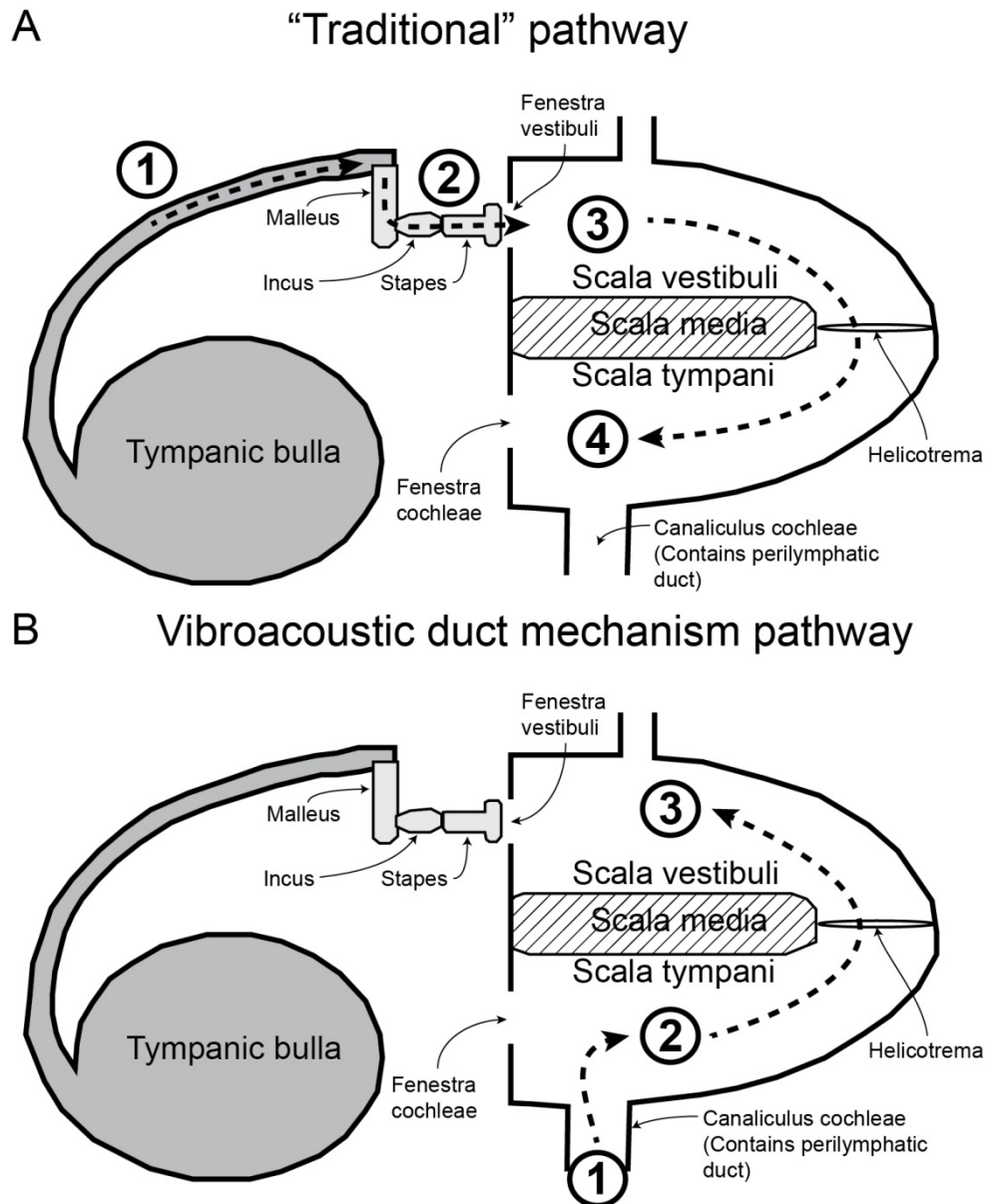
Fig 7.3. Schematic view of the tympanoperiotic complex demonstrating alternative routes of cochlear stimulation. A, the traditional pathway where vibrations of the tympanic bulla (1) set the middle ear ossicles into motion (2). The sound then travels to the cochlear apex via the scala vestibuli (3) before returning to the base via the scala tympani (4); B, the vibroacoustic mechanism where vibrations travel along the perilymphatic duct (1) and travel to the cochlear apex via the scala tympani (2) and returns to the base via the scala vestibuli (3).

March et al. (2015) initially proposed the vibroacoustic duct mechanism for a ziphiid, based on its hypertrophied canaliculus cochleae. They also noted that physeterids and ziphiids retain a bony connection to the skull through a pneumatized posterior process (Cranford & Krysl 2015; March et al. 2015). Combining these observations with the fact that *Physeter* and ziphiids also possess a tympanal recess, there is the tantalising possibility that

these odontocetes are also capable of detecting low frequencies using the bone conduction and vibroacoustic duct mechanisms. This hypothesis remains untested at present.

7.4. Estimating frequency ranges in cetaceans

One of the primary goals of this thesis has been to determine as accurately as possible what frequency ranges early neocetes were capable of detecting. There have been multiple methods employed with varying degrees of precision. Features such as number of turns and length of the secondary spiral laminae indicate general high versus low frequency abilities, although more accurate estimates of frequencies detected by living odontocetes coupled with secondary spiral laminae measurements may yet prove to be a useful indicator of interspecific differences in hearing abilities.

A more precise method of estimating low frequency limits was proposed by Manoussaki et al. (2008). The radii ratio, the radius of the cochlea at its base divided by the radius of the cochlea at its apex, is a value that when entered into the authors' equation, gives the lowest frequency a given mammal can detect. This has been employed by several other authors (Ekdale & Racicot 2015; Ekdale 2016; Ketten et al. 2016) and also in Chapters 2, 3 and 4 of this thesis. Results have thus far been generally consistent with previous estimates of low frequency limits. Nevertheless, estimates of low frequency limits in aquatic mammals using this equation should be considered tentative for now as it based primarily on the hearing of terrestrial animals in air. A useful avenue of future research would be to validate this equation using only aquatic mammals, something that may not be possible in the immediate future due to the lack of recorded audiograms for mysticetes.

A third method takes advantage of the fact that basilar membrane width is a proxy of basilar membrane stiffness, which is positively correlated with frequency i.e. the wider the membrane width, the lower the frequency. The strength of this relationship can be tested by linear regression (e.g. Ketten et al. 2016). As the basilar membrane is a soft tissue structure,

the basilar membrane width can also be estimated using the laminar gap (the distance between the primary and secondary bony laminae) in fossil taxa and modern specimens with skeletal material only. Whilst the laminar gap has been used to infer the width of the basilar membrane in the past (Fleischer 1976; Luo & Eastman 1995; Luo & Marsh 1996; Geisler & Luo 1996), Ketten (2000) cautions against using the laminar gap as a direct correlate of basilar membrane width, noting that membrane width can be overestimated by 110% at the base of the cochlea and 26% at the apex in mysticetes and odontocetes respectively.

In Chapter 2 I adapt this method in a novel manner by adjusting laminar gap measurements by the amount of the error margins stated by Ketten (2000) prior to performing the linear regressions, with the aim of improving the accuracy of basilar membrane width estimates from laminar gap measurements. These basilar membrane width estimates were then used to perform regressions of basal and apical membrane widths against maximum and minimum frequency limits respectively. Basal width and maximum frequency are strongly correlated ($R^2 = 0.7826$), whereas apical width and minimum frequency have a much weaker correlation ($R^2 = 0.2863$). Using the equations derived from these regressions I was then able to estimate the maximum and minimum frequency ranges of fossil taxa. It should be noted however, that the error margins given by Ketten (2000) each appear to be from either single specimens or perhaps only a few at most. Future work should increase this sample size using a broad sample of mysticete and odontocete species, determining whether there are different inter-specific and inter-ordinal relationships.

Lastly, an attempt to use the shape of the mandible to predict frequency ranges in Chapter 5 did not return any useful results. The methods listed above are, at present, the most accurate available.

References

Au WWL, Hastings HC. 2008. Principles of Marine Bioacoustics. Springer Science & Media LLC, New York, 679 p.

Barnes LG, Goedert JL, Furusawa H. 2001. The earliest known echolocating toothed whales (Mammalia; Odontoceti): preliminary observations of fossils from Washington State. Mesa Southwest Bulletin 8, 91–100.

Berta A, Sumich JL, Kovacs KM. 2015. Marine Mammals Evolutionary Biology (3rd ed). Academic Press, London, 726 p.

Churchill M, Martínez-Cáceres M, de Muizon C, Mnieckowski J, Geisler JH. 2016. The Origin of High-Frequency Hearing in Whales. Current Biology http://dx.doi.org/10.1016/j.cub.2016.06.004.

Cranford TW, Krysl P. 2015. Fin Whale Sound Reception Mechanisms: Skull Vibration Enables Low-Frequency Hearing. PLoS ONE 10, e0116222.

Curry BE, Brownell Jr RL. 2014. Balaenidae. In Wilson DE, Mittermeier RA, eds, Handbook of the mammals of the world 4: Sea mammals. Lynx Publishing, Barcelona, pp. 186–213.

Ekdale EG. 2013. Comparative anatomy of the bony labyrinth (inner ear) of placental mammals. PLoS ONE 8, e66624.

Ekdale EG. 2016. Morphological diversity among the inner ears of extinct and extant baleen whales (Cetacea: Mysticeti). Journal of Morphology 277, 1599–1615.

Ekdale EG, Racicot RA. 2015. Anatomical evidence for low frequency sensitivity in an archaeocete whale: comparison of the inner ear of *Zygorhiza kochii* with that of crown Mysticeti. Journal of Anatomy 226, 22–39.

El Adli JJ, Deméré TA, Boessenecker RW. 2014. *Herpetocetus morrowi* (Cetacea: Mysticeti), a new species of diminutive baleen whale from the Upper Pliocene

(Piacenzian) of California, USA, with observations on the evolution and relationships
of the Cetotheriidae. Zoological Journal of the Linnean Society 170, 400–466.

Fleischer G. 1976. Hearing in extinct cetaceans as determined by cochlear structure. Journal
of Paleontology 50, 133–152.

Fordyce RE, Marx FG. 2013. The pygmy right whale *Caperea marginata*: the last of the
cetotheres. Proceedings of the Royal Society B: Biological Sciences 280, 20122645.

Geisler JH, Luo ZX. 1996. The petrosal and inner ear of *Herpetocetus* sp. (Mammalia:
Cetacea) and their implications for the phylogeny of hearing of archaic mysticetes.
Journal of Paleontology 70, 1045–1066.

Geisler JH, Colbert MW, Carew JL. 2014. A new fossil species supports an early origin for
toothed whale echolocation. Nature 508, 383–386.

Godfrey SJ, Uhen MD, Osborne JE, Edwards LE. 2016. A new specimen of *Agorophius
pygmaeus* (Agorophiidae, Odontoceti, Cetacea) from the early Oligocene Ashley
Formation of South Carolina, USA. Journal of Paleontology 90, 154–169.

Goldbogen JA, Calambokidis J, Shadwick RE, Oleson EM, McDonald MA, Hildebraud JA.
2006. Kinematics of foraging dives and lunge-feeding in fin whales. Journal of
Experimental Biology 209, 1231–1244.

Goldbogen JA, Pyenson ND, Shadwick RE. 2007. Big gulps require high drag for fin whale
lunge feeding. Marine Ecology Progress Series 349, 289–301.

Gutstein CS, Figueroa-Bravo CP, Pyenson ND, Yury-Yañez RE, Cozzuol MA, Canals M.
2014. High frequency echolocation, ear morphology, and the marine–freshwater
transition: A comparative study of extant and extinct toothed whales.
Palaeogeography, Palaeoclimatology, Palaeoecology 400, 62–74.

Ketten DR, Arruda J, Cramer S, Yamato M. 2016. Great ears: Low-frequency sensitivity
correlates in land and marine leviathans. In Popper AN, Hawkins A, eds, The Effects

of Noise on Aquatic Life II. Springer Science & Business Media, New York, pp. 529–538.

Lambertsen RH, Ulrich N, Straley J. 2005. Functional morphology of the mouth of the bowhead whale and its implications for conservation. Journal of Mammalogy 82, 342–353.

Luo ZX, Eastman ER. 1995. Petrosal and inner ear of a squalodontoid whale: implications for evolution of hearing in odontocetes. Journal of Vertebrate Paleontology 15, 431–442.

Luo ZX, Marsh K. 1996. Petrosal (periotic) and inner ear of a Pliocene kogiine whale (Kogiinae, Odontoceti): Implications on relationships and hearing evolution of toothed whales. Journal of Vertebrate Paleontology 16, 328–348.

Manoussaki D, Chadwick RS, Ketten DR, Arruda J, Dimitriadis EK, O'Malley JT. 2008. The influence of cochlear shape on low-frequency hearing. Proceedings of the National Academy of Sciences 105, 6162–6166.

March D, Brown D, Gray R, Curthoys I, Wong C, Higgins DP. 2015. Auditory anatomy of beaked whales and other odontocetes: Potential for cochlear stimulation via a "vibroacoustic duct mechanism". Marine Mammal Science 32, 552–567.

McAlpine DF. 2014. Kogiidae. In Wilson DE, Mittermeier RA, eds, Handbook of the mammals of the world 4: Sea mammals. Lynx Publishing, Barcelona, pp. 318–325.

Mead JG. 2009. Beaked Whales, Overview (Ziphiidae). In Perrin WF, Wursig B, Thewissen JGM, eds, Encyclopedia of Marine Mammals (2nd ed). Academic Press, Burlington, pp. 94–97.

Norris KS. 1968. The evolution of acoustic mechanisms in odontocete cetaceans. In Drake ET, ed, Evolution and environment, Yale University Press, New Haven, pp. 297–324.

Sanders AE, Geisler JH. 2015. A new basal odontocete from the Upper Rupelian of South

Carolina, U.S.A., with contributions to the systematics of *Xenorophus* and *Mirocetus*

(Mammalia, Cetacea). Journal of Vertebrate Paleontology 35, e890107.

Watkins WA, Daher MA, Fristrup KM, Howald TJ. 1993. Sperm whales tagged with

transponders and tracked underwater by sonar. Marine Mammal Science 9, 55–67.

Yamato M, Pyenson ND. 2015. Early development and orientation of the acoustic funnel

provides insight into the evolution of sound reception pathways in cetaceans. PLoS

ONE 10, e0118582.

Yamato M, Ketten DR, Arruda J, Cramer S, Moore K. 2012. The auditory anatomy of the

minke whale (Balaenoptera acutorostrata): a potential fatty sound reception pathway

in a baleen whale. Anatomical Record 295, 991–998.

8. Conclusions

The two living cetacean groups Odontoceti (toothed whales) and Mysticeti (baleen whales) have highly disparate acoustic capabilities, with odontocetes hearing and producing ultrasonic signals for echolocation, and mysticetes possessing low frequency or infrasonic hearing and vocalisations. While fossil evidence shows that the earliest cetaceans (archaeocetes) possessed low frequency hearing and archaic odontocetes likely used high frequency echolocation, there is a fundamental lack of data on hearing in the earliest phase of mysticete evolution, which included the critical transition from predation using teeth to filtering with baleen. This thesis investigated the morphological basis for underwater hearing in these toothed mysticetes plus related aspects of hearing in other Neoceti that provide greater context to the evolution of hearing in the group. The thesis achieved this by examining the auditory pathway in toothed mysticetes as three functional modules: the mandible, the basicranium/middle ear, and the inner ear. This thesis fills this critical gap in our knowledge of cetacean hearing.

Toothed mysticetes possess a cochlear morphology very similar to those of basilosaurids and modern mysticetes, indicating that they could detect low frequency sounds and lacked the ability to echolocate. This suggests that toothed mysticetes retained the plesiomorphic condition in their cochleae and that their inner ears have remained relatively unchanged over the last 34 million years, having low frequency hearing prior to the evolution of other signature mysticete characteristics including filter feeding, baleen and giant body size, with the high frequency hearing of odontocetes being derived.

Building on the techniques used to examine the inner ears of toothed mysticetes in Chapter 2, I performed the first anatomical description of the cochlea of the pygmy right whale (*Caperea*). This now means that every living genus of mysticete has an anatomical description of its inner ear. Comparing it to modern and fossil mysticetes with the hope of

resolving ongoing confusion over its phylogenetic position, I found that the shape of the cochlea is consistent with the detection of low frequency sounds but the variability of features on the cochlea mean it does not shed new light on its phylogenetic position.

Looking at another functional module of the toothed mysticete auditory pathway, the basicranium, I found that the overall plesiomorphic morphology of basilosaurids is retained in toothed mysticetes and even eomysticetids, mirroring the pattern established for toothed mysticete cochleae in Chapter 2. It is only with the advent of crown mysticetes that extensive modifications to both the air sinuses around the ear bones and the level of articulation of the ear bones with the skull. It appears that toothed mysticetes and eomysticetids therefore shared the same auditory pathway as basilosaurids, which in turn is the same as odontocetes, where sounds were transmitted to the middle and inner ear via the acoustic fat pad in the enlarged mandibular foramen. Modern mysticetes, on the other hand, display substantial changes in their basicranial morphology that are indicative of a switch to using bone conduction as the primary method of directing sounds to the middle and inner ear, although a secondary pathway incorporating acoustic fats is also employed. Despite the similarity of toothed mysticete and modern mysticete cochleae, I predict that the switch to predominantly using bone conduction was the evolutionary innovation that enabled mysticetes to detect infrasonic frequencies and that toothed mysticetes could hear low but not infrasonic frequencies.

Toothed mysticetes probably shared a common entry point of the auditory pathway with basilosaurids, other fossil mysticetes and odontocetes: a large fat pad housed in the expanded mandibular foramen. However, odontocetes hear high frequency sounds whereas archaeocetes and toothed mysticetes were sensitive to low frequency sounds as demonstrated by their cochleae and basicrania. I therefore tested whether there was a relationship between mandible shape and the frequencies that an odontocete can detect using 3D geometric morphometrics. The results indicate that there is a weak relationship between some aspects of

the shape of the mandibular foramen and frequency range, but overall mandible shape is influenced much more strongly by feeding ecology.

Finally, I established in Chapter 2 that mysticetes had cochleae adapted for detecting low frequencies in the earliest members of their lineage. However, it had yet to be confirmed whether the earliest odontocetes had cochleae capable of detecting the high frequencies used in echolocation. To determine this I examined the cochlea of an Oligocene xenorophid, one of the earliest diverging stem odontocete groups. I showed that archaic odontocetes had a cochlea specialized for sensing high-frequency sound, indicating that the most archaic toothed whales possessed a functional biosonar system, contrasting with the plesiomorphic low frequency cochleae seen in early mysticetes. The acoustic abilities of both neocete groups were established soon after their divergence.

This thesis has provided a new understanding of the evolution of hearing in cetaceans by combining traditional anatomical studies and more recent quantitative and statistical analytical techniques. I have endeavoured to synthesise my own research with multiple lines of evidence on both fossil and modern cetaceans in order to produce a model of how the mysticete auditory pathway has changed over time. Likewise, I have confirmed just how rapidly odontocetes adapted to high frequency hearing and echolocation.

There are still many questions that remain unanswered; many of which concern living cetaceans, whose acoustic biology we still do not comprehend. Promisingly, the field of cetacean acoustics as a whole is undergoing a surge in research effort as new technologies are being applied to these unanswered questions. Ascertaining how living species hear sound is a necessary prerequisite for addressing how it has evolved. As we gain a clearer picture of this, the hypotheses presented in this thesis can be tested more fully. Thinking more broadly, the skills I have acquired in the completion of this body of work can be applied to other aquatic mammals, and the investigation of their sensory systems. Aquatic mammal sensory evolution

is an area rich with the promise of new discoveries. I look forward to being a part of that quest.

References

Adams DC, Otarola-Castillo E. 2016. geomorph: an R package for the collection and analysis of geometric morphometric shape data. Methods in Ecology and Evolution 4, 393–399.

Allin EF, Hopson JA. 1992. Evolution of the Auditory System in Synapsida ("Mammal-Like Reptiles" and Primitive Mammals) as Seen in the Fossil Record. In Webster DB, Fay RR, Popper AN, eds, The Evolutionary Biology of Hearing. Springer-Verlag, New York, pp. 587–614.

Andersen S. 1970. The auditory sensitivity of the harbor porpoise, *Phocoena phocoena*. In Pilleri G, ed, Investigations on Cetacea, Berne-Bumpliz, Berne, pp. 255–259.

Aroyan JL. 2001. Three-dimensional modelling of hearing in *Delphinus delphis*. The Journal of the Acoustical Society of America 110, 3305–3318.

Au WWL, Hastings HC. 2008. Principles of Marine Bioacoustics. Springer Science & Media LLC, New York, 679 p.

Bajpai S, Thewissen JGM, Conley RW. 2011. Cranial Anatomy of Middle Eocene *Remingtonocetus* (Cetacea, Mammalia) from Kutch, India. Journal of Paleontology 85, 703–718.

Barnes LG, Goedert JL, Furusawa H. 2001. The earliest known echolocating toothed whales (Mammalia; Odontoceti): preliminary observations of fossils from Washington State. Mesa Southwest Bulletin 8, 91–100.

Barroso C, Cranford TW, Berta A. 2012. Shape analysis of odontocete mandibles: functional and evolutionary implications. Journal of Morphology 273, 1021–1030.

Berta A, Sumich JL, Kovacs KM. 2015. Marine Mammals Evolutionary Biology (3rd ed). Academic Press, London, 726 p.

Bischoff N, Nickle B, Cronin TW, Velasquez S, Fasick JI. 2012. Deep-sea and pelagic rod visual pigments identified in the mysticete whales. Visual Neuroscience 29, 95–103.

Bisconti M. 2006. *Titanocetus*, a new baleen whale from the Middle Miocene of northern Italy (Mammalia, Cetacea, Mysticeti). Journal of Vertebrate Paleontology 26, 344–354.

Bisconti M. 2015. Anatomy of a new cetotheriid genus and species from the Miocene of Herentals, Belgium, and the phylogenetic and palaeobiogeographical relationships of Cetotheriidae s.s. (Mammalia, Cetacea, Mysticeti). Journal of Systematic Palaeontology 13, 377–395.

Bisconti M, Bosselaers M. 2016. *Fragilicetus velponi*: a new mysticete genus and species and its implications for the origin of Balaenopteridae (Mammalia, Cetacea, Mysticeti). Zoological Journal of the Linnean Society London 177, 450–474.

Bisconti M, Lambert O, Bosselaers M. 2013. Taxonomic revision of *Isocetus depauwi* (Mammalia, Cetacea, Mysticeti) and the phylogenetic relationships of archaic cetothere mysticetes. Palaeontology 56, 95–127.

Boessenecker RW, Fordyce RE. 2015. Anatomy, feeding ecology, and ontogeny of a transitional baleen whale: a new genus and species of Eomysticetidae (Mammalia: Cetacea) from the Oligocene of New Zealand. PeerJ 3, e1129.

Boessenecker RW, Fordyce RE. 2016. A new eomysticetid from the Oligocene Kokoamu Greensand of New Zealand and a review of the Eomysticetidae (Mammalia, Cetacea). Journal of Systematic Palaeontology http://dx.doi.org/10.1080/14772019.2016.1191045.

Brill RL, Sevenich ML, Sullivan TJ, Sustman JD, Witt RE. 1988. Behavioral evidence for hearing through the lower jaw by an echolocating dolphin (Tursiops truncatus). Marine Mammal Science 4, 223–230.

Buchholtz EA. 2011. Vertebral and rib anatomy in Caperea marginata: implications for

    evolutionary patterning of the mammalian vertebral column. Marine Mammal Science

    27, 382–397.

Bullock TH, Grinnell AD, Ikezono F, Kameda K, Katsuki Y, Nomoto M, Sato O, Suga N,

    Yanagisava K. 1968. Electrophysiological studies of the central auditory mechanisms

    in cetaceans. Zeitschrift für Vergleichende Physiologie 59, 117–156.

Carter RT, Adams RA. 2016. Integrating ontogeny of echolocation and locomotion gives

    unique insights into the origin of bats. Journal of Mammalian Evolution.

Churchill M, Berta A, Deméré TA. 2012. The systematics of right whales (Mysticeti:

    Balaenidae). Marine Mammal Science 28, 497-521.

Churchill M, Martínez-Cáceres M, de Muizon C, Mnieckowski J, Geisler JH. 2016. The

    Origin of High-Frequency Hearing in Whales. Current Biology

    http://dx.doi.org/10.1016/j.cub.2016.06.004.

Clementz MT, Goswami A, Gingerich PD, Koch PL. 2006. Isotopic records from early

    whales and sea cows: contrasting patterns of ecological transition. Journal of

    Vertebrate Paleontology 26, 355–70.

Costidis A, Rommel SA. 2012. Vascularization of Air Sinuses and Fat Bodies in the Head of

    the Bottlenose Dolphin (*Tursiops truncatus*): Morphological Implications on

    Physiology. Frontiers in Physiology 3, 243.

Cranford TW, Krysl P. 2015. Fin Whale Sound Reception Mechanisms: Skull Vibration

    Enables Low-Frequency Hearing. PLoS ONE 10, e0116222.

Cranford TW, Amundin M, Norris KS. 1996. Functional morphology and homology in the

    odontocete nasal complex: Implications for sound generation. Journal of Morphology

    228, 223–285.

Cranford TW, Krysl P, Hildebrand JA. 2008. Acoustic pathways revealed: Simulated sound transmission and reception in Cuvier's beaked whale (*Ziphius cavirostris*). Bioinspiration & Biomimetics 3, 1–10.

Cranford TW, Krysl P, Amundin M. 2010. A new acoustic portal into the odontocete ear and vibrational analysis of the tympanoperiotic complex. PLoS ONE 5, e11927.

Cummings WC, Thompson PO. 1971. Underwater sounds from the blue whale, *Balaenoptera musculus*. The Journal of the Acoustical Society of America 50, 1193–1198.

Curry BE, Brownell Jr RL. 2014. Balaenidae. In Wilson DE, Mittermeier RA, eds, Handbook of the mammals of the world 4: Sea mammals. Lynx Publishing, Barcelona, pp. 186–213.

Deméré TA, Berta A. 2008. Skull anatomy of the Oligocene toothed mysticete *Aetiocetus weltoni* (Mammalia; Cetacea): implications for mysticete evolution and functional anatomy. Zoological Journal of the Linnean Society of London 154, 302–352.

Deméré TA, McGowen MR, Berta A, Gatesy J. 2008. Morphological and molecular evidence for a stepwise evolutionary transition from teeth to baleen in mysticete whales. Systematic Biology 57, 15–37.

Denny MW. 1993. Air and water: the biology and physics of life's media. Princeton University Press, New Jersey, 341 p.

Echteler SM, Fay RR, Popper AN. 1994. Structure of the Mammalian Cochlea. In Fay RR, Popper AN, eds, Comparative Hearing: Mammals. Springer-Verlag, New York, pp. 134–171.

Ekdale EG. 2013. Comparative anatomy of the bony labyrinth (inner ear) of placental mammals. PLoS ONE 8, e66624.

Ekdale EG. 2016. Form and function of the mammalian inner ear. Journal of anatomy. 228, 324–337.

Ekdale EG. 2016. Morphological diversity among the inner ears of extinct and extant baleen whales (Cetacea: Mysticeti). Journal of Morphology 277, 1599–1615.

Ekdale EG, Racicot RA. 2015. Anatomical evidence for low frequency sensitivity in an archaeocete whale: comparison of the inner ear of *Zygorhiza kochii* with that of crown Mysticeti. Journal of Anatomy 226, 22–39.

Ekdale EG, Berta A, Deméré TA. 2011. The Comparative Osteology of the Petrotympanic Complex (Ear Region) of Extant Baleen Whales (Cetacea: Mysticeti). PLoS ONE 6, e21311.

El Adli JJ, Deméré TA, Boessenecker RW. 2014. *Herpetocetus morrowi* (Cetacea: Mysticeti), a new species of diminutive baleen whale from the Upper Pliocene (Piacenzian) of California, USA, with observations on the evolution and relationships of the Cetotheriidae. Zoological Journal of the Linnean Society London 170, 400–466.

Evans, HE. 1993. The ear. In Evans HE, ed, Miller's Anatomy of the Dog, (3rd ed). Saunders, Philadelphia, pp. 988–1008.

Fahlke J, Gingerich PD, Welsh RC, Wood AR. 2011. Cranial asymmetry in Eocene archaeocete whales and the evolution of directional hearing in water. Proceedings of the National Academy of Sciences 108, 14545–14548.

Fitzgerald EMG. 2006. A bizarre new toothed mysticete (Cetacea) from Australia and the early evolution of baleen whales. Proceedings of the Royal Society B: Biological Sciences 273, 2955–2963.

Fitzgerald EMG. 2010. The morphology and systematics of *Mammalodon colliveri* (Cetacea: Mysticeti), a toothed mysticete from the Oligocene of Australia. Zoological Journal of the Linnean Society 158, 367–476.

Fitzgerald EMG. 2012 Possible neobalaenid from the Miocene of Australia implies a long evolutionary history for the pygmy right whale *Caperea marginata* (Cetacea, Mysticeti). Journal Vertebrate Paleontology 32, 976–980.

Fleischer G. 1975. Über das spezialisierte Gehörorgan von Kogia breviceps (Odontoceti). Zeitschrift für Säugetierkunde, 40, 89–102.

Fleischer G. 1976. Hearing in extinct cetaceans as determined by cochlear structure. Journal of Paleontology 50, 133–152.

Fleischer G. 1976. Über Beziehungen zwischen Hörvermögen und Schädelbau bei Walen. Säugetierkundliche Mitteilungen 24, 48–59.

Fleischer G. 1978. Evolutionary Principles of the Mammalian Middle Ear. Advances in Anatomy, Embryology, and Cell Biology, 55, 1–70.

Fordyce RE. 1994. *Waipatia maerewhenua*, new genus and new species (Waipatiidae, new Family), an archaic Late Oligocene dolphin (Cetacea: Odontoceti: Platanistoidea) from New Zealand. In Berta A, Deméré TA, eds, Contributions in marine mammal paleontology honoring Frank C. Whitmore, Jr. Proceedings of the San Diego Society of Natural History 29, 147–176.

Fordyce RE. 2002. *Simocetus rayi* (Odontoceti: Simocetidae, New Family): A bizarre new archaic Oligocene dolphin from the eastern Pacific. In Emry RE, ed, Cenozoic Mammals of Land and Sea, Tributes to the Career of Clayton E. Ray. Smithsonian Contributions to Paleobiology 93, 185–222.

Fordyce RE. 2009. Neoceti. In Perrin WF, Wursig B, eds, Encyclopaedia of Marine Mammals (2nd ed), Academic Press, London, pp. 758–763.

Fordyce RE, Marx FG. 2013. The pygmy right whale *Caperea marginata*: the last of the cetotheres. Proceedings of the Royal Society London B: Biological Sciences 280, 20122645.

Fordyce RE, de Muizon C. 2001. Evolutionary history of cetaceans: a review. In Mazin JM,

   Buffrénil, eds, Secondary Adaptation of Tetrapods to Life in Water. Verlag Dr.

   Fredrich Pfeil, Munich, pp. 169–233.

Fraas E. 1904. Neue Zeuglodonten aus dem unteren Mitteleociin vom Mokattam bei Cairo.

   Geologische und Palaontologische Abhandlungen, Jena, Neue Folge, 6, 197– 220.

Fraser FC, Purves PE. 1960. Hearing in cetaceans: Evolution of the accessory air sacs and the

   structure of the outer and middle ear in Recent cetaceans. Bulletin of the British

   Museum (Natural History), Zoology 7, 1–140.

Freckleton RP, Harvey PH, Pagel M. 2002. Phylogenetic analysis and comparative data: a

   test and review of evidence. American Naturalist 160, 712–726.

Geisler JH, Luo ZX. 1996. The petrosal and inner ear of *Herpetocetus* sp. (Mammalia:

   Cetacea) and their implications for the phylogeny of hearing of archaic mysticetes.

   Journal of Paleontology 70, 1045–1066.

Geisler JH, Sanders AE. 2003. Morphological evidence for the phylogeny of Cetacea. Journal

   of Mammalian Evolution 10, 23–129.

Geisler JH, Godfrey SJ, Lambert O. 2012. A new genus and species of late Miocene inioid

   (Cetacea, Odontoceti) from the Meherrin River, North Carolina, USA. Journal of

   Vertebrate Paleontology 32, 198–211.

Geisler JH, Colbert MW, Carew JL. 2014. A new fossil species supports an early origin for

   toothed whale echolocation. Nature 508, 383–386.

Gingerich, PD, Wells N, Russell D, Shah SM. 1983. Origin of whales in epicontinental

   remnant seas: new evidence from the early Eocene of Pakistan. Science 220, 403–

   406.

Gingerich PD, Arif M, Clyde WC. 1995. New archaeocetes (Mammalia, Cetacea) from the

   middle Eocene Domanda Formation of the Sulaiman Range, Punjab (Pakistan).

Contributions of the Museum of Paleontology of the University of Michigan 29, 291–
330.

Gingerich PD, Haq MU, Zalmout IS, Khan IH, Malakani MS. 2001. Origin of whales from
early artiodactyls: hands and feet of Eocene Protocetidae from Pakistan. Science 293,
2239–2242.

Gingerich PD, ul-Haq M, von Koenigswald W, Sanders WJ, Smith BH, Zalmout ES. 2009.
New protocetid whale from the middle Eocene of Pakistan: birth on land, precocial
development, and sexual dimorphism. PLoS One 4, e4366.

Godfrey SJ, Uhen MD, Osborne JE, Edwards LE. 2016. A new specimen of *Agorophius
pygmaeus* (Agorophiidae, Odontoceti, Cetacea) from the early Oligocene Ashley
Formation of South Carolina, USA. Journal of Paleontology 90, 154–169.

Goldbogen JA, Calambokidis J, Shadwick RE, Oleson EM, McDonald MA, Hildebraud JA.
2006. Kinematics of foraging dives and lunge-feeding in fin whales. Journal of
Experimental Biology 209, 1231–1244.

Goldbogen JA, Pyenson ND, Shadwick RE. 2007. Big gulps require high drag for fin whale
lunge feeding. Marine Ecology Progress Series 349, 289–301.

Gol'din P, and Steeman ME. 2015. From problem taxa to problem solver: a new Miocene
family, Tranatocetidae, brings perspective on baleen whale evolution. PLoS ONE 10,
e0135500.

Goswami A. 2006. Cranial modularity shifts during mammalian evolution. American
Naturalist 168, 270–280.

Grafen A. 1989. The phylogenetic regression. Philosophical Transactions of the Royal
Society B: Biological Sciences 326, 119–157.

Gutstein CS, Figueroa-Bravo CP, Pyenson ND, Yury-Yañez RE, Cozzuol MA, Canals M.
2014. High frequency echolocation, ear morphology, and the marine–freshwater

transition: A comparative study of extant and extinct toothed whales. Palaeogeography, Palaeoclimatology, Palaeoecology 400, 62–74.

Heyning JE. 1989. Comparative facial anatomy of beaked whales (Ziphiidae) and a systematic revision among the families of extant Odontoceti. Contributions in Science, Natural History Museum of Los Angeles County 405, 1–64.

Hooker SK. 2009. Toothed Whales, Overview. In Perrin WF, Wursig B, eds, Encyclopaedia of Marine Mammals (2nd ed), Academic Press, London, pp. 1173–1179.

Houser DS, Finneran JJ. 2006. A comparison of underwater hearing sensitivity in bottlenosed dolphins (*Tursiops truncatus*) determined by electrophysiological and behavioural methods. The Journal of the Acoustical Society of America 120, 1713–1722.

Hulbert Jr RC 1998a. Postcranial osteology of the North American middle Eocene protocetid *Georgiacetus*. In Thewissen JGM, ed, The Emergence of Whales, Evolutionary Patterns in the Origin of Cetacea. Plenum Press, New York, pp. 235–267.

Hulbert Jr RC, Petkewich RM, Bishop GA, Bukry D, Aleshire DP, 1998b. A new middle Eocene protocetid whale (Mammalia: Cetacea: Archaeoceti) and associated biota from Georgia. Journal of Paleontology 72, 907–27.

Jacobs DW, Hall JD. 1972. Auditory thresholds of a freshwater dolphin, *Inia geoffrensis* Blainville. The Journal of the Acoustical Society of America 51, 530–533.

Jefferson TA, Webber MA, Pitman RL. 2008. Marine mammals of the world: A comprehensive guide to their identification. Academic Press, San Diego, 592 p.

Kasuya T. 1973. Systematic consideration of recent toothed whales based on morphology of tympanoperiotic bone. Scientific Reports of the Whale Research Institute, Tokyo, 25, 1–103.

Kellogg AR. 1924. Description of a new genus and species of whalebone whale from the Calvert Cliffs, Maryland. Proceedings of the United States National Museum 63, 1–14.

Kellogg R. 1928. The history of whales—Their adaptation to life in the water (concluded). The Quarterly Review of Biology 3, 174–208.

Kellogg AR. 1936. A review of the Archaeoceti. Carnegie Institution of Washington Publication 482, 1–366.

Kellogg AR. 1968. Fossil marine mammals from the Miocene Calvert Formation of Maryland and Virginia: Part 6. A hitherto unrecognized Calvert cetothere. United States National Museum Bulletin 247, 133–161.

Kellogg AR. 1969. Cetothere skeletons from the Miocene Choptank Formation of Maryland and Virginia. United States National Museum Bulletin 294, 1–40.

Kemper CM. 2009. Pygmy right whale *Caperea marginata*. In: Perrin WF, Würsig B, Thewissen JGM, eds, Encyclopedia of Marine Mammals, (2nd ed). Academic Press, Burlington, pp. 939–941.

Kemper CM, Middleton JF, van Ruth PD. 2012. Association between pygmy right whales (*Caperea marginata*) and areas of high marine productivity off Australia and New Zealand. New Zealand Journal of Zoology 40, 102–128.

Ketten DR. 1992. The marine mammal ear: specializations for aquatic audition and echolocation. In Webster DB, Fay RR, Popper AN, eds, The Evolutionary Biology of Hearing. Springer-Verlag, New York pp. 717–750.

Ketten DR. 1993. The cetacean ear: Form frequency and evolution. In Thomas JA, Kastelein RA, Supin AY, eds, Marine Mammal Sensory Systems. Springer Science & Business Media, New York, pp. 53–75.

Ketten DR. 1994. Functional analyses of whale ears: Adaptations for underwater hearing. IEEE Proceedings in Underwater Acoustics 1, 264–270.

Ketten DR. 1997. Structure and function in whale ears. Bioacoustics 8, 103–135.

Ketten DR. 2000. Cetacean ears. In Au WWL, Popper AN, Fay RR, eds, Hearing by whales and dolphins. Springer-Verlag, New York, pp. 43–108.

Ketten DR, Wartzok D. 1990. Three dimensional reconstructions of the dolphin ear. In Thomas JA, Kastelein RA, eds, Sensory abilities of Cetaceans. Plenum Press, New York, pp. 81–105.

Ketten DR, Arruda J, Cramer S, Yamato M. 2016. Great ears: Low-frequency sensitivity correlates in land and marine leviathans. In Popper AN, Hawkins A, eds, The Effects of Noise on Aquatic Life II. Springer Science & Business Media, New York, pp. 529–538.

Kimura T, Sakamoto O, Hasegawa Y. 1998. A cetothere from the Miocene Chichibumachi Group, Saitama Prefecture, Japan. Bulletin of Saitama Museum of Natural History 16, 1–13.

Klingenberg CP. 2016. Size, shape, and form: concepts of allometry in geometric morphometrics. Development Genes and Evolution 226, 113–137.

Klishin VO, Popov VV, Supin AY. 2000. Hearing capabilities of a beluga whale, *Delphinapterus leucas*. Aquatic Mammals 26, 212–228.

Kumar K, Sahni A. 1986. *Remingtonocetus harudiensis*, new combination, a middle Eocene archaeocete (Mammalia, Cetacea) from western Kutch, India. Journal of Vertebrate Paleontology 6, 326–349.

Lambert O, Bianucci G, Post K, de Muizon C, Salas-Gismondi R, Urbina M, Reumer J. 2010. The giant bite of a new raptorial sperm whale from the Miocene epoch of Peru. Nature 466, 105–108.

Lambertsen RH, Ulrich N, Straley J. 2005. Functional morphology of the mouth of the
bowhead whale and its implications for conservation. Journal of Mammalogy 82,
342–353.

Lancaster WC, Ary WJ, Krysl P, Cranford TW. 2015. Precocial development within the
tympanoperiotic complex in cetaceans. Marine Mammal Science 31, 369–75.

Lillie DG. 1910. Observations on the anatomy and general biology of some members of the
larger Cetacea. Proceedings of the Zoological Society of London 1910, 769–792.

Lillie DG. 1915. Cetacea. In, British Antarctic ("Terra Nova") Expedition, 1910. Natural
History Report Zoology British Museum (Natural History), London 3, 85–124.

Lilljeborg W. 1861. Hvalben funna i jorden på Gräsön I Roslagen i Sverige. Forhandlinger
ved de Skandinaviske Naturforskeres, Ottende Møde 8, 599–616.

Lindberg DR, Pyenson ND. 2007. Things that go bump in the night: Evolutionary
interactions between cephalopods and cetaceans in the Tertiary. Lethaia 40, 335–343.

Luo ZX. 1998. Homology and transformation of cetacean ectotympanic structures. In
Thewissen JGM, ed, The emergence of whales: evolutionary patterns in the origin of
Cetacea. Kluwer Academic/Plenum, New York, pp. 269–301.

Luo ZX, Eastman ER. 1995. Petrosal and inner ear of a squalodontoid whale: implications for
evolution of hearing in odontocetes. Journal of Vertebrate Paleontology 15, 431–442.

Luo ZX, Marsh K. 1996. Petrosal (periotic) and inner ear of a Pliocene kogiine whale
(Kogiinae, Odontoceti): Implications on relationships and hearing evolution of
toothed whales. Journal of Vertebrate Paleontology 16, 328–348.

Luo ZX, Gingerich PD. 1999. Terrestrial Mesonychia to aquatic Cetacea: transformation of
the basicranium and evolution of hearing in whales. University of Michigan Papers on
Paleontology 31, 1–98.

Lydekker R. 1894. Cetacean skulls from Patagonia. Anales del Museo de la Plata 2, 1–13.

MacPhee RD. 1981. Auditory regions of primates and eutherian insectivores. Contributions
to Paleobiology 18, 1–282.

Madar SI. 2007. The postcranial skeleton of early Eocene pakicetid cetaceans. Journal of
Paleontology 81, 176–200.

Manley GA. 2012. Evolutionary Paths to Mammalian Cochleae. Journal of the Association
for Research in Otarlaryngology 13, 733–743.

Mann D, Hill-Cook M, Manire C, Greenhow D, Montie E, Powell J, Wells R, Bauer G,
Cunningham-Smith P, Lingenfelser R, DiGiovanni R, Stone A, Brodsky M, Stevens
R, Kieffer G, Hoetjes P. 2010. Hearing loss in stranded odontocete dolphins and
whales. PLoS ONE 5, e13824.

Manoussaki D, Chadwick RS, Ketten DR, Arruda J, Dimitriadis EK, O'Malley JT. 2008. The
influence of cochlear shape on low-frequency hearing. Proceedings of the National
Academy of Sciences 105, 6162–6166.

March D, Brown D, Gray R, Curthoys I, Wong C, Higgins DP. 2015. Auditory anatomy of
beaked whales and other odontocetes: Potential for cochlear stimulation via a
"vibroacoustic duct mechanism". Marine Mammal Science 32, 552–567.

Marino L, Uhen MD, Frohlich B, Aldag JM, Blane C, Bohaska D, Whitmore Jr FC. 2000.
Endocranial volume of mid-late Eocene archaeocetes (Order: Cetacea) revealed by
computed tomography: implications for cetacean brain evolution. Journal of
Mammalian Evolution 7, 81–94.

Martínez-Cáceres M, de Muizon C. 2011. A new basilosaurid (Cetacea, Pelagiceti) from the
late Eocene to early Oligocene Otuma Formation of Peru. Comptes Rendus Palevol
10, 517–26.

Martins EP, Hansen TF. 1997. Phylogenies and the comparative method: a general approach to incorporating phylogenetic information into the analysis of interspecific data. American Naturalist 149, 646–667.

Marx FG, Fordyce RE. 2015. Baleen boom and bust: a synthesis of mysticete phylogeny, diversity and disparity. Royal Society Open Science 2, 140434.

Marx FG, Fordyce RE. 2016. A link no longer missing: New evidence for the cetotheriid affinities of *Caperea*. PLoS ONE 11, e0164059.

Marx FG, Tsai C-H, Fordyce RE. 2015. A new Early Oligocene toothed 'baleen' whale (Mysticeti: Aetiocetidae) from western North America: one of the oldest and the smallest. Royal Society Open Science 2, 150476.

Marx FG, Lambert O, Uhen MD. 2016. Cetacean Paleobiology. John Wiley & Sons, Chichester, 345 p.

Marx FG, Bosselaers MEJ, Louwye S. 2016. A new species of *Metopocetus* (Cetacea, Mysticeti, Cetotheriidae) from the Late Miocene of the Netherlands. PeerJ 4, e1572.

Marx FG, Hocking DP, Park T, Ziegler T, Evans AR, Fitzgerald EMG. 2016. Suction feeding preceded filtering in baleen whale evolution. Memoirs of Museum Victoria 75: 71–82.

McAlpine DF. 2014. Kogiidae. In Wilson DE, Mittermeier RA, eds, Handbook of the mammals of the world 4: Sea mammals. Lynx Publishing, Barcelona, pp. 318–325.

McGowen MR, Spaulding M, Gatesy J. 2009. Divergence date estimation and a comprehensive molecular tree of extant cetaceans. Molecular Phylogenetics and Evolution 53, 891–906.

Mead JG. 2009. Beaked Whales, Overview (Ziphiidae). In Perrin WF, Wursig B, Thewissen JGM, eds, Encyclopedia of Marine Mammals (2nd ed). Academic Press, Burlington, pp. 94–97.

Mead JG, Fordyce RE. 2009. The therian skull: a lexicon with emphasis on the odontocetes. Smithsonian Contributions to Zoology 627, 1–248.

Meredith RW, Gatesy J, Emerling CA, York VM, Springer MS. 2013. Rod monochromacy and the coevolution of cetacean retinal opsins. PLoS Genetics 9, e1003432.

Milinkovitch MC. 2005. Molecular phylogeny of cetaceans prompts revision of morphological transformations. Trends in Ecology and Evolution 10, 328–334.

Miller GS Jr. 1923. The telescoping of the cetacean skull. Smithsonian Miscellaneous Collections 76, 1–70.

Montgomery SH, Geisler JH, McGowen MR, Fox C, Marino L, Gatesy J. 2013. The evolutionary history of cetacean brain and body size. Evolution 67, 3339–3353.

Montie EW, Manire CA, Mann DA. 2011. Live CT imaging of sound reception anatomy and hearing measurements in the pygmy killer whale, *Feresa attenuata*. The Journal of Experimental Biology 214, 945–955.

Mooney TA, Yamato M, Branstetter BK. 2012. Hearing in Cetaceans: From Natural History to Experimental Biology. Advances in Marine Biology 63, 197–246.

Muller, J. 1954. Observations on the orbital region of the skull of the Mystacoceti. Zoologische Mededelingen (Leiden) 32, 279–290.

Nachtigall PE, Yuen MML, Mooney TA, Taylor KA. 2005. Hearing measurements from a stranded infant Risso's dolphin, *Grampus griseus*. The Journal of Experimental Biology 208, 4181–4188.

Norris KS. 1964. Some problems of echolocation in cetaceans. In Tavolga WN, ed, Marine Bioacoustics. Pergamon, New York, pp. 316–336.

Norris KS. 1968. The evolution of acoustic mechanisms in odontocete cetaceans. In Drake ET, ed, Evolution and environment, Yale University Press, New Haven, pp. 297–324.

Norris KS, Harvey GW. 1974. Sound transmission in the porpoise head. The Journal of the
Acoustical Society of America 56, 659–664.

Nummela S, Thewissen JGM, Bajpai S, Hussain ST, Kumar K. 2004. Eocene evolution of
whale hearing. Nature 430, 776–778.

Nummela S, Hussain ST, Thewissen JGM. 2006. Cranial anatomy of Pakicetidae (Cetacea,
Mammalia). Journal of Vertebrate Paleontology 26, 746–759.

Nummela S, Thewissen JGM, Bajpai S, Hussain T, Kumar K. 2007. Sound transmission in
archaic and modern whales: anatomical adaptations for underwater hearing.
Anatomical Record 290, 716–733.

O'Higgins P, Jones N. 2006. Morphologika 2, v. 2.4. Hull York Medical School, York.

Okazaki Y. 2012. A new mysticete from the upper Oligocene Ashiya Group, Kyushu, Japan
and its significance to mysticete evolution. Bulletin of the Kitakyushu Museum of
Natural History and Human History Series A: Natural History 10, 129–152.

Orme D, Freckleton R, Thomas G, Petzoldt T, Fritz S, Isaac N, Pearse W. 2013. caper:
Comparative Analyses of Phylogenetics and Evolution in R. R package version 0.5.2.

Otsuka H, Ota Y. 2008. Cetotheres from the early Middle Miocene Bihoku Group in Shobara
District, Hiroshima Prefecture, West Japan. Miscellaneous Reports of Hiwa Museum
of Natural History 49, 1–66.

Pacini AF, Nachtigall PE, Quintos CT, Schofield TD, Look DA, Levine GA, Turner JP.
2011. Audiogram of a stranded Blainville's beaked whale (*Mesoplodon densirostris*)
measured using auditory evoked potentials. The Journal of Experimental Biology
214, 2409–2415.

Pagel M. 1997. Inferring evolutionary processes from phylogenies. Zoologica Scripta 26,
331–348.

Pagel M. 1999. Inferring the historical patterns of biological evolution. Nature 401, 877–884.

Park T, Fitzgerald EMG, Evans AR. 2016. Ultrasonic hearing and echolocation in the earliest toothed whales. Biology Letters 12, 20160060.

Park T, Fitzgerald EMG, Gallagher SJ, Evans AR. 2017. Low frequency hearing preceded the evolution of giant body size and filter feeding in baleen whales. Proceedings of the Royal Society B: Biological Sciences 284, 20162528.

Perrin WE. 1975. Variation of spotted and spinner porpoise (genus *Stenella*) in the eastern tropical Pacific and Hawaii. Bulletin of the Scripps Institution of Oceanography 21, 1–206.

Pihlström H. 2008. Comparative anatomy and physiology of chemical senses in aquatic mammals. In Thewissen JGM, Nummela S, eds, Sensory Evolution on the Threshold: Adaptations in secondarily aquatic vertebrates. University of California Press, Berkeley, 95–109.

Pompeckj JF. 1922. Das Ohrskelett von Zeuglodon. Senckenbergiana, 4, 44–100.

Pyenson ND, Sponberg SN. 2011. Reconstructing body size in extinct crown Cetacea (Neoceti) using allometry, phylogenetic methods and tests from the fossil record. Journal of Mammalian Evolution 18, 269–288.

Pyenson ND, Vermeij GJ. 2016. The rise of ocean giants: maximum body size in Cainozoic marine mammals as an indicator for productivity in the Pacific and Atlantic Oceans. Biology Letters 12, 20160186.

R Core Team. 2015. R: A language and Environment for Statistical Computing. R Foundation for Statistical Computing, Vienna.

Rado R, Himelfarb M, Arensburg B, Terkel J, Wollberg Z. 1989. Are seismic communication signals transmitted by bone conduction in the blind mole rat? Hearing Research 41, 23–30.

Ridewood WG. 1922. Observations on the skull in foetal specimens of whales of the genera *Megaptera* and *Balaenoptera*. Philosophical Transactions of the Royal Society of London. Series B, Containing Papers of a Biological Character 211, 209–272.

Robert McNeel & Associates. 2015. Rhinoceros 3D, Version 5.0. Robert McNeel & Associates, Seattle, USA.

Rohlf FJ. 2001. Comparative methods for the analysis of continuous variables: geometric interpretations. Evolution 55, 2143–2160.

Ross GJB, Best PB, Donnelly BG. 1975. New records of the pygmy right whale (*Caperea marginata*) from South Africa, with comments on distribution, migration, appearance, and behavior. Journal of the Fisheries Research Board of Canada 32, 1005–1017.

Roth F. 1978. *Mesocetus argillarius* sp.n. (Cetacea, Mysticeti) from Upper Miocene of Denmark, with Remarks on the Lower Jaw and t,he Echolocation System in Whale Phylogeny.

Sanders AE, Barnes LG. 2002a. Paleontology of the Late Oligocene Ashley and Chandler Bridge Formations of South Carolina, 3: Eomysticetidae, a new family of primitive mysticetes (Mammalia: Cetacea). In Emry RJ, ed, Cenozoic mammals of land and sea: tributes to the career of Clayton E. Ray. Smithsonian Contributions to Paleobiology 93, 313–356.

Sanders AE, Barnes LG. 2002b. Paleontology of the Late Oligocene Ashley and Chandler Bridge Formations of South Carolina, 2: *Micromysticetus rothauseni*, a primitive cetotheriid mysticete (Mammalia: Cetacea). In Emry RJ, ed. Cenozoic mammals of land and sea: tributes to the career of Clayton E. Ray. Smithsonian Contributions to Paleobiology 93, 271–293.

Sanders AE, Geisler JH. 2015. A new basal odontocete from the Upper Rupelian of South

    Carolina, U.S.A., with contributions to the systematics of *Xenorophus* and *Mirocetus*

    (Mammalia, Cetacea). Journal of Vertebrate Paleontology 35, e890107.

Sekiguchi K, Best PB, Kaczmaruk BZ. 1992. New information on the feeding habits and

    baleen morphology of the pygmy right whale *Caperea marginata*. Marine Mammal

    Science 8, 288–293.

Steeman ME. 2007. Cladistic analysis and a revised classification of fossil and recent

    mysticetes. Zoological Journal of the Linnean Society 150, 875–894.

Steeman ME. 2009. A new baleen whale from the Late Miocene of Denmark and early

    mysticete hearing. Palaeontology 52, 1169–1190.

Steeman ME, Hebsgaard MB, Fordyce RE, Ho SYW, Rabosky DL, Nielsen R, Rahbek C,

    Glenner H, Sørensen MV, Willerslev E. 2009. Radiation of extant cetaceans driven by

    restructuring of the oceans. Systematic Biology 58, 573–585.

Symonds MRE, Blomberg SP. 2014. In Garamszegi LZ ed, Modern phylogenetic

    comparative methods and their application in evolutionary biology. Concepts and

    Practice. Springer, London, pp. 105–130.

Szymanski MD, Bain DE, Kiehl K, Pennington S, Wong S, Henry KR. 1999. Killer whale

    (*Orcinus orca*) hearing: Auditory brainstem response and behavioural audiograms.

    The Journal of the Acoustical Society of America 106, 1134–1141.

Tanaka Y, Fordyce RE 2016. Awamokoa tokarahi, a new basal dolphin in the Platanistoidea

    (late Oligocene, New Zealand). Journal of Systematic Palaeontology

    http://dx.doi.org/10.1080/03036758.2016.1156552.

Thewissen JGM. 2014. The Walking Whales. From Land to Water in Eight Million Years.

    University of California Press, Oakland, 256 p.

Thewissen JGM, Hussain ST. 1993. Origin of underwater hearing in whales. Nature 361,
444–445.

Thewissen JGM, Bajpai S, 2009. New skeletal material of *Andrewsiphius* and *Kutchicetus*,
two Eocene cetaceans from India. Journal of Paleontology 83, 635–63.

Thewissen JGM, Madar SI, Hussain ST. 1996. *Ambulocetus natans*, an Eocene cetacean
(Mammalia) from Pakistan. Courier Forschungsinstitut Senckenberg 191, 1–86.

Tsai CH, Ando T. 2016. Niche partitioning in Oligocene toothed mysticetes (Mysticeti:
Aetiocetidae). Journal of Mammalian Evolution 23, 33–41.

Tsai CH, Fordyce RE. 2016. Archaic baleen whale from the Kokoamu Greensand: earbones
distinguish a new late Oligocene mysticete (Cetacea: Mysticeti) from New Zealand.
Journal of the Royal Society of New Zealand
http://dx.doi.org/10.1080/14772019.2016.1202339.

Tsai CH, Kohno N. 2016. Multiple origins of gigantism in stem baleen whales. Science and
Nature 103, 89.

Uhen MD. 2004. Form, function, and anatomy of Dorudon atrox (Mammalia, Cetacea): an
archaeocete from the middle to late Eocene of Egypt. University of Michigan Papers
in Paleontology 34, 1–222.

Uhen MD. 2008. A new Xenorophus-like odontocete cetacean from the Oligocene of North
Carolina and a discussion of the basal odontocete radiation. Journal of Systematic
Palaeontology 6, 433–452.

Uhen MD. 2010. The origin(s) of whales. Annual Review of Earth and Planetary Sciences 38,
189–219.

Uhen MD, Pyenson ND, Devries TJ, Urbina M, Renne PR. 2011. New Middle Eocene
whales from the Pisco Basin of Peru. Journal of Paleontology 85, 955–969.

Vandenberghe N, Hilgen FJ, Speijer RP, Ogg JG, Gradstein FM, Hamer, Hollis CJ, Hooker JJ.. 2012. Chapter 28 - The Paleogene Period. In Gradstein FM, Ogg JG, Schmitz MD, Ogg GM, eds, The Geologic Time Scale. Elsevier, Boston, pp. 855–921.

Van Kampen PN. 1905. Die Tympanalgegend des Säugetierschädels. Morphologisches Jahrbuch 34, 1–6.

Varansi U, Feldman HR, Malins, DC. 1975. Molecular basis for formation of lipid sound lens in echolocating cetaceans. Nature 255, 340–343.

Vater M, Meng J, Fox RC. 2004. Hearing Organ Evolution and Specialization: Early and Later Mammals. In Manley GA, Popper AN, Fay RR, eds, Evolution of the Vertebrate Auditory System. Springer-Verlag, New York, pp. 256–288.

Visualization Sciences Group – a FEI Company. 2013. Avizo: 3D Analysis Software for Scientific and Industrial Data, Standard Edition 8.0.0. Berlin: Konrad-Zuse-Zentrum für Informationstechnik.

Wang D, Wang K, Ziao Y, Sheng G. 1992. Auditory sensitivity of a Chinese river dolphin (Lipotes vexillifer). In Thomas JA, Kastelein RA, Supin AY, eds, Marine Mammal Sensory Systems. Plenum Press, New York, pp. 213–221.

Watkins WA, Daher MA, Fristrup KM, Howald TJ. 1993. Sperm whales tagged with transponders and tracked underwater by sonar. Marine Mammal Science 9, 55–67.

Wartzok D, Ketten DR. 1999. Marine mammal sensory systems. In, Reynolds JE, Rommel SE, eds, Biology of marine mammals. Washington, D.C, Smithsonian Institution Press, 117–175.

Werth AJ. 2006. Mandibular and dental variation and the evolution of suction feeding in Odontoceti. Journal of Mammalogy 87, 579–88.

Whitmore FC, Barnes LG. 2008. The Herpetocetinae, a new subfamily of extinct baleen whales (Mammalia, Cetacea, Cetotheriidae). Virgina Museum of Natural History Special Publication 14, 141–180.

Yamada MU. 1953. Contribution to the anatomy of the organ of hearing of whales. Scientific Reports of the Whales Research Institute 8, 1–79.

Yamada M, Yoshizaki F. 1959. Osseous labyrinth of Cetacea. Scientific Reports of the Whales Research Institute 14, 291–304.

Yamato M, Pyenson ND. 2015. Early development and orientation of the acoustic funnel provides insight into the evolution of sound reception pathways in cetaceans. PLoS ONE 10, e0118582.

Yamato M, Ketten DR, Arruda J, Cramer S, Moore K. 2012. The auditory anatomy of the minke whale (*Balaenoptera acutorostrata*): a potential fatty sound reception pathway in a baleen whale. Anatomical Record 295, 991–998.

Yoshida K, Kimura T, Hasegawa Y. 2003. New cetothere (Cetacea: Mysticeti) from the Miocene Chichibumachi Group, Japan. Bulletin of Saitama Museum of Natural History 20-21, 1–10.

Yuen MML, Nachtigall PE, Breese M, Supin AY. 2005. Behavioral and auditory evoked potential audiograms of a false killer whale (*Pseudorca crassidens*). The Journal of the Acoustical Society of America 118, 2688–2695.

Appendix 1

Supplementary Material (ESM) for Chapter 2

Travis Park[1,2], Alistair R. Evans[1,2], Stephen J. Gallagher[3] and Erich M. G. Fitzgerald[2,4,5]

[1]School of Biological Sciences, Monash University, Melbourne, Australia.

[2]Geosciences, Museums Victoria, Melbourne, Australia.

[3] School of Earth Sciences, University of Melbourne, Melbourne, Australia.

[4]Department of Vertebrate Zoology, National Museum of Natural History, Smithsonian Institution, Washington, DC, USA.

[5]Department of Life Sciences, Natural History Museum, London, UK.

Contents

A1.1. Supplementary Material and Methods

    a. Scanning protocols

    b. Analysis protocols

    c. Additional institutional abbreviations

A1.2. Supplementary Results

    a. Systematic palaeontology

A1.3. Supplementary Figures

A1.4. Supplementary Tables

A1.1. Supplementary Material and Methods

(a) Scanning protocols

The three toothed mysticete specimens and the single modern odontocete specimen were scanned using a Zeiss Xradia 520Versa at the Monash University X-ray Microscopy Facility for Imaging Geo-materials (XMFIG) (table A1.1). Due to their larger size, the modern mysticete specimens were scanned using a Siemens 128-slice PET-CT scanner at the Melbourne Brain Centre Imaging Unit (table A1.1).

(b) Analysis protocols

Basic measurements of the internal structures of the cochlea were taken using the Measure, Slice and Spline Probe tools in the Avizo software following the protocols of Fleischer (1976). These included: cochlear height; cochlear width; number of turns; cochlear canal length; extent of the secondary spiral lamina; cochlear volume; width of the primary spiral lamina; width of the secondary spiral lamina; maximum radius of spiral ganglion canal (not measured in the modern mysticetes due to the resolution of the CT scans); area of the fenestra cochlearis and wall thickness between adjacent turns (table A1.1).

The internal structures of the cochlea, especially the secondary spiral lamina, are incredibly delicate and as a result it is often broken in fossil specimens. Fortunately the base of the secondary spiral lamina is more robust and can be used to determine the extent of the secondary spiral lamina along the length of the cochlea, even if the length of the lamina itself is unable to be measured. The extent of the spiral laminae can be used as a proxy for the stiffness of the basilar membrane, the structure which supports the organ of hearing, known as the organ of Corti. The extension (%) of the SSL was measured by dividing length of the cochlear canal at the apical-most point of the SSL by the total length of the cochlear canal. This is slightly different to the method used by Ekdale and Racicot (2015) where they use the length of the SSL divided by the cochlear length. This latter method overestimates the

extension of the SSL due to the SSL measurement being taken from the outer edge of the cochlea (an inherently larger spiral) rather than along the centre of it as is the cochlear canal length measurement.

From these initial measurements, several ratios were calculated that help to give a quantitative description of the cochlear morphology. The axial pitch is the height of the cochlea divided by the number of turns of the cochlea. This is found to be generally negatively proportional to frequency (Ketten & Wartzok 1990). The basal ratio is the height of the cochlea divided by the basal diameter of the cochlea. This is found to be generally negatively proportional to frequency (Ketten & Wartzok 1990). Geisler and Luo (1996) note that values for the basal ratio may vary across different studies, depending on how the diameter is measured. In this study, the methods of Ekdale (2013) were followed when measuring cochlear diameter and height. The cochlear slope is the height of the cochlea divided by the length of the cochlear canal divided by the number of turns (Ketten & Wartzok 1990). The radii ratio (graded curvature of the cochlea in Ekdale & Racicot (2015)) is the radius of the cochlea at its base divided by the radius of the cochlea at its apex. Manoussaki et al. (2008) found this to be strongly correlated with low frequency hearing limits. The radius measurements were taken using the Slice tool in the Avizo software following the methods of Ekdale & Racicot (2015). This method differs slightly from that used by Ketten et al. (2016) in the measurement of the apical radius where this study measures to the outer wall of the apical point of the cochlea and Ketten et al. (2016) measure only to the midpoint of the basilar membrane. This could account for their radii ratio values being marginally larger than those of similar taxa in this study and also in Ekdale and Racicot (2015).

The low frequency limit of hearing was estimated for all taxa using the equation derived by Manoussaki et al. (2008):

$$f = 1507\exp(-0.578[\rho-1])$$

where f = low frequency hearing limit at 60 dB re 20 µPa in air and 120 dB re 1 µPa in water and ρ = radii ratio value. However, this equation was derived mainly from terrestrial mammals in air and should therefore be considered tentative until audiograms of mysticetes can be collected (Ekdale & Racicot 2015).

To estimate the maximum frequency limit, a linear regression was performed using basilar membrane width and maximum frequency. Basilar membrane width is a proxy of basilar membrane stiffness, which is positively correlated with frequency (Wever et al. 1971; Pye 1972). As the basilar membrane is a soft tissue structure, the basilar membrane width was estimated using the laminar gap (the distance between the primary and secondary bony laminae) in fossil taxa and modern specimens with skeletal material only. See Fig A1.7 for an example of the measurement of the laminar gap. The laminar gap has been used to infer the width of the basilar membrane in the past (Fleischer 1976; Luo & Eastman 1995; Geisler & Lo 1996; Luo & Marsh 1996). Taking this into consideration, I sought to counteract these overestimates by adjusting our laminar gap measurements by this amount before performing the linear regression. The analysis was performed in R 3.2.2, using the stats package (R Core Team 2015). Values were log-transformed prior to performing the analysis. The results of this linear regression can be seen in Fig A1.5 and table A1.5. I also performed the same regression with *Balaena mysticetus* excluded (Fig A1.6). The maximum frequency f_{max} was then estimated for the fossil taxa using the equation derived from the linear regression:

$$\log(f_{max}) = -1.2545\log(bmw) + 4.0400$$

where bmw = the log of the estimated basilar membrane width.

The protocol for the principal component analysis (PCA) followed that of Churchill et al. (2016) using R 3.2.2 (R Core Team 2015) and the package FactoMineR (Le et al.2008).

The R module MissMDA (Josse & Husson 2016) was used to calculate missing values in the analysis.

(c) Additional institutional abbreviations

ChM PV, Charleston Museum Vertebrate Palaeontology collection (Charleston); NMVC, Museums Victoria Mammalogy collection (Melbourne); NMVP, Museums Victoria Vertebrate Palaeontology collection (Melbourne); USNM, Department of Paleobiology, National Museum of Natural History, Smithsonian Institution, (Washington, DC).

A1.2. Supplementary Results

(a) Systematic palaeontology

Cetacea Brisson, 1762

Mysticeti Gray, 1864

Mammalodontidae Mitchell, 1989

Mammalodontidae, gen. et sp. indet.

Referred specimen. NMV P173220, an isolated left periotic collected by Arthur Collins, 11 January 1962 (Fig A1.2).

Locality, horizon and age. Fishermans Steps, near Jan Juc, Victoria, southeast Australia. Jan Juc Marl, late Oligocene (27.9–23.0 Ma) (McLaren et al. 2009).

Diagnosis. A mysticete with a periotic having: a relatively short and transversely inflated anterior process; a strongly developed lateral tuberosity; a pars cochlearis with a flat anteroventral surface; a dorsomedially elongated pars cochlearis; a dorsally elongated and anteroposteriorly thick crista transversa that isolates the proximal opening of the facial canal from the rest of the internal acoustic meatus; an indistinct superior process reduced to a low dorsal crest. None of these characters represent unambiguous synapomorphies of Mammalodontidae, but this combination of periotic characters is found only in taxa assigned to that clade.

Comparisons. NMV P173220 differs from the periotic of *Mammalodon colliveri* (see Fitzgerald (2010)) by having: a transversely narrower and less medially inflected anterior process; a shorter anteroexternal sulcus; an accessory ossicle fused to the body of the periotic; a bulbous eminence anterolateral to the base of the posterior process; and an aperture for the vestibular aqueduct that extends medially between the posterior edge of the internal acoustic meatus and the aperture for the cochlear aqueduct. NMV P173220 differs from the periotic of

Janjucetus hunderi (see Fitzgerald (2006)) by having: an anterior process with a flat medial surface; and a shorter lateral tuberosity.

Aetiocetidae Emlong, 1966

Aetiocetidae, gen. et sp. indet.

Referred specimen. NMV P229119, a partial skeleton (including an incomplete cranium, tympanic bulla, periotic, mandibles and teeth) collected by James L. Goedert, 3 February 1990 (Fig A1.2).

Locality, horizon and age. Coastal section between Shipwreck Point and the mouth of the Sekiu River, Clallam County, Olympic Peninsula, Washington, USA. Collected as a small concretion (<1 m in length) from the upper Makah Formation, early Oligocene (33.2–31.0 Ma) (Prothero et al. 2009; Nesbitt et al. 2010; Marx & Fordyce 2015).

Ontogenetic age. The cervical and thoracic vertebral epiphyses are either not fused or only partially fused to the vertebral bodies (via the centre of the intervertebral disc), indicating that NMV P229119 is not a physically mature individual (Moran et al. 2015). The lateral edge of the supra-exoccipital suture is closed in NMV P229119, but there is a broken region of thin bone (perhaps fontanelles) more medially. Furthermore, the sphenoccipital synchondrosis between the basioccipital and basisphenoid is not closed. In modern mysticetes the latter cranial sutures ossify before the age of one (Walsh & Berta 2011). These features suggest that NMV P229119 is either a juvenile individual, or that it is paedomorphic as suggested for other aetiocetids (Sanders & Barnes 2002; Marx & Fordyce 2015).

Diagnosis. A mysticete with the following characters that place it in Aetiocetidae: an embayment for the lacrimal bone in the lateral border of the ascending process of the maxilla; a transversely wide intertemporal region; zygomatic process of squamosal expanded near its anterior margin and at its posterior end but dorsoventrally narrow in the middle (Fig A1.1); a symphyseal groove developed medially along the anterior portion of the mandible; and

enamel ornament present only on the lingual side of the cheek teeth. A more detailed analysis of the morphology and relationships of NMV P229119 within Aetiocetidae is currently in preparation.

A1.3. Supplementary Figures
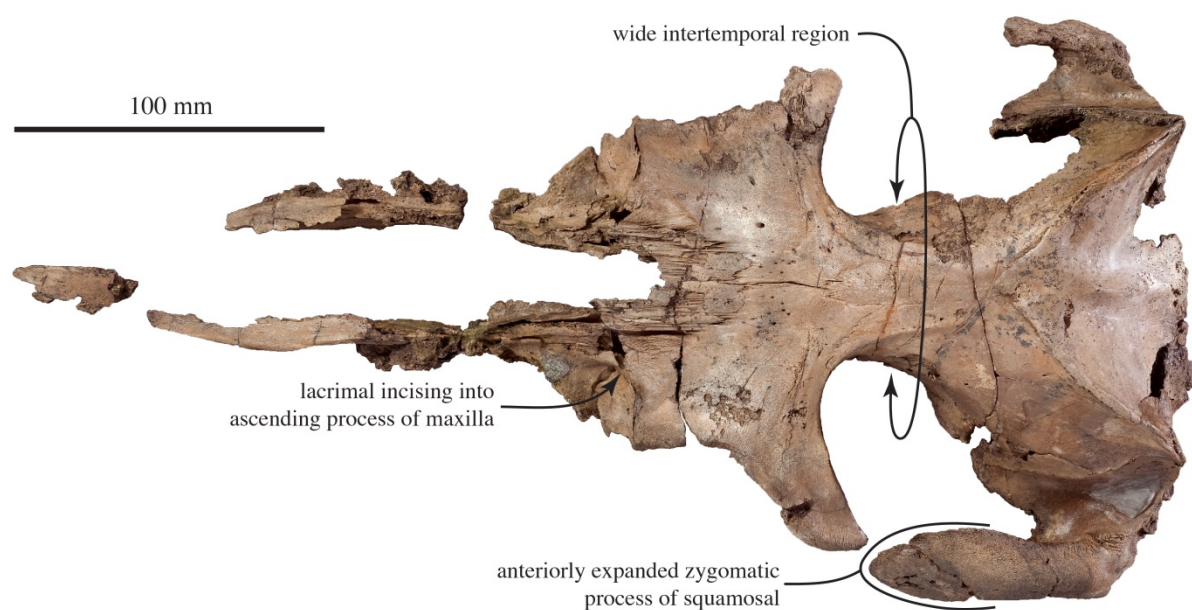
Fig A1.1. NMV P229119, Aetiocetidae indet. cranium in dorsal view, illustrating diagnostic aetiocetid characters.
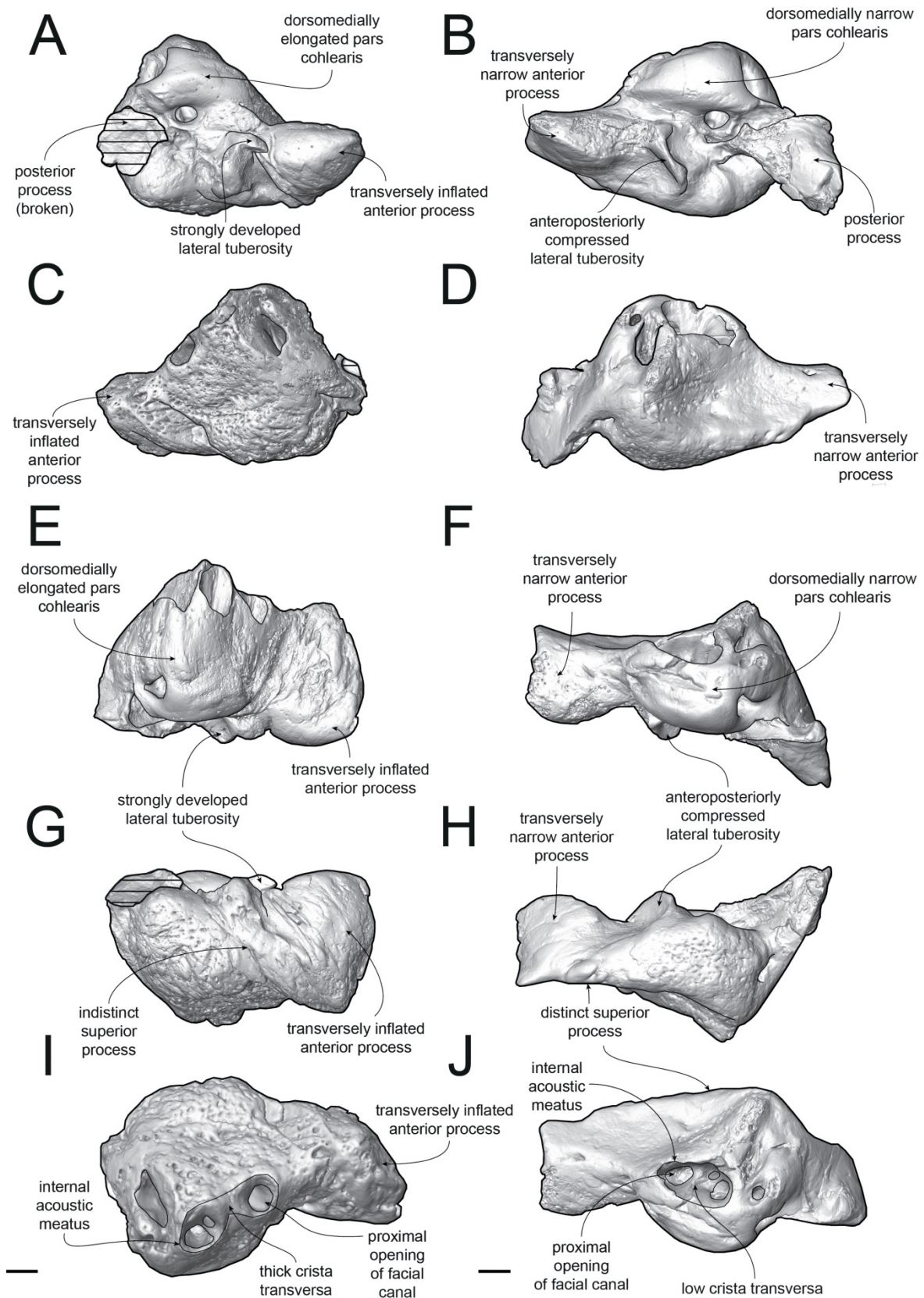
Fig A1.2. Left periotic of Mammalodontidae indet. (NMV P173220) (left), and right periotic of Aetiocetidae indet. (NMV P229119) (right), showing morphological differences. Digital models reconstructed from microCT data in (A,B) ventral, (C,D) dorsal, (E,F) medial, (G,H) lateral, and (I,J) cerebral views. Hatching indicates major breaks. Scale bars represent 5 millimetres. For corresponding figures of the holotype periotic of *Mammalodon colliveri* see Fitzgerald (2010).
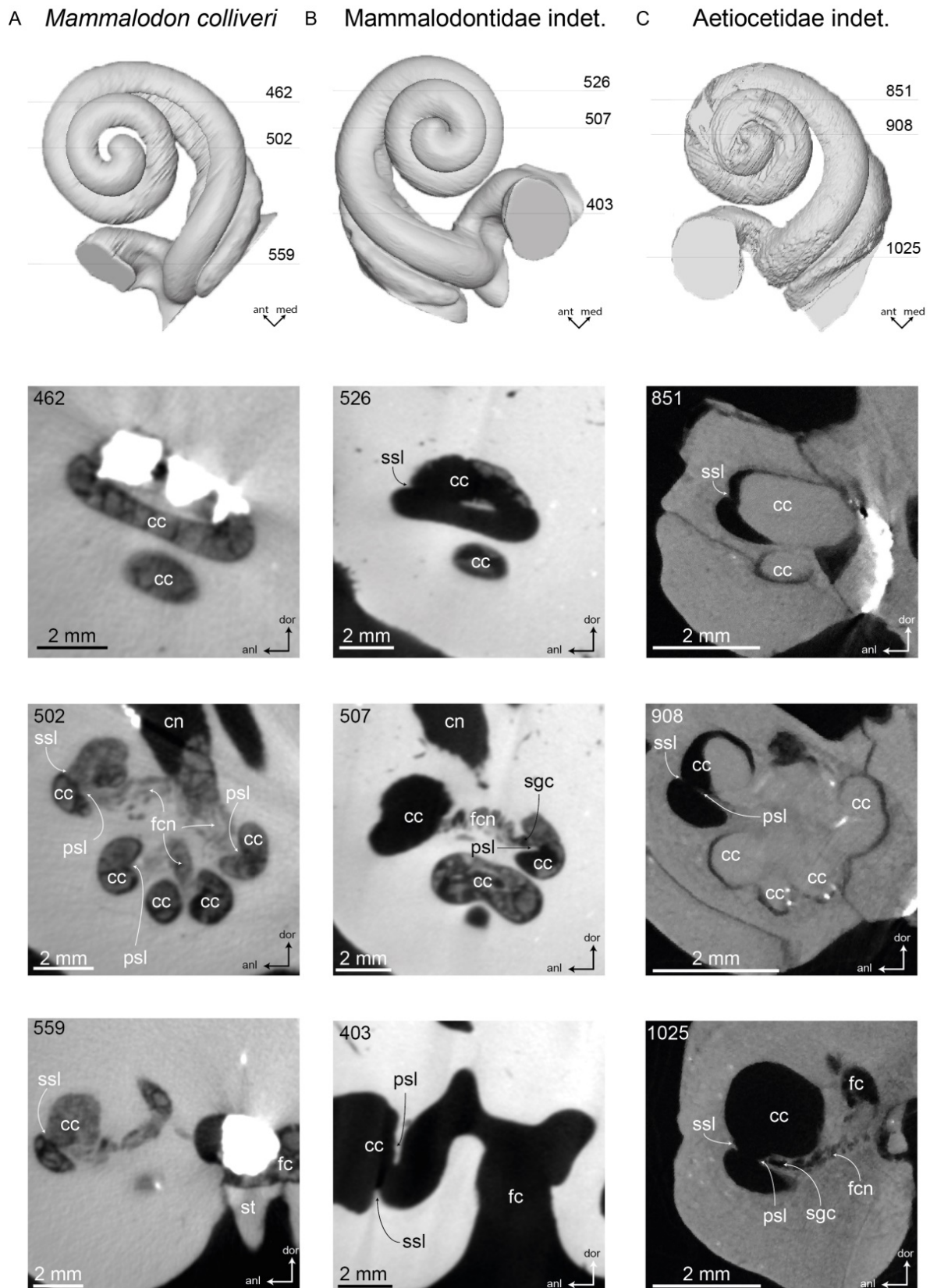
Fig A1.3. Raw microCT slices through right pars cochlearis of periotic in: A, *Mammalodon colliveri*; B, left periotic of NMV P173220 (Mammalodontidae indet.); and C, right periotic of NMV P229119 (Aetiocetidae indet.). Numbers indicate respective slice in cochlea above. anl, anterolateral; ant, anterior; cc, cochlear canal; cn, canal for cranial nerve VIII; fc, fenestra cochleae; fcn, foramina for the cochlear nerves; med, medial; pos, posterior; psl, primary spiral lamina; sgc, spiral ganglion canal; ssl, secondary spiral lamina; st, stapes.

Fig A1.4. Digital endocasts of archaeocete, odontocete and modern mysticete cochleae showing variation in cochlear morphology in: (*a*) anterior, (*b*) lateral, (*c*) dorsal, (*d*) vestibular views. Phylogeny based on Marx & Fordyce (2015). All specimens are shown as right cochlea with specimens from the left side reversed. cc, canaliculus cochleae; fc, fenestra cochleae; fv, fenestra vestibuli; psl, primary spiral lamina; ssl, secondary spiral lamina; tr, tympanal recess.

Fig A1.5. Linear regression of log basal basilar membrane width vs log maximum frequency. BM, basilar membrane; Max freq, maximum frequency.
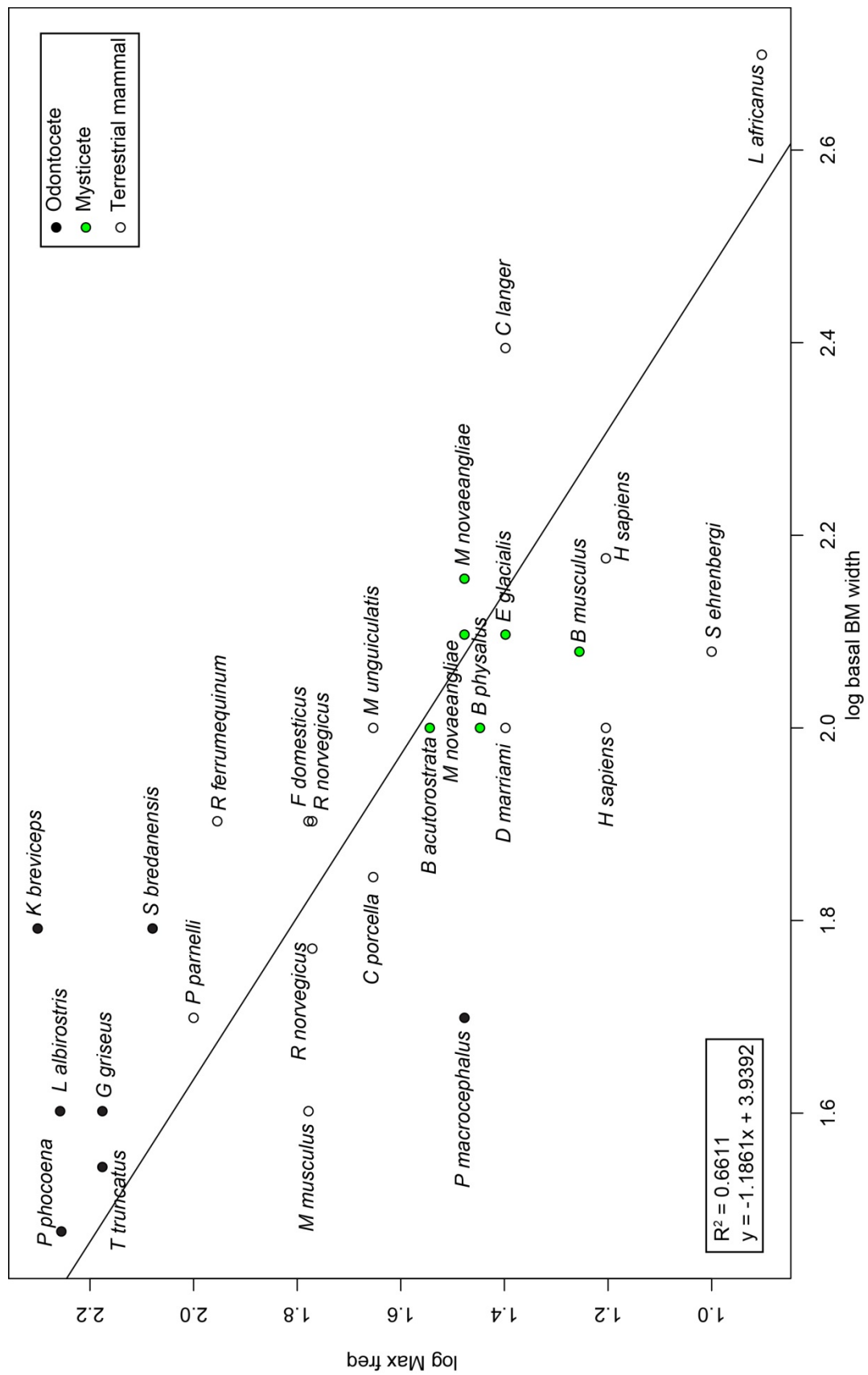
Fig A1.6. Linear regression of log basal basilar membrane width vs log maximum frequency excluding *Balaena mysticetus*. BM, basilar membrane; Max freq, maximum frequency.
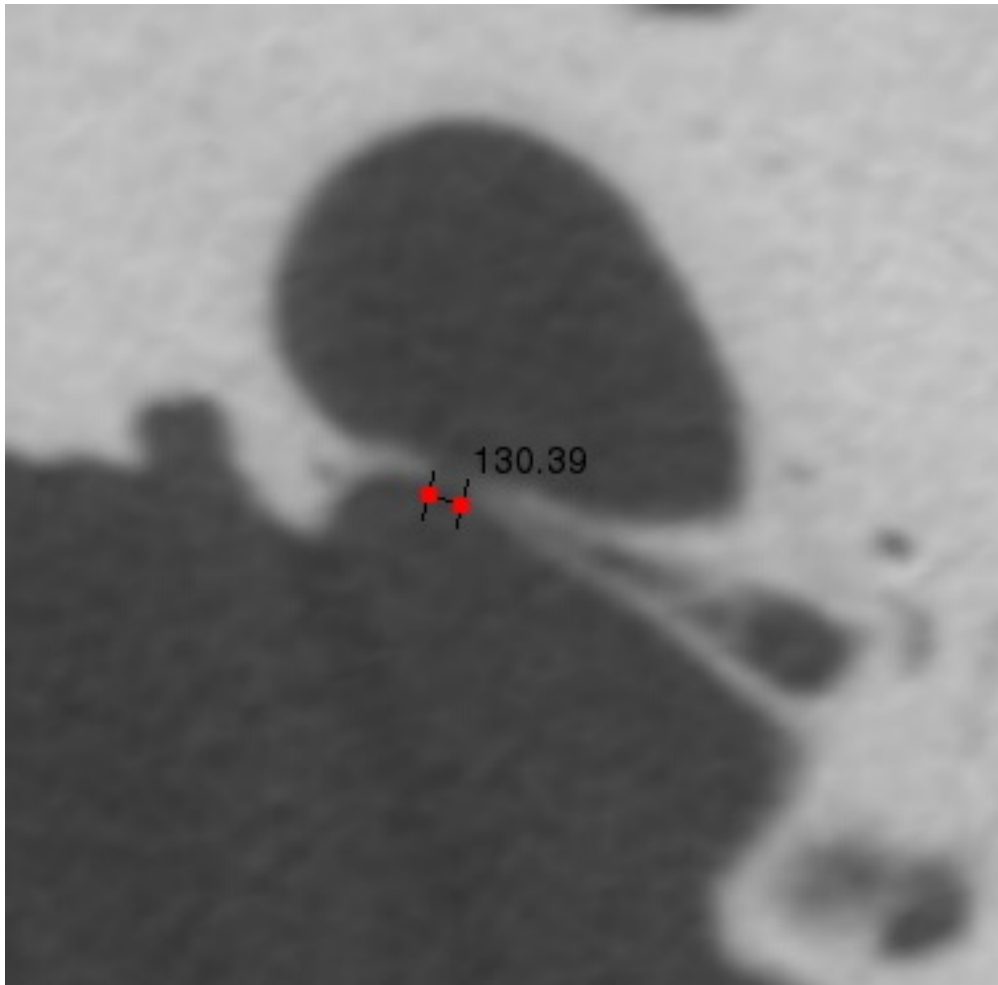
Figure A1.7. Cross section of the basal turn of the cochlea of *Steno bredanensis* (NMVC 36961) showing the measurement (in mm) of the laminar gap.

A1.4. Supplementary Tables

Table A1.1. Complete measurements for cochleae sampled in this study. AP, axial pitch; BR, basal ratio; CBA, cannot be ascertained; CH, cochlear height; CL, canal length; CW, cochlear width; Estd. LFL, estimated low frequency limit; FC, area of fenestra cochlearis; GAN, maximum radius of spiral ganglion canal; ITD, thickness of bone between basal and apical turns; R_{max}, basal radius of cochlea; R_{min}, apical radius of cochlea; RR, radi ratio; S#, specimen number; SSL, secondary spiral lamina; T, number of turns; Vol., volumeW2, width of cochlea perpendicular to maximum cochlea width; % SSL, % extent of SSL .

| Taxon	S#	Side	T	CL (mm)	T*CL	Rmax (mm)	Rmin (mm)	ITD (mm)	GAN (mm)	FC (mm2)	
Steno bredanensis	NMV C36961	Left	1.5	30.32	45.48	4.91	1.45	1.82	0.33	3.49	
Balaenoptera acutorostrata	NMV C24936	Left	2.25	42.78	96.25	8.08	0.98	1.76	CBA	9.07	
Balaenoptera borealis	NMV P166415	Right	2.25	69.56	156.51	8.8	1.2	1.01	CBA	15.53	
Balaenoptera edeni	NMV P171502	Left	2	70.74	141.49	10.85	1.48	1.44	CBA	21.44	
Eubalaena australis	NMV C27879	Left	2.25	52.01	117.03	7.94	1.1	1	CBA	35.45	
Megaptera novaeangliae	NMV C28892	Right	2	56.35	112.7	9.02	1.27	2.11	CBA	13.53	
Aetiocetidae indet.	NMV P229119	Right	2.5	15.18	37.96	2.79	0.37	0.35	CBA	1.91	
Mammalodon colliveri	NMV P199986	Right	2.25	33.15	74.58	5.56	0.82	1.41	CBA	6.53	
Mammalodontidae indet.	NMV P173220	Left	2.5	29.26	73.14	5.24	0.81	1.01	0.32	7.15	
Zygorhiza kochii	USNM 214433	Right	2.5	32.83	82.08	5.82	0.6	1.2	0.4	10.14	

Taxon	RR	SSL (mm)	% SSL	BR	AP	Slope	CH (mm)	CW (mm)	W2	Vol. (mm³)	Estd. LFL (Hz)
Steno bredanensis	3.39	22.49	74.18	0.5	3.47	0.11	5.21	10.46	8.9	154.85	378.31
Balaenoptera acutorostrata	8.24	18.9	44.17	0.53	3	0.07	6.76	12.65	11.44	412.34	22.88
Balaenoptera borealis	7.33	22.86	32.86	0.47	3.56	0.05	8	16.95	15.77	790.72	38.75
Balaenoptera edeni	7.33	22.04	31.15	0.51	4.22	0.06	8.44	16.66	15.9	797.4	38.8
Eubalaena australis	7.22	11.72	22.53	0.64	4.28	0.08	9.62	15.03	12.28	748.64	41.42
Megaptera novaeangliae	7.1	21.64	38.4	0.5	4.39	0.08	8.77	17.44	14.49	804.95	44.29
Aetiocetidae indet.	7.47	5.94	39.09	0.6	1.31	0.09	3.28	5.48	3.95	CBA	35.9
Mammalodon colliveri	6.77	11.04	33.29	0.55	2.57	0.08	5.79	10.5	7.85	145.57	53.81
Mammalodontidae indet.	6.44	12.41	42.41	0.58	2.23	0.08	5.57	9.53	6.67	162.13	65.07
Zygorhiza kochii	9.63	13.7	41.72	0.67	3.02	0.09	7.54	11.31	6.95	259.14	10.26

Table A1.2. Parameters of CT scans of cetacean periotics in this study. kV, kilovolt; μm, micrometres.

Taxon	Specimen No	Scan power (kV)	No. of slices	Voxel size (μm)
Odontoceti				
Steno bredanensis	NMVC36961	90	3201	32.97
Mysticeti				
Balaenoptera acutorostrata	NMVC24936	140	856	146
Balaenoptera borealis	NMVP166415	140	911	242
Balaenoptera edeni	NMVP171502	140	1611	307
Eubalaena australis	NMVC27879	140	1346	386
Megaptera novaeangliae	NMVC28892	140	1101	200
Aetiocetidae indet.	NMV229119	120	1601	47.94
Mammalodon colliveri	NMVP199986	120	1601	51.36
Mammalodontidae indet.	NMVP173220	120	3201	45.05
Archaeoceti				
Zygorhiza kochii	USNM214433	120	1601	51.35

Table A1.3. Measurements (in mm) of the periotic of *Mammalodon colliveri* (NMV P199986), a mammalodontid (NMV P173220) and an aetiocetid (NMV P229119) used in this study. Dimensions and measurements of *M. colliveri* are from Fitzgerald (2010).

Measurement	*Mammalodon colliveri*	NMV P173220	NMV P229119
Maximum length of the periotic (excluding posterior process)	38.7	39.5	33.8
Maximum transverse diameter of periotic	23.5	23.8	21.7
Anteroposterior diameter of anterior process	18.0	15.3	13.8
Transverse diameter of anterior process	14.2	11.4	7.3
Dorsoventral diameter of anterior process	23.4+	22.5	11.8
Anteroposterior diameter of pars cochlearis	25.0	22.3	18.9
Transverse diameter of pars cochlearis	12.0	10.9	8.3
Maximum dorsoventral diameter of pars cochlearis	25.9	25.6	13.7
Distance between aperture for cochlear aqueduct and fenestra rotunda	10.6	7.3	3.8
Distance between aperture for vestibular aqueduct and fenestra rotunda	13.3	11.1	5.7
Distance between fenestra ovalis and fenestra rotunda	5.4	5.5	4.8
Minimum distance between edge of fundus of internal acoustic meatus and the aperture for vestibular aqueduct	5.9	2.4	4.2
Minimum distance between edge of fundus of internal acoustic meatus and the aperture for cochlear aqueduct	3.1	4.7	3.3

Table A1.4. Scores from the principal component analysis.

	PC1	PC2	PC3	PC4	PC5	PC6	PC7	PC8
Choeropsis iberiensis	-1.724	1.768	-0.038	0.279	-0.784	-0.424	0.016	0.056
Hippopotamus amphibious	0.289	2.989	-0.420	0.297	-0.293	-0.166	0.237	0.141
cf. *Cynthiacetus*	-0.219	1.027	-0.919	-0.843	0.499	0.090	-0.118	-0.081
Zygorhiza kochii	-0.655	0.890	-0.921	-0.130	0.020	0.434	0.134	-0.112
Eubalaena australis	2.241	3.658	0.532	1.579	0.036	0.071	-0.101	-0.025
Piscobalaena nana	-0.104	2.062	-0.671	-0.036	0.395	0.342	-0.235	0.201
Balaenoptera physalus	4.818	2.627	0.280	-1.538	-0.259	-0.085	0.394	-0.124
Echovenator sandersi	-0.645	-0.043	0.665	0.573	0.329	0.162	0.264	-0.098
Squalodon calvertensis	-1.581	-0.519	-0.042	0.348	0.149	-0.422	-0.249	-0.049
Kogia breviceps	-2.018	-0.799	-0.322	-0.224	-0.280	0.450	0.068	0.183
Physeter macrocephalus	5.882	-2.673	-1.771	0.550	-0.398	-0.076	-0.138	0.043
Ziphius cavirostris	1.893	-1.346	-0.700	0.234	0.091	0.147	0.094	-0.307
Hyperoodon ampullatus	2.940	-1.017	-0.469	0.261	0.511	0.064	0.034	0.019
Zarhachis flagellator	-0.079	-0.789	0.145	0.092	0.647	-0.348	0.254	0.155
Lipotes vexillifer	0.043	-0.646	-0.011	-0.692	0.051	-0.031	-0.187	0.216
Kentriodon pernix	-2.131	-0.583	0.251	-0.114	-0.235	0.197	0.111	-0.028
Inia geoffrensis	0.185	-0.674	0.883	-0.105	-0.814	-0.090	-0.377	-0.316
Pontoporia blainvillei	-1.513	-0.432	0.826	-0.150	-0.119	0.504	-0.123	0.031
Monodon monoceros	1.083	-0.333	0.284	-0.072	-0.346	0.442	-0.274	0.125
Delphinapterus leucas	3.351	-0.232	2.032	-0.024	0.654	0.077	-0.291	-0.001
Phocoena phocoena	-1.758	-0.725	-0.041	0.129	-0.125	0.224	0.142	-0.097
Phocoenoides dalli	-1.675	-1.130	-0.153	0.572	0.056	0.071	0.398	-0.010
Leucopleurus acutus	-0.888	-0.782	0.220	-0.310	-0.124	-0.242	-0.139	0.190
Sousa chinensis	-0.281	-1.253	0.632	-0.127	0.275	-0.363	0.316	-0.058
Tursiops truncatus	-0.259	-1.152	0.455	-0.013	-0.058	-0.193	0.085	0.060
Phocageneus sp.	0.996	-1.207	0.750	-0.072	-0.471	-0.109	0.219	0.165
Aetiocetidae indet.	-4.819	0.152	-0.342	0.070	0.093	0.044	0.002	-0.105
Mammalodontidae indet.	-1.252	0.416	-0.737	-0.102	0.126	-0.571	-0.276	0.001
Mammalodon colliveri	-2.120	0.742	-0.397	-0.432	0.372	-0.199	-0.257	-0.175

Table A1.5. Data and sources used for linear regression of basal basilar membrane width vs maximum frequency. freq, frequency; kHz, kilohertz; μm, micrometres; * = value calculated by adjusting laminar gap measurement by the error margin given in Ketten (2000).

Taxon	basal BMW (μm)	log basal BMW	Max freq (kHz)	log Max freq	Data source
Terrestrial mammals					
Cavia porcella	70	1.85	45	1.65	Fernández (1952)
Chinchilla langer	248	2.39	25	1.40	Lim (1980)
Dipodymus marriami	100	2.00	25	1.40	Webster & Webster (1977)
Felis domesticus	80	1.90	60	1.78	Nadol (1988)
Homo sapiens	150	2.18	16	1.20	Ketten (2000)
Homo sapiens	100	2.00	16	1.20	Nadol (1988)
Loxodonta africana	500	2.70	8	0.90	Payne et al. (1986); Langbauer et al. (1981)
Meriones unguiculatus	100	2.00	45	1.65	Plassmann et al. (1987)
Mus musculus	40	1.60	60	1.78	Ehret & Frankenreiter (1977)
Pteronotus parnellii	50	1.70	100	2.00	Ketten (2000)
Rattus norvegicus	80	1.90	59	1.77	Ketten (2000)
Rattus norvegicus	59	1.77	59	1.77	Burda et al. (1988)
Rhinolophus ferrumequinum	80	1.90	90	1.95	Bruns (1976)
Spalax ehrenbergi	120	2.08	10	1.00	Bruns et al. (1988)
Odontoceti					
Grampus griseus	40	1.60	150	2.18	Ketten (2000); Nachtigall et al. (2005)
Kogia breviceps	61.90*	1.79	200	2.30	(Caldwell & Caldwell (1987); Santoro et al. (1989); this study
Lagenorhynchus albirostris	40	1.60	181	2.26	Ketten (2000); Nachtigall et al. (2008)
Phocoena phocoena	30	1.48	180	2.26	Ketten (2000); Kastelein et al. (2002)
Physeter macrocephalus	50	1.70	30	1.48	Watkins (1980); Ketten (2000)
Steno bredanensis	61.90*	1.79	120	2.08	Mann et al. (2010); this study
Tursiops truncatus	25	1.40	150	2.18	Wever et al. (1971); Houser & Finneran 2006
Mysticeti					
Balaena mysticetus	120.00	2.08	4.00	0.60	Ketten (2000); Tervo et al. (2012)
Balaenoptera acutorostrata	100.00	2.00	35	1.54	Ketten (2000); Ketten et al. (2016)
Balaenoptera musculus	120	2.08	18	1.26	Ketten et al. (2016)
Balaenoptera physalus	100	2.00	28	1.45	Thompson et al. (1979); Ketten (2000)
Eubalaena australis	900.00*	2.95	2.2	0.34	Cummings et al. (1972); this study
Eubalaena glacialis	125.00	2.10	25	1.40	Ketten (2000); Ketten et al. (2016)
Megaptera novaeangliae	142.86	2.15	30	1.48	Ekdale & Racicot (2015); Ketten et al. (2016)
Megaptera novaeangliae	125	2.10	30	1.48	Ketten et al. (2016)
Fossil cetaceans					
Mammalodon colliveri	190.48*	2.21	17.37	1.24	This study
Mammalodontidae indet.	161.90*	2.65	4.59	0.66	This study
Xenorophidae indet.	447.62*	1.68	86.18	1.94	Park et al. (2016)
Zygorhiza kochii	47.62*	2.28	14.04	1.14	This study

References

Bruns V. 1976. Peripheral auditory tuning for fine frequency analysis by the CF-FM bat, *Rhinolophus ferrumequinum*. I. Mechanical specializations of the cochlea. Journal of Comparative Physiology A l06, 77–86.

Bruns V, Muller M, Hofer W, Heth G, Nevo E. 1988. Inner ear structure and electrophysiological audiograms of the subterranean mole rat, *Spalax ehrenbergi*. Hearing Research 33, 1–10.

Burda H, Ballast L, Bruns V. 1988. Cochlea in old world mice and rats (Muridae). Journal of Morphology 198, 269–285.

Caldwell DK, Caldwell MC. 1987. Underwater echolocation-type clicks by captive stranded pygmy sperm whales, *Kogia breviceps*. Abstracts of the 7th Biennial Conference on the Biology of Marine Mammals, p. 8.

Churchill M, Martínez-Cáceres M, de Muizon C, Mnieckowski J, Geisler JH. 2016. The Origin of High-Frequency Hearing in Whales. Current Biology http://dx.doi.org/10.1016/j.cub.2016.06.004.

Cummings WC, Fish F, Thompson PO. 1972. Sound production and other behavior of southern right whales, *Eubalaena australis*. Transactions of the San Diego Society of Natural History 17, 1–13.

Ehret G, Frankenreiter M. 1977. Quantitative analysis of cochlear structures in the house mouse in relation to mechanisms of acoustical information processing. Journal of Comparative Physiology A 122, 65–85.

Ekdale EG. 2013. Comparative anatomy of the bony labyrinth (inner ear) of placental mammals. PLoS ONE 8, e66624.

Ekdale EG, Racicot RA. 2015. Anatomical evidence for low frequency sensitivity in an archaeocete whale: comparison of the inner ear of *Zygorhiza kochii* with that of crown Mysticeti. Journal of Anatomy 226, 22–39.

Fernández C. 1952. Dimensions of the cochlea (guinea pig). Journal of the Acoustical Society of America 24, 519–523.

Fitzgerald EMG. 2006. A bizarre new toothed mysticete (Cetacea) from Australia and the early evolution of baleen whales. Proceedings of the Royal Society B: Biological Sciences 273, 2955–2963.

Fitzgerald EMG. 2010. The morphology and systematics of *Mammalodon colliveri* (Cetacea: Mysticeti), a toothed mysticete from the Oligocene of Australia. Zoological Journal of the Linnean Society 158, 367–476.

Fleischer G. 1976. Hearing in extinct cetaceans as determined by cochlear structure. Journal of Paleontology 50, 133–152.

Geisler JH, Luo ZX. 1996. The petrosal and inner ear of *Herpetocetus* sp. (Mammalia: Cetacea) and their implications for the phylogeny of hearing of archaic mysticetes. Journal of Paleontology 70, 1045–1066.

Houser DS, Finneran JJ. 2006. A comparison of underwater hearing sensitivity in bottlenosed dolphins (*Tursiops truncatus*) determined by electrophysiological and behavioural methods. The Journal of the Acoustical Society of America 120, 1713–1722.

Josse J, Husson F. 2016. missMDA: A package for handling missing values in multivariate data analysis. Journal of Statistical Software 70, 1–31.

Kastelein RA, Bunskoek P, Hagedoorn M, Au WWL, de Haan D. 2002. Audiogram of a harbor porpoise (*Phocoena phocoena*) measured with narrow-band frequency-modulated signals. Journal of the Acoustical Society of America 112, 334–344.

Ketten DR, 2000. Cetacean ears. In Au WWL, Popper AN, Fay RR, eds, Hearing by whales and dolphins. Springer-Verlag, New York, pp. 43–108.

Ketten DR, Wartzok D. 1990. Three dimensional reconstructions of the dolphin ear. In Thomas JA, Kastelein RA, eds, Sensory abilities of Cetaceans. Plenum Press, New York, pp. 81–105.

Ketten DR, Arruda J, Cramer S, Yamato M. 2016. Great ears: Low-frequency sensitivity correlates in land and marine leviathans. In Popper AN, Hawkins A, eds, The Effects of Noise on Aquatic Life II. Springer Science & Business Media, New York, pp. 529–538.

Langbauer WR, Payne K, Charif R, Rappaport E, Osborn F. 1991. African elephants respond to distant playbacks of low-frequency conspecific calls. Journal of Experimental Biology 157, 35–46.

Le S, Josse J, Husson F. 2008. FactoMineR: An R package for multivariate analysis. Journal of Statistical Software 25, 1–18.

Lim DJ. 1980. Cochlear anatomy related to cochlear micromechanics. A review. Journal of the Acoustical Society of America 67, 1686–1695.

Luo ZX, Eastman ER. 1995. Petrosal and inner ear of a squalodontoid whale: implications for evolution of hearing in odontocetes. Journal of Vertebrate Paleontology 15, 431–442.

Luo ZX, Marsh K. 1996. Petrosal (periotic) and inner ear of a Pliocene kogiine whale (Kogiinae, Odontoceti): Implications on relationships and hearing evolution of toothed whales. Journal of Vertebrate Paleontology 16, 328–348.

Mann D, Hill-Cook M, Manire C, Greenhow D, Montie E, Powell J, Wells R, Bauer G, Cunningham-Smith P, Lingenfelser R, Di Giovanni R, Stone A, Brodsky M, Stevens R, Kieffer G, Hoetjes P. 2010. Hearing loss in stranded odontocete dolphins and whales. PLoS ONE 5, e13824.

Manoussaki D, Chadwick RS, Ketten DR, Arruda J, Dimitriadis EK, O'Malley JT. 2008. The influence of cochlear shape on low-frequency hearing. Proceedings of the National Academy of Sciences 105, 6162–6166.

Marx FG, Fordyce RE. 2015. Baleen boom and bust: a synthesis of mysticete phylogeny, diversity and disparity. Royal Society Open Science 2, 140434.

McLaren, S, Wallace, MW, Gallagher, SJ, Dickinson, JA, McAllister, A. 2009. Age constraints on Oligocene sedimentation in the Torquay Basin, southeastern Australia. Australian Journal of Earth Sciences 56, 595–604.

Moran M, Bajpai S, George JC, Suydam R, Usip S, Thewissen JGM. 2015. Intervertebral and epiphyseal fusion in the postnatal ontogeny of cetaceans and terrestrial mammals. Journal of Mammalian Evolution 22, 93–109.

Nachtigall PE, Yuen MML, Mooney TA, Taylor KA. 2005. Hearing measurements from a stranded infant Risso's dolphin, *Grampus griseus*. The Journal of Experimental Biology 208, 4181–4188.

Nachtigall PE, Mooney TA, Taylor KA, Miller LA, Rasmussen M, Akamatsu T, Teilmann J, Linnenschidt M, Vikingsson GA. 2008. Shipboard measurements of the hearing of the white-beaked dolphin, *Lagenorynchus albirostris*. Journal of Experimental Biology 211, 642–647.

Nadol J. 1988. Comparative anatomy of the cochlea and auditory nerve in mammals. Hearing Research 34, 253–266.

Nesbitt EA, Martin RA, Carroll NP, Grieff J. 2010. Reassessment of the Zemorrian foraminiferal stage and Juanian molluscan stage north of the Olympic Mountains, Washington State and Vancouver Island. Newsletters on Stratigraphy 43, 275–291.

Park T, Fitzgerald EMG, Evans AR. 2016. Ultrasonic hearing and echolocation in the earliest toothed whales. Biology Letters 12, 20160060.

Payne KB, Langbauer WJ Jr, Thomas EM. 1986. Infrasonic calls of the Asian elephant, *Elephas maximus*. Behavioral Ecology and Sociobiology 18, 297–301.

Plassmann W, Peetz W, Schmidt M. 1987. The cochlea of gerbilline rodents. Brain, Behavior and Evolution 30, 82–101.

Prothero DR, Draus E, Burns C. 2009. Magnetostratigraphy and tectonic rotation of the Eocene-Oligocene Makah and Hoko River Formations, northwest Washington, USA. International Journal of Geophysics 2009, 1–15.

Pye A. 1972. Variations in the structure of the ear in different mammalian species. Sound 6, 14–18.

R Core Team. 2015. R: A language and Environment for Statistical Computing. R Foundation for Statistical Computing, Vienna.

Sanders AE, Barnes LG. 2002 Paleontology of the Late Oligocene Ashley and Chandler Bridge Formations of South Carolina, 2: *Micromysticetus rothauseni*, a primitive cetotheriid mysticete (Mammalia: Cetacea). Smithsonian Contributions to Paleobiology 93, 271–293.

Santoro AK, Marten KL, Cranford TW. 1989. Pygmy sperm whale sounds *Kogia breviceps*. Abstracts of the 8th Biennial Conference on the Biology of Marine Mammals, p. 59.

Tervo OM, Christoffersen MF, Simon M, Miller LA, Jensen FH, Parks SE, Madsen PT. 2012. High source levels and small active space of high-pitched song in bowhead whales (*Balaena mysticetus*). PLoS ONE 7, e52072.

Thompson TJ, Wmn HE, Perkins PJ. 1979. Mysticete sounds. In Winn HE, Olla BL, eds, Behavior of Marine Animals, Current Perspectives in Research, Vol. 3: Cetaceans. Plenum, New York, pp. 403–431.

Walsh BM, Berta A. 2011. Occipital ossification of balaenopteroid mysticetes. Anatomical Record 294, 391–398.

Watkins WA. 1980. Acoustics and the behavior of sperm whales. In Busnel RG, Fish F eds,

Animal Sonar Systems. Plenum Press, New York, pp. 283–290.

Webster DB, Webster M. 1977. Auditory systems of Heteromyidae: cochlear diversity.

Journal of Morphology 152,153–170.

Wever EG, McCormick JG, Palin J, Ridgway SH. 1971. Cochlea of the Dolphin, *Tursiops

truncatus*: The Basilar Membrane. Proceedings of the National Academy of Sciences

68, 2708–2711.

Appendix 2

Supplementary material for Chapter 3

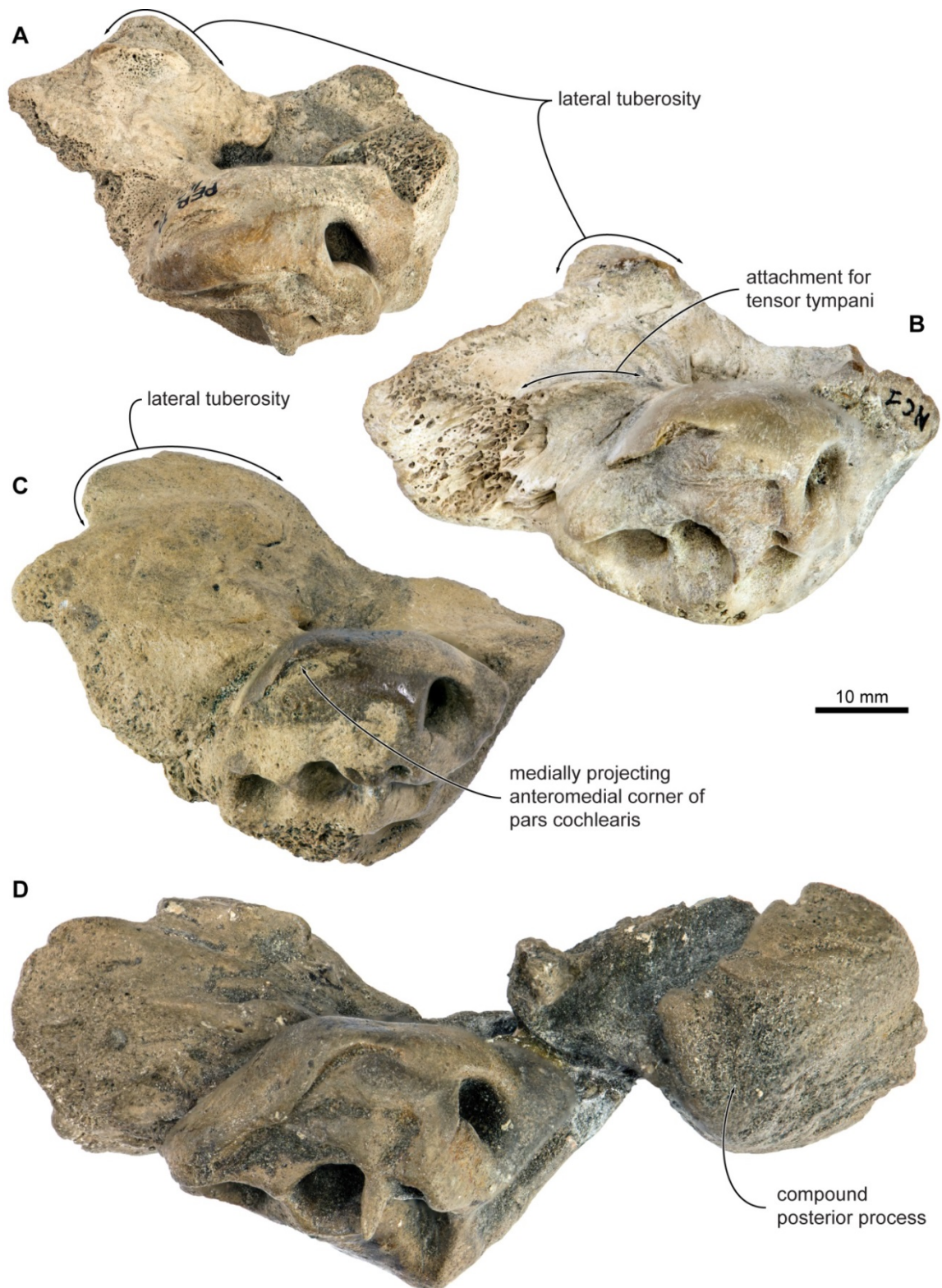

Fig. A2.1. Periotics of *Herpetocetus* scanned for this study, all in medial view. (**A**) *Herpetocetus* cf. *transatlanticus*, IRSNB V00373; (**B**) *Herpetocetus* cf. *transatlanticus*, IRSNB V00372; (**C**) *Herpetocetus* sp., IRSNB V00376 (photograph mirrored to facilitate comparisons); (**D**) *Herpetocetus* sp., IRSNB V00377.

Appendix 3

Supplementary material for Chapter 5

Table A3.1. Results of the PGLS regressions. BCW, bicondylar width; ML, mandible length; PC, principal component; SL, symphysis length.

Both mandibles	PC1		PC2		PC3		PC4		ML	
	p	r²	p	r²	p	r²	p	r²	p	r²
Maxfreq	0.478	0.051	0.112	0.233	0.053	0.325	0.877	0.003	0.297	0.108
Minfreq	0.478	0.052	0.299	0.107	0.324	0.097	0.689	0.017	0.127	0.217
Meanfreq	0.485	0.050	0.124	0.221	0.069	0.294	0.883	0.002	0.341	0.091
Freqrange	0.476	0.052	0.103	0.244	0.041	0.354	0.877	0.003	0.260	0.125
	SL		BCW		Area		Volume		Centroid size	
	p	r²	p	r²	p	r²	p	r²	p	r²
Maxfreq	0.246	0.132	0.115	0.229	0.254	0.128	0.325	0.097	0.420	0.066
Minfreq	0.158	0.189	0.286	0.113	0.156	0.190	0.173	0.177	0.698	0.016
Meanfreq	0.283	0.114	0.127	0.217	0.287	0.112	0.356	0.086	0.412	0.068
Freqrange	0.215	0.149	0.106	0.239	0.226	0.142	0.299	0.107	0.430	0.063

Left mandible	PC1		PC2		PC3		PC4		ML	
	p	r²	p	r²	p	r²	p	r²	p	r²
Maxfreq	0.310	0.103	0.191	0.165	0.460	0.056	0.807	0.006	0.259	0.126
Minfreq	0.788	0.008	0.302	0.106	0.185	0.169	0.363	0.083	0.654	0.021
Meanfreq	0.271	0.120	0.158	0.189	0.367	0.082	0.883	0.002	0.239	0.135
Freqrange	0.513	0.044	0.662	0.020	0.037	0.366	0.272	0.119	0.259	0.125
	SL		BCW		Area		Volume		Centroid size	
	p	r²	p	r²	p	r²	p	r²	p	r²
Maxfreq	0.489	0.049	0.699	0.016	0.812	0.006	0.744	0.011	0.952	0.000
Minfreq	0.579	0.032	0.871	0.003	0.807	0.006	0.932	0.001	0.333	0.094
Meanfreq	0.441	0.060	0.676	0.018	0.798	0.007	0.749	0.011	0.989	0.000
Freqrange	0.215	0.149	0.106	0.240	0.226	0.143	0.299	0.107	0.506	0.045

Mandibular foramen	PC1		PC2		PC3		PC4		ML	
	p	r²	p	r²	p	r²	p	r²	p	r²
Maxfreq	0.810	0.006	0.488	0.049	0.725	0.013	0.889	0.002	0.259	0.126
Minfreq	0.521	0.042	0.175	0.176	0.024	0.414	0.700	0.016	0.654	0.021
Meanfreq	0.800	0.007	0.389	0.075	0.644	0.022	0.892	0.002	0.239	0.135
Freqrange	0.516	0.043	0.232	0.139	0.992	0.000	0.591	0.030	0.259	0.125
	SL		BCW		Area		Volume		Centroid size	
	p	r²	p	r²	p	r²	p	r²	p	r²
Maxfreq	0.489	0.049	0.699	0.016	0.812	0.006	0.744	0.011	0.761	0.010
Minfreq	0.579	0.032	0.871	0.003	0.807	0.006	0.932	0.001	0.309	0.103
Meanfreq	0.441	0.060	0.676	0.018	0.798	0.007	0.749	0.011	0.788	0.008
Freqrange	0.215	0.149	0.106	0.240	0.226	0.143	0.299	0.107	0.271	0.120

Appendix 4

Supplementary Material for Chapter 6

Travis Park[1,2], Erich M. G. Fitzgerald[2,3], Alistair R. Evans[1,2]

[1]School of Biological Sciences, Monash University, Australia.

[2]Geosciences, Museum Victoria, Australia.

[3]National Museum of Natural History, Smithsonian Institution, USA.

Contents

A4.1. Supplementary Material and Methods

(a) Scanning protocols

All specimens were scanned using a Zeiss Xradia 520Versa at the Monash University X-ray Microscopy Facility for Imaging Geo-materials (XMFIG) except for *Physeter macrocephalus* (NMVP218431) and *Balaenoptera acutorostrata* (NMVC24936). Due to their larger size, these two specimens were scanned using a Siemens 128-slice PET-CT scanner at the Melbourne Brain Centre Imaging Unit. Basic measurements of the internal structures of the cochlea were taken using the Measure, Slice and Spline Probe tools in the Avizo software following the methods of Fleischer (1976). These included: cochlear height; cochlear width; number of turns; cochlear canal length; extent of the secondary spiral lamina; cochlear volume; width of the primary spiral lamina; width of the secondary spiral lamina; the distance between the tips of the primary and secondary spiral laminae (known as the laminar gap); diameter of the spiral ganglion canal and wall thickness between adjacent turns. For laminar lengths, laminar gaps and spiral ganglion canal diameters, the measurements were taken at every quarter turn along the length of the cochlea, with the initial measurement taken immediately internal to the fenestra rotunda, following the method of Ekdale & Racicot (2015).

(b) Analysis protocols

The extension (%) of the SSL was measured by dividing length of the cochlear canal at the apical-most point of the SSL by the total length of the cochlear canal. This is slightly different to the method used by Ekdale and Racicot (2015) where they use the length of the SSL divided by the cochlear length.

The laminar gap (the distance between the two spiral laminae) has been used to infer the width of the basilar membrane in the past Fleischer 1976; Luo & Eastman 1995; Geisler & Luo 1996; Luo & Marsh 1996).

From these initial measurements, several ratios were calculated that give a quantitative description of the cochlear morphology. The axial pitch is the height of the cochlea divided by the number of turns of the cochlea. This is found to be generally negatively proportional to frequency (1990). The basal ratio is the height of the cochlea divided by the basal diameter of the cochlea. This is found to be generally negatively proportional to frequency (1990). Geisler and Luo (1996) note that values for the basal ratio may vary across different studies, depending on how the diameter is measured. In this study, the methods of Ekdale (2013) were followed when measuring cochlear diameter and height. The cochlear slope is the height of the cochlea divided by the length of the cochlear canal divided by the number of turns (Ketten & Wartzok 1990). The radii ratio (graded curvature of the cochlea in Ekdale and Racicot (2015)) is the radius of the cochlea at its base divided by the radius of the cochlea at its apex. Manoussaki et al. (2008) found this to be strongly correlated with low frequency hearing limits. The radius measurements were taken using the Slice tool in the Avizo software following the methods of Ekdale and Racicot (2015).

The low frequency limit of hearing was estimated for USNM 534010 using the equation derived by Manoussaki et al. (2008):

$$f = 1507\exp(-0.578[\rho-1])$$

where f = low frequency hearing limit at 60 dB re 20 μPa in air and 120 dB re 1 μPa in water and ρ = radii ratio value.

Another qualitative indicator of whether or not the more apical turns of the cochlea overlapped the basal turns was taken using the Avizo software. The procedure for this followed that of Ekdale and Racicot (2015), where the positional relationships between the basal and more apical turns of the cochlea were observed qualitatively from re-sliced images through the axis of rotation of the cochlea.

(c) Additional institutional abbreviations

Additional institutional abbreviations: MCZ = Museum of Comparative Zoology, Harvard University, Cambridge, USA; NMVC, Museum Victoria Mammalogy collection (Melbourne); NMVP, Museum Victoria Vertebrate Palaeontology collection. USNM = Department of Paleobiology, National Museum of Natural History, Smithsonian Institution, Washington, DC, USA.

A4.2. Supplementary Results

(a) Systematic palaeontology

Order Cetacea Brisson (1762)

Suborder Odontoceti Flower, 1865, *sensu* Flower (1867)

Family Xenorophidae Uhen 2008 *sensu* Sanders and Geisler (2015)

Xenorophidae indet.

Referred specimen. USNM 534010, an isolated right periotic from the Upper Oligocene Belgrade Formation at Onslow Beach, Camp Lejeune Marine Base, Onslow County, North Carolina, USA. USNM 534010 is mostly complete, lacking the distal end of the posterior process and the lateral/anterolateral edge of the lateral tuberosity.

(b) Comparisons based on external morphology of the periotic

USNM 534010 represents a grade of periotic morphology seen in Xenorophidae and two non-xenorophid archaic odontocetes, *Simocetus rayi* Fordyce, 2002 and an unnamed odontocete (USNM 205491) from the Oligocene Alsea Formation of Oregon (Whitmore & Sanders 1977; Fordyce 2002).

Comparisons of USNM 534010 and USNM 205491. Primitive features on the periotic of USNM 534010 provide superficial similarity with USNM 205491, an unnamed "non-squalodontid odontocete" according to Whitmore and Sanders (1977: Fig 2B), and an archaic odontocete of uncertain affinities (Whitmore & Sanders 1977; Fordyce 2002). The right

periotic of USNM 205491 was figured in ventral view by Fordyce (2002: Fig 14). Periotic symplesiomorphies include a transversely compressed hatchet-shaped anterior process, narrow and shallow anterior bullar facet on the anterior process, and a marked anteroexternal sulcus. USNM 534010 is more derived than the periotic of USNM 205491 in having an even narrower, blade-like, anterior process, elongated lateral tuberosity, and salient pyramidal process. The periotic of USNM 205491 is more derived than USNM 534010 in its pars cochlearis having a more rounded outline in ventral view, having relatively narrow bone between the internal acoustic meatus and the anterior edge of the pars cochlearis, lacking a distinct suprameatal fossa, and having a vestigial dorsal crest. The plesiomorphies shared by USNM 534010 and USNM 205491, plus the specialized features of each specimen, do not suggest a close relationship.

Comparisons of USNM 534010 and Simocetus rayi. Comparisons between USNM 534010 and *Simocetus* are restricted to characters on the ventral and medial aspects of the periotic due to the periotic being tightly articulated with the basicranium in the type specimen of *S. rayi*. USNM 534010 and the periotic of *Simocetus* are similar in possessing a primitive elongated morphology of the anterior process. However, USNM 534010 is more specialized than the periotic of *Simocetus* in having a transversely thin, blade-like anterior process and an elongate lateral tuberosity. The periotic of *Simocetus* possesses the following apomorphies absent in USNM 534010: a more transversely inflated anterior process, more strongly developed anterior bullar facet, and a relatively wide fovea epitubaria (Fordyce 2002: Figs 14,15). These comparisons argue against a close relationship between USNM 534010 and *Simocetus*.

Comparisons of USNM 534010 and Xenorophidae. Only three xenorophid species have been described from specimens including the periotic: *Archaeodelphis patrius*, *Albertocetus meffordorum* and *Cotylocara macei* (Allen 1921; Uhen 2008; Geisler et al. 2014).

Comparisons between USNM 534010 and both *Ar. patrius* and *Al. meffordorum* are restricted to characters on the ventral and medial aspects of the periotic due to the periotics being tightly articulated with the basicranium in the type specimens of the latter taxa (Fig A4.5); there are no visible noteworthy differences between USNM 534010 and the periotics of *Ar. patrius* and *Al. meffordorum*. USNM 534010 shares two apomorphies with the periotics of *Ar. patrius*, *Al. meffordorum*, and *C. macei*: a transversely thin, blade-like anterior process and an elongate lateral tuberosity. Primitive characters shared by USNM 534010 and the periotic of *C. macei* include an indistinct anterior bullar facet, poorly defined fovea epitubaria, a pars cochlearis with a trapezoidal outline in ventral view, thick bone between the internal acoustic meatus and the anterior edge of the pars cochlearis, a distinct suprameatal fossa, and a salient dorsal crest. USNM534010 is almost identical in size to the periotic of *C. macei* but differs by having a more strongly salient pyramidal process.

Two specialized periotic characters (transversely thin blade-like anterior process, and an elongate lateral tuberosity) are shared by all described xenorophid periotics plus USNM 534010, and may represent xenorophid synapomorphies. The apomorphies shared with xenorophids, twinned with its lack of specializations in the superficially similar periotics of other archaic odontocetes (*Simocetus* and USNM 205491), show that USNM 534010 represents a xenorophid periotic. Comparisons between USNM 534010 and the periotics of described xenorophids reveal relatively little qualitative morphological variation between taxa. Although USNM534010 was collected from the same locality and horizon as *Al. meffordorum*, I could not identify any potential synapomorphies that unite the latter fossils to the exclusion of other xenorophids. Hence, I provisionally refer USNM534010 to Xenorophidae, gen. et sp. indet.

(c) Comparisons of the cochleae

The cochlea of USNM 534010 completes two turns. Modern odontocetes possess cochleae that range from 1.5 turns (*Kogia breviceps*) to 2.5 turns (*Lagenorhynchus albirostris* (Ketten & Wartzok 1990)), with the majority being 1.75–2 turns. USNM 534010 therefore falls within the range of modern taxa. It is also greater than the 1.5 turns found in the squalodontoid examined by Luo and Eastman (1995). The small size of the fenestra rotunda is also similar to what is found in modern odontocete taxa. The fenestra rotunda and the cochlear aqueduct are enclosed in separate passages, which appears to be the normal condition for all studied cetaceans except for *Eschrichtius*, which possesses an undivided perilymphatic foramen (Ekdale & Racicot 2015).

The apical-most half turn overlaps the basal turn. This is a higher degree of overlap than is seen in modern odontocetes, who display little to no overlap of their turns. Mysticetes and archaeocetes, in contrast, display a high degree of overlap in their turns. The degree of overlap is reflected in the thickness of the walls between the basal and apical turns. USNM 534010 has a thinner wall between its apical and basal turns, more similar to that of mysticetes and archaeocetes than modern odontocetes. USNM 534010 lacks a tympanal recess, which is present in balaenopteroids and, as I show for the first time, ziphiids and physeterids.

The basal ratio of USNM 534010 is 0.48. This value is within the range found for modern odontocetes in this study (0.42 – 0.56). Whilst the mysticete examined in this study (*Balaenoptera acutorostrata*) had a basal ratio of 0.53, the mysticetes examined in Ekdale and Racicot (2015) have higher values in the rage 0.49 – 0.65, reflecting the higher spirals found in mysticetes. *Zygorhiza* was found to have a value of 0.66. The squalodontoid examined by Luo and Eastman (1995) has an abnormally high basal ratio value of 0.83, reflecting the unusually tall height of the cochlea.

The cochlear volume of USNM 534010 is 122.29 mm^3. This is within the range of modern odontocetes (88.51 mm^3 – 204.11 mm^3) with the exception of the two largest odontocete taxa in the sample, *Tasmacetus shepherdi* (684.79 mm^3) and *Physeter macrocephalus* (828.91 mm^3). Excluding the latter species, the cochlear volumes of odontocetes are much smaller than those of *Zygorhiza* (259.14 mm^3) and *B. acutorostrata* (412.34 mm^3).

The radii ratio value can give an indication of the low frequency sensitivity of a taxon (Manoussaki et al. 2008). In having a value of 5.04, USNM 534010 is higher than those calculated for the modern odontocetes in this study (3.39 – 4.91), excepting for the two ziphiid taxa *Mesoplodon grayi* (8.52) and *T. shepherdi* (9.60) and is also close to the value of *Physeter macrocephalus* (4.91) (Table S1). This suggests that xenorophids may have been able to hear lower frequencies than most modern odontocetes.

With an estimated low frequency hearing limit of 145.91 Hz, USNM 534010 could hear lower frequencies than any modern odontocete (excluding ziphiids). The ability of USNM 534010 to detect lower frequencies than most modern odontocetes is also indicated by the shorter extent of its secondary spiral lamina, which would have meant a more flexible basilar membrane. At 50% of the total length of the cochlear canal it is shorter than any modern odontocete and only slightly shorter than the squalodontoid examined by Luo and Eastman (1995), which had a secondary spiral lamina that extended for just over 50% of the cochlear canal length. It is however, much longer than *B. acutorostrata* (33%) and *Zygorhiza* (25%).

## A4.3. Supplementary Figures
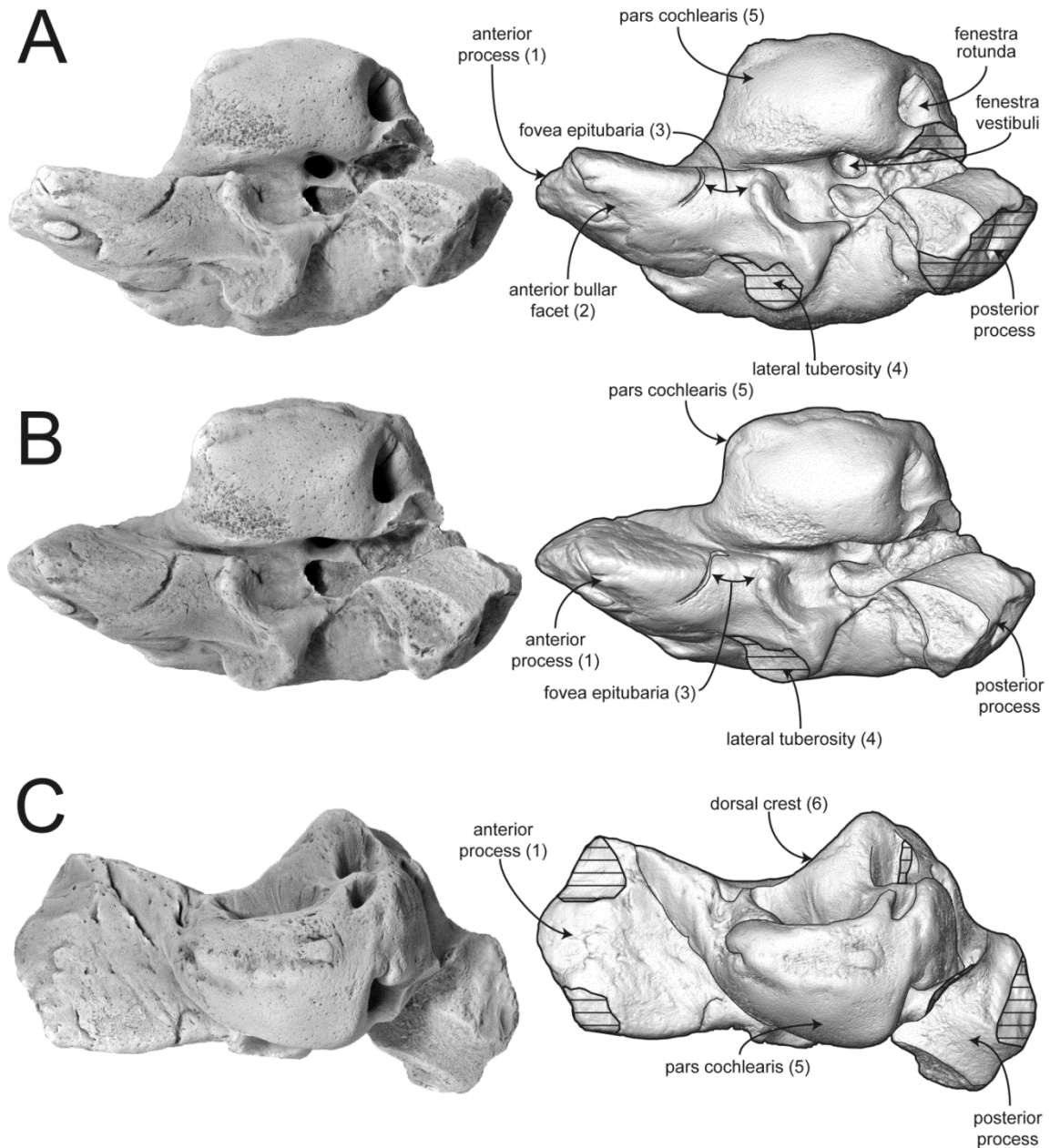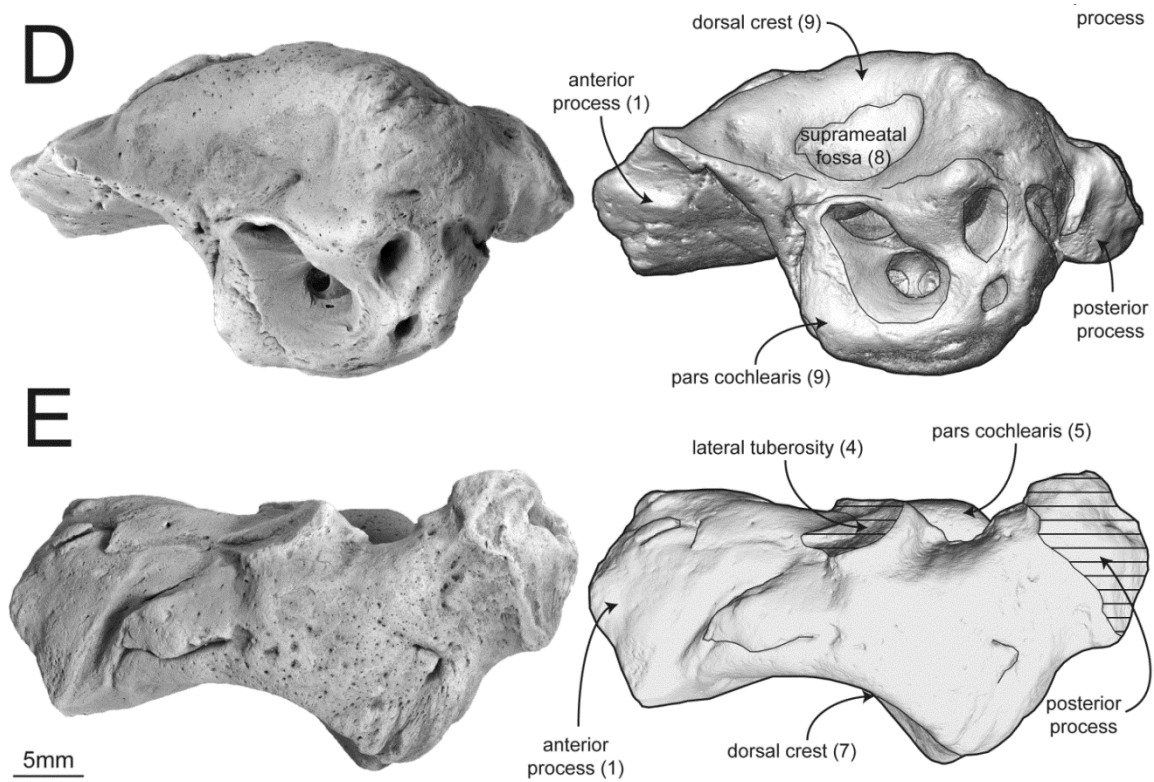
Fig A4.1. USNM 534010, Xenorophidae indet., right periotic, photograph of original specimen (left) and digital model reconstructed from microCT data (right) in (A) ventral, (B) ventromedial, (C) medial, (D) cerebral view, (E) lateral view. Hatching indicates major breaks. Numbers in parentheses indicate character states listed in the Results section of the main text.
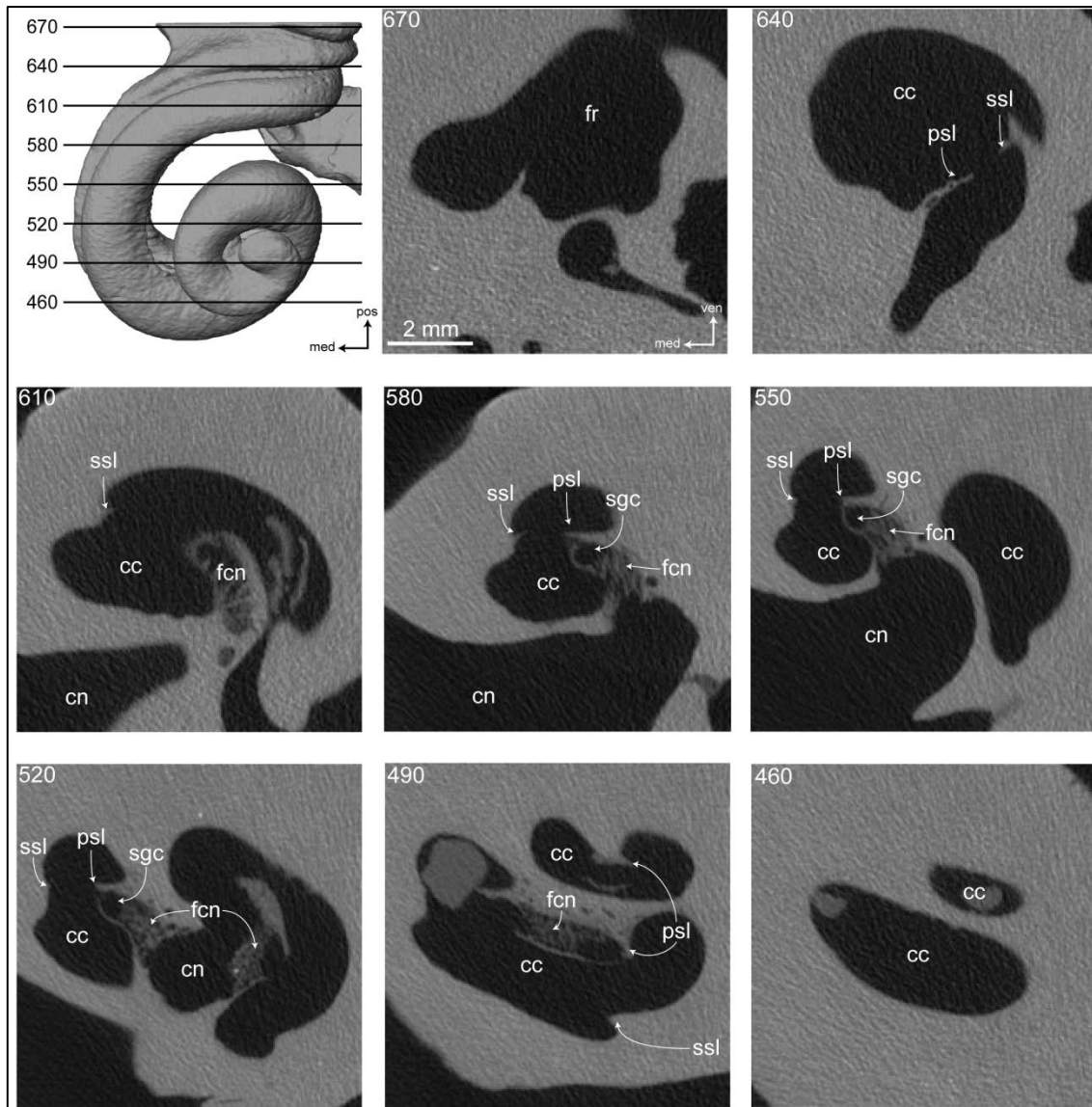
Fig A4.2. Raw microCT slices through right inner ear of USNM 534010. Numbers indicate slice indicated in top left. cc, cochlear canal; cn, canal for cranial nerve VIII (auditory nerve); fcn, foramina for the cochlear nerves; fr fenestra rotunda; med, medial; pos, posterior; psl, primary spiral lamina; sgc, spiral ganglion canal; ssl, secondary spiral lamina; vc, vestibular curve; ven, ventral.
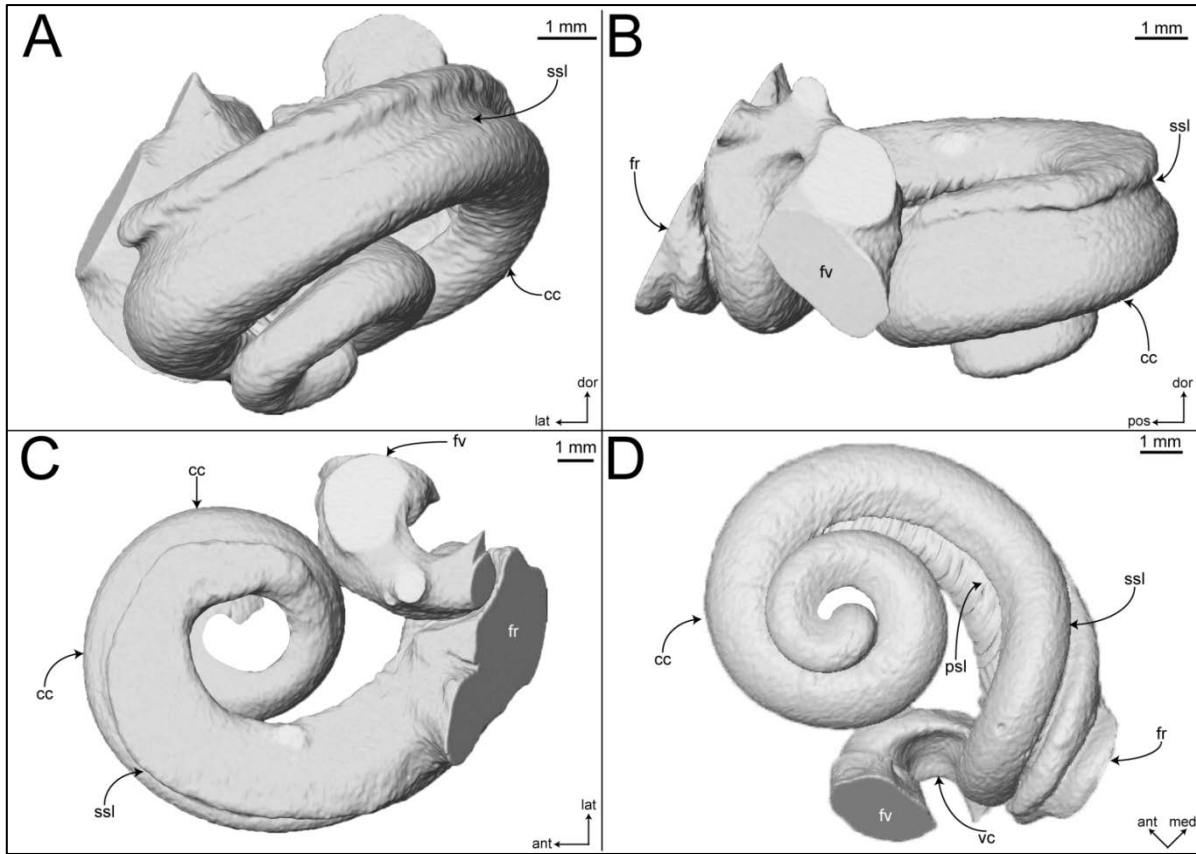
Fig A4.3. Digital endocast of right cochlea of USNM 534010 reconstructed from microCT data in (*a*) anterior, (*b*) lateral, (*c*) dorsal, (*d*) vestibular views. ant, anterior; cc, cochlear canal; dor, dorsal; fr, fenestra rotunda; fv, fenestra vestibuli; lat, lateral; med, medial; pos, posterior; psl, primary spiral lamina; ssl, secondary spiral lamina; vc, vestibular curve.
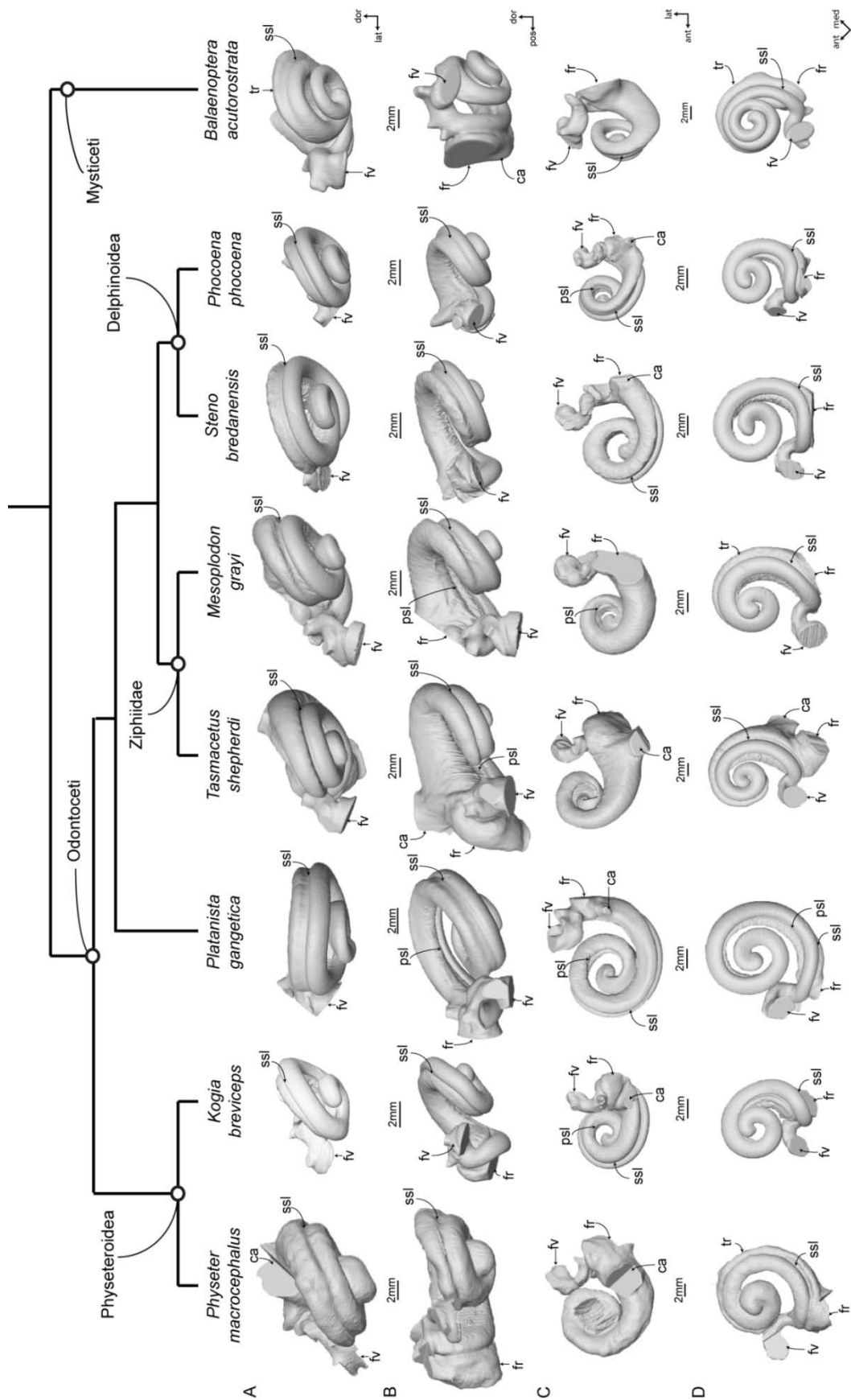
Fig A4.4. Digital endocasts of extant odontocete cochleae in: A, anterior; B, lateral; C, dorsal; D, vestibular views. Specimens shown as right cochlea, specimens from left side reversed. ca, cochlear aqueduct; fr, fenestra rotunda; fv, fenestra vestibuli; psl, primary spiral lamina; ssl, secondary spiral lamina; tr, tympanal recess.
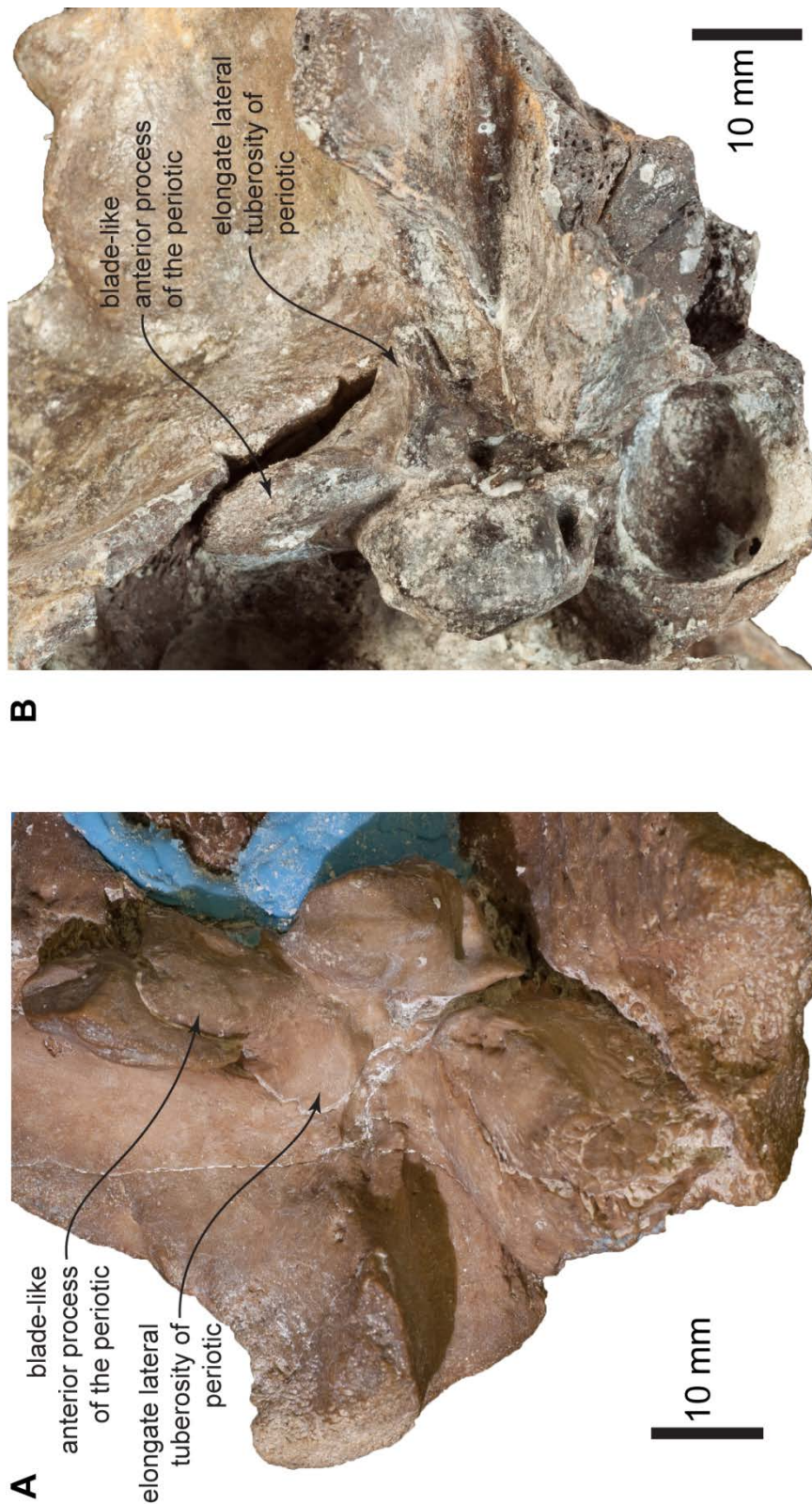
Figure A4.5. Periotic morphology of Xenorophidae. (*a*): MCZ 15749, *Archaeodelphis patrius*, right auditory region of the cranium (including periotic) in ventral view. (*b*): USNM 525001, *Albertocetus meffordorum*, left auditory region of the cranium (including periotic) in ventral view.

A4.4. Supplementary Tables

Table A4.1. Measurements for the cochleae sampled in this study. AP, axial pitch; Ar, apical radius; Br, basal radius; BR, basal ratio; CH, cochlea height; CL, canal length; CW, cochlea width; Est. LFL, estimated low frequency limit; Hz, hertz; T, number of turns; S#, specimen number; Sl, slope; SSL, secondary spiral lamina; Vol., volume.

Taxon	S#	T	CL (mm)	T*CL	Br (mm)	Ar (mm)	RR	% SSL	BR	AP	Sl	CH (mm)	CW (mm)	Vol. (mm³)	Est. LFL (Hz)
Odontoceti															
Xenorophidae indet.	USNM 534010	2	28.83	57.65	5.68	1.13	5.04	50	0.48	2.41	0.08	4.82	9.97	122.29	146
Kogia breviceps	NMVC 24976	1.5	27.12	40.68	4.87	1.07	4.54	83	0.45	2.79	0.10	4.18	9.32	109.54	195
Mesoplodon cf. *grayi*	NMVC 31378	1.75	25.36	44.38	5.84	0.69	8.52	57	0.62	3.63	0.14	6.36	10.32	204.11	20
Phocoena phocoena	NMVC 27654	1.5	23.06	34.59	4.04	1.02	3.97	66	0.56	2.94	0.13	4.41	7.91	85.51	271
Physeter macrocephalus	NMVP 218431	1.75	45.53	79.68	8.01	1.63	4.91	57	0.55	4.83	0.11	8.45	15.25	828.91	157
Platanista gangetica	NMVC 27417.2	2	40.69	81.39	6.92	1.64	4.23	63	0.42	2.71	0.07	5.41	12.84	198.14	233
Steno bredanensis	NMVC 36961	1.5	30.32	45.48	4.91	1.45	3.39	66	0.50	3.47	0.11	5.21	10.46	154.85	378
Tasmacetus shepherdi	NMVC 37967.6	1.75	33.66	58.90	9.06	0.94	9.60	57	0.47	4.12	0.12	7.21	15.48	684.79	10
Mysticeti															
Balaenoptera acutorostrata	NMVC 24936	2.25	42.78	96.25	8.08	0.98	8.24	33	0.53	3.00	0.07	6.76	12.65	412.34	23

Table A4.2. Parameters of CT scans of cetacean periotics in this study. kV, kiloelectron volt; µm, micrometres.

Taxon	Specimen Number	Scan power (kV)	No. of slices	Pixel size (µm)
Xenorophidae indet.	USNM 534010	100	401	38.04
Kogia breviceps	NMV C24976	90	1601	33.07
Mesoplodon cf. *grayi*	NMV C31378	90	1601	44.02
Phocoena phocoena	NMV C27654	90	1601	33.08
Physeter macrocephalus	NMV P218431	140	731	119.14
Platanista gangetica	NMV C27417.2	100	1601	41.50
Steno bredanensis	NMV C36961	90	3201	32.97
Tasmacetus shepherdi	NMV C37967.6	120	1601	58.28
Balaenoptera acutorostrata	NMV C24936	140	856	146.50

Table A4.2 Measurements (in mm) of the periotic of
Xenorophidae indet. (USNM534010).

Measurement	USNM534010
Maximum length of the periotic	41
Maximum transverse diameter of periotic	23
Anteroposterior diameter of anterior process	15.5
Transverse diameter of anterior process	7.3
Dorsoventral diameter of anterior process	14.5
Anteroposterior diameter of pars cochlearis	18.0
Transverse diameter of pars cochlearis	10.0
Maximum dorsoventral diameter of pars cochlearis	14.8
Distance between aperture for cochlear aqueduct and fenestra rotunda	6.1
Distance between aperture for vestibular aqueduct and fenestra rotunda	9.0
Distance between fenestra ovalis and fenestra rotunda	4.3
Minimum distance between edge of fundus of internal acoustic meatus and the aperture for vestibular aqueduct	2.6
Minimum distance between edge of fundus of internal acoustic meatus and the aperture for cochlear aqueduct	3.0

References

Allen GM. 1921. A new fossil cetacean. Bulletin of the Museum of Comparative Zoology at Harvard College 65, 1–14.

Ekdale EG. 2013 Comparative anatomy of the bony labyrinth (inner ear) of placental mammals. PLoS ONE 8, e66624.

Ekdale EG, Racicot RA. 2015. Anatomical evidence for low frequency sensitivity in an archaeocete whale: comparison of the inner ear of Zygorhiza kochii with that of crown Mysticeti. Journal of Anatomy 226, 22–39.

Fleischer G. 1976. Hearing in extinct cetaceans as determined by cochlear structure. Journal of Paleontology 50, 133–152.

Fordyce RE. 2002. *Simocetus rayi* (Odontoceti: Simocetidae, New Family): A bizarre new archaic Oligocene dolphin from the eastern Pacific. In Emry RE, ed, Cenozoic Mammals of Land and Sea, Tributes to the Career of Clayton E. Ray. Smithsonian Contributions to Paleobiology 93, 185–222.

Fordyce RE, Fitzgerald EMG, González Barba G. 2012. Long-tusked archaic Oligocene odontocetes from Oregon and Baja California Sur, Eastern Pacific Margin. Society of Vertebrate Paleontology Program and Abstracts 2012, 95.

Geisler JH, Luo ZX. 1996. The petrosal and inner ear of Herpetocetus sp. (Mammalia: Cetacea) and their implications for the phylogeny of hearing of archaic mysticetes. Journal of Paleontology 70, 1045–1066.

Geisler JH, Colbert MW, Carew JL. 2014. A new fossil species supports an early origin for toothed whale echolocation. Nature 508, 383–386.

Ketten DR, 2000. Cetacean ears. In Au WWL, Popper AN, Fay RR, eds, Hearing by whales and dolphins. Springer-Verlag, New York, pp. 43–108.

Ketten DR, Wartzok D. 1990. Three dimensional reconstructions of the dolphin ear. In

    Thomas JA, Kastelein RA, eds, Sensory abilities of Cetaceans. Plenum Press, New

    York, pp. 81–105.

Luo ZX, Eastman ER. 1995. Petrosal and inner ear of a squalodontoid whale: implications for

    evolution of hearing in odontocetes. Journal of Vertebrate Paleontology 15, 431–442.

Luo ZX, Marsh K. 1996. Petrosal (periotic) and inner ear of a Pliocene kogiine whale

    (Kogiinae, Odontoceti): Implications on relationships and hearing evolution of

    toothed whales. Journal of Vertebrate Paleontology 16, 328–348.

Manoussaki D, Chadwick RS, Ketten DR, Arruda J, Dimitriadis EK, O'Malley JT. 2008. The

    influence of cochlear shape on low-frequency hearing. Proceedings of the National

    Academy of Sciences 105, 6162–6166.

Uhen MD. 2008. A new *Xenorophus*-like odontocete cetacean from the Oligocene of North

    Carolina and a discussion of the basal odontocete radiation. Journal of Systematic

    Palaeontology 6, 433–452.

Whitmore FC Jr, Sanders AE. 1977. A Review of the Oligocene Cetacea. Systematic

    Zoology 25, 304–320.